Bone marrow-derived cells in renal repair

Broekema, Martine

Publication date:
2007

[Link to publication in University of Groningen/UMCG research database](#)

Bone marrow-derived
cells in renal repair

Martine Broekema

Bone Marrow-Derived Cells in Renal Repair

Stellingen behorende bij het proefschrift

Bone Marrow-Derived Cells in Renal Repair

1   Aangezien beenmergafkomstige cellen slechts sporadisch inbouwen in het tubulusepitheel, is het onwaarschijnlijk dat deze cellen een structurele rol spelen in tubulair herstel na schade. *(dit proefschrift)*

2   Beenmergafkomstige cellen zouden, door te differentiëren tot interstitiële myofibroblasten, kunnen bijdragen aan het onstaan van nierfibrose. *(dit proefschrift)*

3   De profibrotische bijwerking van ciclosporine is niet het gevolg van toegenomen myofibroblast differentiatie van beenmergafkomstige cellen. *(dit proefschrift)*

4   De multipotente differentiatiecapaciteit van beenmergafkomstige cellen maakt de therapeutische toepassing van deze cellen een riskante onderneming. *(dit proefschrift)*

5   (W)eten is een primaire levensbehoefte van de mens.

6   Het betrekkelijk lage aantal nieuwe donoren dat naar aanleiding van BNN's "Grote Donorshow" is geregistreerd, geeft aan dat het tekort aan donoren niet het gevolg is van een tekort aan publiciteit, maar eerder te wijten valt aan de apathie van de potentiële donorpopulatie.

7   Wijziging van de huidige wet op de orgaandonatie door de invoering van het Actief Donorregistratiesysteem (ADR) is op dit moment de enige manier om het aantal orgaandonoren te verhogen.

8   De wereld is een boek en zij die niet reizen, lezen slechts één bladzijde.
(H. Augustinus van Hippo)

9   Het leven is een feest, maar je moet wel zelf de slingers ophangen.

10   Het feit dat het dankwoord van een proefschrift op de laatste pagina staat, zorgt ervoor dat (tot en met) de laatste pagina doorgelezen wordt.

Martine Broekema
14 november 2007
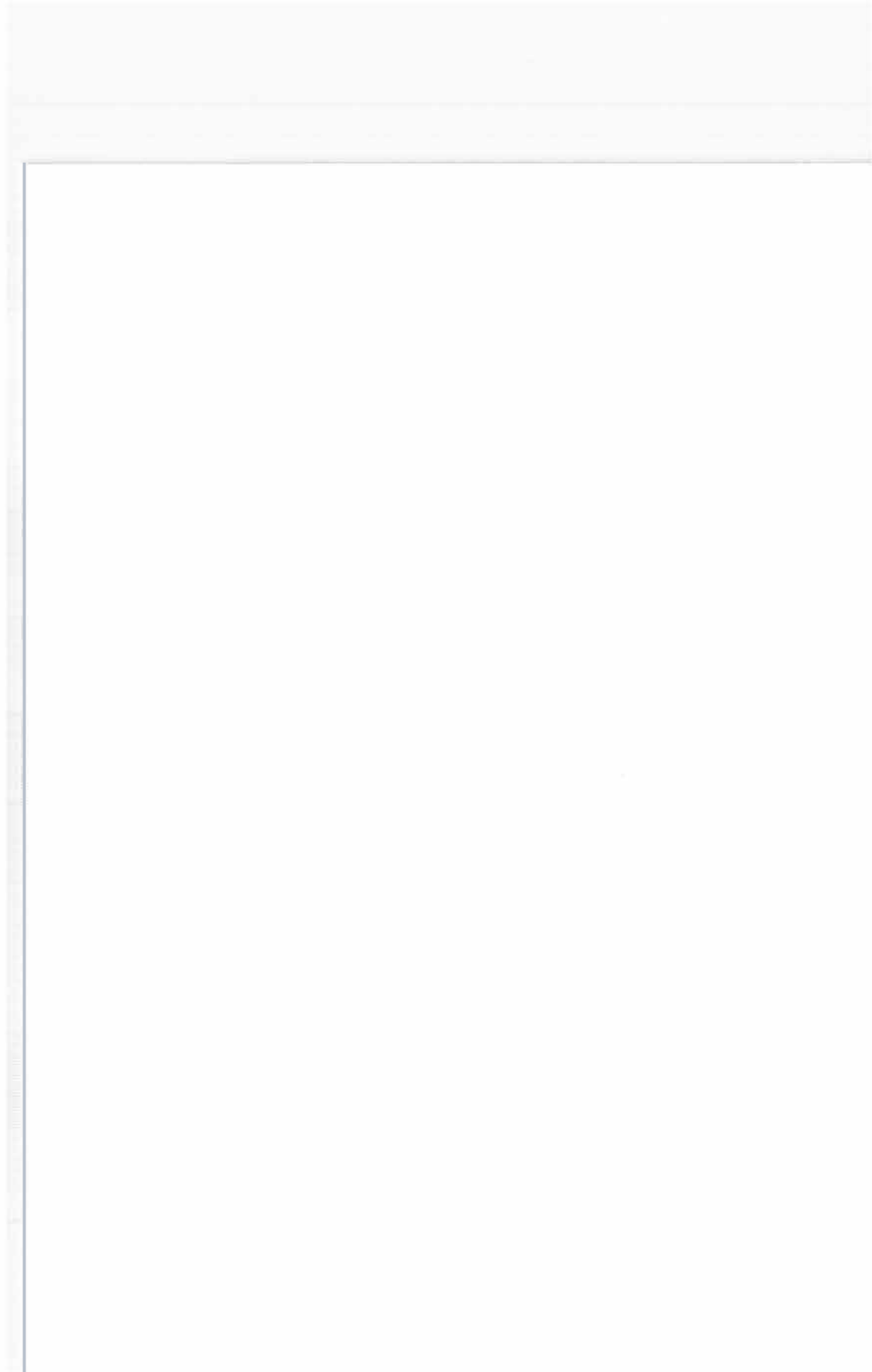
RIJKSUNIVERSITEIT GRONINGEN

Bone Marrow-derived Cells in Renal Repair

Proefschrift

ter verkrijging van het doctoraat in de
Medische Wetenschappen
aan de Rijksuniversiteit Groningen
op gezag van de
Rector Magnificus, dr. F. Zwarts,
in het openbaar te verdedigen op
woensdag 14 november 2007
om 16:15 uur

door

Martine Broekema

geboren op 9 december 1978
te Veendam

Paranimfen: Machteld van Amerongen
Lyanne Brouwer

Contents

Chapter 1

Introduction to the thesis

The kidney can recover after acute renal injury due to its highly effective endogenous regenerative capacity. However, under certain conditions the balance between injury and repair can get disturbed. This can ultimately lead to chronic renal failure, which is an increasing problem in the clinical setting. Therapy for renal failure has greatly improved over the years, especially by the introduction of kidney transplantation. Nevertheless, due to the shortage of donor organs and the relatively low long-term success rate after kidney transplantation, new therapeutic strategies are highly desirable. Bone marrow-derived cells (BMDC) might offer a therapeutic solution for renal failure. In this thesis we explored the differentiation choices of BMDC after acute renal injury. First, we will introduce some general aspects of renal damage, repair, and the possible therapeutic potential of BMDC therein and we will discuss the research questions addressed in this thesis.

Acute renal failure

Acute renal failure (ARF), which affects up to 5% of all long-term hospital patients (1), can be triggered by various insults, among which ischemia/reperfusion injury (IRI) holds a forefront role. The pathophysiology of IRI involves renal endothelial and tubular epithelial injury, oxidative stress, inflammation and wound healing. Post-ischemic endothelial damage results, due to an imbalance in the production of endothelin (2) and NO (3), in intra-renal vasoconstriction, which is assumed to contribute to loss of renal function. However, the use of renal vasodilators, which return renal blood flow to normal in experimental IRI, do not improve renal function, therefore the vasomotor component may not be the culprit.

Studies on the mechanisms mediating IRI have been primarily focused on the renal tubule. The straight segment of the proximal tubule (S_3 segment, pars recta) is most susceptible to ischemic injury (4). Both the deprivation of oxygen during ischemia and the restoration of oxygen supply during reperfusion cause tubular damage (Figure 1). The damage caused by renal ischemia depends largely on the duration of oxygen deprivation. Upon ischemia, oxygen deprivation of the tubular cell leads to depletion of cellular ATP, which initiates a cascade of biochemical events that lead to mitochondrial damage, impaired solute and ion transport, loss of cell polarity, and cytoskeletal disruption (5). In case of severe ischemia these events lead to cell death, shedding and excretion of proximal tubule brush border membranes and tubular epithelial cells into the urine (6). Histologically, ischemic damage is represented by patchy and focal loss of tubular epithelial cells, resulting in areas of denuded basement membrane, and the presence of intraluminal casts (7).

Although restoration of blood flow during reperfusion is essential for survival of the kidney, it leads to further cellular damage. Reperfusion is therefore known as the "reflow paradox". The mechanism of reperfusion injury includes the generation of reactive oxygen species (ROS) (8). ROS have numerous deleterious effects on cells, such as lipid peroxidation, oxidation of cell proteins, and damage to DNA (9). Moreover, generation of ROS causes endothelial activation and recruitment of leukocytes through the upregulation of chemokines (10) and the proinflammatory cytokines interleukin-1 (IL-1), IL-2, IL-8, tumor necrosis factor-alpha (TNF-α) and interferon-γ (IFN-γ) by affected cells (11-13). Adhesion molecules, such as intercellular adhesion molecule-1 (ICAM-1),

vascular cell adhesion molecule (VCAM) and P-selectin are upregulated during IRI and promote endothelial-leukocyte interactions. These adhesion molecules facilitate inflammation by increasing the infiltration of mainly neutrophils and macrophages in the renal interstitium early after ischemic injury (14), while later phases are characterized by infiltration of macrophages and T lymphocytes (15;16). The infiltration of leukocytes leads to a vicious circle of inflammation by secondary activation of leukocytes which release mediators, such as free oxygen radicals, proteases, and cytokines that further aggravate tissue damage.

Kidney transplantation can also lead to acute renal injury and consequently, delayed graft function. Renal transplantation is the treatment of choice for end stage renal failure (17). Due to the introduction of immunosuppressive therapy (especially of ciclosporin (CsA) in the 1980's) and improvements in HLA matching (18), ischemic times and organ preservation (19), graft survival after kidney transplantation has improved to about 90% at 1 year post-transplantation (20). Despite major short-term graft survival, 30% of all renal transplant recipients experience acute rejection, which is the strongest risk factor for development of chronic renal transplant failure. Beside acute rejection, transplant injury is caused by cold and warm ischemia and nephrotoxicity from immunosuppressive medication. IRI augments the specific immune response to the allograft through the upregulation of MHC class II and adhesion molecule expression in the allografted kidney, thereby increasing the risk of acute rejection (21). In principle, IRI of the donor kidney is unavoidable, especially when a kidney of a deceased donor is transplanted. However, when ischemic times are short, for example during transplantation of a kidney of a living donor, IRI and the risk for delayed graft function is substantially reduced.

Acute rejection is primarily a cell-mediated immune-response of the recipient against the alloantigens present in the renal graft. Histologically, acute rejection is characterized by interstitial inflammatory infiltrates, tubulitis and various degrees of arteritis. For diagnostic purposes, the abnormalities are classified in renal biopsies according to the Banff classification (22). Acute rejection is initiated when recipient CD8+ T-cells recognize allogeneic MHC class I-molecules on the tubular epithelium, endothelium or mesangial cells of the donor kidney. Upon costimulation by professional antigen-presenting cells (APCs) or cytokines provided by CD4+ helper T-cells, CD8+ T-cells differentiate to cytotoxic T-cells (CTLs). These alloreactive CTLs directly lyse target cells of the donor kidney. Activation of CD4+ helper T-cells, by recognition of MHC class II molecules on APCs, results in secretion of cytokines and activation of macrophages, B cells and CD8+ T-cells, thereby maintaining inflammation and further aggravating graft injury. Not only cell-mediated, but also a humoral immune response against allo-antigens contributes to rejection. Allo-antibodies bind to endothelium, activate the complement system and injure graft blood vessels.

Renal repair mechanisms after acute injury

After acute renal injury innate mechanisms are activated that result in replacement of damaged tubular epithelial cells and deposition of extracellular matrix (ECM) to restore renal morphology and function. Better understanding of these innate mechanisms of repair will uncover new therapeutic targets.

Acute tubular injury is usually reversible. The prevailing theory is that the innate repair mechanisms of the kidney are dependent on surviving proximal tubular epithelial cells (Figure 1). After injury the surviving tubular cells have the ability to repair themselves by re-polarization and restoration of their cytoskeleton, mitochondria and solute and ion transport system. In addition, surviving tubular cells serve to replace lost tubular cells. In the scenario of replacement, sublethally injured tubular cells dedifferentiate to mesenchymal cells (23;24). Subsequently, the dedifferentiated tubular epithelial cells proliferate rapidly and extensively to restore original epithelial cell number (25-27). The dedifferentiated cells spread and migrate over the basement membrane to denuded areas (28;29) where they differentiate to tubular epithelial cells, leading to restoration of morphology and function (30). Several growth factors have been identified that may facilitate these regenerative responses, such as epidermal growth factor (EGF), insulin-like growth factor-1 (IGF-1), hepatocyte growth factor (HGF), vascular endothelial growth factor (VEGF) and fibroblast growth factor (FGF) (31).

Repair of the kidney after acute injury depends not only on epithelialization of the denuded basement membrane, but also on wound healing. Wound healing is the process of structural remodeling in order to maintain tissue integrity. Fibroblasts and myofibroblasts participate in wound healing by producing ECM components and by responding to and synthesizing cytokines, chemokines and other mediators of inflammation. When wound healing is completed, fibroblasts and myofibroblasts generally disappear by apoptosis (32). However, when apoptosis is lacking and proliferation and/or activation of fibroblasts and myofibroblasts is out of control, this can result in the excessive deposition ECM components. Long-term consequence of the disturbed balance between ECM production and degradation is interstitial fibrosis and chronic renal failure.

Chronic renal failure

If innate renal repair mechanisms are inadequately controlled, this can eventually lead to chronic renal failure (CRF). CRF is characterized by the progressive loss of renal function and can result in end-stage renal disease and the need for replacement therapy, i.e. dialysis or transplantation. Renal interstitial fibrosis is the hallmark of CRF because the extent of renal interstitial fibrosis correlates with loss of renal function (33). As discussed above, renal interstitial fibrosis is the result of inadequately controlled wound healing. Control over wound healing is lost when transforming growth factor-β (TGF-β), generally regarded as the inducer of fibrosis, is overexpressed in the kidney. TGF-β increases expression of connective tissue growth factor (CTGF) (34), which induces proliferation of (myo)fibroblasts (35). Similar to CTGF, TGF-β causes upregulation of basic fibroblast growth factor-2 (FGF-2) in renal interstitial (myo)fibroblasts, inducing proliferation of these cells (36). The downstream effect of TGF-β upregulation and subsequent (myo)fibroblast proliferation is excessive interstitial accumulation of ECM components, such as fibronectin, collagen I, III and proteoglycans. Formation of peptide bonds between these ECM components is catalyzed by transglutaminases, resulting in extensively cross linked protein polymers, which are resistant to degradation. Together with excessive production of ECM, this will lead to a disturbance in the balance between production and degradation of ECM

components, resulting in interstitial scarring and suppression of tubular epithelial cells (Figure 1).

Myofibroblasts are considered the major producers of ECM components during renal interstitial fibrosis (37). These cells possess phenotypical characteristics of both fibroblasts and smooth muscle cells. The origin of the myofibroblast remains subject of discussion. Several options for their origin have been reported, i.e. that myofibroblasts may represent an activated population of resident fibroblasts (38), or that myofibroblasts originate from injured tubular epithelial cells by epithelial-to-mesenchymal transition (EMT) (39), from perivascular smooth muscle cells (40) or from BMDC (41) (Figure 1).

Chronic renal injury can also occur in the renal transplant and thus lead to graft loss. Despite the excellent clinical perspective at 1 year post-transplantation, half of the transplanted kidneys are lost within 10 years after engraftment (42). The most important cause of graft loss is chronic allograft nephropathy (CAN); progressive deterioration of renal function ultimately leading to graft loss. Histopathologically, CAN is characterized by mononuclear cell infiltration, glomerulosclerosis, interstitial fibrosis, tubular atrophy, perivascular inflammation, vascular obliteration and vascular wall thickening. In contrast to the allo-antigen-driven event of acute rejection, CAN is the consequence of both immune factors, such as acute rejection episodes, and non-immune factors, such as donor-related factors (e.g. age, brain death), IRI during transplantation and immunosuppressive drug-induced toxicity (43). To date, there is no effective way to prevent or treat CAN.

Currently, preventing or treating renal failure by simulating or promoting the innate capacity of the kidney to reverse acute tubular injury, has attracted interest as a new therapeutic strategy.

Bone marrow-derived cells (BMDC) in renal repair

The BMDC population is heterogeneous, consisting mainly of inflammatory cells, i.e. neutrophils, macrophages and T lymphocytes that infiltrate the kidney upon injury. Besides inflammatory cells, the BMDC population contains small numbers of stem cells and/or progenitor cells. A large body of evidence supports the idea that stem- and progenitor cells can infiltrate multiple organs and engraft tissue structures upon injury. BMD stem- and progenitor cells were reported to show the plasticity to differentiate towards cells from any of the three germ layers. The potential of BMDC subpopulations to replace damaged tissue cells by engraftment and differentiation, favors therapeutic cell therapy with BMDC.

The bone marrow contains two stem cell populations that were believed to serve only as the blood-forming compartment of the body. However, multiple investigators have suggested that these stem cells mediate tissue repair by repopulation and differentiation in injured tissues. Firstly, hematopoietic stem cells (HSC), appeared capable to differentiate to multiple cell types (44). HSC are lineage-uncommitted (Lin) bone marrow cells that are characterized in human and mice by the expression of the cell surface markers CD34, Sca-1 and c-kit (45;46). Secondly, mesenchymal stem cells or marrow stromal cells (MSC) that are typically characterized as plastic adherent, non-hematopoietic bone marrow cells that can be cultured *in vitro* and maintained
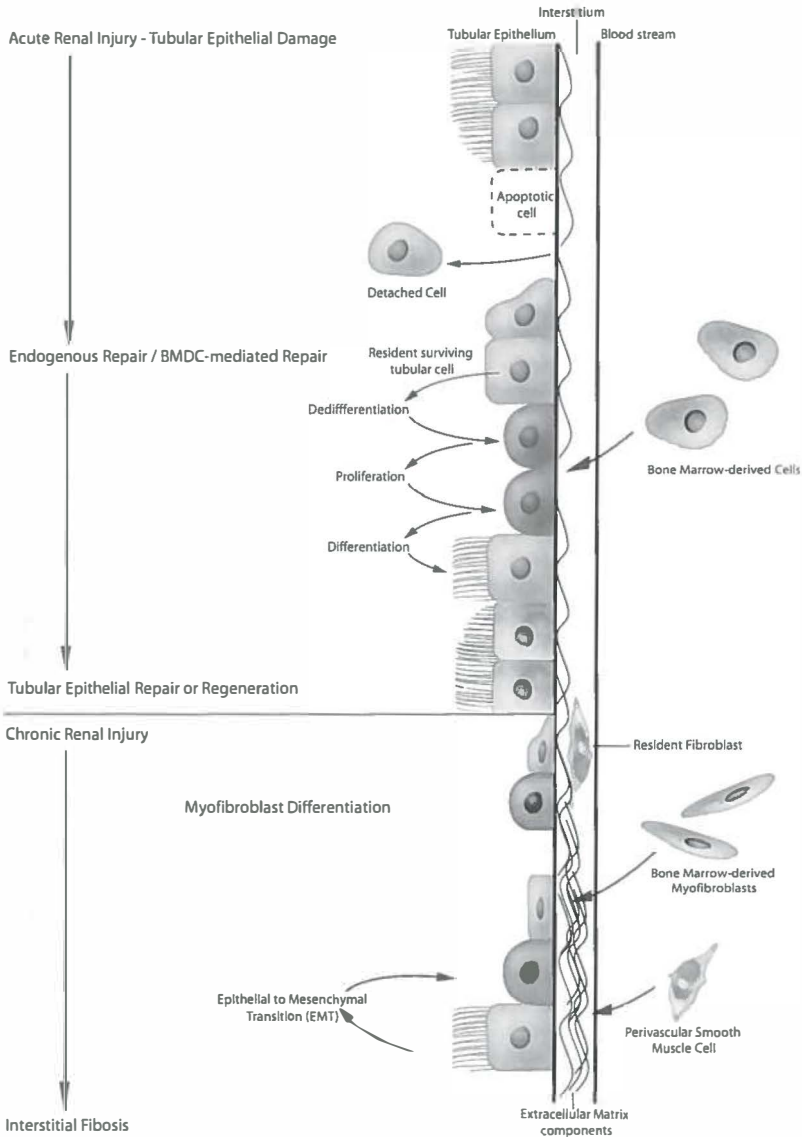
Figure 1. *Schematic representation of BMDC in acute and chronic renal injury. Acute renal injury will lead to tubular epithelial damage, loss of tubular epithelial cells and areas of denuded basement membrane. Acute renal injury elicits activation of endogenous renal repair, i.e. restoration of cell physiology or dediffferentiation, proliferation and differentiation of surviving tubular cells to replace the lost tubular cells. Another option for tubular repair after acute renal injury is recruitment of BMDC from the bone marrow upon injury and subsequent engraftment and replacement of lost tubular cells. However, a disturbed balance between renal injury and repair can lead to chronic renal injury. Myofibroblasts, originating from differentiated resident fibroblasts, BMDC, perivascular smooth muscle cells or tubular epithelium cells by epithelial-to-mesenchymal transition, produce ECM components in the renal interstitium. Interstitial fibrosis, the hallmark of chronic renal injury, occurs when apoptosis of myofibroblasts is lacking, proliferation of myofibroblasts is out to control, leading to excessive deposition, cross linking and dysregulated degradation of ECM in the renal interstitium. Adapted from: Krause, D. and Cantley, L.G.: J Clin Invest 115: 1705-8, 2005.*

as fibroblast-like cells. MSC have the potential to differentiate into mesenchymal lineages such as chondrocytes, osteocytes and adipocytes, but also into other, non-mesenchymal cell lineages such as endothelial and muscle cells (47). Possibly, these bone marrow-derived (BMD) stem cell populations have the ability to mediate kidney repair by differentiation towards tubular epithelial cells.

Besides stem cells, progenitor cells can be part of the BMDC population that infiltrates the kidney upon injury. While progenitor cells share many common features with stem cells, they are more restricted in terms of plasticity and self renewal. Endothelial progenitor cells (EPC) are BMD progenitor cells that, based on their expression of a restricted set of surface markers (CD34, VEGF-R2 and/or CD133), can be isolated from bone marrow, umbilical vein blood and peripheral blood. *In vitro*, EPC differentiate into endothelial cells and in animal models of ischemia, EPC were shown to incorporate into sites of active angiogenesis and mediate neovascularization (48;49). This potential renders the EPC an attractive candidate for therapeutic application to achieve endothelial repair in the injured kidney.

In several organs BMDC or BMD stem- or progenitor cells were reported to engraft and differentiate towards tissue specific cell types. Since in most studies bone marrow transplantation was performed with whole bone marrow, the investigators were unable to define which BMDC subpopulation differentiated. In the infarcted heart, lineage-depleted, c-kit$^+$ BMDC have been shown to differentiate into cardiomyocytes and vascular structures, thereby ameliorating the function of the infarcted heart (50;51). In the damaged liver an undefined BMDC subpopulation was shown to infiltrate and differentiate to hepatocytes, thereby improving liver function (52;53). Furthermore, undefined BMDC subpopulations have been reported to differentiate into endocrine β cells of the pancreas (54;55), cells of the central nervous system, such as neurons, oligodendrocytes and astrocytes (56-59), skeletal muscle cells (60) and intestinal epithelial cells (44;61). The recurrent hypothesis in all mentioned organ system is that upon injury, inflammation leads to the recruitment of BMDC subpopulations to the site of injury, where some BMDC subpopulations can repopulate the damaged structure by engraftment and differentiation into tissue specific cell-types.

The hypothesis that BMDC can infiltrate and repopulate the damaged organ upon injury was also tested in the kidney. In experimental studies, BMDC are usually detected by bone marrow transplantation with labeled bone marrow cells to allow tracing of BMDC in an injured organ. In humans, bone marrow transplantation with sex- or MHC-mismatched bone marrow followed by renal injury would allow tracing BMDC in the injured kidney. Since this sequence of events is not likely to occur, the presence of recipient-derived cells after sex- or MHC- mismatched kidney transplantation was investigated instead. In these studies, the presence of recipient-derived cells was reported in vessels and tubuli of the renal transplant (62-68). Recipient-derived cells that engrafted the tubular epithelium adopted a tubular epithelial phenotype (63;65;66). Since the extent of engraftment of recipient-derived cells in donor epithelium or endothelium correlated with the severity of sustained graft damage (64;67), it was suggested that recipient-derived cells mediate graft repair by replacing damaged graft cells. Moreover, since the recipient-derived cells are extra-renal and showed plasticity to differentiate *in vivo*, these cells were suggested to represent a BMD population of stem- or progenitor cells.

Outline of the thesis

In this thesis we explored the differentiation choices of BMDC after acute renal injury in rats. Since we performed bone marrow transplantation with whole bone marrow, we could not study subpopulations of BMDC but we studied the differentiation choices of the total BMDC population instead. Therefore, the differentiation fates of BMDC described in this thesis might represent differentiation of stem-, progenitor cells or other BMDC subpopulations.

Acute renal damage is, when not too severe, reversible. Innate mechanisms of regeneration and remodeling of the kidney result in recovery of function and morphology of the tubular epithelium. BMD stem- or progenitor cells possibly mediate tubular epithelial repair by their differentiation potential and may provide a therapeutic solution for acute renal injury. Therefore, we investigated the capacity of BMDC to differentiate towards tubular epithelial cells and thereby their possible contribution to tubular epithelial repopulation (Figure 1). Remodeling of the kidney after acute renal injury may, due to an uncontrolled balance between synthesis and degradation of ECM proteins, result in interstitial fibrosis. Myofibroblasts contribute to the onset of interstitial fibrosis by producing ECM components. Therefore, we studied the capacity of BMDC to differentiate to renal interstitial myofibroblasts and thereby their possible contribution to ECM synthesis (Figure 1).

For correct interpretation of the functional contribution of BMDC in renal repair *in vivo* tracking of BMDC is crucial. Many different tracking methods, with variable experimental outcomes, have been reported. In *chapter 2* we provided an overview of the different tracking methods and discussed their advantages and drawbacks for use in renal injury models. Besides differences in reporter systems, differences in the extent of renal damage might also be a determinant for BMDC-mediated repair. In *chapter 3* we investigated whether the severity of damage and post-ischemic recovery time determines the extent of BMDC engraftment in tubular epithelium. Moreover, we studied the balance between endogenous and BMDC-mediated tubular cell replacement. Besides tubular epithelial regeneration, acute renal injury also elicits ECM production. In *chapter 4* we determined the capacity of BMDC to differentiate towards ECM-producing interstitial myofibroblasts. Moreover, we investigated the presence of BMD myofibroblasts over time and their ability to produce ECM components and the pro-fibrotic growth factor TGF-β. Myofibroblast differentiation is known to be stimulated by several pro-fibrotic stimuli. The immunosuppressive agent ciclosporin (CsA), widely used after kidney transplantation, is known for its pro-fibrotic potential. We investigated in *chapter 5* whether myofibroblast differentiation of BMDC was stimulated by CsA. Besides the influence of pro-fibrotic stimuli on BMDC differentiation, transplantation injury factors, i.e. IRI and rejection-associated injury, may influence differentiation. Therefore, we investigated in *chapter 6* the differentiation choices of recipient-derived cells after experimental kidney transplantation. Moreover, in *chapter 7* we studied the effects of kidney transplantation on circulating BMD progenitor cells. We determined the number of EPC in the circulation of kidney transplant recipients with and without complications. Finally, the results described in this thesis are summarized and future perspectives are discussed in *chapter 8*.

References

1) Nony PA, Schnellmann RG. Mechanisms of renal cell repair and regeneration after acute renal failure. J Pharmacol Exp Ther 2003 Mar;304(3):905-12.

2) Chan L, Chittinandana A, Shapiro JI, Shanley PF, Schrier RW. Effect of an endothelin-receptor antagonist on ischemic acute renal failure. Am J Physiol 1994 Jan;266(1 Pt 2):F135-F138.

3) Lieberthal W, Wolf EF, Rennke HG, Valeri CR, Levinsky NG. Renal ischemia and reperfusion impair endothelium-dependent vascular relaxation. Am J Physiol 1989 May;256(5 Pt 2):F894-F900.

4) Sutton TA, Molitoris BA. Mechanisms of cellular injury in ischemic acute renal failure. Semin Nephrol 1998 Sep;18(5):490-7.

5) Bush KT, Keller SH, Nigam SK. Genesis and reversal of the ischemic phenotype in epithelial cells. J Clin Invest 2000 Sep;106(5):621-6.

6) Thadhani R, Pascual M, Bonventre JV. Acute renal failure. N Engl J Med 1996 May 30;334(22):1448-60.

7) Solez K, Morel-Maroger L, Sraer JD. The morphology of "acute tubular necrosis" in man: analysis of 57 renal biopsies and a comparison with the glycerol model. Medicine (Baltimore) 1979 Sep;58(5):362-76.

8) Walker LM, York JL, Imam SZ, Ali SF, Muldrew KL, Mayeux PR. Oxidative stress and reactive nitrogen species generation during renal ischemia. Toxicol Sci 2001 Sep;63(1):143-8.

9) Ichikawa I, Kiyama S, Yoshioka T. Renal antioxidant enzymes: their regulation and function. Kidney Int 1994 Jan;45(1):1-9.

10) Ishibashi N, Weisbrot-Lefkowitz M, Reuhl K, Inouye M, Mirochnitchenko O. Modulation of chemokine expression during ischemia/reperfusion in transgenic mice overproducing human glutathione peroxidases. J Immunol 1999 Nov 15;163(10):5666-77.

11) Donnahoo KK, Meng X, Ayala A, Cain MP, Harken AH, Meldrum DR. Early kidney TNF-alpha expression mediates neutrophil infiltration and injury after renal ischemia-reperfusion. Am J Physiol 1999 Sep;277(3 Pt 2):R922-R929.

12) Donnahoo KK, Meldrum DR, Shenkar R, Chung CS, Abraham E, Harken AH. Early renal ischemia, with or without reperfusion, activates NFkappaB and increases TNF-alpha bioactivity in the kidney. J Urol 2000 Apr;163(4):1328-32.

13) Goes N, Urmson J, Ramassar V, Halloran PF. Ischemic acute tubular necrosis induces an extensive local cytokine response. Evidence for induction of interferon-gamma, transforming growth factor-beta 1, granulocyte-macrophage colony-stimulating factor, interleukin-2, and interleukin-10. Transplantation 1995 Feb 27;59(4):565-72.

14) De Greef KE, Ysebaert DK, Ghielli M, Vercauteren S, Nouwen EJ, Eyskens EJ, De Broe ME. Neutrophils and acute ischemia-reperfusion injury. J Nephrol 1998 May;11(3):110-22.

15) Klausner JM, Paterson IS, Goldman G, Kobzik L, Rodzen C, Lawrence R, Valeri CR, Shepro D, Hechtman HB. Postischemic renal injury is mediated by neutrophils and leukotrienes. Am J Physiol 1989 May;256(5 Pt 2):F794-F802.

16) Takada M, Nadeau KC, Shaw GD, Tilney NL. Prevention of late renal changes after initial ischemia/reperfusion injury by blocking early selectin binding. Transplantation 1997 Dec 15;64(11):1520-5.

17) Wolfe RA, Ashby VB, Milford EL, Ojo AO, Ettenger RE, Agodoa LY, Held PJ, Port FK. Comparison of mortality in all patients on dialysis, patients on dialysis awaiting transplantation, and recipients of a first cadaveric transplant. N Engl J Med 1999 Dec 2;341(23):1725-30.

18) Opelz G, Wujciak T, Dohler B, Scherer S, Mytilineos J. HLA compatibility and organ transplant survival. Collaborative Transplant Study. Rev Immunogenet 1999;1(3):334-42.

19) Stubenitsky BM, Booster MH, Nederstigt AP, Kievit JK, Jacobs RW, Kootstra G. Kidney preservation in the next millenium. Transpl Int 1999;12(2):83-91.

20) Halloran PF. Immunosuppressive drugs for kidney transplantation. N Engl J Med 2004 Dec 23;351(26):2715-29.

21) Land W. Postischemic reperfusion injury and allograft dysfunction: is allograft rejection the result of a fateful confusion by the immune system of danger and benefit? Transplant Proc 1999 Feb;31(1-2):332-6.

22)   Racusen LC, Solez K, Colvin RB, Bonsib SM, Castro MC, Cavallo T, Croker BP, Demetris AJ, Drachenberg CB, Fogo AB, Furness P, Gaber LW, Gibson IW, Glotz D, Goldberg JC, Grande J, Halloran PF, Hansen HE, Hartley B, Hayry PJ, Hill CM, Hoffman EO, Hunsicker LG, Lindblad AS, Yamaguchi Y, . The Banff 97 working classification of renal allograft pathology. Kidney Int 1999 Feb;55(2):713-23.

23)   Abbate M, Brown D, Bonventre JV. Expression of NCAM recapitulates tubulogenic development in kidneys recovering from acute ischemia. Am J Physiol 1999 Sep;277(3 Pt 2):F454-F463.

24)   Witzgall R, Brown D, Schwarz C, Bonventre JV. Localization of proliferating cell nuclear antigen, vimentin, c-Fos, and clusterin in the postischemic kidney. Evidence for a heterogenous genetic response among nephron segments, and a large pool of mitotically active and dedifferentiated cells. J Clin Invest 1994 May;93(5):2175-88.

25)   Cuppage FE, Chiga M, Tate A. Cell cycle studies in the regenerating rat nephron following injury with mercuric chloride. Lab Invest 1972 Jan;26(1):122-6.

26)   Houghton DC, Hartnett M, Campbell-Boswell M, Porter G, Bennett W. A light and electron microscopic analysis of gentamicin nephrotoxicity in rats. Am J Pathol 1976 Mar;82(3):589-612.

27)   Wallin A, Zhang G, Jones TW, Jaken S, Stevens JL. Mechanism of the nephrogenic repair response. Studies on proliferation and vimentin expression after 35S-1,2-dichlorovinyl-L-cysteine nephrotoxicity in vivo and in cultured proximal tubule epithelial cells. Lab Invest 1992 Apr;66(4):474-84.

28)   Kartha S, Toback FG. Adenine nucleotides stimulate migration in wounded cultures of kidney epithelial cells. J Clin Invest 1992 Jul;90(1):288-92.

29)   Pawar S, Kartha S, Toback FG. Differential gene expression in migrating renal epithelial cells after wounding. J Cell Physiol 1995 Dec;165(3):556-65.

30)   Toback FG, Kartha S, Walsh-Reitz MM. Regeneration of kidney tubular epithelial cells. Clin Investig 1993 Oct;71(10):861-6.

31)   Wang S, Hirschberg R. Role of growth factors in acute renal failure. Nephrol Dial Transplant 1997 Aug;12(8):1560-3.

32)   Desmouliere A, Redard M, Darby I, Gabbiani G. Apoptosis mediates the decrease in cellularity during the transition between granulation tissue and scar. Am J Pathol 1995 Jan;146(1):56-66.

33)   Bohle A, Strutz F, Muller GA. On the pathogenesis of chronic renal failure in primary glomerulopathies: a view from the interstitium. Exp Nephrol 1994 Jul;2(4):205-10.

34)   Grotendorst GR, Okochi H, Hayashi N. A novel transforming growth factor beta response element controls the expression of the connective tissue growth factor gene. Cell Growth Differ 1996 Apr;7(4):469-80.

35)   Kothapalli D, Grotendorst GR. CTGF modulates cell cycle progression in cAMP-arrested NRK fibroblasts. J Cell Physiol 2000 Jan;182(1):119-26.

36)   Strutz F, Zeisberg M, Renziehausen A, Raschke B, Becker V, van KC, Muller G. TGF-beta 1 induces proliferation in human renal fibroblasts via induction of basic fibroblast growth factor (FGF-2). Kidney Int 2001 Feb;59(2):579-92.

37)   Qi W, Chen X, Poronnik P, Pollock CA. The renal cortical fibroblast in renal tubulointerstitial fibrosis. Int J Biochem Cell Biol 2006 Jan;38(1):1-5.

38)   Wiggins R, Goyal M, Merritt S, Killen PD. Vascular adventitial cell expression of collagen I messenger ribonucleic acid in anti-glomerular basement membrane antibody-induced crescentic nephritis in the rabbit. A cellular source for interstitial collagen synthesis in inflammatory renal disease. Lab Invest 1993 May;68(5):557-65.

39)   Ng YY, Huang TP, Yang WC, Chen ZP, Yang AH, Mu W, Nikolic-Paterson DJ, Atkins RC, Lan HY. Tubular epithelial-myofibroblast transdifferentiation in progressive tubulointerstitial fibrosis in 5/6 nephrectomized rats. Kidney Int 1998 Sep;54(3):864-76.

40)   Desmouliere A, Gabbiani G. Myofibroblast differentiation during fibrosis. Exp Nephrol 1995 Mar;3(2):134-9.

41)   Friedenstein AJ, Chailakhjan RK, Lalykina KS. The development of fibroblast colonies in monolayer cultures of guinea-pig bone marrow and spleen cells. Cell Tissue Kinet 1970 Oct;3(4):393-403.

42)   Chapman JR, O'Connell PJ, Nankivell BJ. Chronic renal allograft dysfunction. J Am Soc Nephrol 2005 Oct;16(10):3015-26.

43) Merville P. Combating chronic renal allograft dysfunction : optimal immunosuppressive regimens. Drugs 2005;65(5):615-31.

44) Krause DS, Theise ND, Collector MI, Henegariu O, Hwang S, Gardner R, Neutzel S, Sharkis SJ. Multi-organ, multi-lineage engraftment by a single bone marrow-derived stem cell. Cell 2001 May 4;105(3):369-77.

45) Spangrude GJ, Heimfeld S, Weissman IL. Purification and characterization of mouse hematopoietic stem cells. Science 1988 Jul 1;241(4861):58-62.

46) Wolf NS, Kone A, Priestley GV, Bartelmez SH. In vivo and in vitro characterization of long-term repopulating primitive hematopoietic cells isolated by sequential Hoechst 33342-rhodamine 123 FACS selection. Exp Hematol 1993 May;21(5):614-22.

47) Pittenger MF, Mackay AM, Beck SC, Jaiswal RK, Douglas R, Mosca JD, Moorman MA, Simonetti DW, Craig S, Marshak DR. Multilineage potential of adult human mesenchymal stem cells. Science 1999 Apr 2;284(5411):143-7.

48) Asahara T, Murohara T, Sullivan A, Silver M, van der Zee R, Li T, Witzenbichler B, Schatteman G, Isner JM. Isolation of putative progenitor endothelial cells for angiogenesis. Science 1997 Feb 14;275(5302):964-7.

49) Asahara T, Masuda H, Takahashi T, Kalka C, Pastore C, Silver M, Kearne M, Magner M, Isner JM. Bone marrow origin of endothelial progenitor cells responsible for postnatal vasculogenesis in physiological and pathological neovascularization. Circ Res 1999 Aug 6;85(3):221-8.

50) Orlic D, Kajstura J, Chimenti S, Jakoniuk I, Anderson SM, Li B, Pickel J, McKay R, Nadal-Ginard B, Bodine DM, Leri A, Anversa P. Bone marrow cells regenerate infarcted myocardium. Nature 2001 Apr 5;410(6829):701-5.

51) Orlic D, Kajstura J, Chimenti S, Limana F, Jakoniuk I, Quaini F, Nadal-Ginard B, Bodine DM, Leri A, Anversa P. Mobilized bone marrow cells repair the infarcted heart, improving function and survival. Proc Natl Acad Sci U S A 2001 Aug 28;98(18):10344-9.

52) Petersen BE, Bowen WC, Patrene KD, Mars WM, Sullivan AK, Murase N, Boggs 55, Greenberger JS, Goff JP. Bone marrow as a potential source of hepatic oval cells. Science 1999 May 14;284(5417):1168-70.

53) Lagasse E, Connors H, Al Dhalimy M, Reitsma M, Dohse M, Osborne L, Wang X, Finegold M, Weissman IL, Grompe M. Purified hematopoietic stem cells can differentiate into hepatocytes in vivo. Nat Med 2000 Nov;6(11):1229-34.

54) Hess D, Li L, Martin M, Sakano S, Hill D, Strutt B, Thyssen S, Gray DA, Bhatia M. Bone marrow-derived stem cells initiate pancreatic regeneration. Nat Biotechnol 2003 Jul;21(7):763-70.

55) Ianus A, Holz GG, Theise ND, Hussain MA. In vivo derivation of glucose-competent pancreatic endocrine cells from bone marrow without evidence of cell fusion. J Clin Invest 2003 Mar;111(6):843-50.

56) Brazelton TR, Rossi FM, Keshet GI, Blau HM. From marrow to brain: expression of neuronal phenotypes in adult mice. Science 2000 Dec 1;290(5497):1775-9.

57) Kopen GC, Prockop DJ, Phinney DG. Marrow stromal cells migrate throughout forebrain and cerebellum, and they differentiate into astrocytes after injection into neonatal mouse brains. Proc Natl Acad Sci U S A 1999 Sep 14;96(19):10711-6.

58) Mezey E, Chandross KJ, Harta G, Maki RA, McKercher SR. Turning blood into brain: cells bearing neuronal antigens generated in vivo from bone marrow. Science 2000 Dec 1;290(5497):1779-82.

59) Mezey E, Key S, Vogelsang G, Szalayova I, Lange GD, Crain B. Transplanted bone marrow generates new neurons in human brains. Proc Natl Acad Sci U S A 2003 Feb 4;100(3):1364-9.

60) Ferrari G, Cusella-De AG, Coletta M, Paolucci E, Stornaiuolo A, Cossu G, Mavilio F. Muscle regeneration by bone marrow-derived myogenic progenitors. Science 1998 Mar 6;279(5356):1528-30.

61) Okamoto R, Yajima T, Yamazaki M, Kanai T, Mukai M, Okamoto S, Ikeda Y, Hibi T, Inazawa J, Watanabe M. Damaged epithelia regenerated by bone marrow-derived cells in the human gastrointestinal tract. Nat Med 2002 Sep;8(9):1011-7.

62) Bai HW, Shi BY, Qian YY, Na YQ, Cai M, Zeng X, Zhong DR, Wu SF, Chang JY, Zhou WQ. Does endothelial chimerism correlate with renal allograft rejection? Transplant Proc 2006 Dec;38(10):3430-3.

63) Gupta S, Verfaillie C, Chmielewski D, Kim Y, Rosenberg ME. A role for extrarenal cells in the regeneration following acute renal failure. Kidney Int 2002 Oct;62(4):1285-90.

64) Lagaaij EL, Cramer-Knijnenburg GF, van Kemenade FJ, van Es LA, Bruijn JA, van Krieken JH. Endothelial cell chimerism after renal transplantation and vascular rejection. Lancet 2001 Jan 6;357(9249):33-7.

65) Mengel M, Jonigk D, Marwedel M, Kleeberger W, Bredt M, Bock O, Lehmann U, Gwinner W, Haller H, Kreipe H. Tubular chimerism occurs regularly in renal allografts and is not correlated to outcome. J Am Soc Nephrol 2004 Apr;15(4):978-86.

66) Poulsom R, Forbes SJ, Hodivala-Dilke K, Ryan E, Wyles S, Navaratnarasah 5, Jeffery R, Hunt T, Alison M, Cook T, Pusey C, Wright NA. Bone marrow contributes to renal parenchymal turnover and regeneration. J Pathol 2001 Sep;195(2):229-35.

67) Sinclair RA. Origin of endothelium in human renal allografts. Br Med J 1972 Oct 7;4(5831):15-6.

68) van Poelgeest EP, Baelde HJ, Lagaaij EL, Sijpkens YW, de Heer E, Bruijn JA, Bajema IM. Endothelial cell chimerism occurs more often and earlier in female than in male recipients of kidney transplants. Kidney Int 2005 Aug;68(2):847-53.

Chapter 2

Searching for bone marrow-derived cells in experimental models for renal injury: reporter systems revisited

Martine Broekema, Martin C. Harmsen, Eliane R. Popa

Department of Pathology and Laboratory Medicine, Medical Biology section, University Medical Center Groningen, University of Groningen, The Netherlands

Abstract

At this time point renal injury, ultimately resulting in renal failure, can not be therapeutically cured by endothelial, glomerular or tubular regeneration. Over the last five years, several reports appeared in which the replacement of damaged renal cells by bone marrow-derived cells (BMDC) was shown, thereby suggesting a therapeutic role for BMDC in renal regeneration. For correct interpretation of the function of these cells in renal repair, *in vivo* tracking of BMDC is crucial. Since various tracking methods with variable experimental outcomes have been reported, we will provide an overview of these methods and discuss their advantages and drawbacks for experimental renal disease models.

Introduction

At this time point renal injury, ultimately resulting in renal failure, can not be therapeutically cured by endothelial, glomerular and tubular regeneration. Bone marrow-derived cells (BMDC) might provide a therapeutic role in renal regeneration by replacement of damaged cells. In various models of renal injury, BMDC have been shown to be recruited from the circulation to the affected kidney, where they engraft and can adopt epithelial, endothelial or mesangial phenotypes, which suggests that damaged cells are actually replaced (1-6). However, due to the low and variable number of BMDC that differentiated to renal-specific cell types in these models, the functional relevance of BMDC engraftment in renal repair is still subject of debate. One of the reasons for the variation in BMDC engraftment and differentiation may be the use of different BMDC tracking models. Moreover, there are reports suggesting that several BMDC tracking models are unreliable for identification of these engrafted cells *in vivo* (7;8). Since BMDC tracking models are important for investigating possible therapeutic applications of BMDC in renal repair, we provide an overview and review the advantages and drawbacks of reporter systems used for tracing BMDC in the kidney (Tabel 1).

Reporter systems can generally be divided in two groups, i.e. those using genetic tracking devices that are present or newly introduced in the genome, and those using *ex vivo* labeling of cells.

BMDC tracking in the kidney using bone marrow transplantation

The most commonly used technique to track BMDC and study their role of BMDC after renal injury is transplantation of bone marrow from rodents that are genetically distinguishable from the recipient, into bone marrow-ablated recipients. After bone marrow transplantation, the transplanted bone marrow cells stably reconstitute the recipient's bone marrow compartment. In practice, the efficiency of bone marrow ablation and reconstitution with donor bone marrow is never 100% and a certain degree of underestimation of, for example the actual number of renal infiltrated BMDC, is always present. Another issue to consider is that bone marrow transplantation experiments with newly introduced genetically modified BMDC can elicit immunological rejection. However, the possibility of an interfering immune response has not been studied in bone marrow transplantation experiments described in this article.

Genetic "tracking devices"

Y chromosome detection

Male to female bone marrow transplantation offers a reliable, but laborious approach for tracking BMDC in the kidney. Several studies describe detection of male BMDC using Y-chromosome *in situ* hybridization (Y-ISH) to determine the bone marrow origin of cells engrafting the female kidney (2;4;9-12). Y-chromosome detection is also used to study extra-renal, host-derived cells in tissue biopsy or autopsy material after sex-mismatched kidney transplantation (13-15), or to study renal infiltrated BMDC in patients after sex-mismatched bone marrow transplantation (16). Thus, beside the

CHAPTER 2

Tabel 1: *Reporter systems and their andvantages and drawbacks*

Reporter	Promoter	Advantages (+) and drawbacks (-) *	Circumvented by
Y-chrom.	-	+ Applicable in sex-mismatched patient material (13-16) - Unreliable in female to male combination - Underestimation due to thickness of sections (17) - Complicated, time-consuming (9) - Incorrect detection due to aggregates of fluorescent probe (9)	Correction factor
MHC/ Blood group	-	+ Applicable in mismatched patient material (6,14) + Simple detection techniques (14) - Mismatch can cause immune rejection (6)	
β-Gal	ROSA26	+ Enzymatic and immunohistochemical detection (9,30,31) + High sensitivity + Quantification using soluble color substrates + Ubiquitous renal expression (27) - Incorrect detection due to expression of mammalian- and senescence-associated β-Gal (9,28,29,32,33,35,36)	Adjust buffer pH Use β-Gal antibody
EGFP	chicken β-actin	+ Direct detection by microscopy/flow cytometry (38) + Detection in living cells (38) + Ubiquitous renal expression (38) + Rat reporter model available (5,46,47) + No endogenous EGFP expression (9) + Spectral variants of EGFP available (37,44,45) - Renal autofluorescence in the green spectrum (45) - EGFP in tissues often too weak for direct detection	Confocal micoscopy Spectral variants Use EGFP antibody
hPAP	ROSA26	+ Enzymatic and immunohistochemical detection (50,51) + Ubiquitous renal expression (26) + Stable expression in isolated cells in culture (52) + Rat reporter model available (26) - Endogenous alkaline phosphatase (48,49)	hPAP distinguished by heat stability
Firefly lucifer- ase	hCMV immedi- ate early gene	+ *In vivo*, real-time, non-invasive detection (53,55-57) + No animal-to-animal variation (56) + Ubiquitous renal expression (53) + Stable expression in isolated cells in culture (54) + High sensitivity - Exact localization can not be determined *in vivo* (57)	*Ex vivo* analysis on tissue samples
Epi- thelial specific EGFP	Ksp-cad- herin	+ Detection of tubular epithelial cells + Specific and permanent expression in mature tubular epithelium (42) + Additional phenotypical analysis not necessary - Mosaic expression pattern (42)	

Reporter	Promoter	Advantages (+) and drawbacks (-) *	Circumvented by
Fibro-blast-specific EGFP	FSP-1	+ Detection of fibroblasts + Specific and permanent expression in FSP-1⁺ cells (60) + Additional phenotypical analysis not necessary - Specificity FSP-1 debatable	
Pro-COL1A2 specific lucifer-ase/ β-Gal	Pro-COL1A2	+ Detection of Pro-collagen1A2 + Specific and permanent expression in Pro-collagen 1-producing BMDC (35) + Additional analysis for Coll I production not necessary	
CFDA	-	+ Detection of *ex vivo* labeled cells + Label retained during development, meiosis, *in vivo* tracing, cell division, fusion (64) + Not transferred to adjacent cells (64) - Reduction of fluorescence level after cell division - Limited stability of the fluorescence, up to 20 days (66) - *In vivo* detection not possible (64) - Exact localization can not be determined *in vivo*	Expose kidney (64) *Ex vivo* analysis on tissue samples (64)
Iron-dextran particles	-	+ Detection of *ex vivo* labeled cells + Non-invasive, *in vivo*, real-time detection with MRI (65) - MRI is laborious and requires equipment and train personnel - Possible clearance via fagocytosis - Exact localization can not be determined *in vivo*	*Ex vivo* analysis on tissue samples (65)

* References are given between brackets

use in animals after sex-mismatched bone marrow transplantation, Y-chromosome detection is used for recipient-derived cell detection in humans, in which the introduction of transgene-expressing cells, by for example bone marrow transplantation, is not possible.

The ISH method is laborious and may yield variable results, explaining the contradicting results of detection (2;4;9;10;12). In a study by Duffield and colleagues (9), stating that post-ischemic tubular epithelial restoration occurs independently of BMDC, confocal laser fluorescent microscopy was used to show that Y⁺ tubular cells often were artifacts. These artifacts were due to leukocytes overlying renal tubular structures, intratubular monocytes or nonspecific aggregates of fluorescent probe. This also suggests that the Y-chromosome positive tubular cells detected in previous studies in female mice following transplantation of bone marrow from male donor mice could be artifacts of imaging.

A drawback of this reporter system is that ISH is necessary to detect Y chromosome-positive cells in tissues. This technique is time consuming and requires extensive pre-treatment of the sections, which affects tissue morphology and epitopes and therefore reduces the possibility to perform double-stainings for further characterization of the engrafted cells. Moreover, the method of Y-ISH for detection of BMDC can lead to an underestimation of Y-chromosome presence by distribution of the nucleus over

multiple thin tissue sections, and loss of the Y chromosome for detection in some of the sections. Because of these bottlenecks, detection of the Y-chromosome in male tissue sections is never 100%, as it should be. Therefore, the exact number of Y chromosome-positive cells can only be estimated using a correction factor, as was done in a study by Direkze (17). In this study radiation-induced injury was shown to elicit differentiation of BMDC to myofibroblasts in multiple organs, including the kidney. Using Y-ISH, the authors showed that only 50% of all male cells were Y chromosome-positive, which should have been 100%. Therefore, the observed number of renal Y chromosome-positive BMDC in the female kidney was corrected by dividing by 0.5 to estimate the exact number of renal BMDC. This approach is not very accurate since this is only an estimation and not the exact number of BMDC. Together with the fact that bone marrow transplantation is never 100% efficient, this estimation can lead to incorrect interpretation of data. Another limitation of sex-mismatched BMDC tracking, especially in the clinical setting, is that female to male detection is more difficult and unreliable, thereby excluding female to male transplantations for detection of recipient-derived cells. Therefore, the use of sex-mismatched bone marrow transplantation for tracking of BMDC can be regarded as a limited and insensitive method.

MHC and ABO blood group antigen detection

Although all reporter markers that are incorporated in the genome can be detected using *in situ* hybridization, other, less complicated methods for detection of recipient-derived cells in human tissue biopsies or post-mortem tissue are possible, e.g. MHC or ABO blood group antigen detection by immunohistochemistry (14). Besides in patient studies, this strategy was also applied in rat studies, e.g. by Rookmaaker *et al.* (6), who used a rat allogenic BM transplant model in BN rats with WR rats as bone marrow donors to generate rat BM chimeras. In the model of anti-Thy-1.1-glomerulonephritis, BMDC were traced using a donor-specific major histocompatibility complex class-I monoclonal antibody and were found to differentiate towards glomerular endothelial and mesangial cells (6). Although it was not reported in this study, possible immune rejection of MHC mismatched bone marrow and the necessity for immunosuppressive therapy can be a limiting factor of this detection method.

Transgenic reporters

Transgenic reporters under the control of ubiquitous promoters

Tracing of BMDC in the kidney using reporter genes relies on the expression of the reporter gene (i.e. the transgene) by the BMDC. Expression of the reporter gene at all times can only be accomplished if the gene is driven by a promoter of a ubiquitously expressed gene, such as mouse metallothionein (18;19), β-actin from human (20), rat (21) and chicken (22), ubiquitin (23), simian virus 40 (24), cytomegalovirus immediate-early (25) or ROSA 26 (26).

β-Galactosidase

Bacterial β-galactosidase-transgenic mice expressing the *E.coli*-derived LacZ gene (27), are frequently used as reporters for tracing BMDC. The presence of this reporter

gene can be visualized by enzymatic detection of the bacterial β-galactosidase by X-gal staining or by immunohistochemical detection with an antibody against bacterial β-galactosidase. In the enzymatic detection, X-gal is converted by β-galactosidase to a blue reaction product which precipitates *in situ*. β-Galactosidase is among the most sensitive of reporter enzymes because only a few molecules of this enzyme readily convert X-gal in amounts that are detectable by light microscopy. An advantage of β-galactosidase is, that also soluble color substrates such as ONPG (o-nitrophenyl-β-D-galactopyranoside) exist that are employed to determine relative or total amount of reporter protein in tissue extracts.

Using this technique, previous studies have reported large numbers of X-gal^{+} tubular cells after ischemic renal injury (1;2), thereby suggesting that BMDC play an important role in repair of renal injury. However, many mammalian tissues, including the kidney (28;29), contain endogenous β-galactosidase, an enzyme important for the enzymatic digestion of glycolipids (30;31). This mammalian enzyme has an acidic pH optimum (32;33), whereas the bacterial β-galactosidase enzyme has a neutral pH optimum (34). In most published protocols, a weak buffer such as phosphate-buffered saline (PBS) was used, which may have become acidic during the exposure of fixed tissues to X-gal. Moreover, after ischemia the kidney becomes acidic due to disturbed pH regulation. At low pH, endogenous β-galactosidase is detected and, thereby, false positive cells. Several studies indeed showed that, using the enzymatic detection method of β-galactosidase at low pH (6.5), endogenous β-galactosidase could not be distinguished from the bacterial β-galactosidase in injured kidneys (9),(35). Therefore, X-gal^{+} tubular cells reported in previous studies (1;2) may have been detected as a result of increased intrinsic β-galactosidase activity, rather than the presence of β-galactosidase-positive bone marrow cells. Another disturbance in the detection of β-galactosidase is the presence of senescence-associated β-galactosidase (SA-β-gal), which is defined as β-galactosidase activity detectable at pH 6.0, in senescent cells (36).

Despite these detection problems, β-galactosidase can still be used as a reliable reporter, as long as bacterial β-galactosidase is clearly distinguished from endogenous mammalian β-galactosidase. This can be achieved by a simple modification of the X-gal method, raising the pH of the X-gal solution to weakly alkaline pH (29), or by using a commercially produced β-gal staining set which is designed to minimize staining from mammalian β-galactosidase (9). Another method is based on immunolabeling with anti-bacterial β-galactosidase antibody instead of enzymatic detection of the reporter by X-gal staining. The study of Duffield (9) showed that, using anti-β-galactosidase, it was possible to discriminate between endogenous mammalian β-galactosidase activity and that resulting from LacZ gene expression. Therefore, β-galactosidase can be reliably detected without interference of endogenous mammalian β-galactosidase.

Enhanced Green Fluorescent Protein (EGFP)

Green fluorescent protein (GFP) is responsible for the green bioluminescence of the jellyfish *Aequorea Victoria*. Using this protein, transgenic mouse lines were generated, in which all tissues emitted green light under excitation. However, the first generation GFP transgenic mice proved to be unsuitable for use in experimental renal disease models, since GFP was, in the healthy animal, not expressed in all renal components (7;37). If, in the setting of GFP[+] bone marrow transplantation, BMDC regulate GFP in a

similar way as kidney cells and BMDC differentiate to kidney cells, this would result in an underestimation of GFP expressing, bone marrow-derived, kidney cells. Therefore, mutants of the first generation of GFP transgenic mice were constructed that had about 35-fold brighter fluorescence, termed 'enhanced' GFP (EGFP) (37). These mutants were the result of double amino acid substitutions in the wild-type GFP cDNA construct, placed under the control of the same chicken β-actin promoter and a cytomegalovirus enhancer as in the first generation of GFP transgenes. EGFP transgenic mice do express EGFP in all renal components, as well as in other tissues, with the exception of erythrocytes, hair (38) and some leukocytes (personal observation).

Chimeric mice reconstituted with EGFP bone marrow are commonly and successfully used to trace BMDC in renal disease models (39-43). The advantage of EGFP as a reporter is that introduction of a substrate is not required, unlike other commonly used reporters such as β-galactosidase and alkaline phosphatase, allowing to monitor the presence of EGFP by sole illumination of tissue sections or living cells (38). Moreover, EGFP is not disturbed by expression of endogenous EGFP and because the excitation optimum for EGFP is close to 488 nm, the transgenic cells can also be analyzed by flow cytometry. A drawback of EGFP is that in tissue sections EGFP is often too weak for direct fluorescence microscopy, making antibody labeling necessary for detection (personal observation, confirmed by other researchers). Moreover, the utility of EGFP as a reporter in renal disease models is limited by the fact that the kidney possesses intensive auto-fluorescence, which complicates detection of EGFP* cells, unless confocal microscopy is used. This problem can also be overcome by using one of the spectral variants of GFP, emitting blue, cyan or yellow light (37;44;45). Moreover, these spectral variants of GFP can be very useful for achieving *in vivo* double-labeling.

Besides EGFP transgenic mice, rats expressing EGFP ubiquitously were generated. EGFP transgenic rats were originally established using the same construct and technique described for the production of EGFP transgenic mice (38). Rats are, in comparison to mice, preferable in certain renal disease models, such as experimental kidney transplantation (easier microsurgical procedure) and anti-Thy1 antibody-mediated glomerulonephritis model (Thy1 is a well-established rat-specific mesangial marker, EGFP rat BM chimeras with Thy1 nephritis are described in references (5;46;47)). Therefore, the EGFP transgenic rat is an important tool for studying BMDC in renal disease.

Several characteristics of EGFP, its reliable detection, possibility of detection without introduction of a substrate in living cells and the availability of spectral variants of EGFP to avoid green autofluorescence or to simultaneously label multiple cell types, make this reporter an attractive option for use in BMDC tracking in renal disease models.

human Placental Alkaline Phosphatase (hPAP)

Alkaline phosphatase (AP) dephosphorylates many types of phosphorylated molecules, for example nucleotides and proteins. Besides this functional property, which is extensively used in molecular biology, AP is used as a label in enzyme immunoassays. In humans, AP is present in all tissues throughout the body, but is particularly concentrated in liver, bile duct, kidney, bone and placenta. The advantage of human placental alkaline phosphatase (hPAP) is its heat stability, which allows to distinguish the placental form from other forms of AP (48;49).

Transgenic rats have been generated in which hPAP is placed under control of the ubiquitously active ROSA26 gene promoter (26). The hPAP transgenic rat shows ubiquitous expression of hPAP in the kidney (Figure 1A) and is therefore suitable for BM transplantation experiments and subsequent tracking of BMDC in renal disease models.

We have used hPAP as a marker molecule to track BMDC in the post-ischemic rat kidney and showed BMDC differentiation towards tubular epithelial cells and myofibroblasts (50;51). To allow for renal BMDC tracking, we reconstituted lethally irradiated F344 rats with ROSA26-hPAP transgenic bone marrow cells and subsequently studied infiltrating BMD (hPAP+) cells in the kidney after unilateral ischemia/reperfusion injury. The heat-stability of the hPAP enzyme allowed reliable detection of hPAP+ cells, without interference of endogenous AP, which is abundantly present in the kidney. In our model, we showed that heat-inactivation of endogenous AP resulted in complete absence of substrate conversion by this enzyme, without destroying the reactivity of hPAP (Figure 1B) (50;51).

2

A   B
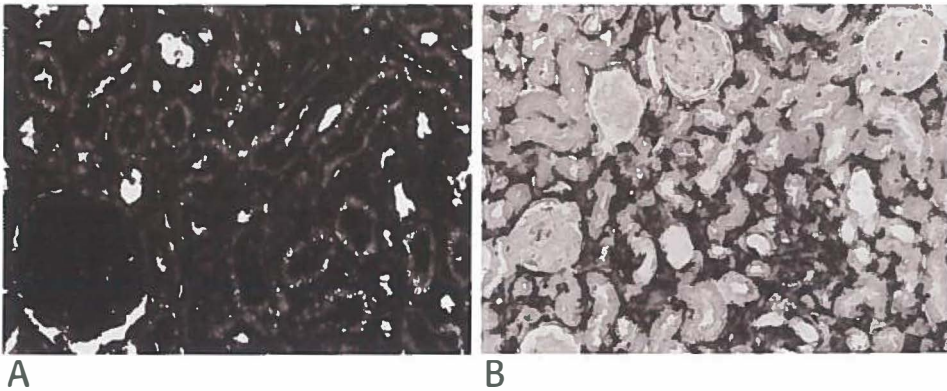
Figure 1. *Renal expression of ROSA26-hPAP in transgenic rats and bone marrow chimeras. Expression of the ROSA26-hPAP gene was assessed by enzymatic hPAP staining on kidney sections. hPAP is ubiquitously expressed in the kidney of a healthy ROSA26-hPAP transgenic rat (A). ROSA26-hPAP expression can be easily detected on renal infiltrating hPAP+ BMDC (black) in ROSA26-hPAP bone marrow chimeric rats 7 days after induction of ischemia (B). No interference of endogenous AP was observed. Lens magnification 200x (B) and 400x (A).*

Detection of hPAP+ BMDC in renal tissue sections by (immuno)histochemical staining was confirmed by BMDC labeling and fluorescence-activated cell sorting (Figure 2). It has also been described that the expression of hPAP is stable in isolated cells in culture (52).

The stable and ubiquitous expression of hPAP, its applicability in rat models and simple detection methods, make the ROSA26-hPAP transgene a reliable reporter for studies on the fate of BMDC after renal injury.

Figure 2. *hPAP expression determined by FACS. ROSA26-hPAP transgenic bone marrow cells were detected by flow cytometry after isolation and labeling with anti-hPAP and a FITC-labeled conjugate. The graph shows FITC expression in bone marrow cells of a non-transgenic F344 rat (left), and of a ROSA26-hPAP rat (right).*

Firefly luciferase

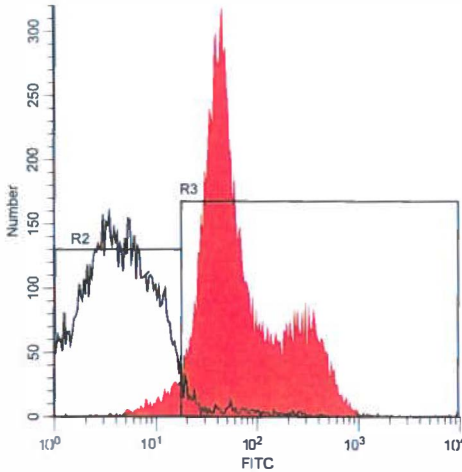Transgenic mice ubiquitously expressing luciferase from the North-American firefly (*Photinus pyralis*) have been generated, in which the firefly luciferase gene is controlled by promoter and enhancer elements of the human cytomegalovirus major immediate early gene (53). Firefly luciferase, an enzyme that causes light emission from yellow to green wavelengths in the presence of a substrate (luciferin), oxygen, ATP and magnesium (54), is the most commonly used bioluminescent reporter in biomedical research. The fast rate of firefly luciferase enzyme turnover in the presence of the substrate luciferin and its short half-life allows for real-time measurements, because firefly luciferase does not accumulate intracellularly to the extent of other reporters (55). Moreover, luciferase expression has been shown to be stable in isolated cells in culture (54).

The greatest advantage of the use of the bioluminescent firefly luciferase gene as a reporter protein is that the internal biological light source provided by luciferase can penetrate relatively easy through tissues, allowing *in vivo* detection using *in vivo* imaging techniques. Therefore, luciferase-produced bioluminescence can be non-invasively and repetitively measured in real-time in the same animal, thereby reducing the interference of animal-to-animal variation and requiring fewer animals per study (56).

A short-coming of the currently available techniques is that it is not possible to accomplish the imaging of real-time luciferase expression within individual cells within living organisms (57). *In vivo* imaging can provide information on the renal localization of luciferase, but cellular localization must be determined, similar to other reporters, in (post-mortem) tissue sections or cell lysates. Nevertheless, sensitive noninvasive imaging of firefly luciferase gene expression makes this reporter suitable for studying BMDC recruitment to the circulation and homing to the injured kidney in a living organism.

Despite these advantages, bone marrow transplantation of ubiquitous luciferase-expressing bone marrow to study renal infiltrating BMDC has not been described.

However, the use of a murine mesenchymal stem cell line transfected with a retroviral construct encoding firefly luciferase to study homing of these cells to the ischemic kidney was recently described (abstract by Kielstein J.T. *et al.* J. Am. Soc. Nephrol. 2007; 17: 527A). Detection of selectively luciferase-expressing BMDC was reported in the kidney (35) and will be discussed in the section on transgenic reporters under control of tissue or cell type-specific promoters. Moreover, the recently generated firefly luciferase/EGFP double transgenic mouse (58) will be very useful in studies on BMDC fate in the renal disease.

Transgenic reporters under the control of tissue or cell type-specific promoters

Phenotypical changes or functional properties of renal infiltrating BMDC are mostly studied by combined immunohistochemistry detecting the reporter marker in conjunction with a cell type-specific marker. Another option is to perform bone marrow transplantation with transgenic bone marrow in which the reporter gene is driven by a cell type-specific promoter. Since differentiation of BMDC to that specific cell type will elicit activation of the promoter and expression of the reporter marker, this allows, in addition to mere localization of the BMDC, to evaluate potential differentiation of the BMDC to a certain cell type in a more reliable way. A problem that can be encountered when using these tissue or cell type-specific promoters is that activation of the promoter and thus expression of the reporter is not as specifically as it should be. However, when expression is cell-type-specific within the organ of interest, the reporter can be utilized. For example, in the first version of the GFP expressing 'green' mice, GFP was expressed in the renal podocytes, skeletal muscle, pancreas and heart (37). Although GFP expression was not exclusively observed in renal podocytes, these mice could be used to study differentiation of BMDC to podocytes (7;59).

Epithelial-specific expression of EGFP

Lin *et al.* (42) crossed two mouse strains to accomplish conditional tubular epithelial specific expression of EGFP to study the contribution of intra-renal and BMDC to post-ischemic tubular regeneration. The first mouse strain, Z/EG, is a double reporter mouse. The first reporter, lacZ, is linked to a ubiquitous promoter and is flanked by two loxP sites. The second reporter, EGFP, resides further downstream. The EGFP gene will only be activated in the presence of cre recombinase, resulting in recombination between the loxP sites and subsequent deletion of the lacZ sequence. Once activated, EGFP expression is irreversible and inheritable, irrespective of the continued presence of cre recombinase.

The second transgenic mouse strain, cre[ksp], expresses cre recombinase under the control of the renal tubular epithelial-specific Ksp-cadherin promoter. Crosses between these two mouse strains result in the cre[ksp];Z/EG transgenic mice which specifically and permanently express EGFP in mature tubular epithelial cells (42). In cre[ksp];Z/EG bone marrow chimeric mice, differentiation of BMDC to tubular epithelial cells would be visible by EGFP expression. However, the cre[ksp];Z/EG transgenic mice that were used in this study showed a mosaic expression pattern of EGFP, due to inefficient cre/loxP recombination and non-ubiquitous expression of the Z/EG promoter. Therefore BMDC fate could not be determined reliably using this reporter marker (42).

Fibroblast-specific expression of EGFP

To determine the source of renal interstitial fibroblasts in renal fibrosis, Iwano *et al.* (60) used FSP1.GFP bone marrow chimeras. In these chimeras, renal infiltrating BMDC express GFP under control of the FSP1 (fibroblast specific protein 1) promotor, and therefore, express GFP upon conversion to a fibroblast phenotype. Although Iwano demonstrated differentiation of BMDC to FSP-1+ cells after unilateral ureter obstruction (UUO), the question remains if FSP-1 is specifically expressed by fibroblasts.

The use of transgenic mice constitutively expressing a reporter molecule under the control of an endothelial-specific promoter for bone marrow transplantation studies has, to the best of our knowledge, not been described in renal disease models. In cardiovascular research however, the use of bone marrow chimeras in which β-galactosidase expression is transcriptionally regulated by endothelial-specific promotors Flk-1 or Tie-2 has been proven suitable to study BMDC differentiation to an endothelial phenotype (61). Moreover, the use of transgenic mice in which a reporter gene is placed under the control of a podocyte-specific promoter, such as nephrin or podocin, will also be a useful tool to extend our knowledge on BMDC differentiation in renal injury models.

Pro-collagen 1A2-specific expression of luciferase/β-galactosidase

The use of reporters driven by cell-type specific promoters for BMDC detection can give information about differentiation fates of BMDC. However, another important question is whether BMDC are functional in their differentiated state. This question was addressed in a study by Roufosse (35), using the UUO model of renal fibrosis to study the functional contribution of BMDC to fibrosis by determination of their capacity to produce collagen. To this end, a transgenic mouse was generated that expressed both luciferase and β-galactosidase reporter genes under the control of a promoter and enhancer element of the gene encoding pro-COL1A2 (coding for the α2 chain of the pro-collagen type 1). Roufosse demonstrated the unreliability of β-galactosidase in this model (see also β-galactosidase section). However, detection of pro-collagen 1 could still be accomplished by luciferase. The presence of luciferase was determined by measurement of luminescence or luciferase protein, or by *in situ* hybridization for luciferase mRNA, the latter allowing the authors to determine the exact location of luciferase activity and co-expression with other markers (35).

In the study of Roufosse, *in vivo* imaging techniques were not used to determine luciferase activity. When performed on living animals *in vivo* bioluminescence imaging would have provided information on renal luciferase activity and would have allowed for non-invasive tracing of luciferase activity in time in the same animal.

Stability of transgene expression

It may occur that a transgene is not expressed, that expression disappears in subsequent generations of the transgenic rodent, despite the presence of the transgene in the genome, or that expression is or becomes variable in different tissues. This phenomenon can be caused by gene silencing, which causes the loss of transcription of the particular gene (62). Gene silencing can be the result of DNA

methylation and/or histon deacetylation, causing alterations in chromatin structure by as yet unknown but cell-type restricted mechanisms. Both cause the shutting-off of gene transcription (63).

Gene silencing can also take place on a post-transcriptional level (62). This occurs when mRNA of the transgene is degraded or blocked prior to translation e.g. by microRNA. Alternatively, the stability of transgenic protein may be affected, causing a high degradation rate, e.g. by increased ubiquitination.

The possibility of gene silencing in transgenic bone marrow transplantation models is often not considered and is likely to be an underestimated problem.

Ex vivo labeling of BMDC

Besides the use of bone marrow transplantation to study the role of BMDC in renal disease models, local or systemic infusion of BMDC, or a sub-set of BMDC, has been used. This approach does not require total body irradiation and is more relevant in pre-clinical, rather than experimental, studies. However, since the native bone marrow is not replaced by bone marrow transplantation, the infused BMDC will compete with physiologically recruited BMDC, which might hamper the interpretation of BMDC function.

Infusion of BMDC can be performed using the same genetically labeled reporter cells as used in bone marrow transplantation models, i.e. Y-chromosome, β-galactosidase, EGFP and hPAP. To allow detection of the infused cells in the kidney, non-genetic labeling methods have been applied, e.g. infusion of CFDA fluorescence labeled (64) or iron-dextran labeled cells (65).

Long-lasting dyes - CFDA

In a study by Tögel (64), carboxy-fluorescein diacetate (CFDA; Vybrant cell tracer kit, Molecular Probes) pre-labeled mesenchymal stem cells were infused in the left carotid artery to study their contribution to post-ischemic renal recovery. CFDA enters the cell by passive diffusion and starts to fluoresce after conversion by intracellular esterases, and is therefore suitable for marking living cells. The label is retained during development, meiosis and *in vivo* tracing, and is inherited by daughter cells after division or fusion, but is not transferred to adjacent cells in a population. However, after each cell division the fluorescence level is two-fold reduced. The major drawback of this labeling method and other comparable fluorescent labels is the limited stability of the fluorescence. *In vivo,* the label could be traced up to 20 days after labeling (66) and is, therefore, not suitable for use in longer-term experiments. The emitted fluorescence of CFDA does not penetrate deep enough through tissue to allow for *in vivo* detection of the label. However, when the kidney was exposed and renal vasculature was visualized using rhodamine-dextran or FITC-albumin, BMDC within the renal vasculature could be observed *in vivo* using two-photon confocal microscopy (64).

Particles - Iron-dextran labeled particles

Lange *et al.* (65) infused mesenchymal stem cells, pre-labeled with carboxy-dextran-coated iron oxide nanoparticles ("Resovist", Schering), into the thoracic aorta via a carotid artery after ischemia. These non-toxic iron-dextran particles are smaller than erythrocytes and are readily taken up by rat mesenchymal stem cells (65). An advantage of this method is the non-invasive detection of the labeled cells by Magnetic Resonance Imaging (MRI), which allows for real-time imaging in the living animal. However, MRI is a laborious technique which requires equipment and trained personnel. Besides *in vivo* detection with MRI, *ex vivo* histological identification of the iron-labeled cells by Prussian blue staining can be used to determine the exact location of the cells. It is unknown how these iron-dextran particles, likely to be cleared by phagocytosis, influence the inflammatory response. In the study by Lange (65), the particles did not elicit an immune response, were stable and detectable in a non-invasive way, therefore, providing an elegant method for *ex vivo* labeling of cells.

Summary and future perspectives

Various detection methods have been described to study the functional relevance of renal infiltrating BMDC. Provided that the essential prerequisites of enzymatic staining are met, all above mentioned reporters would seem applicable and useful for tracing BMDC in renal disease models. Some have, however, advantages over others. EGFP and luciferase both can be detected in living cells, which is an advantage for functional studies. The advantage of EGFP as a reporter molecule over luciferase is that detection of the protein can be accomplished without the introduction of a substrate. Luciferase needs a substrate for excitation, but it does not require external light excitation and, therefore, is less susceptible to background noise than EGFP. The background noise of EGFP, which is especially problematic in the kidney, can be overcome by the use of one of its spectral variants (cyan-, blue- and yellow fluorescent protein). These spectral variants also allow simultaneous labeling of multiple cell types. Both luciferase and EGFP have their advantages and disadvantages. However, a considerable disadvantage of EGFP is that, in contrast to firefly luciferase, it does not penetrate tissues enough for non-invasive *in vivo* detection of the signal in the living animal. Firefly luciferase does provide the opportunity to *in vivo*, real-time, repetitive measurements in the same animal. Where reporter molecules previously limited investigators to study the presence of BMDC only *ex vivo*, bioluminescent imaging (used for luciferase detection), magnetic resonance imaging (MRI) and Positron Emission Tomography (PET) techniques now allow for *in vivo* tracking of BMDC in living animals. Advantage of bioluminescent imaging over MRI and PET is that the use of light for bioluminescent imaging is safe and not subject to radioactive decay, as are the tracers used in PET, and does not require the introduction of particles or contrast fluids, as are required for MRI (56). A major short-coming of the currently available imaging techniques is that their resolution is not sufficient for visualization of individual cells or nephrons (57). Therefore, additional phenotypical analysis on tissue section will be necessary to study differentiation fates of BMDC.

In conclusion, most described reporter molecules can, knowing their strong and weak sides, be reliably applied for detection of renal infiltrating BMDC. The application

determines which reporter is most suitable. Firefly luciferase would be suitable for *in vivo* detection of BMDC mobilization and homing to the damaged kidney. However, for phenotypical analysis of BMDC to determine their functional relevance in renal repair, EGFP has been described as the reporter marker with the most opportunities.

2

Acknowledgements

References

1)   Kale S, Karihaloo A, Clark PR, Kashgarian M, Krause DS, Cantley LG. Bone marrow stem cells contribute to repair of the ischemically injured renal tubule. J Clin Invest 2003 Jul;112(1):42-9.

2)   Lin F, Cordes K, Li L, Hood L, Couser WG, Shankland SJ, Igarashi P. Hematopoietic stem cells contribute to the regeneration of renal tubules after renal ischemia-reperfusion injury in mice. J Am Soc Nephrol 2003 May;14(5):1188-99.

3)   Morigi M, Imberti B, Zoja C, Corna D, Tomasoni S, Abbate M, Rottoli D, Angioletti S, Benigni A, Perico N, Alison M, Remuzzi G. Mesenchymal stem cells are renotropic, helping to repair the kidney and improve function in acute renal failure. J Am Soc Nephrol 2004 Jul;15(7):1794-804.

4)   Poulsom R, Forbes SJ, Hodivala-Dilke K, Ryan E, Wyles S, Navaratnarasah S, Jeffery R, Hunt T, Alison M, Cook T, Pusey C, Wright NA. Bone marrow contributes to renal parenchymal turnover and regeneration. J Pathol 2001 Sep;195(2):229-35.

5)   Ito T, Suzuki A, Imai E, Okabe M, Hori M. Bone marrow is a reservoir of repopulating mesangial cells during glomerular remodeling. J Am Soc Nephrol 2001 Dec;12(12):2625-35.

6)   Rookmaaker MB, Smits AM, Tolboom H, Van 't WK, Martens AC, Goldschmeding R, Joles JA, Van Zonneveld AJ, Grone HJ, Rabelink TJ, Verhaar MC. Bone-marrow-derived cells contribute to glomerular endothelial repair in experimental glomerulonephritis. Am J Pathol 2003 Aug;163(2):553-62.

7)   Akagi Y, Isaka Y, Akagi A, Ikawa M, Takenaka M, Moriyama T, Yamauchi A, Horio M, Ueda N, Okabe M, Imai E. Transcriptional activation of a hybrid promoter composed of cytomegalovirus enhancer and beta-actin/beta-globin gene in glomerular epithelial cells in vivo. Kidney Int 1997 Apr;51(4):1265-9.

8)   Duffield JS, Park K, Hsaio L, Kelley V, Bonventre J. Tubular cell replenishment is independent of bone marrow stem cells (BMSCs) in the post-ischemic mouse kidney. J.Am.Soc.Nephrol. 15, 38A. 2004. Ref Type: Abstract

9)   Duffield JS, Park KM, Hsiao LL, Kelley VR, Scadden DT, Ichimura T, Bonventre JV. Restoration of tubular epithelial cells during repair of the postischemic kidney occurs independently of bone marrow-derived stem cells. J Clin Invest 2005 Jul;115(7):1743-55.

10) Fang TC, Alison MR, Cook HT, Jeffery R, Wright NA, Poulsom R. Proliferation of Bone Marrow-Derived Cells Contributes to Regeneration after Folic Acid-Induced Acute Tubular Injury. J Am Soc Nephrol 2005 Jun;16(6):1723-32.

11) Krause DS, Theise ND, Collector MI, Henegariu O, Hwang S, Gardner R, Neutzel S, Sharkis SJ. Multi-organ, multi-lineage engraftment by a single bone marrow-derived stem cell. Cell 2001 May 4;105(3):369-77.

12) Szczypka MS, Westover AJ, Clouthier SG, Ferrara JL, Humes HD. Rare incorporation of bone marrow-derived cells into kidney after folic Acid-induced injury. Stem Cells 2005;23(1):44-54.

13) Gupta S, Verfaillie C, Chmielewski D, Kim Y, Rosenberg ME. A role for extrarenal cells in the regeneration following acute renal failure. Kidney Int 2002 Oct;62(4):1285-90.

14) Lagaaij EL, Cramer-Knijnenburg GF, van Kemenade FJ, van Es LA, Bruijn JA, van Krieken JH. Endothelial cell chimerism after renal transplantation and vascular rejection. Lancet 2001 Jan 6;357(9249):33-7.

15) Grimm PC, Nickerson P, Jeffery J, Savani RC, Gough J, McKenna RM, Stern E, Rush DN. Neointimal and tubulointerstitial infiltration by recipient mesenchymal cells in chronic renal-allograft rejection. N Engl J Med 2001 Jul 12;345(2):93-7.

16) Nishida M, Kawakatsu H, Shiraishi I, Fujimoto S, Gotoh T, Urata Y, Ono T, Hamaoka K. Renal tubular regeneration by bone marrow-derived cells in a girl after bone marrow transplantation. Am J Kidney Dis 2003 Nov;42(5):E10-E12.

17) Direkze NC, Forbes SJ, Brittan M, Hunt T, Jeffery R, Preston SL, Poulsom R, Hodivala-Dilke K, Alison MR, Wright NA. Multiple organ engraftment by bone-marrow-derived myofibroblasts and fibroblasts in bone-marrow-transplanted mice. Stem Cells 2003;21(5):514-20.

18) Rhim JA, Sandgren EP, Degen JL, Palmiter RD, Brinster RL. Replacement of diseased mouse liver by hepatic cell transplantation. Science 1994 Feb 25;263(5150):1149-52.

19) Stevens ME, Meneses JJ, Pedersen RA. Expression of a mouse metallothionein-Escherichia coli beta-galactosidase fusion gene (MT-beta gal) in early mouse embryos. Exp Cell Res 1989 Aug;183(2):319-25.

20) Nilsson E, Lendahl U. Transient expression of a human beta-actin promoter/lacZ gene introduced into mouse embryos correlates with a low degree of methylation. Mol Reprod Dev 1993 Feb;34(2):149-57.

21) Beddington RS, Morgernstern J, Land H, Hogan A. An in situ transgenic enzyme marker for the midgestation mouse embryo and the visualization of inner cell mass clones during early organogenesis. Development 1989 May;106(1):37-46.

22) Sands AT, Hansen TN, Demayo FJ, Stanley LA, Xin L, Schwartz RJ. Cytoplasmic beta-actin promoter produces germ cell and preimplantation embryonic transgene expression. Mol Reprod Dev 1993 Feb;34(2):117-26.

23) Schorpp M, Jager R, Schellander K, Schenkel J, Wagner EF, Weiher H, Angel P. The human ubiquitin C promoter directs high ubiquitous expression of transgenes in mice. Nucleic Acids Res 1996 May 1;24(9):1787-8.

24) Takeda S, Toyoda Y. Expression of SV40-lacZ gene in mouse preimplantation embryos after pronuclear microinjection. Mol Reprod Dev 1991 Oct;30(2):90-4.

25) Boshart M, Weber F, Jahn G, Dorsch-Hasler K, Fleckenstein B, Schaffner W. A very strong enhancer is located upstream of an immediate early gene of human cytomegalovirus. Cell 1985 Jun;41(2):521-30.

26) Kisseberth WC, Brettingen NT, Lohse JK, Sandgren EP. Ubiquitous expression of marker transgenes in mice and rats. Dev Biol 1999 Oct 1;214(1):128-38.

27) Zambrowicz BP, Imamoto A, Fiering S, Herzenberg LA, Kerr WG, Soriano P. Disruption of overlapping transcripts in the ROSA beta geo 26 gene trap strain leads to widespread expression of beta-galactosidase in mouse embryos and hematopoietic cells. Proc Natl Acad Sci U S A 1997 Apr 15;94(8):3789-94.

28) Ahern-Rindell AJ, Prieur DJ, Murnane RD, Raghavan SS, Daniel PF, McCluer RH, Walkley SU, Parish SM. Inherited lysosomal storage disease associated with deficiencies of beta-galactosidase and alpha-neuraminidase in sheep. Am J Med Genet 1988 Sep;31(1):39-56.

29) Weiss DJ, Liggitt D, Clark JG. Histochemical discrimination of endogenous mammalian beta-galactosidase activity from that resulting from lac-Z gene expression. Histochem J 1999 Apr;31(4):231-6.

30) Conchie J, Findlay J, Levvy GA. Mammalian glycosidases; distribution in the body. Biochem J 1959 Feb;71(2):318-25.

31) Pearson B, Wolf PL, Vazquez J. A comparative study of a series of new indolyl compounds to lokalize beta-galactosidase in tissues. Lab Invest 1963 Dec;12:1249-59.

32) Cohen RB, Tsou KC, Rutenburg SH, Seligman AM. The colorimetric estimation and histochemical demonstration of beta-d-galactosidase. J Biol Chem 1952 Mar;195(1):239-49.

33) Lojda Z. Indigogenic methods for glycosidases. II. An improved method for beta-D-galactosidase and its application to localization studies of the enzymes in the intestine and in other tissues. Histochemie 1970;23(3):266-88.

34) Lederberg J. The beta-d-galactosidase of Escherichia coli, strain K-12. J Bacteriol 1950 Oct;60(4):381-92.

35) Roufosse C, Bou-Gharios G, Prodromidi E, Alexakis C, Jeffery R, Khan S, Otto WR, Alter J, Poulsom R, Cook HT. Bone Marrow-Derived Cells Do Not Contribute Significantly to Collagen I Synthesis in a Murine Model of Renal Fibrosis. J Am Soc Nephrol 2006 Feb 8.

36) Lee BY, Han JA, Im JS, Morrone A, Johung K, Goodwin EC, Kleijer WJ, DiMaio D, Hwang ES. Senescence-associated beta-galactosidase is lysosomal beta-galactosidase. Aging Cell 2006 Apr;5(2):187-95.

37) Ikawa M, Yamada S, Nakanishi T, Okabe M. 'Green mice' and their potential usage in biological research. FEBS Lett 1998 Jun 23;430(1-2):83-7.

38) Okabe M, Ikawa M, Kominami K, Nakanishi T, Nishimune Y. 'Green mice' as a source of ubiquitous green cells. FEBS Lett 1997 May 5;407(3):313-9.

39) Herrera MB, Bussolati B, Bruno S, Fonsato V, Romanazzi GM, Camussi G. Mesenchymal stem cells contribute to the renal repair of acute tubular epithelial injury. Int J Mol Med 2004 Dec;14(6):1035-41.

40) Imasawa T, Utsunomiya Y, Kawamura T, Zhong Y, Nagasawa R, Okabe M, Maruyama N, Hosoya T, Ohno T. The potential of bone marrow-derived cells to differentiate to glomerular mesangial cells. J Am Soc Nephrol 2001 Jul;12(7):1401-9.

41) Iwasaki M, Adachi Y, Minamino K, Suzuki Y, Zhang Y, Okigaki M, Nakano K, Koike Y, Wang J, Mukaide H, Taketani S, Mori Y, Takahashi H, Iwasaka T, Ikehara S. Mobilization of bone marrow cells by G-CSF rescues mice from cisplatin-induced renal failure, and M-CSF enhances the effects of G-CSF. J Am Soc Nephrol 2005 Mar;16(3):658-66.

42) Lin F, Moran A, Igarashi P. Intrarenal cells, not bone marrow-derived cells, are the major source for regeneration in postischemic kidney. J Clin Invest 2005 Jul;115(7):1756-64.

43) Stokman G, Leemans JC, Claessen N, Weening JJ, Florquin S. Hematopoietic stem cell mobilization therapy accelerates recovery of renal function independent of stem cell contribution. J Am Soc Nephrol 2005 Jun;16(6):1684-92.

44) Cormack B, Valdivia R, Falkow S. FACS-optimized mutants of the green fluorescent protein (GFP). Gene 1996;173(1):33-8.

45) Ellenberg J, Lippincott-Schwartz J, Presley JF. Dual-colour imaging with GFP variants. Trends Cell Biol 1999 Feb;9(2):52-6.

46) Ikarashi K, Li B, Suwa M, Kawamura K, Morioka T, Yao J, Khan F, Uchiyama M, Oite T. Bone marrow cells contribute to regeneration of damaged glomerular endothelial cells. Kidney Int 2005 May;67(5):1925-33.

47) Li B, Morioka T, Uchiyama M, Oite T. Bone marrow cell infusion ameliorates progressive glomerulosclerosis in an experimental rat model. Kidney Int 2006 Jan;69(2):323-30.

48) Neale FC, Clubb JS, Hotchkis D, Posen S. Heat stability of human placental alkaline phosphatase. J Clin Pathol 1965 May;18:359-63.

49) Posen S, Cornish CJ, Horne M, Saini PK. Placental alkaline phosphatase and pregnancy. Ann N Y Acad Sci 1969 Oct 14;166(2):733-44.

50) Broekema M, Harmsen MC, Koerts JA, Petersen AH, van Luyn MJ, Navis G, Popa ER. Determinants of tubular bone marrow-derived cell engraftment after renal ischemia/reperfusion in rats. Kidney Int 2005 Dec;68(6):2572-81.

51) Broekema M, Harmsen MC, van Luyn MJ, Koerts JA, Petersen AH, van Kooten TG, van Goor H, Navis G, Popa ER. Bone Marrow-Derived Myofibroblasts Contribute to the Renal Interstitial Myofibroblast Population and Produce Procollagen I after Ischemia/Reperfusion in Rats. J Am Soc Nephrol 2007 Jan;18(1):165-75.

52) Mujtaba T, Han SS, Fischer I, Sandgren EP, Rao MS. Stable expression of the alkaline phosphatase marker gene by neural cells in culture and after transplantation into the CNS using cells derived from a transgenic rat. Exp Neurol 2002 Mar;174(1):48-57.

53) Geusz ME, Fletcher C, Block GD, Straume M, Copeland NG, Jenkins NA, Kay SA, Day RN. Long-term monitoring of circadian rhythms in c-fos gene expression from suprachiasmatic nucleus cultures. Curr Biol 1997 Oct 1;7(10):758-66.

54) Hastings JW. Chemistries and colors of bioluminescent reactions: a review. Gene 1996;173(1 Spec No):5-11.

55)   Naylor LH. Reporter gene technology: the future looks bright. Biochem Pharmacol 1999 Sep 1;58(5):749-57.

56)   Contag PR. Whole-animal cellular and molecular imaging to accelerate drug development. Drug Discov Today 2002 May 15;7(10):555-62.

57)   Greer LF, III, Szalay AA. Imaging of light emission from the expression of luciferases in living cells and organisms: a review. Luminescence 2002 Jan;17(1):43-74.

58)   Cao YA, Bachmann MH, Beilhack A, Yang Y, Tanaka M, Swijnenburg RJ, Reeves R, Taylor-Edwards C, Schulz S, Doyle TC, Fathman CG, Robbins RC, Herzenberg LA, Negrin RS, Contag CH. Molecular imaging using labeled donor tissues reveals patterns of engraftment, rejection, and survival in transplantation. Transplantation 2005 Jul 15;80(1):134-9.

59)   Imai E, Akagi Y, Isaka Y, Ikawa M, Takenaka M, Hori M, Okabe M. Glowing podocytes in living mouse: transgenic mouse carrying a podocyte-specific promoter. Exp Nephrol 1999 Jan;7(1):63-6.

60)   Iwano M, Plieth D, Danoff TM, Xue C, Okada H, Neilson EG. Evidence that fibroblasts derive from epithelium during tissue fibrosis. J Clin Invest 2002 Aug;110(3):341-50.

61)   Asahara T, Masuda H, Takahashi T, Kalka C, Pastore C, Silver M, Kearne M, Magner M, Isner JM. Bone marrow origin of endothelial progenitor cells responsible for postnatal vasculogenesis in physiological and pathological neovascularization. Circ Res 1999 Aug 6;85(3):221-8.

62)   Finnegan EJ, Wang M, Waterhouse P. Gene silencing: fleshing out the bones. Curr Biol 2001 Feb 6;11(3):R99-R102.

63)   Pannell D, Ellis J. Silencing of gene expression: implications for design of retrovirus vectors. Rev Med Virol 2001 Jul;11(4):205-17.

64)   Togel F, Hu Z, Weiss K, Isaac J, Lange C, Westenfelder C. Administered mesenchymal stem cells protect against ischemic acute renal failure through differentiation-independent mechanisms. Am J Physiol Renal Physiol 2005 Feb 15.

65)   Lange C, Togel F, Ittrich H, Clayton F, Nolte-Ernsting C, Zander AR, Westenfelder C. Administered mesenchymal stem cells enhance recovery from ischemia/reperfusion-induced acute renal failure in rats. Kidney Int 2005 Oct;68(4):1613-7.

66)   Karrer FM, Reitz BL, Hao L, Lafferty KJ. Fluorescein labeling of murine hepatocytes for identification after intrahepatic transplantation. Transplant Proc 1992 Dec;24(6):2820-1.
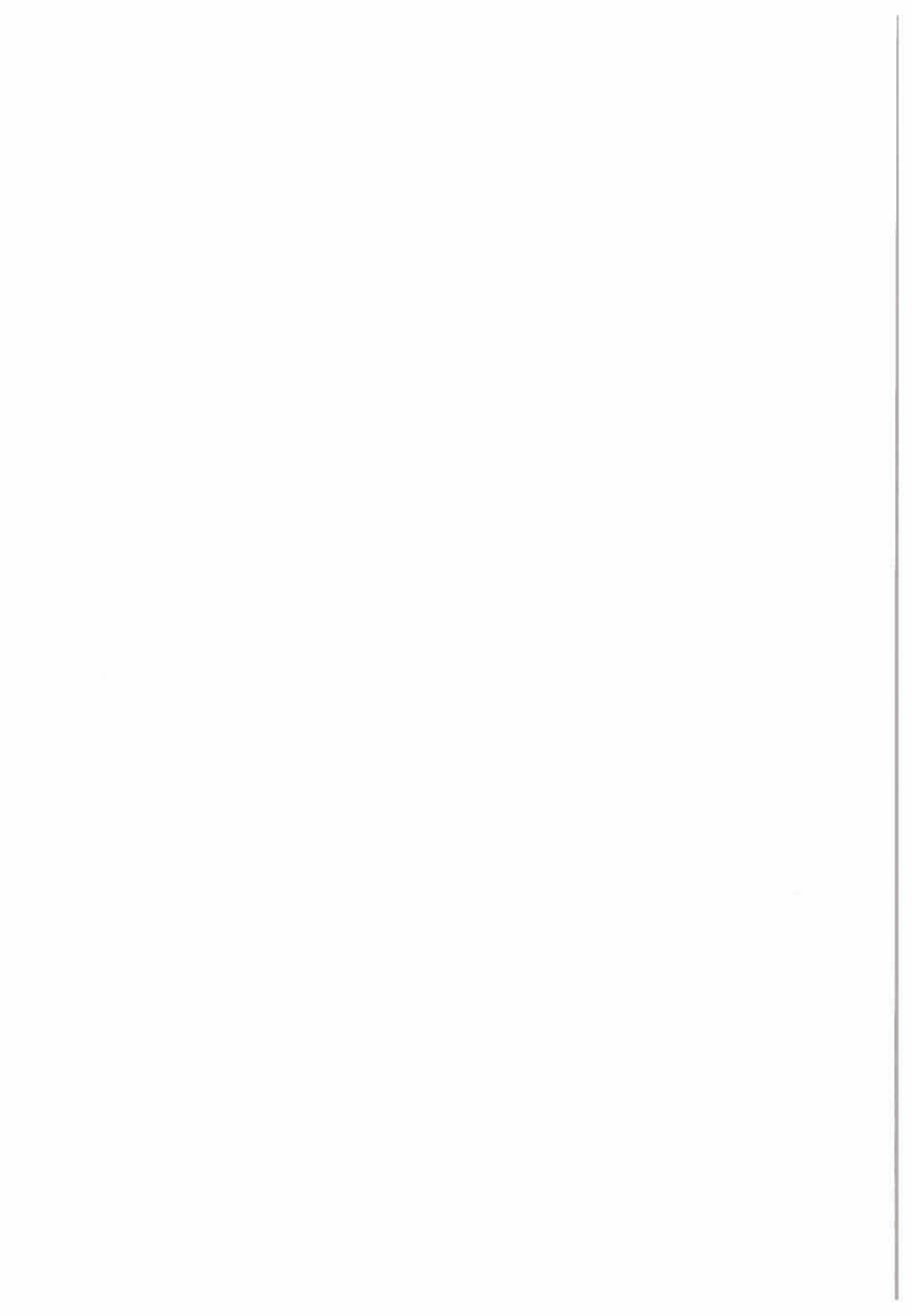
Chapter 3

Determinants of tubular bone marrow-derived cell engraftment after renal ischemia/reperfusion in rats

Martine Broekema[1], Martin C. Harmsen[1], Jasper A. Koerts[1], Arjen H. Petersen[1], Marja J. A. van Luyn[1], Gerjan Navis[2], Eliane R. Popa[1]

[1]Department of Pathology and Laboratory Medicine, Medical Biology section, [2]Department of Nephrology, University Medical Center Groningen, University of Groningen, The Netherlands

Abstract

Ischemia/reperfusion injury (IRI) is a major cause of acute renal failure (ARF). ARF is reversible, due to an innate regenerative process, which is thought to depend partly on bone marrow-derived progenitor cells. The significance of these cells in the repair process has been questioned in view of their relatively low frequency. Here, we hypothesize that the severity of renal damage and the post-ischemic recovery time are determinants of tubular bone marrow-derived cell (BMDC) engraftment.

We used a model of unilateral renal ischemia/reperfusion in F344 rats reconstituted with R26-hPAP transgenic bone marrow, in which we quantified and characterized tubular BMDC engraftment with increasing severity of damage and in time.

After IRI, BMDC engrafted the tubular epithelium and acquired an epithelial phenotype. Tubular epithelial BMDC engraftment increased with longer ischemic time, indicating that tubular epithelial BMDC engraftment increases with the severity of damage. The number of circulating progenitor cells doubled early after IRI and was followed by a transient increase in tubular epithelial BMDC engraftment. The latter positively correlated with morphological recovery of the kidney over time.

The extent of tubular BMDC engraftment depends on the severity of renal damage and follows a distinct time course after IRI. Therefore, the severity of damage and time course need to be taken into account when interpreting data on the role of tubular BMDC engraftment in renal repair after IRI.

Introduction

Renal ischemia/reperfusion injury (IRI) is a major cause of acute renal failure (ARF), a condition affecting up to 5% of long-term hospital patients (1), and, additionally, posing a potential post-operative problem for kidney transplant patients. Renal IRI is the result of oxygen deprivation and the subsequent cumulative assaults of the ensuing inflammatory reaction on renal vascular and epithelial tissue.

Severe IRI is characterized by tubular epithelial cell death and loss of kidney function (2). Interestingly, however, renal IRI is reversible (3), indicating that innate repair mechanisms are activated upon renal damage. One of these mechanisms is thought to involve bone marrow-derived (BMD) progenitor cells, which have been shown to engraft affected kidneys and to adopt an epithelial phenotype (4-7), possibly replacing damaged tubular epithelial cells. The functional significance of bone marrow-derived cells (BMDC) in renal repair is so far uncertain. Whereas there is data to suggest a contribution to renal repair, it has been pointed out that the number of BMDC detected in the kidney after IRI is low and variable, typically ranging between just 2% and 8%, which led to questioning their functional significance (5;7).

The determinants of the extent of BMDC engraftment have not been explored so far, which hampers the interpretation of previous data. Here, we hypothesize that the extent of BMDC engraftment is modulated by the severity of renal damage and post IRI recovery time. Moreover, the impact of endogenous repair, based on proliferation of surviving renal cells, was investigated. While the impact of these three parameters on renal BMDC engraftment has not yet been explored, they are likely to play a role in renal repair. It is known, for example, that increasing severity of IRI negatively affects renal recovery. Furthermore, studies concerning mobilization kinetics of endothelial progenitor cells (EPC) after acute myocardial infarction demonstrated a gradual increase in numbers of these cells in the circulation, peaking on day 7 post-infarction, suggesting the presence of windows of opportunity for engraftment of these cells in the heart (8). Finally, proliferation of resident tubular epithelial cells that survive renal IRI is thought to contribute to the restoration of kidney morphology and function (9-11).

The hypotheses were tested using a model of unilateral renal ischemia/reperfusion in F344 rats reconstituted with rat R26-hPAP transgenic bone marrow. The unilateral model, with the other kidney remaining *in situ* to ensure residual renal function and survival of the animals, allowed us to study not only mild and moderate, but also severe IRI.

Materials and Methods

Study design

In both experiments, unilateral renal ischemia was induced in R26-hPAP to F344 BM chimeric rats.

To investigate the influence of the severity of renal damage on tubular BMDC engraftment we modulated damage extent by varying ischemic times (20, 30, 45 and 60 min, n=3 per group). The effect of renal damage extent on renal morphology was monitored after 7 days by PAS staining, the effect on renal function and tubular BMDC engraftment after 28 days.

To study the kinetics of tubular epithelial BMDC engraftment in relation to recovery time, we inflicted 45 min of unilateral ischemia and evaluated tubular BMDC engraftment after 1 (n=6), 3 (n=6), 7 (n=6), 14 (n=7), 28 (n=5), 56 (n=3) and 112 (n=3) days of recovery.

Animals

Male, 6 week-old F344 rats (Harlan Nederland, Horst, The Netherlands) were used as BM recipients. R26-hPAP rats (founders were a kind gift of Dr. E. Sandgren; F344 background, 6 week-old), transgenic for human placental alkaline phosphatase (hPAP) (12), were used as BM donors.

Rats were housed in a conventional environment and received standard chow and water ad libitum. Drinking water was supplemented with 1 mg/ml 5-bromo-2-deoxyurdine (BrdU, Sigma, St. Louis, USA), for 3 days before termination.

All animal procedures were approved by the local committee for care and use of laboratory animals and performed according to governmental and international guidelines on animal experimentation.

Irradiation and bone marrow transplantation

Non-transgenic rats received lethal total body irradiation (9 Gy, IBL 637 Cesium-137 gamma ray source) for bone marrow ablation. Subsequently, the rats were housed in filter top cages. Drinking water was supplemented with neomycin (0.35% w/v) starting one week before irradiation, until 2 weeks after irradiation.

Total BM from R26-hPAP rats was isolated by flushing femurs and tibiae with sterile PBS. Erythrocytes were lyzed in 155 mmol/L NH_4Cl, 10mmol/L $KHCO_3$, 0.1 mmol/L Na EDTA, and the BM cell suspension was filtered through a 10 μm cell strainer (Falcon, Becton Dickson). BM isolation was carried out on ice.

Twenty-four hours after irradiation, rats received approximately 1×10^6 R26-hPAP BM cells intravenously and were allowed to recover for 4 weeks. Bone marrow chimerism in recipients was determined by enzymatic hPAP staining (see below) on bone marrow cytospots from recipients and was typically between 80% and 90%.

Surgical procedure

Reconstituted BM recipients were sedated by general isoflurane (2% Forene, Abbot b.v., Hoofddorp, The Netherlands), N_2O (50%), O_2 (50%) anaesthesia. The left renal artery was exposed and clamped with a non-traumatic clamp to induce ischemia. The clamp was removed after specified periods and renal reperfusion was confirmed visually. SHAM-operated control rats underwent bone marrow transplantation followed by a midline incision.

At specified time points after ischemia/reperfusion, rats were anaesthetized. Blood samples were drawn and both kidneys were perfused in situ with cold saline. Kidneys were isolated and divided into quarters by a longitudinal and a transversal section. These quarters were fixed in zinc fixative (0.1M Tris buffer, pH 7.4 with 0.5g $CaCH_2COO$, 5g $(CH_2COO)2Zn*2H_2O$ and 5g $ZnCl_2$ per liter; MERCK, Darmstadt, Germany), or snap-frozen in N_2 and stored at −80°C. Zinc-fixed tissues were processed for paraffin

embedding by standard procedures and used for immunohistochemistry. Snap-frozen tissue was used for immunofluorescence microscopy.

Kidney function

Plasma creatinine levels were determined using a colorimetric test (Merck MEGA® analyzer, Merck).

Detection of lineage negative (Lin⁻) cells

Mobilization of BMD progenitor cells to the circulation was determined using total mononuclear cell (MNC) fractions. Since no monoclonal antibodies (moAbs) specific for rat progenitor cell markers are available, we assessed circulating Lin⁻ cells as a population enriched for potential BMD progenitor cells. Briefly, MNC fractions were isolated by lympholite rat density gradient centrifugation (Cederlane, Uden, The Netherlands). MNCs were stained with a cocktail of PE- or FITC-labeled moAbs against the lineage markers CD3 (T cells, Becton Dickinson, Alphen aan den Rijn, The Netherlands), CD11b/c (myeloid and dendritic cells, BD) and anti-rat κ/λ (B cells, Sigma-Aldrich, Zwijndrecht, The Netherlands). Lin⁻ cells were detected and quantified on day 1 (n=3), 3 (n=3), 7 (n=3) and 14 (n=3) after 45 min of ischemia using MoFlo cytometer (Cytomation Inc., Fort Collins, CO), and WinList 5.0 software (Verity, Topsham, ME).

(Immuno)histochemistry

Enzymatic hPAP staining was used to detect renal infiltration of hPAP⁺ BMDC. Briefly, 5 µm paraffin sections were dewaxed and endogenous alkaline phosphatase was heat-inactivated by incubation in substrate buffer (0.1M Tris-HCl, pH 9.5, 0.1M NaCl, 5mM $MgCl_2$) at 65°C for 30 min (12). Subsequently, sections were incubated in fresh substrate buffer containing 2% (v/v) nitroblue tetrazolium/5-bromo-4-chloro-3-indolyl phosphate (NBT/BCIP, Roche, Woerden, The Netherlands) (5h, room temperature (RT)).

Detection of hPAP⁺ BMDC was confirmed by immunohistochemical staining using a rabbit anti-human Placental Alkaline Phosphatase monoclonal antibody (hPAP, Serotec, Oxford, UK) to detect bone-marrow derived cells. Briefly, 5 µm zinc-fixed paraffin sections were dewaxed and subjected to endogenous alkaline phosphatase inactivation by incubation in substrate buffer at 65°C for 30 min (12). Non-specific protein binding was blocked with 2% BSA for 30 min and endogenous biotin was blocked with biotin blocking kit (Biotin blocking system, DAKO). Rabbit anti-hPAP antibody was applied to the sections for 60 min, at room temperature (RT), followed by biotinylated goat-anti-rabbit conjugate (DAKO, Glostrup, Denmark) and streptavidin-alkaline phosphatase (Southern Biotechnology). Color development was performed with fuchsin substrate-chromogen system according to manufacturer's instructions (DAKO).

The epithelial phenotype of tubular engrafted BMDC, was assessed by immunofluorescent double-staining for hPAP (rabbit-anti-human Placental Alkaline Phosphatase, Serotec) in combination with, respectively, E-cadherin (clone 36, BD Biosciences), pan-cytokeratin (C-11, Abcam, Cambridgeshire, UK) or a cocktail of

the tubular epithelial-specific lectins SBA (biotinylated soybean agglutinin), DBA (biotinylated dolichos biflorus agglutinin) and PNA (biotinylated peanut agglutinin; all from Vector laboratories Inc., Burlingame, CA, USA). Briefly, on 5 µm cryo sections, endogenous biotin was blocked with biotin blocking kit (biotin blocking system) according to manufacturer's instructions (Dako). BMDC were detected by incubation with anti-hPAP moAb (1h, RT), followed by goat-anti-rabbit-FITC conjugate (Southern Biotechnology, Birmingham, USA). Tubular epithelial cells were detected in several ways; by incubation with a mixture of 30 µg/mL biotinylated SBA/DBA/PNA followed by a streptavidin-Cy3 (Zymed Laboratories Inc., San Francisco, USA) conjugate, or by incubation with moAbs against E-cadherin or pan-cytokeratin (1h, RT) followed by biotinylated goat-anti-mouse (IgG2a for E-cadherin and IgG1 for pan-cytokeratin) (Dako) and streptavidin-Cy3 conjugates (Zymed Laboratories Inc).

To confirm that hPAP⁺ cells, engrafted in renal tubuli, were not engrafted BMD leukocytes, we performed double-staining combining hPAP with CD45 (leukocyte marker). Briefly, on 5 µm cryo sections, endogenous biotin was blocked and BMDC were detected as described above. Leukocytes were detected by incubation with mouse anti-rat CD45 moAb (1h, RT, OX-1, culture supernatant), followed by biotinylated goat anti-mouse IgG (Southern Biotechnology) and streptavidin-Cy3 conjugates (Zymed Laboratories Inc).

To detect BrdU incorporation, 5 µm paraffin sections were treated with 0.7M HCl (30 min, 37°C), followed by incubation with 0.025% (w/v) pepsin in 0.35M HCl (15 min, 37°C, Roche). BrdU was detected by incubation with anti-BrdU moAb (1h, RT, Sigma-Aldrich), followed by biotinylated goat anti-mouse IgG (Southern Biotechnology) and streptavidin-conjugated peroxidase (Dako). Color development was performed with 3-amino-9-ethylcarbazole (Sigma-Aldrich) substrate dissolved in N,N-dimethylformamide (MERCK) and 0.5M acetate buffer, pH 4.9.

All conjugate incubations were performed for 30 min, RT, in the dark, and were followed by appropriate washing steps. Immunofluorescence sections were counterstained with DAPI and mounted with citifluor (Agar scientific, Stansted, UK). Immunohistochemically stained sections were counterstained with Mayer's hemalum (MERCK) and mounted in Kaiser's glycerol (MERCK).

Light- and fluorescence microscopy was performed using a Leica DMLB microscope (Leica Microsystems, Rijswijk, The Netherlands), Leica DC300F camera and Leica QWin 2.8 software. To confirm that double positive cells were not the result of overlying cells, confocal microscopy was performed using a Leica TCS SP2 confocal microscope and Leica confocal 2.5 software.

Quantification

The severity of morphological renal damage was assessed using an arbitrary score based on PAS-stained kidney sections. Briefly, the extent of 4 typical IRI-associated damage markers, i.e. dilatation, denudation, intraluminal casts and cell flattening, was expressed in arbitrary units (a.u.) in a range of 0-3.

Tubular engraftment of BMDC in the cortex and outer medulla was assessed by scoring the number of tubulus sections containing at least one hPAP⁺ cell. To be considered an epithelial cell, hPAP⁺ cells had to be integrated in the renal tubule at the luminal side of the basal membrane and have epithelial size and morphology, similar to

that of neighboring, resident tubular cells. Kidney section area was determined by computerized planimetry (Leica QWin 2.8 software) and differences in kidney section area were corrected for by expressing the number of hPAP+ tubuli per 10 mm².

The percentage of the tubular engrafted BMDC which also express a tubular epithelial marker was determined on kidney sections after immunofluorescence staining for hPAP and a tubular epithelial marker.

To determine proliferation-mediated renal repair in the cortex and outer medulla, we first determined the percentage of tubulus sections containing at least one BrdU+ cell. Subsequently, the percentage of BrdU+ nuclei per BrdU+ tubulus section was determined.

Statistics

Statistical tests were performed using GraphPad Prism 4.0 (GraphPad Software, San Diego California, USA) and SPSS 12.0 software (SPSS Inc., Chicago, USA). Two-tailed Mann-Whitney-U tests were performed to determine differences between SHAM and experimental groups. Spearman correlation tests were performed to determine the relationship between different parameters. P-values <0.05 were considered statistically significant.

Results

Morphological and functional damage extent in relation to ischemic time

On day 7, morphological IRI was observed in the tubular epithelium in cortex and outer medulla, while glomeruli were morphologically normal. Increasing ischemic time was associated with increasing renal damage (Figure 1B-D), as apparent from the presence of all classical damage markers, such as proximal epithelial cell flattening or loss, tubular dilatation, and the intraluminal brush border debris and protein casts (13). Tubular denudation was observed after 45 min of ischemia (Figure 1C). Sixty min of ischemia resulted in extensive damage (Figure 1D) and was not further investigated.

The cumulative damage score, assessed on day 28 after 20, 30 and 45 min of ischemia, was higher in the groups with longer ischemic time, thereby validating our model (Figure 2A). The cumulative damage score significantly correlated with ischemic time (Figure 2B). Plasma creatinine levels, assessed on day 28 after 20, 30 and 45 min of ischemia, were slightly but significantly higher than in SHAM controls (Figure 2C).
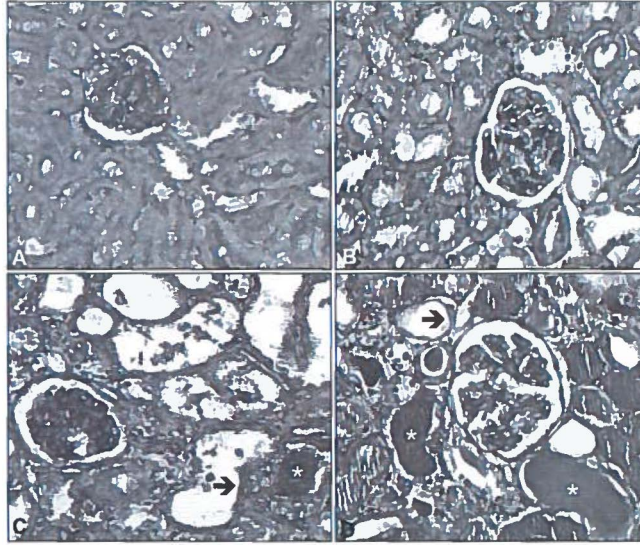
Figure 1. *Morphological kidney damage extent in relation to ischemic time. Representative morphology of a healthy control kidney (A) and of kidneys subjected to 30 (B), 45 (C) and 60 min of ischemia (D) assessed on day 7 after IRI induction by PAS staining of paraffin sections. Arrows indicate examples of tubular membrane denudation. Asterisks indicate examples of intraluminal casts. Lens magnification 200x.*
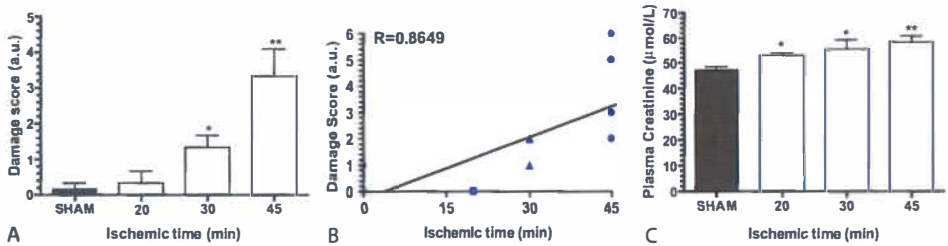
Figure 2. *Morphological and functional kidney damage extent in relation to ischemic time. Severity of damage was determined by an arbitrary score of the presence of 4 typical IRI-associated damage markers, i.e. dilatation, denudation, intraluminal casts and cell flattening and expressed in arbitrary units (a.u.) in a range of 0-3. The severity of damage was assessed on PAS stained kidney sections of rats sacrificed on day 28 after 20, 30 and 45 min of ischemia (A). Correlation between damage score and ischemic time was assessed by a Spearman correlation test (B). SHAM-operated controls = open circles, 20 min of ischemia = squares, 30 min of ischemia = triangles, 45 min of ischemia = closed circles. Plasma creatinine levels were measured on day 28 after 20, 30 and 45 min of ischemia (C). Bars indicate mean + SEM of all experimental animals per group. Statistically significant differences compared to SHAM are indicated as * = P<0.05, ** = P<0.005.*

Tubular epithelial BMDC engraftment in relation to ischemic time

hPAP was ubiquitously expressed in renal cells of R26-hPAP transgenic rats (Figure 3A), and was undetectable in non-transgenic kidneys (not shown) and in post-ischemic kidneys of non-BM transplanted F344 rats (Figure 3B). In ischemic kidneys of R26-hPAP BM transplanted rats, most hPAP+ BMDC formed interstitial infiltrates (Figure 3C). On day 28 after IRI induction, the extent of renal BMDC infiltration was similar in kidneys subjected to 20 and 30 min of ischemia, but more extensive in kidneys subjected to 45 min of ischemia (not shown). Morphological examination of the contralateral kidney demonstrated small interstitial infiltrates of hPAP+ BMDC (not shown).

To determine tubular epithelial BMDC engraftment we sought for hPAP+ cells that were integrated in the renal tubulus, at the luminal side of the basal membrane (Figure 3D). hPAP expression was confirmed by immunohistochemical staining on consecutive slides (Figure 3E). Typically, in engrafted tubuli, we detected one hPAP+ cell per tubulus section and, sporadically, two or three, but never more. In SHAM-operated and contralateral kidneys, BMDC-engrafted tubuli were infrequent and significantly lower compared to ischemic kidneys (Figure 3F). After ischemia, the number of BMDC-engrafted tubuli in cortex and outer medulla increased progressively with ischemic time (Figure 3F) and, moreover, correlated significantly with ischemic time (Figure 3G).

3

Epithelial phenotype of BMDC engrafted in tubuli

The epithelial phenotype of engrafted hPAP+ cells was assessed by immunofluorescence double-staining combining hPAP detection with detection of the epithelial markers E-cadherin, pan-cytokeratin and epithelial-binding lectins (SBA, DBA and PNA). In accordance with the enzymatic detection of tubular engrafted BMDC, engrafted tubuli contained one or two hPAP+ cells. These cells also bound lectins (Figure 4A-C), or co-expressed pan-cytokeratin (Figure 4D-F) or E-cadherin (Figure 4G-I). Independently of the epithelial marker used, an average of 94% of the tubular engrafted BMDC also expressed a tubular epithelial marker. Neither E-cadherin nor pan-cytokeratin expression or epithelial lectin binding was observed within hPAP+ inflammatory cell infiltrates, indicating the specificity of these tubular epithelial markers (not shown).

To confirm that tubular epithelial engrafted BMDC were not incorporated leukocytes, we performed a double-staining combining hPAP with CD45 (leukocyte marker). Cells expressing CD45 were only present in interstitial infiltrates, but were not engrafted in the tubular epithelium (Figure 4J-L).
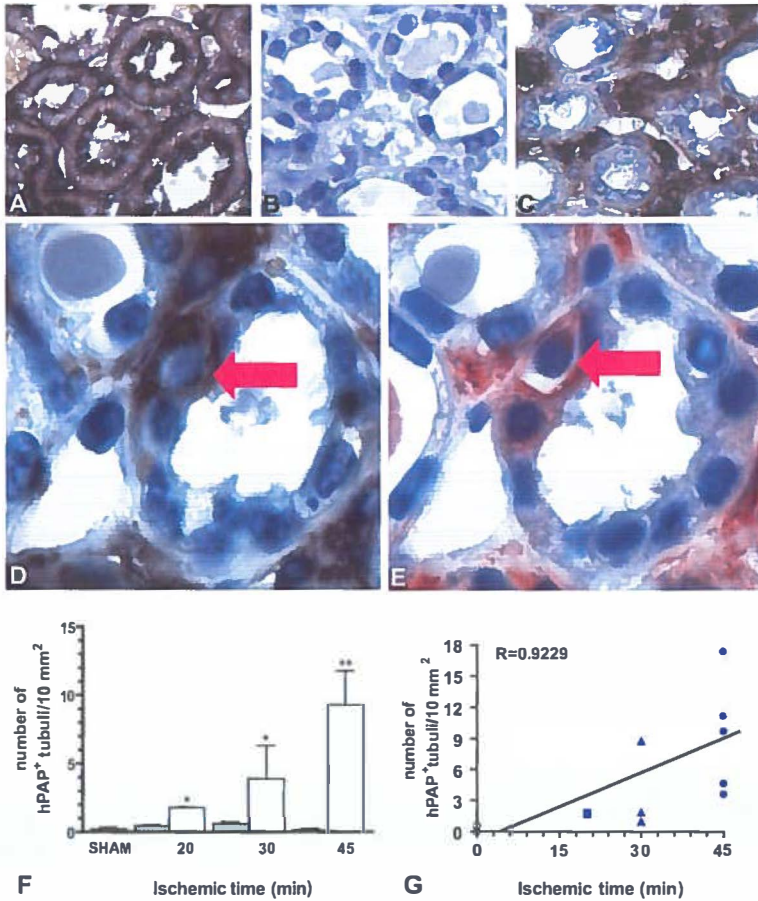
Figure 3. *Tubular epithelial BMDC engraftment in relation to ischemic time. To detect hPAP+, i.e. bone marrow-derived cells, enzymatic staining of hPAP was performed after heat inactivation of endogenous alkaline phosphatase. Ubiquitous expression of hPAP was observed in R26-hPAP transgenic rat kidney (A). hPAP staining was absent in post-ischemic kidneys of non-BM transplanted F344 rats (B). Expression of hPAP was observed on infiltrating BMDC in post-ischemic kidneys of rats, reconstituted with R26-hPAP transgenic bone marrow (C). Lens magnification 400x. Engraftment of hPAP+ cells in tubuli of ischemic kidney was observed on day 28 after 45 min of ischemia with enzymatic hPAP staining (D) and was confirmed by immunohistochemical hPAP staining on a consecutive slide (E). Note similar morphology of hPAP+ cells to that of neighboring, resident tubular cells. Arrows indicate examples of tubular epithelial BMDC engraftment. Lens magnification 1000x. Tubular BMDC engraftment in relation to damage extent was determined on day 28 after IRI induction (F). Tubulus sections containing at least one hPAP+ cell with epithelial morphology were counted in the cortex and outer medulla. Scoring was performed on SHAM (black bars), contralateral (grey bars) and ischemic kidneys (white bars). Bars indicate mean values + SEM of all experimental animals per group. Statistically significant differences compared to SHAM are indicated as * = P<0.05, ** = P<0.005. Correlation between tubular BMDC engraftment and ischemic time was assessed by a Spearman correlation test (G). SHAM-operated controls = open circles, 20 min of ischemia = squares, 30 min of ischemia = triangles, 45 min of ischemia = closed circles.*
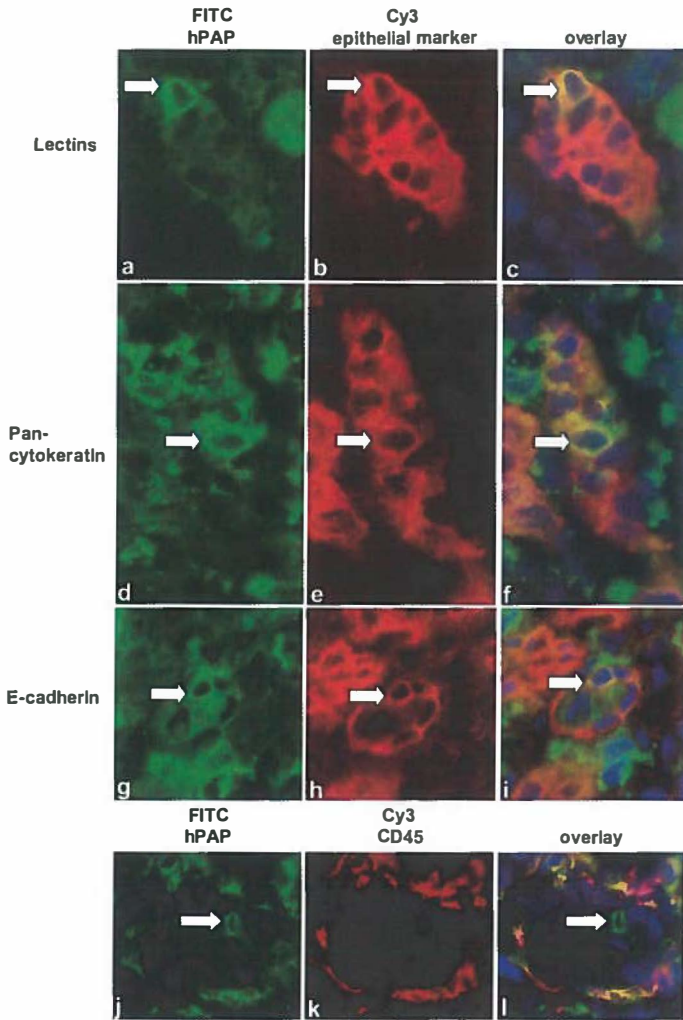
Figure 4. *Epithelial phenotype of BMDC engrafted in tubuli. Epithelial phenotype of BMDC engrafted in tubuli after IRI was confirmed by immunofluorescence co-detection of hPAP (A,D,G) and epithelium-binding lectins SBA, DBA, PNA (cocktail) (B) or the epithelium-specific markers pan-cytokeratin (E) and E-cadherin (H). Double-positive cells are shown in the overlay pictures (C,F,I). To confirm that tubular engrafted BMDC were not leukocytes we used immunofluorescence co-detection of hPAP (J) and CD45 (K, common leukocyte antigen). No double-positive cells were found engrafted in the tubular epithelium (L, overlay). Green = FITC, red = Cy3, blue = DAPI. Arrows indicate examples of tubular engrafted BMDC. Note identical morphology of positive cells in both channels. Lens magnification 400x.*

Tubular epithelial BrdU incorporation in relation with ischemic time

The extent of proliferation in tubular epithelial cells in the cortex and outer medulla was assessed by BrdU incorporation into nuclei of tubular epithelial cells on day 28 after IRI induction. No differences in BrdU incorporation, quantified as the percentage of BrdU$^+$ tubuli and as the percentage of BrdU$^+$ nuclei per BrdU$^+$ tubulus section, were present between SHAM, contralateral and post-ischemic kidneys. In all cases, most BrdU$^+$ nuclei were found within the tubular epithelium and often appeared in pairs. Sporadically, proliferating cells were present in the tubulo-interstitial spaces and in glomeruli (not shown).

Time course of morphological and functional kidney regeneration

To study the time course of renal repair, the ischemic time of 45 min was selected, since this model yielded sufficient renal damage, especially in terms of tubular denudation, but still allowed for regeneration.

On day 1, extensive epithelial cell loss in the cortex and outer medulla was observed (Figure 5A). By day 112, the tubular epithelium was virtually restored and ischemic damage markers, discussed above, were attenuated (Figure 5B). Cumulative severity of damage score showed a gradual morphological recovery in time (Figure 5C). Plasma creatinine levels peaked slightly, but significantly, on day 1, with a gradual decrease towards baseline values afterwards (Figure 5D).
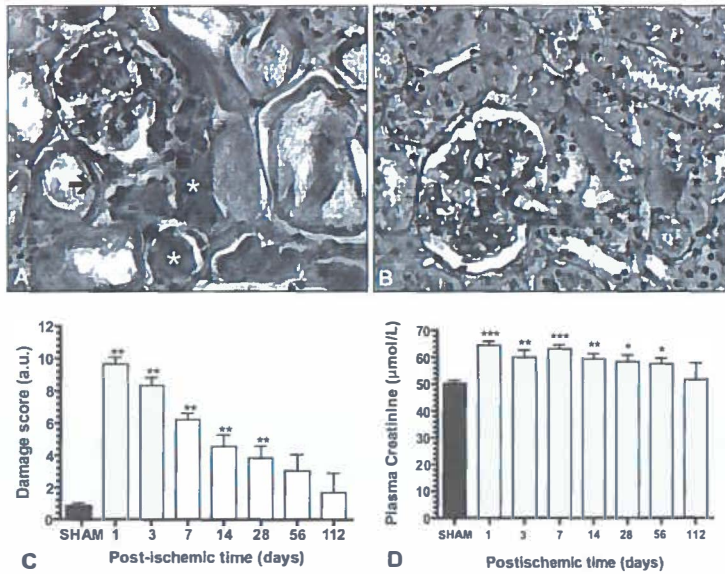
Figure 5. *Time course of morphological and functional kidney regeneration. Representative morphology of a kidney subjected to 45 min of ischemia on day 1 (A) and 112 (B) after IRI induction, was assessed by PAS staining of paraffin sections. Arrows indicate examples of tubular membrane denudation. Asterisks indicate examples of intraluminal casts. Lens magnification 200x. The severity of damage was determined by an arbitrary score, ranging from 0-3 arbitrary units (a.u.), of classic damage markers present in PAS stained kidney sections (C). Plasma creatinine levels were assessed to determine kidney function (D). Bars indicate mean levels + SEM of all experimental animals per group. Statistically significant differences compared to SHAM are indicated as * = P<0.05, ** = P<0.005, *** = P<0.0005.*

Time course of mobilization of BMDC

Tubular epithelial BMDC engraftment is preceded by mobilization of BMD progenitor cells to the circulation. After a reduction on day 1 after IRI, the number of circulating Lin⁻ cells, a population enriched for progenitor cells (Figure 6A), increased and peaked on day 3, compared to controls (Figure 6B). After day 3 the number of Lin⁻ cells gradually decreased and reached control values by day 14.

Time course of tubular epithelial BMDC engraftment

The majority of infiltrating BMDC formed interstitial infiltrates. The infiltrate size peaked by day 7 and gradually decreased after day 14. Small interstitial infiltrates persisted in the kidney until day 112 (not shown).

In engrafted tubuli, typically one hPAP⁺ cell was present per BMDC-engrafted tubulus section. On days 1 and 3 after ischemia, BMDC-engrafted tubuli were infrequent and comparable in number to tubular BMDC engraftment in SHAM and contralateral kidneys (Figure 6C). On day 7 a sharp increase in the number of BMDC-engrafted tubuli was observed, followed by a peak on day 14, gradually decreasing by days 28 and 56, to return to SHAM levels on day 112 (Figure 6C).

The epithelial phenotype of hPAP⁺ cells engrafted in tubuli was confirmed as above. Immunofluorescence double-staining combining hPAP detection with detection of the epithelial markers E-cadherin, pan-cytokeratin and epithelial-binding lectins (SBA, DBA and PNA) was in agreement with the peak of tubular epithelial BMDC engraftment on day 14 and low frequency on day 56 and 112 after IRI induction. Over time we observed, independently of tubular epithelial marker, a slight increase in the percentage of tubular engrafted BMDC which also expressed a tubular epithelial marker ($91 \pm 5\%$ on day 7, $93 \pm 2\%$ on day 14 and $97 \pm 2\%$ on day 28).
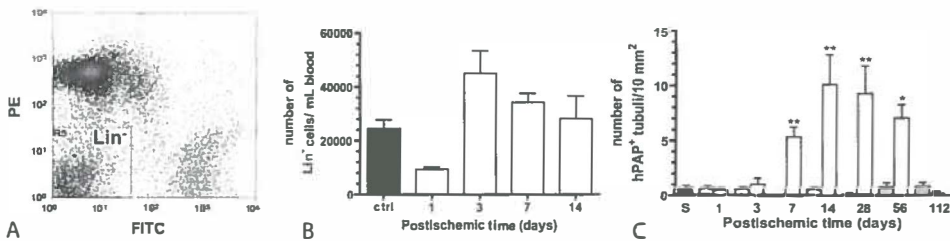
Figure 6. *Time course of recruitment of BMDC to the circulation and the kidney. Circulating lineage-negative (Lin⁻) cells (gated) were detected by flow cytometry after staining of MNC with moAbs against the lineage markers CD3 and CD11b/c (both PE labeled) and anti-rat κ/λ (FITC labeled)(A) and quantified at various time points after 45 min of ischemia (B). Tubular BMDC engraftment was assessed as the number of tubuli containing at least one hPAP⁺ epithelial cell by enzymatic staining for the hPAP enzyme (C). hPAP⁺ tubuli were scored in the cortex and outer medulla of SHAM (black bars), contralateral (grey bars) and ischemic (white bars) kidneys. Bars indicate mean values + SEM of all experimental animals per group. Ctrl. = control, S = SHAM, * = P<0.05, ** = P<0.005.*

Time course of tubular epithelial BrdU incorporation

Most BrdU⁺ nuclei in cortex and outer medulla were found in the tubular epithelium. In SHAM kidneys typically one, and sporadically, two BrdU⁺ nuclei per tubulus section were observed (Figure 7A), in ischemic kidneys, frequently three or more adjacent BrdU⁺ tubular epithelial cells were detected (Figure 7B), with the highest frequency on day 7 after IRI.

The extent of BrdU incorporation was quantified as the percentage of BrdU⁺ tubuli (Figure 7C) and as the percentage of BrdU⁺ nuclei per BrdU⁺ tubulus section (Figure 7D). The percentage of BrdU⁺ tubuli dropped significantly early after IRI to recover to control values from day 7 on. The percentage of BrdU⁺ nuclei per BrdU⁺ tubule was difficult to determine on days 1 and 3 due to extensive tubular denudation and, therefore, absence of nuclei. As a result, not all experimental animals from these time points could be included in the quantification. The percentage of BrdU⁺ nuclei per BrdU⁺ tubule peaked on day 7 and decreased to control values afterwards.
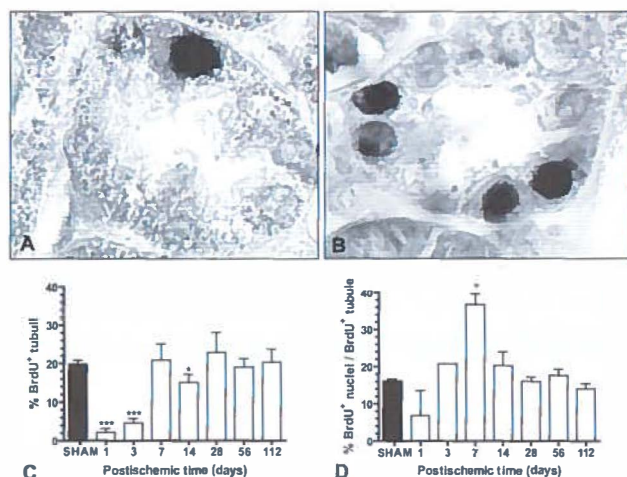
Figure 7. *Time course of tubular epithelial BrdU incorporation. Single BrdU⁺ nuclei (brown) were typically present in tubuli of SHAM kidneys (A). Multiple BrdU⁺ nuclei were present within tubular epithelial cells in ischemic kidneys 7 days after IRI (B). Lens magnification 1000x. To determine the extent of proliferative tubular repair we first determined the percentage of BrdU⁺ tubuli in cortex and outer medulla (C). Secondly, we determined the percentage of BrdU⁺ tubular epithelial cells in 10 tubuli in the cortex and 10 tubuli in the outer medulla (D). BrdU incorporation in ischemic kidney was compared with incorporation in corresponding SHAM kidneys at the respective time point. Bars indicate mean values + SEM of all experimental animals per group. * = P<0.05, *** = P<0.0005.*

Discussion

The current study demonstrates that the severity of renal damage is an important modulator of the extent of tubular epithelial BMDC engraftment after IRI in rats. Moreover, BMDC engraftment follows a distinct time course, different from the time course of proliferation of tubular epithelial cells.

To detect the bone marrow origin of tubular engrafted cells, we used the rat R26-hPAP transgene as a reporter marker. hPAP is one of the few available rat reporter markers and is more reliable than other commonly used reporter molecules, such as GFP and

β-gal. Problems with differential expression in kidney cells, as encountered with renal GFP expression in mice (14), or activation of endogenous protein expression at low pH (e.g. mammalian β-gal expression)(Duffield JS, Park K, Hsaio L, et al: Tubular cell replenishment is independent of bone marrow stem cells (BMSCs) in the post-ischemic mouse kidney (abstract) J.Am.Soc.Nephrol. 15:38A, 2004) were not encountered when using hPAP as a reporter marker.

We modulated the severity of renal damage by exposing the kidneys to different ischemic times. Thus, as apparent from the morphological data, a gradient in the severity of renal damage was obtained, that ranged from relatively moderate in the 20 min group to severe in the 45 min group. As the contralateral kidney remained *in situ*, the acute tubular necrosis did not result in severe acute renal insufficiency, as apparent from the mild rise in plasma creatinine. This allowed the animals to survive the period of acute tubular necrosis, and thus enabled us to study the renal recovery after severe IRI. Whereas the time course of plasma creatinine corresponded to the morphological restoration of the kidney, the contribution of the contralateral kidney to overall renal function precludes conclusions on the functional recovery of the ischemic kidney.

The relationship between the severity of renal damage and extent of tubular BMDC engraftment suggests that the extent of engraftment is determined by increasing need for repair. The mechanism underlying the relationship between the severity of damage and tubular BMDC engraftment was not addressed in our study. However, we propose that the presence and amount of molecular repair mediators in the post-ischemic renal niche is influenced by the severity of damage, thereby influencing the extent of BMDC engraftment.

Documentation of the time course of tubular BMDC engraftment after IRI was the second purpose of our study. We first studied the time course of mobilization of BMD progenitor cells to the circulation. In accordance with data by Kale *et al*. (4), we observed an early increase in the number of circulating Lin⁻ cells after IRI induction, indicating a relationship between renal damage and recruitment of BMD progenitor cells to the circulation. Numbers of circulating Lin⁻ cell peaked on day 3 after IRI. A lag between injury and maximal recruitment of progenitor cells to the circulation was also reported in patients with acute myocardial infarction by Shintani *et al*., who found a peak of circulating endothelial progenitor cells on day 7 after the ischemic event (8). The gradual decrease in numbers of circulating Lin⁻ cells, observed from day 7 after IRI induction on, would be compatible with homing of these cells to the damaged kidney. The appearance of BMD interstitial infiltrates in the kidney by day 7 supports this scenario. Moreover, the number of engrafted BMDC with epithelial phenotype also increased on day 7, demonstrating specific differentiation of some of the infiltrating cells to tubular epithelium. A slight increase in the percentage of tubular engrafted BMDC co-expressing a tubular epithelial marker was observed in time, indicating that differentiation of these cells upon arrival is not immediate.

The long-term follow-up in our study, with follow-up data up to 112 days after IRI, allowed us to investigate tubular epithelial BMDC engraftment during the complete time course of the tubular epithelial restoration process of the kidney after IRI. An interesting finding was the decline in numbers of BMD tubular epithelial cells at long term follow-up. An explanation for this phenomenon may be turn-over, during which tubular engrafted BMDC may be replaced by non-BMD renal cells, resulting in disappearance of the hPAP signal. However, since it was not technically feasible

to perform double staining for hPAP and BrdU, it remains unclear whether tubular engrafted BMDC underwent proliferation in the kidney. Furthermore, it is conceivable that the presence of proper growth factors and adhesion molecules in the ischemic niche would be responsible for creating a compatible situation for tubular epithelial BMDC engraftment and differentiation. Thus, inadequacy or absence of these factors could lead to loss of BMD tubular epithelial cells.

Recently, it has been suggested that BMDC engraftment may be the result of a spontaneous cell fusion process, thereby questioning the biological relevance of stem cell plasticity (15;16). In our study we are not able to distinguish cell transdifferentiation from cell fusion and are, therefore, unable to rule out the possible contribution of cell fusion to tubular BMDC engraftment. Cell fusion, followed by reprogramming of the fusion product and silencing of the hPAP gene, could be a cause for the decline in tubular epithelial BMDC engraftment we observed at later post-ischemic time points. Our data are in agreement with previous studies reporting low numbers of tubular BMDC engraftment in mouse models of renal ischemia (5;7;17). Together with the decline in their numbers at long term follow-up, this could be taken to argue against a functional role of BMDC in tubular epithelial cell replacement. However, it has recently been shown that, when activated by pro-inflammatory cytokines *in vitro*, CD34$^+$ BMD progenitor cells express a variety of immuno-regulatory mediators, thereby exerting a potential modulatory role in their environment (18). Thus, even at low numbers, BMD tubular epithelial cells might have functional significance during the process of renal repair, but further studies are needed to substantiate this issue.

The overall low frequency of tubular BMDC engraftment in the ischemic kidney and the occurrence of complete tubular re-epithelialization indicate that, besides BMDC engraftment, another mechanism must be involved in the repopulation of the denuded tubular membranes. Renal repair most likely occurs as a concerted process involving both tubular engraftment of BMDC and the proliferative activity of surviving renal cells. Indeed, epithelial proliferation increased after IRI and peaked on day 7, illustrating proliferation-mediated tubular repair. Interestingly, the peak in epithelial proliferation preceded that of tubular epithelial BMDC engraftment, which peaked on day 14 post IRI. Thus, tubular re-epithelialization by proliferation appears to be a distinct process with a different time course. In fact, tubular re-epithelialization was already ongoing by the time of emerging tubular epithelial BMDC engraftment, possibly explaining the low number of engrafted BMDC.

In conclusion, we showed that the extent of tubular epithelial BMDC engraftment depends on the severity of damage, and follows a distinct time course after IRI induction. Tubular re-epithelialization by proliferation of renal cells appeared to be a distinct process with a different time course, already ongoing by the time of emerging tubular epithelial BMDC engraftment. Thus, the severity of renal damage, the time course and the contribution of proliferation to renal repair, need to be taken into account when interpreting data on the role of tubular BMDC engraftment in renal repair after IRI.

Acknowledgements

References

1)   Hou SH, Bushinsky DA, Wish JB, Cohen JJ, Harrington JT. Hospital-acquired renal insufficiency: a prospective study. Am J Med 1983 Feb;74(2):243-8.

2)   Schrier RW, Wang W, Poole B, Mitra A. Acute renal failure: definitions, diagnosis, pathogenesis, and therapy. J Clin Invest 2004 Jul;114(1):5-14.

3)   Finn WF, Chevalier RL. Recovery from postischemic acute renal failure in the rat. Kidney Int 1979 Aug;16(2):113-23.

4)   Kale S, Karihaloo A, Clark PR, Kashgarian M, Krause DS, Cantley LG. Bone marrow stem cells contribute to repair of the ischemically injured renal tubule. J Clin Invest 2003 Jul;112(1):42-9.

5)   Lin F, Cordes K, Li L, Hood L, Couser WG, Shankland SJ, Igarashi P. Hematopoietic stem cells contribute to the regeneration of renal tubules after renal ischemia-reperfusion injury in mice. J Am Soc Nephrol 2003 May;14(5):1188-99.

6)   Morigi M, Imberti B, Zoja C, Corna D, Tomasoni S, Abbate M, Rottoli D, Angioletti S, Benigni A, Perico N, Alison M, Remuzzi G. Mesenchymal stem cells are renotropic, helping to repair the kidney and improve function in acute renal failure. J Am Soc Nephrol 2004 Jul;15(7):1794-804.

7)   Poulsom R, Forbes SJ, Hodivala-Dilke K, Ryan E, Wyles S, Navaratnarasah S, Jeffery R, Hunt T, Alison M, Cook T, Pusey C, Wright NA. Bone marrow contributes to renal parenchymal turnover and regeneration. J Pathol 2001 Sep;195(2):229-35.

8)   Shintani S, Murohara T, Ikeda H, Ueno T, Honma T, Katoh A, Sasaki K, Shimada T, Oike Y, Imaizumi T. Mobilization of endothelial progenitor cells in patients with acute myocardial infarction. Circulation 2001 Jul 12;103(23):2776-9.

9)   Bonventre JV. Dedifferentiation and proliferation of surviving epithelial cells in acute renal failure. J Am Soc Nephrol 2003 Jun;14 Suppl 1:S55-S61.

10) El Nahas AM. Plasticity of kidney cells: role in kidney remodeling and scarring. Kidney Int 2003 Nov;64(5):1553-63.

11) Thadhani R, Pascual M, Bonventre JV. Acute renal failure. N Engl J Med 1996 May 30;334(22):1448-60.

12) Kisseberth WC, Brettingen NT, Lohse JK, Sandgren EP. Ubiquitous expression of marker transgenes in mice and rats. Dev Biol 1999 Oct 1;214(1):128-38.

13) Brady HR, Brenner BM, Lieberthal W. Acute renal failure. In: Brenner BM, editor. Brenner and Rector's The Kidney. 6th ed. Philadelphia, United Sates of America: Saunders; 2000. p. 1201-62.

14) Akagi Y, Isaka Y, Akagi A, Ikawa M, Takenaka M, Moriyama T, Yamauchi A, Horio M, Ueda N, Okabe M, Imai E. Transcriptional activation of a hybrid promoter composed of cytomegalovirus enhancer and beta-actin/beta-globin gene in glomerular epithelial cells in vivo. Kidney Int 1997 Apr;51(4):1265-9.

15) Medvinsky A, Smith A. Stem cells: Fusion brings down barriers. Nature 2003 Apr 24;422(6934):823-5.

16) Vassilopoulos G, Russell DW. Cell fusion: an alternative to stem cell plasticity and its therapeutic implications. Curr Opin Genet Dev 2003 Oct;13(5):480-5.

17) Gupta S, Verfaillie C, Chmielewski D, Kim Y, Rosenberg ME. A role for extrarenal cells in the regeneration following acute renal failure. Kidney Int 2002 Oct;62(4):1285-90.

18) Umland O, Heine H, Miehe M, Marienfeld K, Staubach KH, Ulmer AJ. Induction of various immune modulatory molecules in CD34(+) hematopoietic cells. J Leukoc Biol 2004 May;75(4):671-9.

3

Chapter 4

Bone marrow-derived myofibroblasts contribute to the renal interstitial myofibroblast population and produce procollagen I after ischemia/reperfusion in rats

Martine Broekema[1], Martin C. Harmsen[1], Marja J.A. van Luyn[1], Jasper A. Koerts[1], Arjen H. Petersen[1], Theo G. van Kooten[2], Harry van Goor[3], Gerjan Navis[4], Eliane R. Popa[1]

[1] Department of Pathology & Laboratory Medicine, Medical Biology Section; [2] Department of Biomedical Engineering; [3] Department of Pathology; [4] Department of Nephrology, University Medical Center Groningen, University of Groningen, The Netherlands

Abstract

Bone marrow-derived cells (BMDC) have been proposed to exert beneficial effects after renal ischemia/reperfusion injury (IRI) by engraftment in the tubular epithelium. However, BMDC can give rise to myofibroblasts, and may contribute to fibrosis. We investigated BMDC contribution to the renal interstitial myofibroblast population in relation to fibrotic changes after IRI in rats.

We used a model of unilateral renal IRI (45 min of ischemia) in F344 rats reconstituted with R26-human Placental Alkaline Phosphatase (hPAP) transgenic bone marrow to quantify BMDC contribution to the renal interstitial myofibroblast population over time.

After IRI, transient increases in collagen III transcription and interstitial protein deposition were observed, peaking on, respectively, day 7 and day 28. Interstitial infiltrates of BMDC and myofibroblasts reached a maximum on day 7 and gradually decreased afterwards. Over time, an average of 32% of all interstitial α-SMA-positive myofibroblasts co-expressed hPAP and were, therefore, derived from the bone marrow. BMD myofibroblasts produced procollagen I protein and were thus functional. The post-ischemic kidney environment was pro-fibrotic, as demonstrated by increased transcription of TGF-β, and decreased transcription of BMP-7. TGF-β protein was predominantly present in interstitial myofibroblasts, but not in BMD myofibroblasts.

In conclusion, functional BMD myofibroblasts infiltrate in the post-ischemic renal interstitium and are involved in ECM production.

Introduction

Renal tubular ischemia/reperfusion injury (IRI) is, if not too severe, in principle completely reversible (1), indicating that innate repair mechanisms are activated upon damage. Regeneration and remodeling of the kidney results in recovery of renal function and morphology by tubular epithelial cell replacement (2;3). However, tubulointerstitial remodeling can also, due to an uncontrolled balance between synthesis and degradation of extracellular matrix proteins, result in tubulointerstitial fibrosis (4;5), which is an important risk factor for progressive renal function loss (6).

Previously, we and others have shown that after renal IRI low numbers of bone marrow-derived cells (BMDC) engraft tubuli and differentiate to tubular epithelium (7-10), possibly replacing damaged tubular epithelial cells. These data have been taken to support a therapeutic potential for bone marrow-derived (BMD) stem-/progenitor cells in renal tubular IRI. However, adverse effects have also been reported in models of lung and liver injury, where BMD stem-/progenitor cells gave rise to myofibroblasts and contributed to fibrosis (11;12).

Renal interstitial myofibroblasts are regarded as major producers of extracellular matrix (ECM) proteins in fibrosis, and thus play a central role in its pathogenesis. Their origin remains subject of discussion. Myofibroblasts may originate from injured tubular epithelial cells by epithelial-to-mesenchymal transition (EMT) (13), differentiation of resident fibroblasts (14), or migration of perivascular smooth muscle cells (15). However, in mouse models of bone marrow transplantation it was shown that the bone marrow is a source of myofibroblasts for many tissues, including the gut, lung, and kidney (10;16-18). However, functionality of renal BMD myofibroblasts after IRI was not shown.

Here, we investigated the contribution of BMDC to the renal interstitial myofibroblast population. Moreover, we studied the contribution of these cells to ECM production. To this end, we used a rat model of unilateral renal ischemia/reperfusion in F344 rats, reconstituted with R26-hPAP transgenic bone marrow.

Methods

Animals

Male, 6 week-old F344 rats (Harlan, Horst, the Netherlands) and R26-hPAP rats (founders kind gift of Dr. E. Sandgren; F344 background), transgenic for human placental alkaline phosphatase (hPAP) (19) were placed under conventional housing and diet. Drinking water was supplemented with 1 mg/ml 5-bromo-2-deoxyurdine (BrdU, Sigma, St. Louis, USA), for 3 days prior termination. All animal procedures were approved by the local committee for care and use of laboratory animals and performed according to governmental and international guidelines on animal experimentation.

Bone marrow chimeras

In non-transgenic rats BM was ablated by whole-body irradiation (9 Gy, IBL 637 Cesium-137) and reconstituted with total R26-hPAP BM (1x10^6 R26-hPAP cells/recipient, intravenously). Rats were housed in filter top cages and drinking water

was supplemented with neomycin (0.35% w/v) from 1 week before to 2 weeks after irradiation. BM chimerism was determined after termination by enzymatic hPAP staining (see below) on BM cytospots, and was typically between 80% and 90%.

Surgical procedures

Four weeks after BM transplantation, rats were sedated by general isoflurane (2% Forene, Abbot b.v., Hoofddorp, The Netherlands), N_2O (50%), O_2 (50%) anaesthesia. The left renal artery was clamped for 45 min to induce ischemia, followed by reperfusion. SHAM-operated control rats underwent the same procedure, except for clamping of the left renal artery.

One (n=6), 3 (n=6), 7 (n=6), 14 (n=6), 28 (n=5), 56 (n=5) and 112 (n=5) days after ischemia/reperfusion, rats were anaesthetized and kidneys were perfused *in situ*. Kidneys were divided into quarters and fixed in Zinc fixative (0.1M Tris buffer, pH 7.4 with 0.5g $CaCH_2COO$, 5g $(CH_2COO)2Zn*2H_2O$ and 5g $ZnCl_2$ per liter; MERCK, Darmstadt, Germany), or snap-frozen in N_2 and stored at -80°C.

Kidney function

Plasma creatinine levels were determined using the enzymatic colorimetric assay CREA plus (Roche, Woerden, the Netherlands), which is a precise and specific quantification method for creatinine (20).

(Immuno)histochemistry

Immunohistochemistry was performed on 5 μm zinc-fixed, paraffin-embedded sections. Sections were dewaxed and antigen was retrieved by overnight incubation in 0.1 M Tris/HCl buffer at 80°C (for α-SMA and collagen III staining) or incubation with 0.7M HCl at room temperature (RT) for 30 min and 0.025% (w/v) pepsin in 0.35M HCl at RT for 15 min (for BrdU staining). Endogenous AP was heat-inactivated by incubation in substrate buffer (0.1 M Tris/HCl, pH 9.5, 0.1 M NaCl, 5 mM $MgCl_2$) at 65°C for 30 min (19) (for α-SMA/hPAP staining). Endogenous peroxidase was blocked with 0.3% H_2O_2 for 30 min and endogenous biotin was blocked with biotin blocking kit (DAKO, Glostrup, Denmark). Sections were incubated for 1h with primary antibodies, i.e. rabbit anti-rat collagen III (Biogenesis, Poole, UK), rabbit anti-hPAP (Serotec, Oxford, UK), mouse α-SMA (clone 1A4, DAKO) or anti-BrdU (Sigma-Aldrich), followed by appropriate secondary antibodies for 30 min. Color development was performed with 3,3'-diaminobenzidine tetrachloride (α-SMA, collagen III), fuchsin substrate-chromogen system (hPAP) (DAKO) or with 3-amino-9-ethylcarbazole (Sigma-Aldrich) substrate dissolved in N,N-dimethylformamide (MERCK) and 0.5M acetate buffer, pH 4.9 (BrdU).

For enzymatic hPAP staining endogenous AP was heat-inactivated (see above), and sections were incubated in fresh substrate buffer containing 2% (v/v) of the substrate nitroblue tetrazolium/5-bromo-4-chloro-3-indolyl phosphate (NBT/BCIP, Roche) at RT for 5 h.

Sections were counterstained with Mayer's hemalum (MERCK) and mounted in Kaiser's glycerol gelatine (MERCK).

Immunofluorescence staining for confocal microscopy was performed on 5 μm cryostat sections. For double staining of α-SMA and hPAP, the primary antibodies were incubated for 1h followed by development of α-SMA with tyramide-TRITC (PerkinElmer Life Sciences, Boston, USA) via goat anti-mouse HRP (Southern Biotechnology, Birmingham, USA) and hPAP with FITC-labeled goat anti-rabbit conjugate (Southern Biotechnology). Triple staining of α-SMA and hPAP with goat anti-procollagen I (Santa Cruz Biotechnology, Santa Cruz, USA) or goat anti-TGF-β (Santa Cruz Biotechnology) required the use different conjugates to prevent cross reaction. After overnight incubation at 4°C with goat anti-TGF-β and 1h incubation with the other primary antibodies, α-SMA was developed with tyramide-TRITC (PerkinElmer Life Sciences) via donkey anti-mouse HRP (Southern Biotechnology), hPAP with Cy5-labeled donkey anti-rabbit conjugate (Jackson ImmunoResearch, Soham, UK), procollagen I with FITC-labeled donkey anti-goat conjugate (Jackson ImmunoResearch) and TGF-β was developed via biotinylated donkey anti-goat (Abcam, Cambridge, UK) with SA-FITC (DAKO). All possible cross reactions were tested and none were found. Sections were counterstained with 4',6-diamidino-2-phenylindole (DAPI, Sigma-Aldrich, St.Louis, USA) and mounted with citifluor (Agar scientific, Stansted, UK).

Light microscopy was performed using a Leica DMLB microscope (Leica Microsystems, Rijswijk, the Netherlands), Leica DC300F camera and Leica QWin 2.8 software. Fluorescent images were obtained using a LEICA TCS SP2 3-channel confocal laser scanning microscope, equipped with lasers providing 488 nm, 543 nm and 633 nm laser lines. Tissue sections were observed using a 20x 0.70NA oil immersion objective lens, stack sections were chosen to obtain a z-resolution and images were obtained at 1024 x 1024 pixel resolution.

Quantitative RT-PCR

Frozen kidneys were homogenized in 4M guanidinium isothyocyanate (0.7% β-mercaptoethanol). Total RNA was isolated by standard procedures using phenol and chloroform/isoamylalcohol. After DNase treatment (DNA-free Kit, Ambion) RNA integrity and absence of DNA contamination were confirmed by gel electrophoresis. Equal amounts (5 μg) of total RNA from quarters of control and experimental kidneys were reverse-transcribed with M-MuLV Reverse Transcriptase in the presence of random hexamers (First strand cDNA Synthesis Kit, Fermentas Life Sciences, Lithuania). Equal amounts of cDNA (30 ng) were used for all qRT-PCR reactions. To further confirm that RNA was free from genomic DNA, qRT-PCR was also carried out on total RNA.

For qRT-PCR we used TaqMan "assay by demand" primer/probe sets for rat β2-microglobulin, collagen III, TGFβ and BMP-7 (Applied Biosystems, Foster City, CA, USA, www.appliedbiosystems.com). PCR was performed in triplicate in 384-well microtitre plates in a final volume of 10 μl, of which 5 μl TaqMan universal PCR Master Mix (Applied Biosystems), 0.5 μl primer/probe mix, and 4.5 μl cDNA, using an ABI7900HT System (Applied Biosystems). Amplifications were performed starting with a 2 min AmpErase UNG activation step at 50°C, followed by a 10 min Amplitaq Gold Enzyme Activation step at 95°C, followed by 45 cycles of denaturation at 95°C for 15 sec and combined primer annealing/extension at 60°C for 1 min. Cycle thresholds (C_T) for the individual reactions were determined using ABI Prism SDS 2.0 data processing software (Applied Biosystems). C_T values >40 were not included in calculations. C_T values were normalized

against β2-microglobulin expression levels (21). To correct for interassay variance, C_T values were normalized against an external calibrator, consisting of RNA from healthy and ischemic rat kidneys. Differences in expression levels between experimental and control rats were expressed as fold variance of expression, calculated as $2^{-\Delta\Delta\Delta C_T}$ (21). Briefly, fold variance of 1 indicates that there are no transcriptional differences compared to healthy control rats, >1 is considered increased transcription and <1 is considered decreased transcription.

Quantification

Interstitial staining of collagen III, α-SMA and hPAP was measured by a blinded observer, using computerized morphometry (Leica QWin 2.8 software). Stained areas of 15-25 randomly selected fields in cortex and outer medulla were quantified as percentage of total measured area. The quantification was performed at a magnification of 200x for each rat and time point. Vascular and glomerular expression of collagen III and vascular expression of α-SMA was excluded from measurements.

The percentage of hPAP+/α-SMA+ cells was determined by counting by two independent investigators, of all α-SMA+, hPAP+ and double-positive cells in 30 microscope fields in cortex and outer medulla per section, for each rat at a magnification of 200x.

Statistics

Statistical tests were performed using GraphPad Prism 4.0 (GraphPad Software, San Diego California, USA). Differences between controls and experimental groups was determined with One-way ANOVA Dunnett's Multiple Comparison Test. P-values <0.05 were considered statistically significant.

Results

Post-ischemic plasma creatinine levels and renal interstitial collagen III deposition

Plasma creatinine levels were significantly increased until day 28 after IRI. Afterwards plasma creatinine gradually decreased to reach baseline values on day 56 and 112 after IRI (Figure 1).
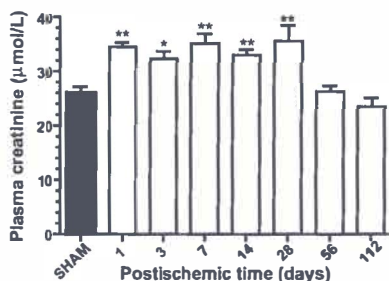

Figure 1. Post-ischemic plasma creatinine levels. Plasma creatinine levels were assessed to determine kidney function. Bars indicate mean levels and SEM of all experimental animals per group. All SHAM groups showed similar results and are therefore shown as one group. Statistically significant differences compared to SHAM are indicated as * = P<0.05, ** = P<0.005.

Presence of collagen III, which is known to be excessively produced during fibrosis, was determined at transcript levels and protein level. Collagen III mRNA transcript levels increased progressively, peaking on day 7 and gradually decreasing afterwards at later time points (Figure 2A).

Deposition of collagen III on day 1 after IRI (Figure 2B, E) was comparable to that in kidneys subjected to a SHAM procedure (Figure 2B, C) and contralateral kidneys (Figure 2B, D). Renal interstitial deposition of collagen III reached a maximum on day 28 (Figure 2B, F) and gradually decreased afterwards but remained elevated as compared to controls (day 112: Figure 2B, G).

Irradiation, required for bone marrow transplantation, did not elicit renal interstitial fibrosis, as determined by negligible collagen III deposition in contralateral kidneys (Figure 2D).

Post-ischemic infiltration of renal interstitial BMDC

Renal interstitial BMDC infiltration was readily visible by the presence of hPAP-positive cells. No alkaline phosphatase activity was observed in the post-ischemic kidney of a non-transgenic F344 rat after heat-inactivation of endogenous alkaline phosphatase (Figure 3A). In R26-hPAP BM-transplanted rats, small renal interstitial BMDC infiltrates were observed in kidneys subjected to SHAM operation (Figure 3B, G), contralateral kidneys (Figure 3C, G) and kidneys on day 1 after IRI (Figure 3D, G). The BMDC infiltrate size strongly increased after day 1, reaching a maximum on day 7 after IRI (Figure 3E, G). The large BMDC infiltrates persisted until day 28 after IRI (Figure 3G) and gradually decreased afterwards, manifesting in small interstitial infiltrates on day 112 (Figure 3F, G). The BMDC infiltrate size in ischemic kidneys remained, however, higher than in contralateral kidneys.

Presence of renal interstitial myofibroblasts

Renal interstitial myofibroblasts were detected using α-SMA staining. Interstitial α-SMA-positive myofibroblasts were sporadically detected in SHAM (Figure 4A, G), contralateral kidneys (Figure 4B, G) and in kidneys isolated on day 1 after IRI (Figure 4C, G). After day 1 we observed a strong increase in renal interstitial α-SMA-stained area, with a peak on day 7 (Figure 4D, G). After day 28 after IRI (Figure 4E, G) the renal interstitial α-SMA-stained area was gradually decreased, up to day 112 (Figure 4F, G).

Irradiation, required for bone marrow transplantation, did not elicit renal interstitial fibrosis, as determined by the absence of myofibroblasts in contralateral kidneys (Figure 4B).
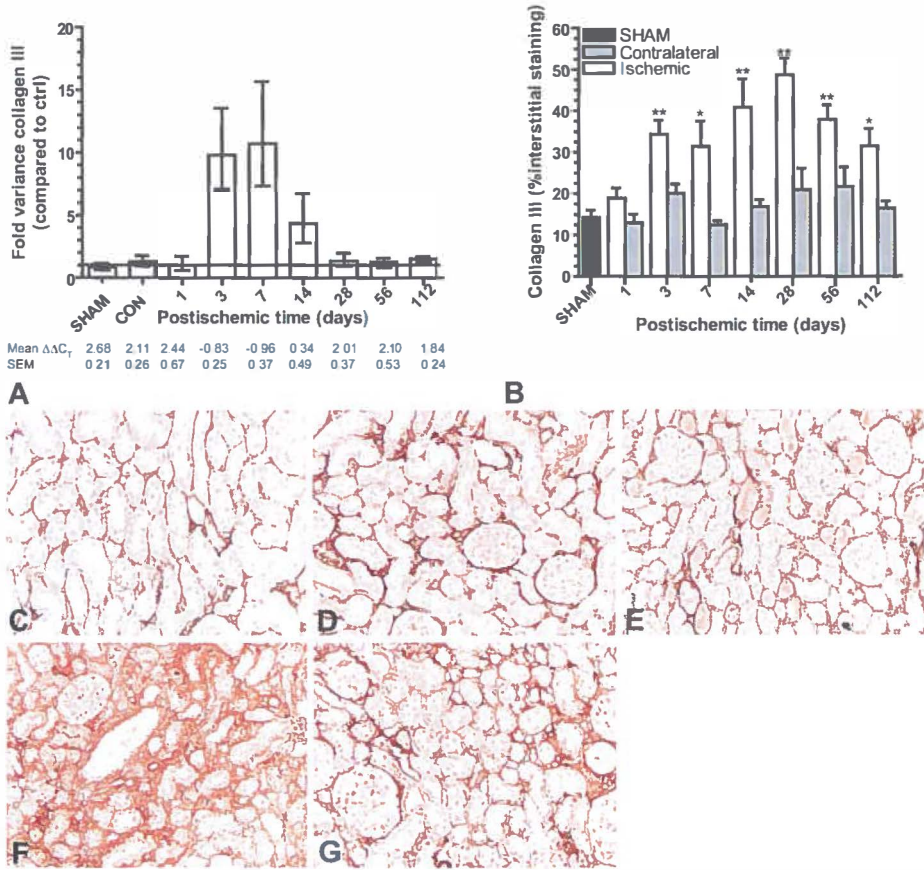
Figure 2. Post-ischemic renal interstitial collagen III deposition. Expression levels of collagen III were determined by quantitative RT-PCR on RNA isolated from kidneys at various time points after IRI induction (A). Mean $\Delta\Delta CT$ values are shown in combination with SEM of all experimental animals per group. Mean $\Delta\Delta CT$ values indicate gene expression CT values normalized against expression levels of an internal calibrator ($\beta 2$-microglobulin) and mRNA expression levels of an external calibrator. Differences in expression levels between experimental and healthy control rats were expressed as fold variance of expression, calculated as $2^{\Delta\Delta CT}$ (21). Fold variance of 1 indicates that there are no transcriptional differences compared to healthy control rats, >1 is considered increased transcription and <1 is considered decreased transcription. Bars indicate mean levels and SEM of all experimental animals per group. Con = contralateral. All SHAM and contralateral groups showed similar results and are therefore shown as one group. In healthy control kidneys the mean $\Delta\Delta CT$ was 2.46 ± 0.40. Post-ischemic collagen III protein deposition was quantified by computerized morphometry (B). Scoring was performed on SHAM (black bars), ischemic (white bars) and contralateral kidneys (grey bars). All SHAM groups showed similar results and are therefore shown as one group. Significant differences compared to SHAM animals are indicated as *= P<0.05, ** = P<0.005. Photomicrographs of collagen III staining are shown of SHAM kidney (day 1) (C), contralateral kidney of an ischemic kidney (day 1) (D) and kidneys subjected to ischemia and isolated on day 1 (E), 28 (F) and 112 (G) after IRI induction. Lens magnification 200x.
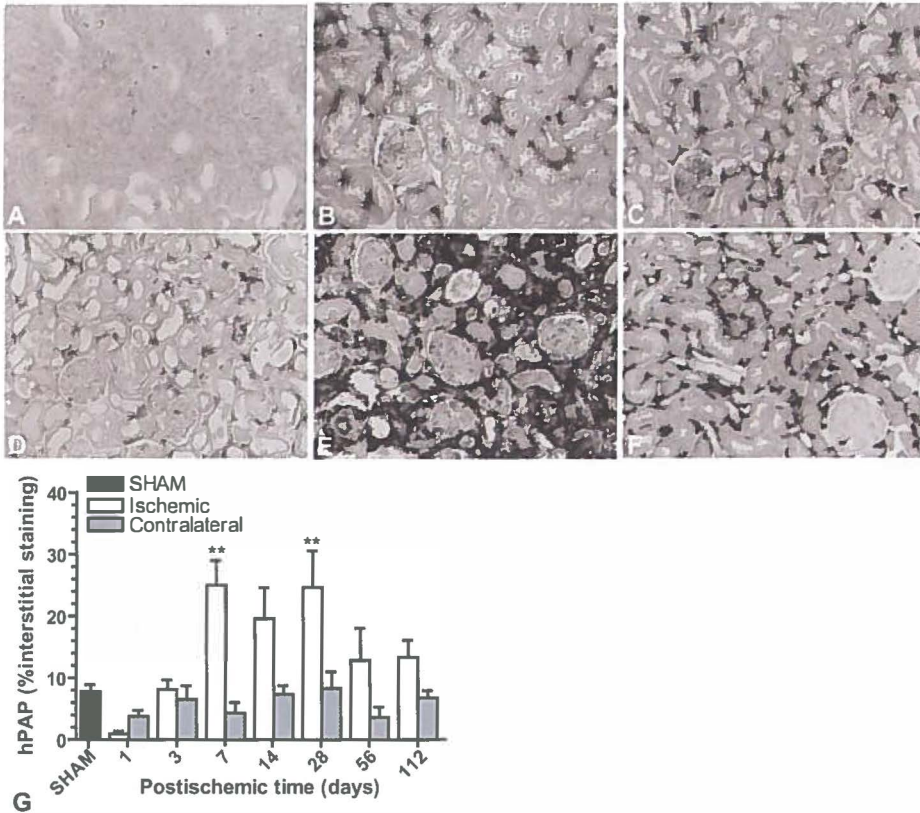
Figure 3. *Post-ischemic infiltration of renal interstitial BMDC. Representative pictures of BMDC infiltration, determined by enzymatic hPAP staining, in a post-ischemic kidney of a non-transgenic F344 rat (A), a kidney of a hPAP BM recipient subjected to SHAM operation (day 3) (B), a contralateral kidney of a hPAP BM recipient after IRI (day 7) (C) and post-ischemic kidneys of a hPAP BM recipient on day 1 (D), 7 (E), and 112 (F) after IRI. Lens magnification 200x. Post-ischemic infiltration of renal interstitial BMDC was quantified by computerized morphometry (G). Bars indicate mean levels and SEM of all experimental animals per group. All SHAM groups showed similar results and are therefore shown as one group. Significant differences compared to BMDC infiltration in SHAM kidneys is indicated as ** = P<0.005.*
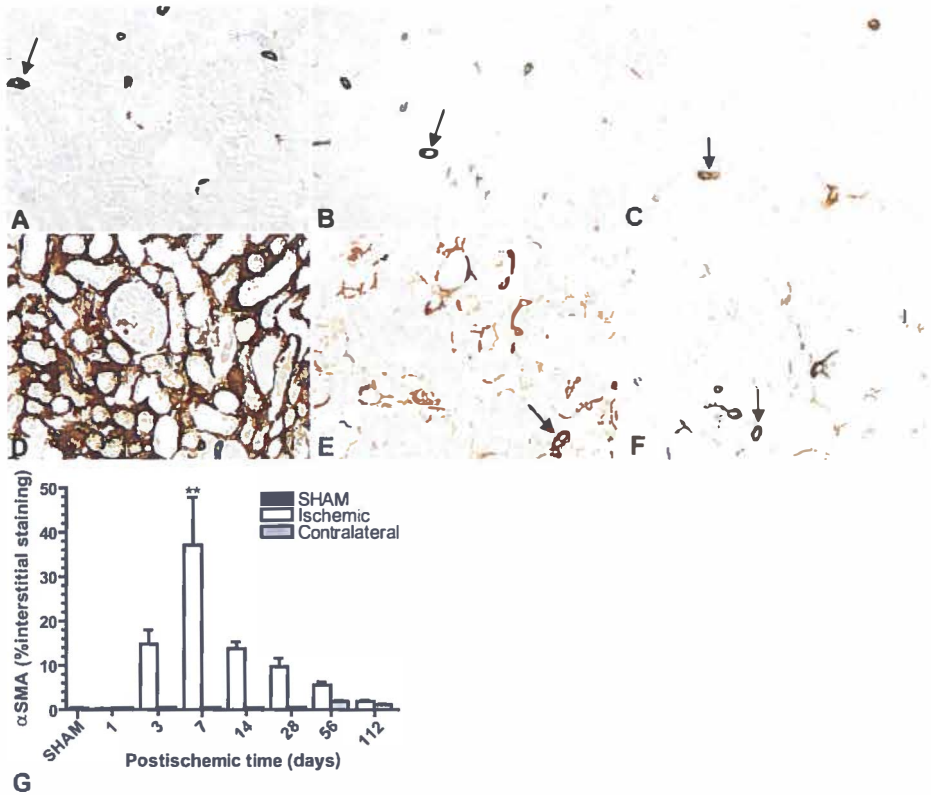
Figure 4. *Post-ischemic presence of renal interstitial myofibroblasts. Presence of renal interstitial myofibroblasts is shown by a-SMA expression in SHAM (day 28) (A), contralateral (day 28) (B) and post-ischemic kidneys on day 1 (C), 7 (D), 28 (E) and 112 (F) after IRI. Arrows indicate examples of a-SMA-positive bloodvessels. All a-SMA-positive vascular structures were excluded from quantitative analysis. Lens magnification 200x. Post-ischemic presence of renal interstitial myofibroblasts was quantified by computerized morphometry (G). Bars indicate mean levels and SEM of all experimental animals per group. All SHAM groups showed similar results and are therefore shown as one group. Significant differences compared to SHAM animals are indicated as ** = P<0.005.*

Proliferation of renal interstitial cells

Proliferation during three days prior to termination of the rats was assessed by BrdU incorporation. After IRI, most BrdU-positive nuclei were present in tubular epithelial cells (7), and were only occasionally found in interstitial cells (Figure 5, day 14 postischemia).

Figure 5. *Proliferation of renal interstitial cells. Proliferation was assessed by BrdU incorporation. BrdU-positive nuclei (black, indicated with arrows), here shown on day 14 after IRI, were mainly present in tubular epithelial cells. The insert shows the presence of BrdU-positive nuclei in interstitial cells. Lens magnification 400x.*

Bone marrow-derived myofibroblasts

After renal ischemia, cells that were double-positive for hPAP (BMDC) and α-SMA (myofibroblasts) were observed, albeit exclusively in the interstitium. From day 7 after IRI on, the number of renal interstitial hPAP-positive BMDC co-expressing α-SMA significantly increased compared to contralateral kidneys (Figure 6A). Over time, the number of renal interstitial hPAP-positive BMDC co-expressing α-SMA remained relatively stable, with an average of 4% of all interstitial hPAP-positive BMDC co-expressing α-SMA (Figure 6A).

On day 3 after IRI, the number of renal interstitial α-SMA-positive myofibroblasts co-expressing hPAP significantly exceeded that in contralateral kidneys (Figure 6B) and further increased until day 14. Over the whole observation period an average of 32% of all renal interstitial α-SMA-positive myofibroblasts co-expressed hPAP (Figure 6B).

To confirm that the observed hPAP/α-SMA double-positive cells were BMDC which differentiated to myofibroblasts and not overlying cells, we used confocal microscopy of hPAP (Figure 6C) and α-SMA (Figure 6D) immunofluorescence staining. Overlap of signal in both channels (Figure 6E) was present in 10 out of 14 consecutive z-planes.

To determine if BMD myofibroblasts expressed ECM proteins, we studied their ability to produce procollagen I. Using fluorescence staining combining α-SMA, procollagen I and hPAP, we confirmed procollagen I production by α-SMA-positive myofibroblasts (Figure 6F-I, arrowheads). In addition, all observed hPAP/α-SMA double-positive cells (BMD myofibroblasts) also stained positive for procollagen I (Figure 6F-I, arrows). Overlap of signal in all three channels was present in 5 of the 6 consecutive z-planes.
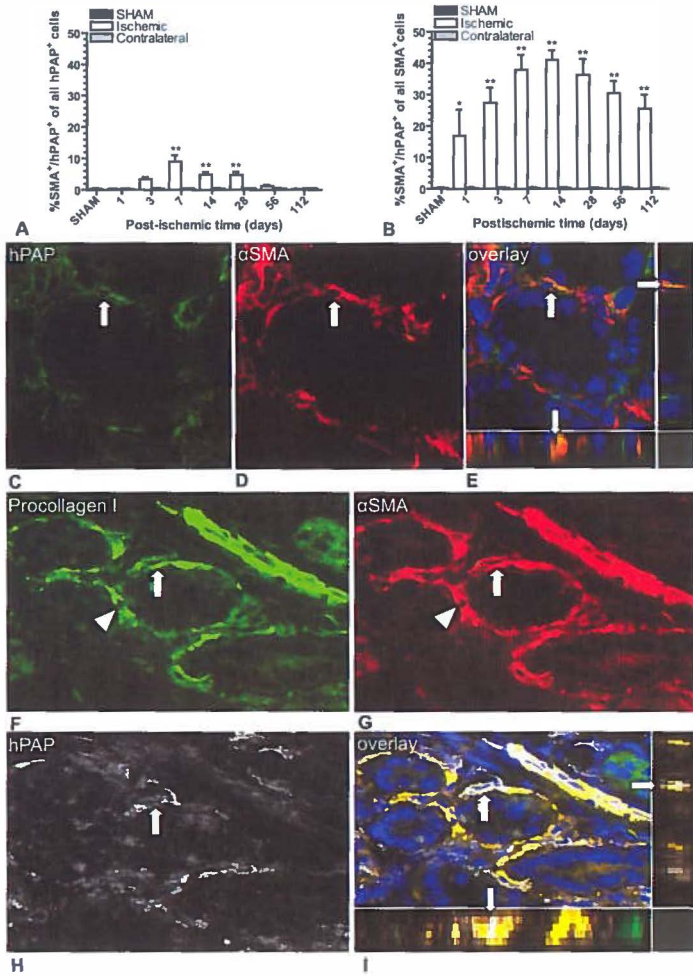
Figure 6. Bone marrow-derived myofibroblasts. Co-expression of BMDC and myofibroblast markers was assessed by immunohistochemical hPAP/a-SMA double staining on post-ischemic kidneys. Co-expression of hPAP and a-SMA was quantified in relation to the renal interstitial population of BMDC (A) and to the renal interstitial myofibroblast population (B). Bars indicate mean levels and SEM of all experimental animals per group. All SHAM groups showed similar results and are therefore shown as one group. Significant differences compared to SHAM kidneys is indicated as *= P<0.05 and ** = P<0.005. BMD myofibroblasts were detected by immunofluorescence staining for hPAP (C) (green) in combination with a-SMA (D) (red) on post-ischemic kidney tissue (shown here: day 7 postischemia). The overlay shows FITC, TRITC and DAPI channels, and the x/z and y/z planes on the right and underneath the merged picture demonstrate true colocalization of the markers (E). Arrows indicate colocalization. Production of procollagen I by BMD myofibroblasts was assessed by immunofluorescence staining for procollagen I (F) (green) in combination with a-SMA (G) (red) and hPAP (H) (white) on postischemic kidney tissue (shown here: day 7 postischemia). The overlay (I) shows FITC, TRITC, Cy5 and DAPI channels, and the x/z and y/z planes on the right and underneath the merged picture demonstrate true colocalization of the three markers. Arrowheads indicate an example of a procollagen-positive myofibroblast (a-SMA/Procollagen I double-positive). Arrow indicates an example of a procollagen I-positive bone marrow-derived myofibroblast (a-SMA/hPAP/procollagen I triple-positive).

Transcript levels of fibrosis-regulating factors TGF-β and BMP-7

Expression levels of TGF-β and BMP-7 in post-ischemic kidneys were normalized against β2-microglobulin expression levels and expression levels of an external calibrator and were expressed as $\Delta\Delta C_T$ values (Figure 7). After IRI, $\Delta\Delta C_T$ values for TGF-β and BMP-7 were at most time points significantly different from $\Delta\Delta C_T$ values of healthy control kidneys (Figure 7). Differences in expression levels between experimental and control rats were expressed as fold variance of expression, calculated as $2^{-\Delta\Delta\Delta C_T}$ (21) (Figure 7). TGF-β transcript levels doubled on day 1, peaked on day 7 (2.7 fold increase) and decreased gradually afterwards, to return to baseline levels on day 56 after IRI (Figure 7A). BMP-7 transcript levels were 10 times decreased on day 1 after IRI, as compared to control values and remained decreased at all studied time points (Figure 7B).
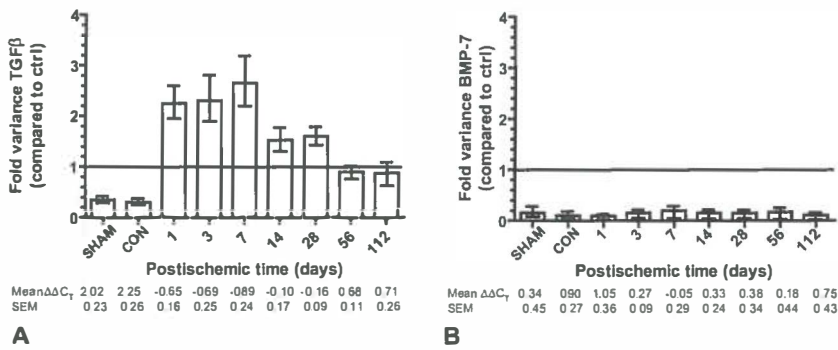

| | Mean $\Delta\Delta C_T$ | 2.02 | 2.25 | -0.65 | -069 | -0.89 | -0.10 | -0.16 | 0.68 | 0.71 |
| | SEM | 0.23 | 0.26 | 0.16 | 0.25 | 0.24 | 0.17 | 0.09 | 0.11 | 0.26 |

A

| | Mean $\Delta\Delta C_T$ | 0.34 | 0.90 | 1.05 | 0.27 | -0.05 | 0.33 | 0.38 | 0.18 | 0.75 |
| | SEM | 0.45 | 0.27 | 0.36 | 0.09 | 0.29 | 0.24 | 0.34 | 0.44 | 0.43 |

B

Figure 7. *Transcript levels of fibrosis-regulating factors TGF-β and BMP-7. Expression levels of TGF-β (A) and BMP-7 (B) were determined by quantitative RT-PCR on RNA isolated from kidneys at various time points after IRI induction. Mean $\Delta\Delta C_T$ values are shown in combination with SEM of all experimental animals per group. Mean $\Delta\Delta C_T$ values indicate gene expression C_T values normalized against expression levels of β2-microglobulin and mRNA expression levels of an external calibrator. Differences in expression levels between experimental and healthy control rats were expressed as fold variance of expression, calculated as $2^{-\Delta\Delta C_T}$ (21). Fold variance of 1 indicates that there are no transcriptional differences compared to healthy control rats, >1 is considered increased transcription and <1 is considered decreased transcription. Bars indicate mean levels and SEM of all experimental animals per group. Con = contralateral. All SHAM and contralateral groups showed similar results and are therefore shown as one group. In healthy controls mean $\Delta\Delta C_T$ of TGF-β was 0.52 ± 0.13 and of BMP-7 was -2.38 ± 0.75.*

Post-ischemic renal presence of TGF-β protein.

To address TGF-β expression at protein level and determine which cells were responsible for the increased TGF-β mRNA expression in post-ischemic kidneys, we used immunofluorescence staining for TGF-β with α-SMA and hPAP. In healthy kidneys TGF-β protein was mainly present in proximal tubular cells, but also in arterial structures and sporadically in interstitial cells (not shown). After ischemic damage renal TGF-β protein was occasionally observed in proximal tubular epithelial cells (Figure 8A-D). However, using triple staining of TGF-β, α-SMA and hPAP, we could identify myofibroblasts (TGF-β & α-SMA double positive, yellow cells) as main producers of TGF-β in post-ischemic kidneys (Figure 8 E-H). We did, however, not observe TGF-β

expression in bone marrow-derived myofibroblasts (TGF-β, α-SMA & hPAP triple positive).

Discussion

Previously, we showed the ability of BMDC to engraft renal tubuli and differentiate to tubular epithelial cells in a rat model of IRI (7). Our current study investigated the contribution of BMD myofibroblasts to the renal interstitial myofibroblast population and, for the first time, their functional capacity to produce ECM proteins after IRI. We show that the contribution of BMDC to the renal myofibroblast population amounted to over 30%. Moreover, BMD myofibroblasts produced procollagen I, suggesting an active role of these cells in the production of extracellular matrix proteins in post-ischemic remodeling. Resident renal myofibroblasts produced TGF-β, thereby possibly contributing to the environment in which BMD myofibroblasts can become functionally active in producing ECM proteins.

Renal remodeling of the ECM after injury initially proceeds as a wound healing process, but can develop into pathologic renal interstitial fibrosis (22). In renal remodeling myofibroblasts, alpha-smooth muscle actin (α-SMA) expressing cells with features of both fibroblasts and smooth muscle cells (23), play a dual role. First, in the early phase after injury, myofibroblasts participate in wound healing by producing ECM components (e.g. collagens I and III, tenascin, fibronectin) (24). Second, persisting inflammation after renal injury can lead to persistent myofibroblast activation (25), and thus to excessive ECM production. In conjunction with reduced ECM degradation, this can result in renal interstitial fibrosis, an important risk factor for progressive renal damage (6). In our IRI model, collagen III mRNA levels and protein deposition increased significantly, peaking on day 7 and 28, respectively, but gradually decreased afterwards. Together with decreasing BMDC infiltrates and improving kidney function, this is likely to reflect the process of wound healing. However, at the latest time point of the study, i.e. day 112, renal interstitial collagen III deposition and BMDC infiltrates still were higher than in control kidneys, which possibly reflect a transition phase between wound healing and fibrosis. Since our model did not result in fibrosis, we determined if BMD myofibroblasts could contribute to ECM deposition during renal remodeling, rather than to fibrosis.

While the central role of myofibroblasts in renal remodeling is established, the origin of these cells is still under investigation. Epithelial-to-mesenchymal transition (EMT) (13;26), differentiation of resident fibroblasts (14), and migration of perivascular smooth muscle cells (15) have been identified as intrarenal mechanisms of myofibroblast formation. However, findings of bone marrow-derived, α-SMA-positive cells in skin (17;27), lung (27), small intestine (16), colon (16), stomach (17), liver (11) and kidney (10;17;18) provide evidence for an additional source of myofibroblasts.

In the current study we investigated the contribution of BMDC to the renal interstitial myofibroblast population and found it to amount to over 30%. This is three times as high as in a study in unilateral ureteral obstruction (UUO) in mice (18). This difference may reflect differences between our respective models. Possibly, the method of Y-chromosome *in situ* hybridization used by Roufosse for detection of BMD myofibroblasts
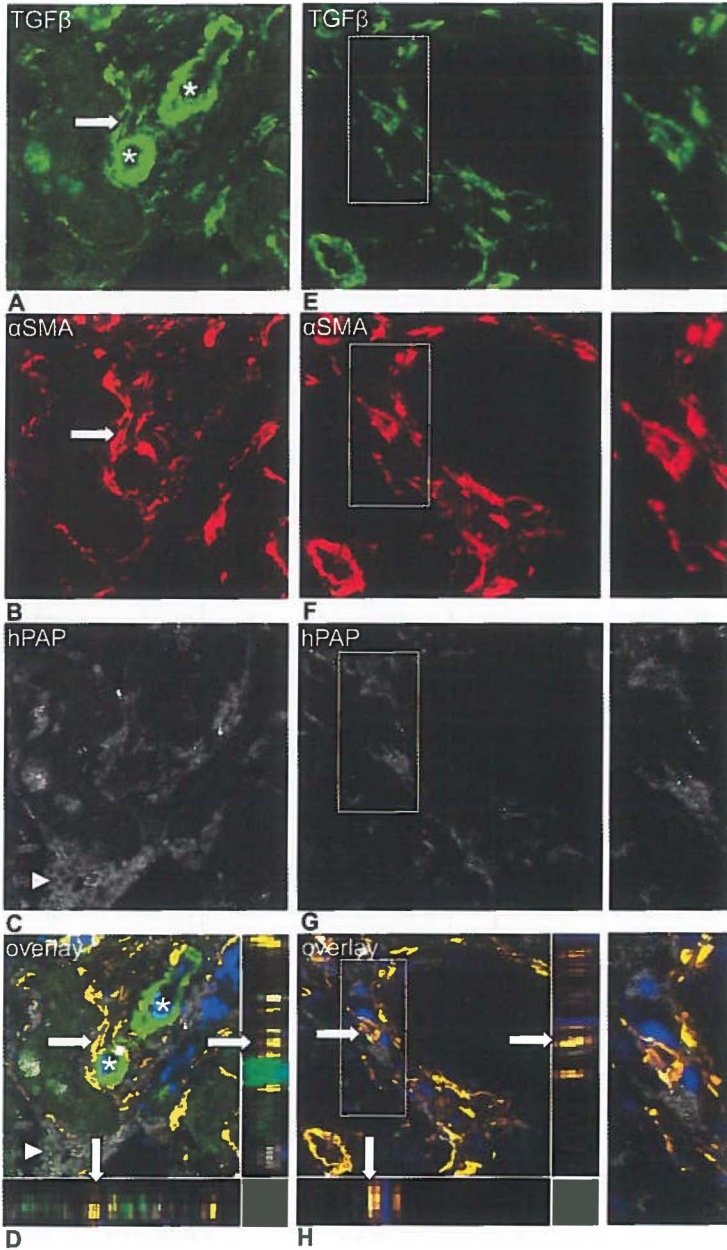
Figure 8. Post-ischemic renal presence of TGF-β protein. TGF-β protein expression in post-ischemic kidneys (A-D day 3 and E-H day 7 postischemia) was determined by immunofluorescence staining combining TGF-β (A, E) (green) with a-SMA (B, F) (red) and hPAP (C, G) (white). Overlays show FITC, TRITC, Cy5 and DAPI channels and the x/z and y/z planes on the right and underneath the merged pictures demonstrate colocalization of TGF-β and a-SMA (D, H). Magnification of the indicated parts are shown on the far right of E-H. Asterisks indicate examples of TGF-β+ tubular structures. Arrowheads indicate infiltrated BMDC (hPAP+). Arrows indicate TGF-β+ myofibroblasts (a-SMA/ TGF-β+).

can lead to an underestimation by division of the nucleus in sections, and loss of the Y chromosome for detection.

BMDC can, in line with their plasticity, differentiate into different cell types, thereby potentially exerting different roles in renal remodeling after IRI. The regulation of these differentiation choices is of pathophysiological relevance. In the present study we observed an altered balance between bone morphogenic protein-7 (BMP-7) and transforming growth factor-ß (TGF-ß), two major regulators of renal interstitial fibrosis (28). While TGF-ß is a well-established inducer of fibrosis by stimulating differentiation to and proliferation of myofibroblasts (29;30), BMP-7 directly counteracts TGF-ß-induced extracellular matrix production and promotes epithelial differentiation (31;32). Thus, the transcriptional increase of TGF-β and decrease of BMP-7 may provide the environmental clues for preferential differentiation of BMDC towards myofibroblasts and subsequent production of extracellular matrix proteins. In the post-ischemic kidney, TGF-β was observed in proximal tubular epithelial cells and arterial structures, but not in BMD myofibroblasts. Resident renal myofibroblasts appeared to be the major producers of TGF-β, suggesting that these cells may contribute to the post-ischemic renal environment in which BMDC differentiate to myofibroblasts.

A prerequisite for a role of BMD myofibroblasts in renal remodeling is the ability of these cells to produce and deposit ECM proteins. We addressed the functionality of renal interstitial BMD myofibroblasts by showing production of procollagen I after IRI. This finding is in agreement with data by Iwano (26), in UUO-induced renal fibrosis, where renal BMD fibroblasts produced collagen I and HSP47, a chaperone molecule for collagen I production. By contrast, Roufosse (18), found no collagen I synthesis in interstitial BMDC in a mouse model of UUO-induced renal fibrosis. The reason for these discrepancies is unclear but might result from differences between the models. UUO is a relatively straightforward model of obstruction-induced fibrosis, whereas our ischemia/reperfusion model leads to wound healing rather than fibrosis. Alternatively, differences in transgenic bone marrow transplantation models (BMDC expressing GFP under the promoter of the FSP-1, luciferase under the promoter of collagen I gene, or hPAP) or specific type of BMDC (BMD myofibroblasts, fibroblasts or all interstitial BMDC) may be involved.

In addition to previous studies showing tubular BMDC engraftment and epithelial differentiation after IRI (7-10), our current study supports the contribution of BMDC to the renal myofibroblast population. Remarkably, the contribution of BMDC to the myofibroblast population largely exceeds their contribution to the tubular epithelial population. This is in accordance with recent studies, showing that post-ischemic repair of tubular epithelium occurs only marginally by differentiation of BMDC but mainly by proliferation of resident epithelial cells (10;33).

The different BMDC phenotypes in the kidney after IRI, point towards different roles in the post-ischemic process, as also supported by differences in the time courses in which the different BMDC phenotypes are present. We previously showed that tubular epithelial BMDC engraftment peaked on day 14, while the peak in tubular epithelial proliferation was observed a week earlier (7). Our present study showed that already on day 3 after IRI 27% of all renal interstitial myofibroblasts was derived from the bone marrow. Taken together, these data suggest that post-ischemic replacement of damaged tubular epithelial cells was already accomplished by proliferation of resident epithelial cells after the first week. Therefore, the BMDC may, possibly influenced by

upregulation of TGF-β in the post-ischemic renal environment, preferably differentiated to myofibroblasts rather than to tubular epithelial cells.

It is not clear what the ontogeny of BMD myofibroblasts and BMD tubular epithelial cells is and if they are derived from the same source. It has been proposed that myofibroblasts differentiate from a circulating precursor cell type, i.e. the circulating fibrocyte (34). The fibrocyte is a distinct mesenchymal cell type that arises in *ex vivo* cultures of peripheral blood and has the capacity to differentiate *in vitro* into α-SMA-positive myofibroblasts (34;35). Although fibrocytes are recruited to the damage site after injury (34;35), it is improbable that they are the only source of renal interstitial BMD myofibroblasts, since the large numbers of BMD myofibroblasts in our study contrasts with the low numbers of circulating fibrocytes (0.1-0.5% of human blood cells) reported previously (34;35). Moreover, the sporadic presence of interstitial cell proliferation argues against local amplification of the myofibroblast population. An alternative source of renal BMD myofibroblasts may be monocytes, since these cells can transdifferentiate (36-38), as well as synthesize and secrete fibrosis-promoting growth factors and cytokines (39).

Data on tubular engraftment of BMDC (7-10;40), as well as promising results after infusion of BMDC (8;41;42), have provided support for the therapeutic potential of BMDC in tubular epithelial recovery after ARF. However, in line with data from others (10;17;18), our current results show that BMDC can differentiate to renal interstitial myofibroblasts as well. By producing ECM proteins, these cells can have a beneficial role in wound healing. However, in case of persistent inflammation and a disturbed balance between ECM production and degradation, these cells can play an adverse role by promoting processes ultimately leading to fibrosis. Therefore, for therapeutic application of BMDC, caution is called for.

Acknowledgements

References

1) Finn WF, Chevalier RL. Recovery from postischemic acute renal failure in the rat. Kidney Int 1979 Aug;16(2):113-23.

2) Mene P, Polci R, Festuccia F. Mechanisms of repair after kidney injury. J Nephrol 2003 Mar;16(2):186-95.

3) Nony PA, Schnellmann RG. Mechanisms of renal cell repair and regeneration after acute renal failure. J Pharmacol Exp Ther 2003 Mar;304(3):905-12.

4) Azuma H, Nadeau K, Takada M, Mackenzie HS, Tilney NL. Cellular and molecular predictors of chronic renal dysfunction after initial ischemia/reperfusion injury of a single kidney. Transplantation 1997 Jul 27;64(2):190-7.

5) Williams P, Lopez H, Britt D, Chan C, Ezrin A, Hottendorf R. Characterization of renal ischemia-reperfusion injury in rats. J Pharmacol Toxicol Methods 1997 Feb;37(1):1-7.

6) Remuzzi G, Bertani T. Pathophysiology of progressive nephropathies. N Engl J Med 1998 Nov 12;339(20):1448-56.

7) Broekema M, Harmsen MC, Koerts JA, Petersen AH, van Luyn MJ, Navis G, Popa ER. Determinants of tubular bone marrow-derived cell engraftment after renal ischemia/reperfusion in rats. Kidney Int 2005 Dec;68(6):2572-81.

8) Kale S, Karihaloo A, Clark PR, Kashgarian M, Krause DS, Cantley LG. Bone marrow stem cells contribute to repair of the ischemically injured renal tubule. J Clin Invest 2003 Jul;112(1):42-9.

9) Lin F, Cordes K, Li L, Hood L, Couser WG, Shankland SJ, Igarashi P. Hematopoietic stem cells contribute to the regeneration of renal tubules after renal ischemia-reperfusion injury in mice. J Am Soc Nephrol 2003 May;14(5):1188-99.

10) Lin F, Moran A, Igarashi P. Intrarenal cells, not bone marrow-derived cells, are the major source for regeneration in postischemic kidney. J Clin Invest 2005 Jul;115(7):1756-64.

11) Forbes SJ, Russo FP, Rey V, Burra P, Rugge M, Wright NA, Alison MR. A significant proportion of myofibroblasts are of bone marrow origin in human liver fibrosis. Gastroenterology 2004 Apr;126(4):955-63.

12) Phillips RJ, Burdick MD, Hong K, Lutz MA, Murray LA, Xue YY, Belperio JA, Keane MP, Strieter RM. Circulating fibrocytes traffic to the lungs in response to CXCL12 and mediate fibrosis. J Clin Invest 2004 Aug;114(3):438-46.

13) Ng YY, Huang TP, Yang WC, Chen ZP, Yang AH, Mu W, Nikolic-Paterson DJ, Atkins RC, Lan HY. Tubular epithelial-myofibroblast transdifferentiation in progressive tubulointerstitial fibrosis in 5/6 nephrectomized rats. Kidney Int 1998 Sep;54(3):864-76.

14) Wiggins R, Goyal M, Merritt S, Killen PD. Vascular adventitial cell expression of collagen I messenger ribonucleic acid in anti-glomerular basement membrane antibody-induced crescentic nephritis in the rabbit. A cellular source for interstitial collagen synthesis in inflammatory renal disease. Lab Invest 1993 May;68(5):557-65.

15) Desmouliere A, Gabbiani G. Myofibroblast differentiation during fibrosis. Exp Nephrol 1995 Mar;3(2):134-9.

16) Brittan M, Hunt T, Jeffery R, Poulsom R, Forbes SJ, Hodivala-Dilke K, Goldman J, Alison MR, Wright NA. Bone marrow derivation of pericryptal myofibroblasts in the mouse and human small intestine and colon. Gut 2002 Jun;50(6):752-7.

17) Direkze NC, Forbes SJ, Brittan M, Hunt T, Jeffery R, Preston SL, Poulsom R, Hodivala-Dilke K, Alison MR, Wright NA. Multiple organ engraftment by bone-marrow-derived myofibroblasts and fibroblasts in bone-marrow-transplanted mice. Stem Cells 2003;21(5):514-20.

18) Roufosse C, Bou-Gharios G, Prodromidi E, Alexakis C, Jeffery R, Khan S, Otto WR, Alter J, Poulsom R, Cook HT. Bone Marrow-Derived Cells Do Not Contribute Significantly to Collagen I Synthesis in a Murine Model of Renal Fibrosis. J Am Soc Nephrol 2006 Feb 8.

19) Kisseberth WC, Brettingen NT, Lohse JK, Sandgren EP. Ubiquitous expression of marker transgenes in mice and rats. Dev Biol 1999 Oct 1;214(1):128-38.

20) Mazzachi BC, Peake MJ, Ehrhardt V. Reference range and method comparison studies for enzymatic and Jaffe creatinine assays in plasma and serum and early morning urine. Clin Lab 2000;46(1-2):53-5.

21) Livak KJ, Schmittgen TD. Analysis of relative gene expression data using real-time quantitative PCR and the 2(-Delta Delta C(T)) Method. Methods 2001 Dec;25(4):402-8.

22) Razzaque MS, Taguchi T. Cellular and molecular events leading to renal tubulointerstitial fibrosis. Med Electron Microsc 2002 Jun;35(2):68-80.

23) Gabbiani G, Ryan GB, Majne G. Presence of modified fibroblasts in granulation tissue and their possible role in wound contraction. Experientia 1971 May 15;27(5):549-50.

24) Gabbiani G. The biology of the myofibroblast. Kidney Int 1992 Mar;41(3):530-2.

25) Boukhalfa G, Desmouliere A, Rondeau E, Gabbiani G, Sraer JD. Relationship between alpha-smooth muscle actin expression and fibrotic changes in human kidney. Exp Nephrol 1996 Jul;4(4):241-7.

26) Iwano M, Plieth D, Danoff TM, Xue C, Okada H, Neilson EG. Evidence that fibroblasts derive from epithelium during tissue fibrosis. J Clin Invest 2002 Aug;110(3):341-50.

27) Ishii G, Sangai T, Sugiyama K, Ito T, Hasebe T, Endoh Y, Magae J, Ochiai A. In vivo characterization of bone marrow-derived fibroblasts recruited into fibrotic lesions. Stem Cells 2005 May;23(5):699-706.

28) Kingsley DM. The TGF-beta superfamily: new members, new receptors, and new genetic tests of function in different organisms. Genes Dev 1994 Jan;8(2):133-46.

29) Desmouliere A, Geinoz A, Gabbiani F, Gabbiani G. Transforming growth factor-beta 1 induces alpha-smooth muscle actin expression in granulation tissue myofibroblasts and in quiescent and growing cultured fibroblasts. J Cell Biol 1993 Jul;122(1):103-11.

30) Creely JJ, DiMari SJ, Howe AM, Haralson MA. Effects of transforming growth factor-beta on collagen synthesis by normal rat kidney epithelial cells. Am J Pathol 1992 Jan;140(1):45-55.

31) Zeisberg M, Hanai J, Sugimoto H, Mammoto T, Charytan D, Strutz F, Kalluri R. BMP-7 counteracts TGF-beta1-induced epithelial-to-mesenchymal transition and reverses chronic renal injury. Nat Med 2003 Jul;9(7):964-8.

32) Zeisberg M, Bottiglio C, Kumar N, Maeshima Y, Strutz F, Muller GA, Kalluri R. Bone morphogenic protein-7 inhibits progression of chronic renal fibrosis associated with two genetic mouse models. Am J Physiol Renal Physiol 2003 Dec;285(6):F1060-F1067.

33) Duffield JS, Park KM, Hsiao LL, Kelley VR, Scadden DT, Ichimura T, Bonventre JV. Restoration of tubular epithelial cells during repair of the postischemic kidney occurs independently of bone marrow-derived stem cells. J Clin Invest 2005 Jul;115(7):1743-55.

34) Abe R, Donnelly SC, Peng T, Bucala R, Metz CN. Peripheral blood fibrocytes: differentiation pathway and migration to wound sites. J Immunol 2001 Jun 15;166(12):7556-62.

35) Bucala R, Spiegel LA, Chesney J, Hogan M, Cerami A. Circulating fibrocytes define a new leukocyte subpopulation that mediates tissue repair. Mol Med 1994 Nov;1(1):71-81.

36) Fujiyama S, Amano K, Uehira K, Yoshida M, Nishiwaki Y, Nozawa Y, Jin D, Takai S, Miyazaki M, Egashira K, Imada T, Iwasaka T, Matsubara H. Bone marrow monocyte lineage cells adhere on injured endothelium in a monocyte chemoattractant protein-1-dependent manner and accelerate reendothelialization as endothelial progenitor cells. Circ Res 2003 Nov 14;93(10):980-9.

37) Rehman J, Li J, Orschell CM, March KL. Peripheral blood "endothelial progenitor cells" are derived from monocyte/macrophages and secrete angiogenic growth factors. Circulation 2003 Mar 4;107(8):1164-9.

38) Urbich C, Heeschen C, Aicher A, Dernbach E, Zeiher AM, Dimmeler S. Relevance of monocytic features for neovascularization capacity of circulating endothelial progenitor cells. Circulation 2003 Nov 18;108(20):2511-6.

39) Nathan CF. Secretory products of macrophages. J Clin Invest 1987 Feb;79(2):319-26.

40) Poulsom R, Forbes SJ, Hodivala-Dilke K, Ryan E, Wyles S, Navaratnarasah S, Jeffery R, Hunt T, Alison M, Cook T, Pusey C, Wright NA. Bone marrow contributes to renal parenchymal turnover and regeneration. J Pathol 2001 Sep;195(2):229-35.

41) Morigi M, Imberti B, Zoja C, Corna D, Tomasoni S, Abbate M, Rottoli D, Angioletti S, Benigni A, Perico N, Alison M, Remuzzi G. Mesenchymal stem cells are renotropic, helping to repair the kidney and improve function in acute renal failure. J Am Soc Nephrol 2004 Jul;15(7):1794-804.

42) Togel F, Hu Z, Weiss K, Isaac J, Lange C, Westenfelder C. Administered mesenchymal stem cells protect against ischemic acute renal failure through differentiation-independent mechanisms. Am J Physiol Renal Physiol 2005 Feb 15.

4

Chapter 5

Ciclosporin does not influence bone marrow-derived cell differentiation to myofibroblasts early after renal ischemia/ reperfusion

Martine Broekema[1], Martin C. Harmsen[1], Jasper A. Koerts[1], Theo G. van Kooten[2], Donald R. A. Uges[3], Arjen H. Petersen[1], Marja J. A. van Luyn[1], Gerjan Navis[4] and Eliane R. Popa[1]

[1]Department of Pathology and Laboratory Medicine, Medical Biology section, [2]Department of Biomedical Engineering, [3]Department of Pharmacy, [4]Department of Nephrology, University Medical Center Groningen, University of Groningen, The Netherlands

Abstract

Ischemia/reperfusion injury (IRI) is a risk factor for the development of interstitial fibrosis after renal transplantation. Previously we showed that after renal IRI, bone marrow-derived cells (BMDC) can differentiate to interstitial myofibroblasts. Here we hypothesized that the immunosuppressant ciclosporin (CsA), known for its pro-fibrotic side-effect, promotes myofibroblast differentiation of BMDC in the post-ischemic kidney.

Using a model of unilateral renal IRI in rats reconstituted with R26-hPAP transgenic bone marrow, CsA was administered in a previously defined critical window for differentiation of BMDC to myofibroblasts. We evaluated fibrotic changes in the kidney and myofibroblast differentiation of BMDC on day 14 after CsA treatment.

CsA treatment for 14 days led to increased TGF-β transcript levels and collagen III deposition in the post-ischemic kidney. However, neither the total number of α-SMA[+] interstitial myofibroblasts, nor the bone marrow-derived fraction thereof was affected by CsA administration, irrespective of dosage and duration of treatment.

In the critical post-ischemic window of BMDC differentiation to myofibroblasts, CsA did not promote BMDC differentiation to myofibroblasts, suggesting that, in the clinical setting, CsA is not involved in myofibroblastic differentiation of BMDC.

Introduction

Ischemia/reperfusion injury (IRI) has been identified as a risk factor for the development of renal interstitial fibrosis, eventually leading to progressive loss of graft function after renal transplantation (1). Moreover, the detrimental effects of IRI can be amplified by fibrotic side-effects of immunosuppressive agents, such as ciclosporin (CsA) (2-4).

Myofibroblasts are recognized as the major producers of extracellular matrix (ECM) components and are, therefore, important in the development of fibrosis (5). Persisting inflammation and increased excretion of pro-fibrotic growth factors (e.g. TGF-β) can result in increased proliferation of myofibroblasts and increased ECM production. When the balance between production and degradation of ECM proteins is disturbed, ECM proteins accumulate in the renal interstitium, resulting in interstitial fibrosis (6,7). We recently reported that, in a rat model of IRI, bone marrow-derived cells (BMDC) differentiated to myofibroblasts, forming a significant proportion (up to 40%) of the total renal interstitial myofibroblast population (8). Moreover, bone marrow-derived myofibroblasts produced ECM components and could, thereby, potentially contribute to fibrosis (8). In the current study we are the first to investigate whether CsA stimulates differentiation of BMDC to myofibroblasts in the kidney, due to its pro-fibrotic potential. We used a previously established model of unilateral renal IRI in rats reconstituted with R26-human Placental Alkaline Phosphatase (hPAP) transgenic bone marrow (BM). In this model we defined an early window of opportunity for BMDC differentiation to myofibroblasts in the first 7-14 days after IRI (8). In this study we administered CsA during this window to determine the effect of CsA on BMDC myofibroblast differentiation. Moreover, to extend our IRI-associated findings to the transplantation setting, in which CsA is commonly used, we also performed a pilot experiment in which we studied the effect of CsA on myofibroblastic BMDC differentiation in syngeneic kidney transplantation, circumventing the confounding influence of immune rejection.

Materials and Methods

Animal experimentation

Male, 6 week-old F344 rats (Harlan, Horst, the Netherlands) and R26-hPAP rats (F344 background), transgenic for hPAP (9) were kept under conventional housing and diet. Non-transgenic F344 rats underwent total body irradiation (9 Gy, IBL 637 Cesium-137) for BM ablation and were reconstituted with total hPAP BM (1×10^6 hPAP cells/recipient, intravenously). After irradiation, rats were housed in filter top cages and drinking water was supplemented with neomycin (0.35% w/v) until 2 weeks after irradiation. BM chimerism, determined by flow cytometric assessment of hPAP expressing BM cells at experimental end points, was typically 76±3%.

Four weeks after BM transplantation, rats were subjected to unilateral renal IRI. Rats were sedated by general isoflurane (2% Forene, Abbot, Hoofddorp, The Netherlands), N_2O (50%), O_2 (50%) anesthesia and the left renal artery was clamped for 45 min. SHAM-operated control rats underwent the same procedure, except for clamping the artery. Immediately after renal IRI, rats (n=5 per group) were administered CsA (Sandimmun, Novartis, Basel, Switzerland) in different dosages, i.e. 0 (saline), 2.5 or 5 mg/kg CsA (all as daily subcutaneous injections for 3 days after IRI) diluted in saline (Figure 1).

These CsA dosages are sufficient to prevent allograft rejection in experimental kidney transplantation (10). In additional experiments, treatment was extended to 10 and 14 days (Figure 1), respectively. Plasma CsA levels were measured after the last administration and varied between 172 and 2010 µg/L, depending on the dose and duration of the treatment. Post-ischemic rats injected with saline served as controls. SHAM-operated rats received similar CsA treatment as rats subjected to IRI. Moreover, healthy rats (no irradiation, no BM transplantation, no IRI) were subjected to similar CsA treatment to determine baseline effects of CsA. For histological analyses, contralateral kidneys of IRI-treated rats served as additional controls.
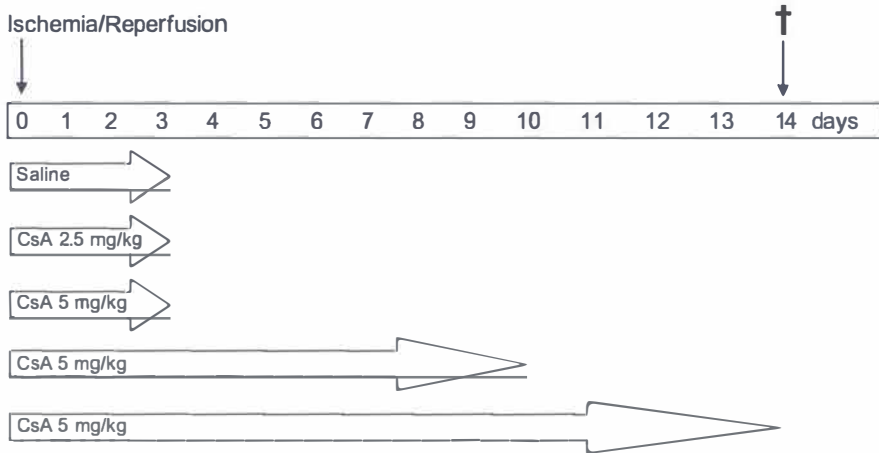

Figure 1. *Study design. Schematic representation of the CsA treatment regime. CsA was administered in different dosages, i.e. 0 (saline), 2,5 or 5 mg/kg, for 3 consecutive days starting after IRI induction. This treatment was applied to rats subjected to renal IRI (n=5 per group), SHAM-operated control rats (n=3 per group) and healthy control rats (n=3 per group). Treatment with 5 mg/kg CsA was also applied during 10 or 14 consecutive days after IRI (n=5 per group).*

Additionally, we performed a pilot experiment with rats receiving syngeneic kidney transplantations. R26-hPAP transgenic rats served as recipients and non-transgenic F344 rats as donors, to allow tracing of recipient-derived cells in the transplanted kidney. After anesthesia, the left kidneys were excised from donors, flushed with cold saline and transplanted orthotopically in hPAP recipient rats by end-to-end anastomosis of the vessels and ureters using 10-0 prolene sutures (Johnson & Johnson Intl., Brussels, Belgium). Cold ischemia by storage in saline on ice was approximately 30 min. Warm ischemia time was 25 min. In recipients, the right kidney was nephrectomized between day 7 and 10 after transplantation. The transplanted rats were divided into two groups. The first group (n=5) did not receive CsA treatment after transplantation. The second group (n=2) received 5 mg/kg CsA for the first 10 days after transplantation.
All rats were terminated on day 14 after IRI. Twenty-four hour urine was collected prior to termination. Blood samples were taken and kidneys were perfused *in situ*. Animal procedures were approved by the local committee for care and use of laboratory

animals and performed according to governmental and international guidelines on animal experimentation.

Kidney function

Creatinine levels were determined in plasma and urine using the enzymatic colorimetric assay CREA plus (Roche, Woerden, the Netherlands) (11). Creatinine clearance (mL/min) was calculated by multiplying the creatinine level of a 24 h urine sample (µmol/L) by the volume of this 24 h urine sample (mL/min) and dividing the resulting value by the plasma creatinine level (µmol/L).

Quantitative RT-PCR

For qRT-PCR we used TaqMan "assay by demand" primer/probe sets for rat β2-microglobulin and TGF-β (Applied Biosystems, Foster City, CA, USA, www.appliedbiosystems.com). RNA isolation from frozen kidneys, cDNA synthesis and qRT-PCR were performed as previously described (8).

Cycle thresholds (C_T) for the individual reactions were determined using ABI Prism SDS 2.2 data processing software (Applied Biosystems). C_T values >40 were not included in calculations. C_T values were normalized against β2-microglobulin expression levels (12). To correct for interassay variance, C_T values were normalized against an external calibrator, consisting of RNA from healthy and ischemic rat kidneys. Differences in expression levels between experimental and saline-treated healthy control rats were expressed as fold variance of expression, calculated as $2^{-\Delta\Delta\Delta CT}$ (12). Briefly, fold variance of 1 indicates that there are no transcriptional differences compared to healthy control rats, >1 is considered increased transcription and <1 is considered decreased transcription.

Detection of circulating progenitor cells

Since no monoclonal antibodies (moAbs) specific for rat progenitor cell markers are available, we assessed circulating lineage-negative (Lin⁻) cells as a population enriched for potential BMD progenitor cells. Briefly, MNC fractions were isolated from peripheral blood by Histopaque-1083 (Sigma-Aldrich, Zwijndrecht, the Netherlands) density gradient centrifugation. MNCs were stained with a cocktail of PE- or FITC-labeled moAbs against the lineage markers rat κ/λ (B cells, Sigma-Aldrich), CD3 (T cells), CD11b/c (myeloid and dendritic cells), CD161a (NK cells) and rat erythroid cells (erythrocytes, all from BD). The non-labeled population (Lin⁻ cells) was gated and quantified using MoFlo cytometer (Cytomation Inc., Fort Collins, CO), and WinList 5.0 software.

Tissue collection, fixation and histological analyses

Immediately after termination, kidneys were divided into quarters and fixed in Zinc fixative (0.1M Tris buffer, pH 7.4 with 0.5g $CaCH_2COO$, 5g $(CH_2COO)2Zn*2H_2O$ and 5g $ZnCl_2$ per liter; MERCK, Darmstadt, Germany) or snap-frozen in N_2 and stored at -80°C. Histological analyses were performed on 5 µm zinc-fixed, paraffin-embedded sections, which were dewaxed before staining. Periodic acid-Schiff (PAS) staining, used to evaluate renal morphology, was performed routinely at the department of Pathology. hPAP was detected by enzymatic or immunohistochemical staining procedures. In cases where infiltration of BMDC needed to be quantified by computer morphometry, we used the

enzymatic staining, which gives a strong signal and no background, which is essential for correct computerized quantification of the stained area. The immunohistological method was used for more detailed examination of individual hPAP+ cells or in cases when double-staining was necessary to determine the phenotype of engrafted BMDC. Enzymatic hPAP detection and inactivation of endogenous alkaline phosphatase (AP) was performed as previously described (8). Immunostaining of hPAP was performed by incubation with rabbit anti-hPAP polyclonal antibody (Serotec, Oxford, UK), followed by incubation with biotinylated goat anti-rabbit conjugate (DAKO, Glostrup, Denmark) and streptavidine-alkaline phosphatase (Southern Biotechnology, Birmingham, USA). Myofibroblasts were detected by α-SMA staining. Briefly, sections were incubated with mouse α-SMA (clone 1A4, DAKO), and subsequent labeled with peroxidase-conjugated rabbit anti-mouse antibody, followed by peroxidase-conjugated swine anti-rabbit antibody (both DAKO) as previously described (8). Collagen III was detected with rabbit anti-rat collagen III (Biogenesis, Poole, UK) and subsequent labeling with peroxidase-conjugated goat anti-rabbit antibody, followed by peroxidase-conjugated rabbit anti-goat (both DAKO) antibody (8). For α-SMA/hPAP double staining, sections were subsequently stained with α-SMA and hPAP (see above), as previously described (8). Color development was performed with fuchsin substrate-chromogen system (hPAP) (DAKO), 3,3'-diaminobenzidine tetrachloride (α-SMA, collagen III). Sections were counterstained with Mayer's hemalum (MERCK) and mounted in Kaiser's glycerol gelatine (MERCK).

All immunofluorescent stainings were performed on 5 µm cryostat sections which were fixed in acetone. Double staining of α-SMA and hPAP was performed by incubation in primary antibodies, development of α-SMA with tyramide-TRITC (PerkinElmer Life Sciences, Boston, USA) via goat anti-mouse HRP (Southern Biotechnology) and development of hPAP with FITC-labeled goat anti-rabbit conjugate (Southern Biotechnology), as previously described (8). Tyramide signal amplification is used to amplify the fluorescent signal. The epithelial phenotype of tubular engrafted BMDC was assessed by double-staining for hPAP in combination with the epithelial marker E-cadherin (clone 36) (Becton Dickinson Biosciences). Briefly, sections were incubated with anti-hPAP and anti-E-cadherin. hPAP was developed with goat anti-rabbit-FITC conjugate (Southern Biotechnology) and E-cadherin with biotinylated goat anti-mouse (IgG2a) (DAKO) and streptavidin-Cy3 conjugate (Zymed Laboratories Inc.). To confirm that hPAP+ cells, engrafted in renal tubuli, were not engrafted leukocytes, we performed double-staining combining hPAP with CD45 (leukocyte marker). hPAP was detected as described above and leukocytes were detected by incubation with mouse anti-rat CD45 monoclonal antibody (OX-1, culture supernatant), followed by biotinylated goat anti-mouse IgG (Southern Biotechnology) and streptavidin-Cy3 conjugate (Zymed Laboratories Inc.).

All antibody incubations were performed for 1 hour at room temperature. For negative controls, sections were processed in the absence of primary antibody. Light and fluorescence microscopy was performed using a Leica DMLB microscope (Leica Microsystems, Rijswijk, the Netherlands), Leica DC300F camera and Leica QWin 2.8 software. Co-localization of hPAP and α-SMA signals within cells was demonstrated with confocal microscopy, using a LEICA TCS SP2 3-channel confocal laser scanning microscope. In each section, 14 consecutive optical sections were scanned at the excitation wavelengths of 488 nm (FITC) and 543 nm (TRITC), thus generating a

sequential Z-series of 14 optical sections. Computerized stacking of these 14 optical sections allowed us to obtain a three-dimensional image of cells of interest. A cell was considered double-positive when the signals for FITC (hPAP) and TRITC (α-SMA) were present concomitantly throughout at least 7/14 consecutive optical sections of the Z-series. This method allowed us to reliably detect double-positive cells and to exclude the possibility that the two markers were expressed by different, neighboring cells.

Quantification

The severity of morphological renal damage (severity of damage) was assessed using an arbitrary score based on PAS-stained kidney sections (13). Briefly, the extent of 4 typical IRI-associated damage markers, i.e. dilatation, denudation, intraluminal casts and cell flattening, was scored arbitrarily and expressed in arbitrary units (a.u.) in a range of 0-3 per damage marker.

Interstitial staining of hPAP, α-SMA and collagen III was measured using computerized morphometry (Leica QWin 2.8 software). Stained areas of 15 randomly selected fields in cortex and outer medulla were quantified at a magnification of 200x and expressed as percentage of total measured area. Vascular and glomerular expression of collagen III and vascular expression of α-SMA was excluded from measurements.

The percentage of hPAP$^+$/α-SMA$^+$ cells was determined by counting all α-SMA$^+$, hPAP$^+$ and double-positive cells in 30 microscope fields in cortex and outer medulla per section, for each rat at a magnification of 400x. Because of the low number of α-SMA$^+$ cells in kidneys of SHAM-operated rats we did not include this group in the quantification.

Tubular epithelial BMDC engraftment was determined by counting the number of hPAP$^+$ cells engrafted in tubular cross-sections and all tubular epithelial cells in a microscope field. Tubular engrafted hPAP$^+$ cells displaying similar shape and morphology as adjacent cells were counted in 10 random microscope fields (400x) in cortex and medulla of each rat.

Statistics

Statistical tests were performed using GraphPad Prism 4.0 (GraphPad Software, San Diego California, USA). Differences between controls and experimental groups were determined with One-way ANOVA Dunnett's Multiple Comparison Test. P-values <0.05 were considered statistically significant.

Results

Severity of renal damage

The impact of CsA treatment (Figure 1) on renal morphology was determined by PAS-stained kidney sections. Healthy control rats (Figure 2A) and SHAM rats, subcutaneously injected with saline for 3 consecutive days showed normal renal morphology, irrespective of CsA dosage. Compared to these control kidneys, kidneys subjected to 45 min of unilateral renal IRI and treatment with saline for 3 consecutive days following IRI (Figure 2B) showed severe damage, characterized by tubular dilatation, intraluminal protein casts, tubular membrane denudation and tubular cell flattening. After treatment with 2.5 (not shown) or 5 mg/kg CsA for 3 consecutive days (Figure
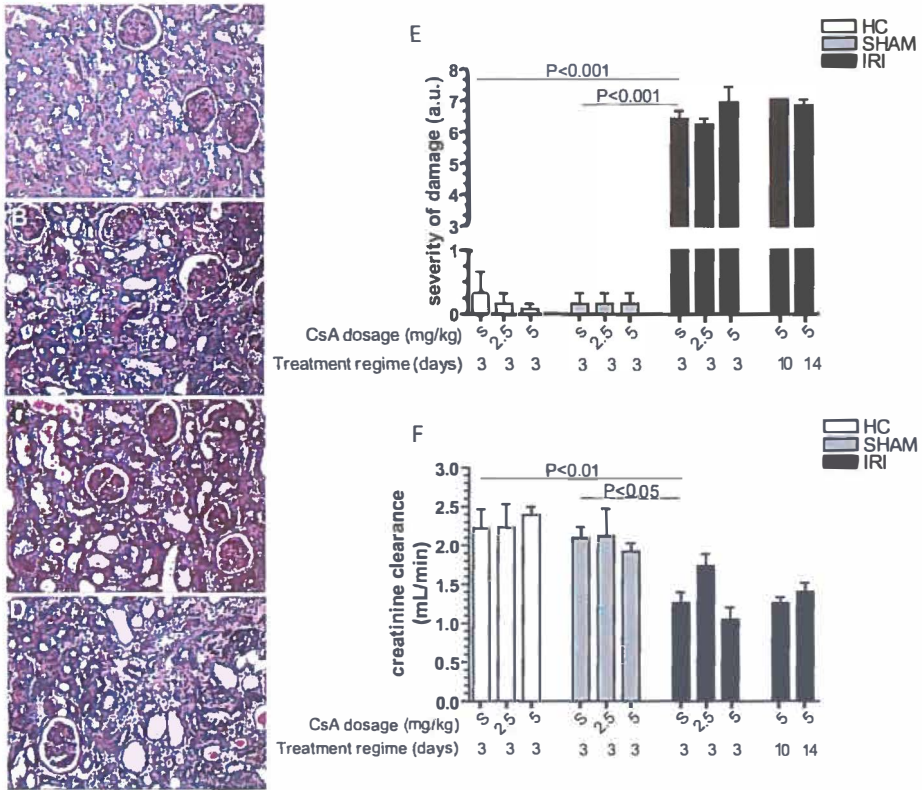
Figure 2. Severity of renal damage. Representative renal morphology is shown by PAS-stained sections of kidneys from a saline-treated rat (A), post-ischemic kidney after saline treatment (B), post-ischemic kidney after treatment with 5 mg/kg for 3 consecutive days (C) and post-ischemic kidney after treatment with 5 mg/kg for 14 consecutive days (D). Lens magnification 200x. Severity of damage was quantified by an arbitrary score of the presence of 4 typical IRI-associated damage markers, i.e. dilatation, denudation, intraluminal casts and cell flattening, expressed in arbitrary units (a.u.) in a range of 0-3 (E). Bars indicate the mean severity of damage per group and SEM. Creatinine clearance was assessed to determine kidney function (F). Bars indicate the mean creatinine clearance per group and SEM. s = saline, HC = Healthy Control, IRI = Ischemia/Reperfusion Injury.

2C) or with 5 mg/kg CsA for 10 (not shown) or 14 consecutive days after IRI (Figure 2D), kidney morphology was comparable to ischemic kidneys from saline-treated rats, without signs of additional damage.

Quantification of morphological damage confirmed absence of damage in healthy and SHAM-operated kidneys, irrespective of CsA treatment, and comparably severe damage in kidneys of saline-treated rats after IRI (Figure 2E). When administered for three consecutive days, CsA did not influence renal damage in healthy rats, rats subjected to SHAM, or IRI operation, irrespective of dose. Because we did not observe changes in renal damage after administration of CsA for 3 days, we extended the treatment duration to 10 and 14 days, which did, however, not influence the severity of damage (Figure 2E).

Creatinine clearance in healthy and SHAM-operated rats was not influenced by administration of CsA for 3 consecutive days, irrespective of dose (Figure 2F). Compared

to healthy controls and SHAM-operated rats, creatinine clearance was significantly lower in saline-treated rats subjected to IRI. However, treatment with CsA in increasing dosages for 3 consecutive days after IRI or treatment with 5 mg/kg CsA for 10 or 14 consecutive days after IRI had no additional effect on creatinine clearance (Figure 2F).

Presence of fibrosis markers

Fibrotic changes in the kidney after CsA treatment were determined by assessing renal TGF-β expression levels, the presence of interstitial myofibroblasts and interstitial collagen III deposition. Differences in TGF-β expression levels between experimental rats and saline-treated healthy control rats were expressed as fold variance of expression, calculated as $2^{-\Delta\Delta\Delta CT}$ (12) (Figure 3A). Compared to healthy control and SHAM-operated rats, TGF-β transcript levels were doubled in rats subjected to IRI and saline treatment (Figure 3A). TGF-β transcript levels were further increased after treatment with 5 mg/kg CsA for 3 or 14 consecutive days after IRI, however no statistical significant difference was found compared to rats treated with saline after IRI (Figure 3A).

Interstitial myofibroblasts were detected using α-SMA immunostaining (Figure 3B-G) and morphometric quantification (Figure 3H). In healthy control kidneys (Figure 3B, H) and SHAM kidneys (Figure 3C, H) after saline treatment and in contralateral kidneys of rats with unilateral IRI (Figure 3D, H) interstitial α-SMA+ cells were observed sporadically, irrespective of CsA dosage (Figure 3H). Compared to control kidneys, a strong increase in α-SMA+ interstitial myofibroblasts was present in saline-treated, post-ischemic kidneys (Figure 3E, H). However, neither treatment with increasing dosages of CsA for 3 consecutive days after IRI (Figure 3F, H) nor treatment for 10 or 14 consecutive days after IRI with 5 mg/kg CsA (Figure 3G, H) influenced numbers of α-SMA+ interstitial myofibroblasts.

Collagen III immunostaining (Figure 3I-N) and morphometric quantification (Figure 3O) showed that the basal presence of collagen III deposition in healthy control kidneys (Figure 3I, O) was comparable to collagen III deposition in SHAM kidneys (Figure 3J, O) and contralateral kidneys of rats with unilateral IRI (Figure 3K, O). Treatment with CsA did not influence collagen III deposition in healthy control kidneys, SHAM-operated kidneys and contralateral kidneys of rats with unilateral IRI, irrespective of dosage (Figure 3O). After IRI induction and saline treatment, renal interstitial collagen III deposition was significantly higher than in healthy controls (Figure 3L, O). No differences in renal collagen III deposition were observed after administration of increasing dosages of CsA for 3 consecutive days after IRI (Figure 3M, O). However, when 5 mg/kg CsA was administered for 14 consecutive days after IRI, collagen III deposition was significantly increased (Figure 3N, O) compared to the saline-treated ischemic rats.

Detection of circulating progenitor cells and renal infiltration of BMDC

To investigate the impact of CsA on BMDC differentiation, we first assessed BMD progenitor (Lin⁻) cell mobilization to the circulation. In healthy control rats, the percentage of circulating Lin⁻ cells was not influenced by CsA treatment, irrespective of dosage (0.1±0.03% in saline-treated vs. 0.08±0.02% Lin⁻ cells in rats treated with 5 mg/kg CsA for 3 days, p>0.05). In SHAM-operated rats, the percentage on Lin⁻ cells
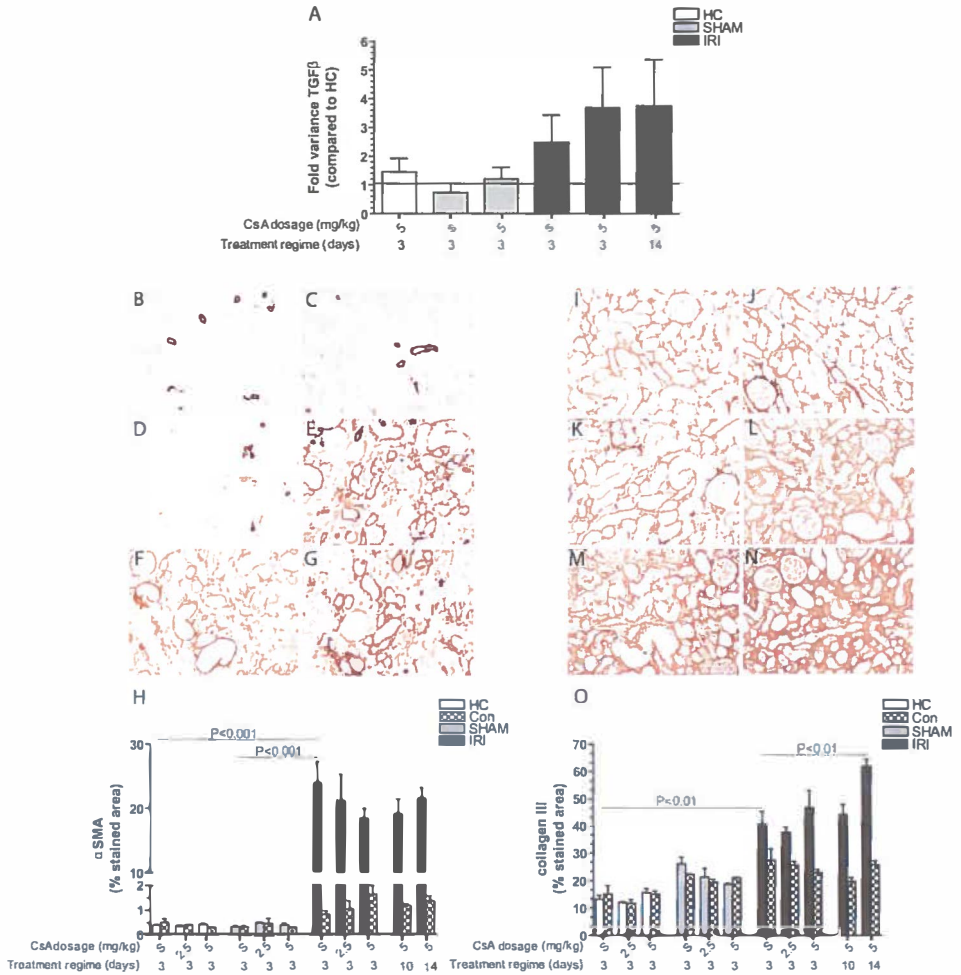
Figure 3. *Presence of fibrosis markers. Expression levels of TGF-β were determined by quantitative RT-PCR on RNA isolated from rat kidneys (A). Differences in expression levels between experimental and healthy control rats were expressed as fold variance of expression, calculated as $2^{\Delta\Delta ct}$ (12). Fold variance of 1 indicates that there are no transcriptional differences compared to healthy control rats, >1 is considered increased transcription and <1 is considered decreased transcription. Bars indicate the mean TGF-β expression levels per group and SEM. The presence of renal interstitial myofibroblasts was detected by staining for a-SMA in saline-treated healthy (B), SHAM (C) and contralateral (D) kidneys. Post-ischemic presence of interstitial myofibroblasts is shown after treatment with saline for 3 consecutive days (E), 5 mg/kg CsA for 3 consecutive days (F) or 5 mg/kg CsA for 14 consecutive days (G). The percentage of a-SMA-stained area was quantified by computerized morphometry (H). Bars indicate the mean a-SMA-stained area per group and SEM. All a-SMA-positive vascular structures were excluded from quantitative analysis. Renal interstitial collagen III protein deposition is shown in healthy control (I), SHAM (J) and contralateral (K) kidneys. Post-ischemic collagen III deposition is shown after treatment with saline 3 consecutive days (L) or 5 mg/kg CsA for 3 consecutive days after IRI (M) or treatment with 5 mg/kg CsA for 14 consecutive days after IRI (N). The percentage of collagen III-stained area was quantified with computerized morphometry (O). Bars indicate the mean percentage of collagen III-stained area per group and SEM. Lens magnification 200x. s = saline, HC = Healthy Control, Con = Contralateral, IRI = Ischemia/Reperfusion Injury.*

was also not influenced by treatment with increasing dosages of CsA (0.06±0.003% in saline-treated vs. 0.09±0.01% Lin⁻ cells in rats treated with 5 mg/kg CsA for 3 days, p>0.05). At day 14 after IRI, percentages of circulating Lin⁻ cells in ischemic, healthy and SHAM-operated controls were comparable. Moreover, the percentage of Lin⁻ cells was not influenced by treatment with increasing dosages of CsA for 3 consecutive days after IRI, or treatment with 5 mg/kg CsA for 10 consecutive days after IRI (0.08±0.02% in saline-treated vs. 0.1±0.01% Lin⁻ cells in rats treated with 5 mg/kg CsA for 10 days, p>0.05).

Staining by enzymatic conversion of substrate by hPAP allowed identification of renal infiltrating BMDC (Figure 4A-F), and subsequent morphometric quantification (Figure 4G). Since healthy controls were not subjected to hPAP BM transplantation, BMDC could not be assessed in these rats. In healthy control kidneys no hPAP signal was observed (Figure 4A). A low number of hPAP⁺ BMDC was observed in the renal interstitium of saline-treated SHAM-operated controls (Figure 4B, G) and in contralateral kidneys of rats after IRI (Figure 4C, G), which was not changed by treatment with increasing dosages of CsA (Figure 4G). Compared to SHAM-operated controls, induction of IRI followed by treatment with saline for 3 consecutive days resulted in a significantly higher number of renal infiltrating BMDC (Figure 4D, G). Treatment with CsA in increasing dosages for 3 consecutive days after IRI did not influence renal BMDC infiltration (Figure 4E, G). Moreover, treatment with 5 mg/kg CsA for 10 or 14 consecutive days after IRI had no additional effect on the number of renal infiltrating BMDC (Figure 4F, G).

Bone marrow-derived myofibroblasts

Differentiation of BMDC into renal interstitial myofibroblasts was detected by double staining combining hPAP with α-SMA. After renal IRI, cells co-expressing hPAP (BMDC, Figure 5A) and α-SMA (myofibroblasts, Figure 5B) were observed in the renal interstitium. In these cells, co-expression of hPAP (FITC) and α-SMA (TRITC) (Figure 5C) was detected in 8/14 consecutive confocal optical sections of the Z-series, confirming the double-positivity of these cells and excluding the possibility that the two markers were expressed by different, neighboring cells.

In ischemic kidneys of rats treated with saline for 3 consecutive days, 40.7% of all renal interstitial α-SMA⁺ myofibroblasts was derived from the BM, confirming our previous findings (8). However, neither treatment with CsA in increasing dosages for 3 consecutive days after IRI, nor treatment with 5 mg/kg CsA for 10 or 14 consecutive days after IRI, influenced the number of BMD myofibroblasts (Figure 5D).
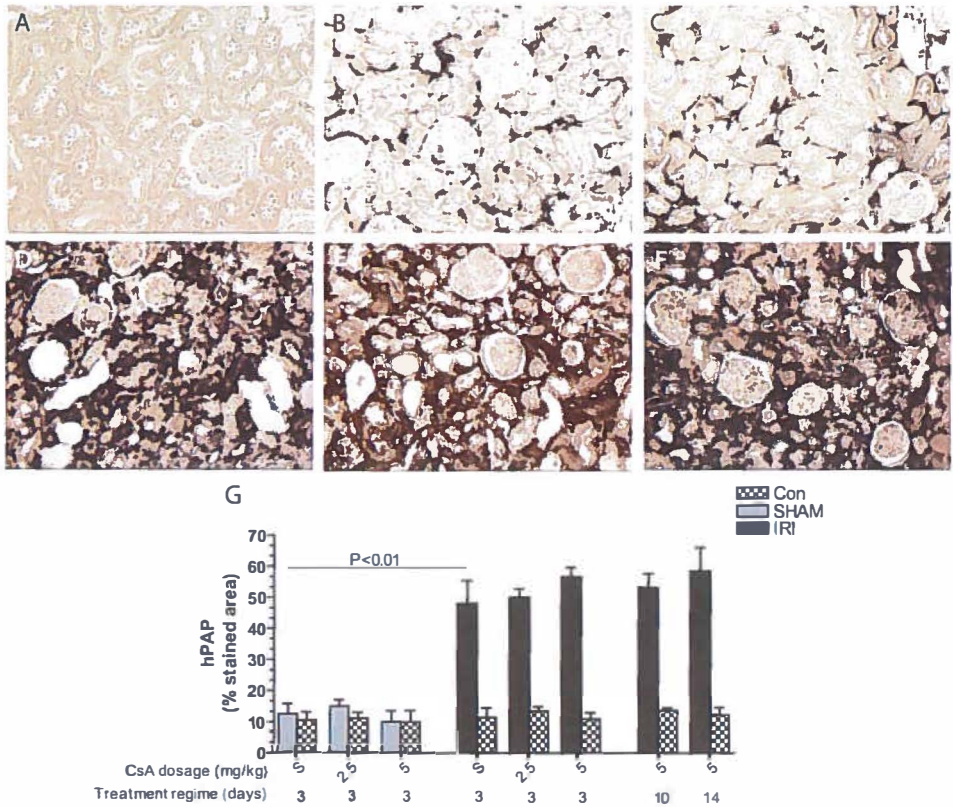
Figure 4. *Renal infiltration of BMDC. BMDC infiltration, determined by enzymatic hPAP staining, is shown in saline-treated, non-transgenic healthy (A), SHAM-operated (B) and contralateral kidney after IRI (C). Post-ischemic renal infiltration of BMDC is shown in kidneys after treatment with saline for 3 consecutive days (D), 5 mg/kg CsA for 3 consecutive days (E) or treatment with 5 mg/kg CsA for 14 consecutive days (F). Lens magnification 200x. The percentage of hPAP stained area was quantified by computerized morphometry (G). Bars indicate the mean percentage of hPAP stained area per group and SEM. s = saline, Con = Contralateral, IRI = Ischemia/Reperfusion Injury.*

Recipient-derived myofibroblasts after experimental kidney transplantation

On day 14 after kidney transplantation (TX), without post-operative CsA treatment, an average of 28% of all renal interstitial myofibroblasts in the donor kidney was recipient-derived (Figure 5D). Treatment with 5 mg/kg CsA for 10 consecutive days after kidney transplantation did not affect the percentage of recipient-derived myofibroblasts (Figure 5D). Moreover, no statistical differences in the numbers of recipient-derived myofibroblasts were found between the IRI and TX groups that did not receive CsA treatment (Figure 5D). IRI rats and kidney transplant recipients treated with 5 mg/kg CsA for 10 consecutive days had similar percentages of hPAP+ myofibroblasts (Figure 5D).
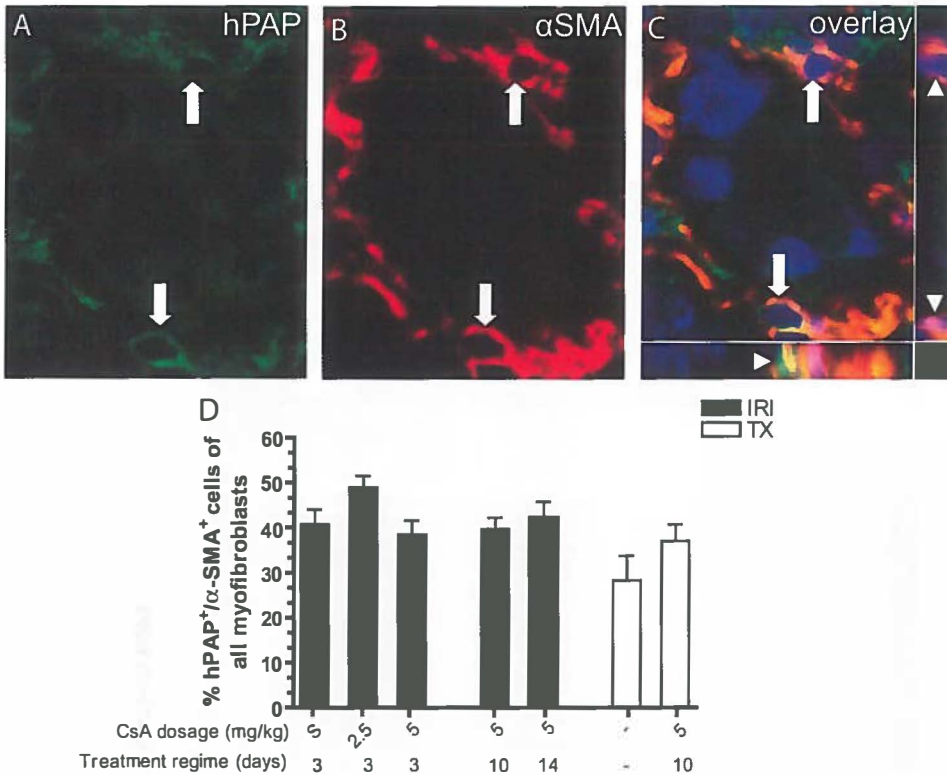
Figure 5. *Bone marrow-derived and recipient-derived myofibroblasts. The presence of BMD myofibroblasts was determined by confocal microscopy of staining for hPAP (FITC) (A) in combination with α-SMA (TRITC) (B) on post-ischemic or post-transplant kidney tissue. The overlay shows FITC, TRITC and DAPI channels and the x/z and y/z planes underneath and on the right of the merged picture demonstrate colocalization of the markers (C). Arrows indicate double-positive cells. Arrowheads indicate co-expression in the x/z and y/z planes. Co-expression of hPAP and α-SMA was quantified in relation to the renal interstitial myofibroblast population in IRI rats and syngeneic kidney transplant recipients (D). Bars indicate the mean percentage hPAP/α-SMA double-positive cells of all α-SMA+ cells per group and SEM. s = saline, IRI = Ischemia/Reperfusion Injury, TX = Transplantation.*

Tubular epithelial engraftment of BMDC

Besides differentiating into myofibroblasts, BMDC have also been shown to engraft into renal tubules and to adopt an epithelial phenotype after IRI (13-16). Therefore, we assessed the influence of CsA on tubular BMDC engraftment. Since healthy controls were not subjected to hPAP BM transplantation, BMDC could not be assessed in these rats. In the kidneys of SHAM-operated control rats, BMDC were present in the interstitium (Figure 6A), however, tubular epithelial BMDC engraftment was observed sporadically. Treatment with increasing dosages of CsA for 3 consecutive days after SHAM operation did not influence the percentage of hPAP+ tubular engrafted cells (Figure 6F). After induction of IRI and treatment with saline for 3 consecutive days, 2% of all tubular epithelial cells were hPAP+ (Figure 6B, F). Epithelial phenotype of the engrafted BMDC was demonstrated by double-staining combining hPAP with the epithelial-specific marker E-cadherin (Figure 6C-E). These engrafted hPAP+ cells did not

express the common leukocyte antigen CD45 (not shown). Neither administration of CsA in increasing dosages for 3 consecutive days, nor treatment with 5 mg/kg CsA for 10 or 14 consecutive days after IRI, did influence tubular BMDC engraftment (Figure 6F).
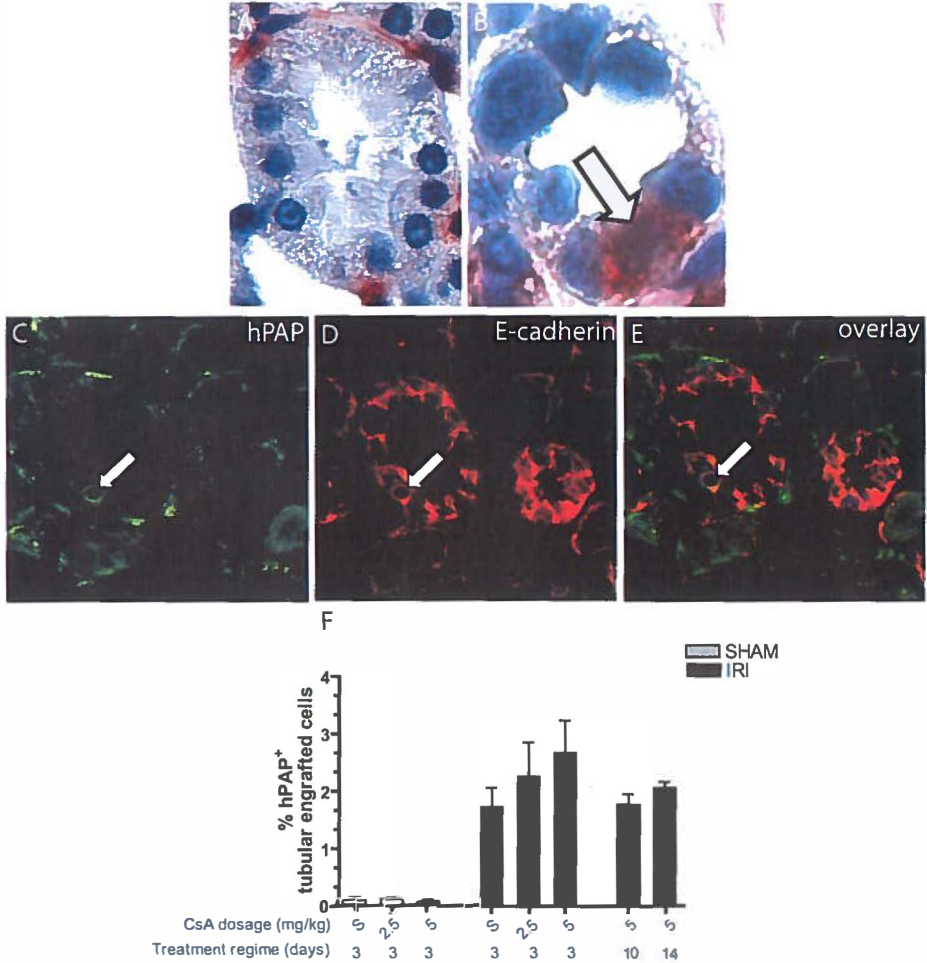

Figure 6. *Tubular epithelial engraftment of BMDC. hPAP staining in SHAM (A) and saline-treated post-ischemic kidney (B) showed occasional tubular BMDC engraftment in the latter. Arrow indicates an example of tubular epithelial BMDC engraftment. Lens magnification 1000x. Epithelial phenotype of the engrafted BMDC was demonstrated by double-staining for hPAP (C) and E-cadherin (D). The overlap of signal is shown in the overlay (E). Arrows indicate double-positive cells. Tubular epithelial BMDC engraftment was quantified as the percentage of hPAP⁺ tubular engrafted cells (F). Bars indicate the mean percentage of hPAP⁺ tubular engrafted cells per group and SEM. s = saline, IRI = Ischemia/Reperfusion Injury.*

Discussion

This study is the first to investigate the effects of CsA on differentiation of BMDC to myofibroblasts after renal IRI. Using a previously validated experimental model of IRI, we found no direct adverse effects of CsA during the critical window of BMDC differentiation to myofibroblasts.

Our previous finding that BMDC contribute up to 40% of the post-ischemic myofibroblast pool raised the question whether differentiation of BMDC to myofibroblasts may be promoted by CsA. Based on the described window of opportunity for BMDC differentiation to myofibroblasts, in the current study we administered CsA for 3, 10 or 14 consecutive days after IRI induction.

Benefiting from a group of unmanipulated (no irradiation, BM transplantation, IRI) healthy rats we showed that CsA had no baseline effects on numbers and mobilization of Lin- progenitor cells, irrespective of dosage and course of administration. Moreover, in conjunction with IRI, the effect of CsA on circulating Lin⁻ cells was not altered. Since CsA was administered during the first 3 days after IRI, in the time frame when mobilization of progenitor cells is at its strongest, this suggests that CsA has no impact on production of Lin⁻ cells in or mobilization of these cells from the BM. This is, to our knowledge, the first report on the influence of CsA on circulating progenitor cells *in vivo*.

Our expectation that the pro-fibrotic action of CsA may promote BMDC differentiation to myofibroblasts was contradicted, irrespective of treatment regimen. Importantly, CsA was administered in the optimal window of opportunity for myofibroblastic differentiation of BMDC in the renal interstitium (8), supporting the concept that CsA does not affect differentiation of BMDC. At short term after IRI, CsA also did not affect numbers of endogenous myofibroblasts. Both findings are intriguing in light of the fact that TGF-β transcription was stimulated by long-term treatment with CsA, demonstrating CsA activity (17,18) and indicating that a pro-fibrotic environment was generated. We previously showed that TGF-β was primarily produced by resident, not BMD, myofibroblasts (8). In the present study, 14 day treatment with maximal CsA dosages resulted in increased collagen III deposition, which is a result of TGF-β production. Since numbers of BMD- and endogenous myofibroblasts were not affected by CsA, it is conceivable that at short-term after IRI, CsA may affect function of myofibroblasts, only.

During transplantation, the setting in which CsA is commonly used, solid organs undergo variable times of both warm and cold ischemia. After having studied the impact of CsA on BMDC differentiation in an established, "clean" model of warm ischemia, we conducted a pilot experiment using a model of syngeneic kidney transplantation, in which the donor kidney was subjected to cold and warm ischemia. This study allowed us to investigate the effects of CsA in a relevant setting, without the confounding influence of immune rejection. In this model too, there were no differences in numbers of BMD-myofibroblasts between CsA-treated and untreated rats, indicating that the agent did not affect differentiation of BMDC or recipient-derived cells within this time frame.

Previously, we showed that, besides differentiating into myofibroblasts, a small percentage of BMDC differentiated into tubular epithelial cells (8,13). Since CsA has been shown to create a renal environment in which proliferation of tubular epithelial

cells is inhibited (19), we asked whether differentiation of BMDC to tubular epithelial cells may be impaired by CsA. Similar numbers of BMD tubular epithelial cells in CsA- and saline-treated rats demonstrated that this was not the case. The fact that tubular regeneration did take place in the post-ischemic kidney, even after CsA treatment, suggests that tubular repair was mediated by epithelial proliferation, as previously shown (13), and was not affected by CsA.

We have previously reported a positive correlation between ischemic time, the extent of renal damage and the contribution of BMDC to tubular repair (13). As discussed above, we have also identified a critical time window in renal repair and remodeling, in which BMDC undergo differentiation fates, probably under the influence of the renal microenvironment. The current study is the first to investigate the effects of CsA on these processes, and shows that, within the crucial early time window after the induction of IRI or kidney transplantation, administration of experimentally relevant dosages of CsA did not stimulate BMDC differentiation to myofibroblasts and thus did not increase the already significant contribution of these cells to the interstitial myofibroblast pool. Based on these data it is reasonable to speculate that, in the clinical setting, CsA does not exert its profibrotic action by stimulation of myofibroblastic differentiation of BMDC.

Acknowledgements

References

1) Merville P. Combating chronic renal allograft dysfunction : optimal immunosuppressive regimens. Drugs 2005;65(5):615-31.

2) Andoh TF, Burdmann EA, Bennett WM. Nephrotoxicity of immunosuppressive drugs: experimental and clinical observations. Semin Nephrol 1997 Jan;17(1):34-45.

3) Calne RY, White DJ, Thiru S, Evans DB, McMaster P, Dunn DC, Craddock GN, Pentlow BD, Rolles K. Cyclosporin A in patients receiving renal allografts from cadaver donors. Lancet 1978 Dec 23;2(8104-5):1323-7.

4) de Mattos AM, Olyaei AJ, Bennett WM. Nephrotoxicity of immunosuppressive drugs: long-term consequences and challenges for the future. Am J Kidney Dis 2000 Feb;35(2):333-46.

5) Gabbiani G. The biology of the myofibroblast. Kidney Int 1992 Mar;41(3):530-2.

6) Azuma H, Nadeau K, Takada M, Mackenzie HS, Tilney NL. Cellular and molecular predictors of chronic renal dysfunction after initial ischemia/reperfusion injury of a single kidney. Transplantation 1997 Jul 27;64(2):190-7.

7) Williams P, Lopez H, Britt D, Chan C, Ezrin A, Hottendorf R. Characterization of renal ischemia-reperfusion injury in rats. J Pharmacol Toxicol Methods 1997 Feb;37(1):1-7.

8) Broekema M, Harmsen MC, van Luyn MJ, Koerts JA, Petersen AH, van Kooten TG, van Goor H, Navis G, Popa ER. Bone Marrow-Derived Myofibroblasts Contribute to the Renal Interstitial Myofibroblast Population and Produce Procollagen I after Ischemia/Reperfusion in Rats. J Am Soc Nephrol 2007 Jan;18(1):165-75.

9) Kisseberth WC, Brettingen NT, Lohse JK, Sandgren EP. Ubiquitous expression of marker transgenes in mice and rats. Dev Biol 1999 Oct 1;214(1):128-38.

10) Kunter U, Floege J, von Jurgensonn AS, Stojanovic T, Merkel S, Grone HJ, Ferran C. Expression of A20 in the vessel wall of rat-kidney allografts correlates with protection from transplant arteriosclerosis. Transplantation 2003 Jan 15;75(1):3-9.

11) Keppler A, Gretz N, Schmidt R, Kloetzer HM, Groene HJ, Lelongt B, Meyer M, Sadick M, Pill J. Plasma creatinine determination in mice and rats: An enzymatic method compares favorably with a high-performance liquid chromatography assay. Kidney Int 2007 Jan;71(1):74-8.

12) Livak KJ, Schmittgen TD. Analysis of relative gene expression data using real-time quantitative PCR and the 2(-Delta Delta C(T)) Method. Methods 2001 Dec;25(4):402-8.

13) Broekema M, Harmsen MC, Koerts JA, Petersen AH, van Luyn MJ, Navis G, Popa ER. Determinants of tubular bone marrow-derived cell engraftment after renal ischemia/reperfusion in rats. Kidney Int 2005 Dec;68(6):2572-81.

14) Kale S, Karihaloo A, Clark PR, Kashgarian M, Krause DS, Cantley LG. Bone marrow stem cells contribute to repair of the ischemically injured renal tubule. J Clin Invest 2003 Jul;112(1):42-9.

15) Lin F, Cordes K, Li L, Hood L, Couser WG, Shankland SJ, Igarashi P. Hematopoietic stem cells contribute to the regeneration of renal tubules after renal ischemia-reperfusion injury in mice. J Am Soc Nephrol 2003 May;14(5):1188-99.

16) Lin F, Moran A, Igarashi P. Intrarenal cells, not bone marrow-derived cells, are the major source for regeneration in postischemic kidney. J Clin Invest 2005 Jul;115(7):1756-64.

17) Khanna A, Kapur S, Sharma V, Li B, Suthanthiran M. In vivo hyperexpression of transforming growth factor-beta1 in mice: stimulation by cyclosporine. Transplantation 1997 Apr 15;63(7):1037-9.

18) Shin GT, Khanna A, Sharma VK, Ding R, Azizlerli S, Li B, Suthanthiran M. In vivo hyperexpression of transforming growth factor-beta 1 in humans: stimulation by cyclosporine. Transplant Proc 1997 Feb;29(1-2):284.

19) Wolf G, Killen PD, Neilson EG. Cyclosporin A stimulates transcription and procollagen secretion in tubulointerstitial fibroblasts and proximal tubular cells. J Am Soc Nephrol 1990 Dec;1(6):918-22.

5

Chapter 6

Tubular engraftment and myofibroblast differentiation of recipient-derived cells after experimental kidney transplantation

Martine Broekema[1], Martin C. Harmsen[1], Jasper A. Koerts[1], Theo G. van Kooten[2], Gerjan Navis[3], Marja J. A. van Luyn[1] and Eliane R. Popa[1]

[1]Department of Pathology & Laboratory Medicine, Medical Biology Section, [2]Department of Biomedical Engineering, [3]Department of Nephrology, University Medical Center Groningen, University of Groningen, The Netherlands

Abstract

In human renal allografts, recipient-derived cells engrafted in various kidney substructures, have been detected at long term after transplantation. Here we investigated tubular engraftment and myofibroblast differentiation of recipient-derived cells at short-term after experimental kidney transplantation, during a previously described window of regeneration and possible onset of renal interstitial fibrosis.

Fisher (F344, syngeneic) and Dark Agouti (DA, allogeneic) kidneys were transplanted into F344-hPAP transgenic recipient rats, which allowed tracing of recipient-derived cells in non-transgenic donor kidneys. We evaluated tubular engraftment and myofibroblast differentiation of recipient-derived cells on day 14 after kidney transplantation.

Kidney transplantation resulted in tubular engraftment of recipient-derived cells. After allogeneic kidney transplantation, 9.7% of tubular cross-sections contained at least one recipient-derived cell, which represented a significant increase in comparison to syngeneic transplantation (4.0%, $p < 0.05$). Moreover, recipient-derived myofibroblasts were present in the renal interstitium of the transplanted kidney. These cells contributed 39% of the total interstitial myofibroblast population in allografts, which was comparable to the syngeneic situation (28%, $p = 0.25$).

In a defined early window of regeneration and possible onset of renal interstitial fibrosis after kidney transplantation, rejection-associated injury, superimposed on ischemic damage, increases tubular engraftment of recipient-derived cells, while it does not affect their relative contribution to the renal interstitial myofibroblast population.

Introduction

Early after kidney transplantation both non-immunologic factors, such as ischemia/reperfusion injury (IRI), and immunologic factors, such as acute rejection episodes, cause endothelial and tubular epithelial damage in the graft. At long term, this can result in interstitial fibrosis, which involves infiltration of inflammatory cells, proximal tubular injury and -death, extracellular matrix (ECM) accumulation and the progressive loss of renal function.

Recipient-derived cells, likely originating from bone marrow-derived (progenitor) cells, have been detected in endothelial or tubular epithelial structures of human renal allografts several months after transplantation (1-8). Since the extent of replacement of donor endothelium or epithelium correlates with the severity of graft damage (3;5), it was postulated that recipient-derived cells mediate graft repair by replacing damaged graft cells. Furthermore, in renal transplants with chronic allograft nephropathy, the presence of recipient-derived myofibroblasts in the tubulointerstitial compartments was demonstrated, indicating a possible role for these cells in renal remodeling after kidney transplantation (2).

Engraftment and differentiation of recipient-derived cells in human allografts has been studied in chronic renal transplant injury, but not early after transplantation. Using a rat model of IRI we previously identified an early window of kidney regeneration, but also of possible onset of fibrosis, during the first two weeks after IRI. In this early window we observed sporadic engraftment of bone marrow-derived cells (BMDC) in tubular cross-sections and differentiation to epithelium, which positively correlated with the severity of damage (9). Moreover, we showed that BMDC contributed significantly to the interstitial myofibroblast population, forming up to 40% of all ECM-producing interstitial α-SMA+ myofibroblasts (10). These results suggest that the potential contribution of BMDC to kidney repair or the onset and progression of chronic injury and repair may be determined early after IRI. Since IRI forms an unavoidable damage event during solid organ transplantation, in the current study we hypothesized that after kidney transplantation engraftment of recipient cells in the graft takes place in this early phase, with possible consequences for graft performance. To address this hypothesis we performed experimental kidney transplantations with F344-R26-hPAP transgenic rats as recipients to investigate, for the first time, differentiation fates of recipient-derived cells in the non-transgenic donor kidney using experimental kidney transplantation.

Materials and Methods

Animal experimentation

Male, 8-12 week-old R26-hPAP rats (F344 background), transgenic for human placental alkaline phosphatase (hPAP) (11), their non-transgenic F344 littermates and Dark Agouti rats (DA/OlaHsd, Harlan, Horst, the Netherlands) were kept under conventional housing and diet.

R26-hPAP transgenic rats were used as recipients to allow tracing of recipient-derived cells in the donor kidney. Non-transgenic F344 rats served as donors in syngeneic kidney transplantation (F344 to F344-hPAP, n=6), DA rats served as donors for allogeneic transplantation (DA to F344-hPAP, n=6). Briefly, rats were sedated by

general isoflurane (2% Forene, Abbot b.v., Hoofddorp, The Netherlands), N_2O (50%), O_2 (50%) anesthesia. After anesthesia, the left kidneys were excised from donors, flushed with cold saline and transplanted orthotopically in hPAP recipient rats by end-to-end anastomosis of the vessels of the donor and recipient and, subsequently, ureters of the donor and recipient using 10-0 prolene sutures (Johnson & Johnson Intl., Brussels, Belgium). Cold ischemia by storage in saline on ice was approximately 30 min. Warm ischemia time was 25 min. Nephrectomy of the right kidney was performed between day 7 and 10 after transplantation. Death of the animals early after transplantation, due to acute graft rejection, was prevented by treatment with 5 mg/kg ciclosporin (CsA, Sandimmun, Novartis, Basel, Switzerland) as daily subcutaneous injections for the first 10 consecutive days after allogeneic kidney transplantation (12).

All rats (n=6 per group) were terminated on day 14 after transplantation. Twenty-four hour urine and blood samples were collected prior to termination. Kidneys were perfused *in situ* with cold saline. Kidney size was not measured. Animal procedures were approved by the local committee for care and use of laboratory animals and performed according to governmental and international guidelines on animal experimentation.

Renal function

Total urine protein was determined using the TCA protein assay (13) and BNII equipment (Dade Behring, Marburg, Germany). Creatinine levels were determined in plasma and urine using the enzymatic colorimetric assay CREA plus (Roche, Woerden, the Netherlands) (14), which is a sensitive and specific quantification method for creatinine (15). Creatinine clearance (mL/min) was calculated by multiplying the creatinine level of a 24 h urine sample (μmol/L) by the volume of this 24h urine sample (mL/min) and dividing the resulting value by the plasma creatinine level (μmol/L). Blood and urine collected from healthy F344 and DA rats served as control samples. These healthy F344 and DA rats were at a later stage used as kidney donors for the syngeneic and allogeneic transplantations.

Tissue collection, fixation and histological analyses

Immediately after termination kidneys were divided into quarters and fixed in Zinc fixative (0.1M Tris buffer, pH 7.4 with 0.5g $CaCH_2COO$, 5g $(CH_2COO)2Zn*2H_2O$ and 5g $ZnCl_2$ per liter; MERCK, Darmstadt, Germany) or snap-frozen in N_2 and stored at -80°C. Histological analyses were performed on 5 μm zinc-fixed, paraffin-embedded sections, which were dewaxed before staining, or on 5 μm acetone-fixed, cryostat sections. Periodic acid-Schiff (PAS) staining, used to evaluate renal morphology, was performed using an automated procedure at the department of Pathology.

hPAP was detected by enzymatic or immunohistochemical staining procedures. In cases where infiltration of recipient-derived cells needed to be quantified by computer morphometry, we used the enzymatic staining, which gives a strong signal and no background, which is essential for correct computerized quantification of the stained area. The immunohistological method was used for more detailed examination of individual hPAP+ cells or in cases when double-staining was necessary to determine the phenotype of engrafted recipient-derived cells. Enzymatic hPAP detection and inactivation of endogenous alkaline phosphatase (AP) was performed as previously described (10). Immunohistochemical detection of hPAP was performed

by incubation with rabbit anti-hPAP polyclonal antibody (Serotec, Oxford, UK), followed by incubation with biotinylated goat anti-rabbit conjugate (DAKO) and streptavidine-alkaline phosphatase (Southern Biotechnology, Birmingham, USA) (10). CD4+ and CD8+ T cells were detected using mouse anti-rat CD4 and CD8 antibodies (OX-35 and OX-8, culture supernatant), followed by incubation with biotinylated goat anti-mouse IgG (Southern Biotechnology) and streptavidin-peroxidase conjugates (DAKO). Renal interstitial myofibroblasts were detected using mouse anti-α-SMA (clone 1A4, DAKO), and subsequent labeling with peroxidase-conjugated rabbit anti-mouse antibody, followed by peroxidase-conjugated swine anti-rabbit antibody (both DAKO, Glostrup, Denmark) as previously described (10). Collagen III was detected with rabbit anti-rat collagen III (Biogenesis, Poole, UK) and subsequent labeling with peroxidase-conjugated goat anti-rabbit antibody (DAKO), followed by peroxidase-conjugated rabbit anti-goat (DAKO) antibody (10). For α-SMA/hPAP double staining, sections were first stained with α-SMA and subsequently for hPAP (see above), as previously described (10). Color development was performed with fuchsin substrate-chromogen system (hPAP) (DAKO), 3,3'-diaminobenzidine tetrachloride (α-SMA, collagen III) or with 3-amino-9-ethylcarbazole (Sigma-Aldrich) substrate dissolved in N,N-dimethylformamide (MERCK) and 0.5M acetate buffer, pH 4.9 (CD4, CD8). Sections were counterstained with Mayer's hemalum (MERCK) and mounted in Kaiser's glycerol gelatine (MERCK).

The epithelial phenotype of tubular engrafted recipient-derived cells, was assessed by immunofluorescent double-staining for hPAP in combination with E-cadherin (clone 36) (Becton Dickinson Biosciences) or a cocktail of the tubular epithelial specific lectins: SBA (biotinylated soybean agglutinin), DBA (biotinylated *Dolichos biflorus* agglutinin), and PNA (biotinylated peanut agglutinin) (all from Vector Laboratories Inc., Burlingame, CA, USA). Briefly, on 5 µm cryosections, recipient-derived cells were detected by incubation with anti-hPAP, followed by goat anti-rabbit-FITC conjugate (Southern Biotechnology). Tubular epithelial cells were detected by incubation with a mixture of 30 µg/mL biotinylated SBA/DBA/PNA followed by a streptavidin-Cy3 (Zymed Laboratories Inc., San Francisco, CA, USA) conjugate, or by incubation with monoclonal antibody against E-cadherin followed by biotinylated goat anti-mouse (IgG2a for E-cadherin) (Dako) and streptavidin-Cy3 conjugates (Zymed Laboratories Inc.). To confirm that hPAP+ cells, engrafted in renal tubuli, were not engrafted leukocytes, we performed double-staining combining hPAP with CD45 (leukocyte marker). hPAP was detected as described above and leukocytes were detected by incubation with mouse anti-rat CD45 monoclonal antibody (OX-1, culture supernatant), followed by biotinylated goat anti-mouse IgG (Southern Biotechnology) and streptavidin-Cy3 conjugates (Zymed Laboratories Inc.). The myofibroblast phenotype of recipient-derived cells was assessed by immunofluorescence double-staining of α-SMA and hPAP. hPAP was detected as described above and α-SMA with tyramide-TRITC (PerkinElmer Life Sciences, Boston, USA) via goat anti-mouse HRP (Southern Biotechnology). Tyramide signal amplification is used to amplify the fluorescent signal. Fluorescently stained sections were counterstained with 4',6-diamidino-2-phenylindole (DAPI, Sigma-Aldrich, St.Louis, USA) and mounted with citifluor (Agar scientific, Stansted, UK).

All antibody incubations were performed for 1 hour at room temperature. For negative controls, sections were processed in the absence of primary antibody. Light and fluorescence microscopy was performed using a Leica DMLB microscope (Leica

6

Microsystems, Rijswijk, the Netherlands), Leica DC300F camera and Leica QWin 2.8 software. Fluorescent images of hPAP/α-SMA were obtained using a LEICA TCS SP2 3-channel confocal laser scanning microscope. Co-localization of hPAP and α-SMA signals within cells in the 5 μm thin cryosections was demonstrated with confocal microscopy, using a LEICA TCS SP2 3-channel confocal laser scanning microscope. In each section, ten consecutive optical sections were scanned at the excitation wavelengths of 488 nm (FITC) and 543 nm (TRITC), thus generating a sequential Z-series of ten optical sections. Computerized stacking of these ten optical sections allowed us to obtain a three-dimensional image of cells of interest. A cell was considered double-positive when the signals for FITC (hPAP) and TRITC (α-SMA) were present concomitantly throughout at least 7/10 consecutive optical sections of the Z-series. This method allowed us to reliably detect double-positive cells and to exclude the possibility that the two markers were expressed by different, neighboring cells.

Quantification

Interstitial staining of hPAP, α-SMA and collagen III was measured using computerized morphometry (Leica QWin 2.8 software). Stained areas of 15 (hPAP, collagen III) or 25 (α-SMA) randomly selected fields in cortex and outer medulla were quantified at a magnification of 200x and expressed as percentage of total measured area. α-SMA expression appeared to be more variable and clustered compared to hPAP and collagen III expression, and was therefore measured in 25, instead of 15, microscope fields. Vascular and glomerular expression of collagen III and vascular expression of α-SMA was excluded from measurements.

The percentage of hPAP$^+$/α-SMA$^+$ cells was determined by two independent investigators by counting all α-SMA$^+$, hPAP$^+$ and double-positive cells in 30 microscope fields in cortex and outer medulla per section, for each rat at a magnification of 400x. In syngeneic transplanted kidneys 3250 interstitial cells (650 interstitial cells/kidney section) and in allogeneic transplanted kidneys 4878 interstitial cells (813 interstitial cells/kidney section) were counted.

Tubular epithelial engraftment of recipient-derived cells was determined by counting the number of tubular cross-sections containing at least one hPAP$^+$ cell of all tubular cross-sections in a microscope field. In syngeneic transplanted kidneys 800 tubular cross sections (133 tubuli/kidney section) and in allogeneic kidneys 786 tubular cross sections (131 tubuli/kidney section) (n=6 rats per group) were counted. The number of tubular engrafted recipient-derived cells was determined by counting the number hPAP$^+$ cells engrafted in tubular cross-sections of all tubular epithelial cells in a microscope field. In both groups a comparable number of tubular cells was counted (1482 tubular cells/kidney in syngeneic vs. 1577 tubular cells/kidney in allogeneic kidneys). Tubular engrafted hPAP$^+$ cells had the same shape and morphology as adjacent cells and were counted in 10 random microscope fields (400x) in cortex and medulla for each rat.

Statistics

Statistical tests were performed using GraphPad Prism 4.0 (GraphPad Software, San Diego California, USA). Differences between control, syngeneic kidney transplantation and allogeneic kidney transplantation groups were determined with One-way ANOVA Bonferroni's Multiple Comparison Test. Between group (syngeneic vs. allogeneic

kidney transplantation) comparison was analyzed using unpaired t-tests. Spearman correlation test was performed to determine the relationship between 2 different parameters. P-values <0.05 were considered statistically significant.

Results

Renal morphology and function

Normal morphology was observed in contralateral right kidneys of the F344 or DA donor (Figure 1A), harvested during transplantation, and nephrectomized right kidneys of the F344-hPAP recipient (Figure 1B), harvested between day 7-10 after transplantation. Based on visual observation, there were no differences in kidney size on day 14 after F344 kidney transplantation into F344-hPAP recipients, i.e. F344 to F344-hPAP or transplantation of DA kidneys into F344-hPAP recipients, i.e. DA to F344-hPAP. After F344 to F344-hPAP transplantation, kidneys showed occasional tubular dilatation (Figure 1C). DA to F344-hPAP kidney transplantation resulted in more severe renal tubular dilatation compared to F344 to F344-hPAP kidney transplantation and large interstitial inflammatory infiltrates (Figure 1D).

Renal function reflected by total urine protein, did not differ significantly between F344 to F344-hPAP transplanted rats and F344 healthy controls and between DA to F344-hPAP transplanted rats and DA healthy controls (Figure 1E). Moreover, total urine protein was similar in rats subjected to F344 to F344-hPAP transplantation and DA to F344-hPAP transplanted rats (Figure 1E). Creatinine clearance in rats after F344 to F344-hPAP kidney transplantation was lower, albeit not significantly lower, compared to F344 healthy controls (Figure 1F). After DA to F344-hPAP kidney transplantation, creatinine clearance decreased significantly compared to DA healthy controls (Figure 1F). Moreover, creatinine clearance was similar in rats after F344 to F344-hPAP and after DA to F344-hPAP kidney transplantation (Figure 1F).

Renal infiltration of recipient-derived cells

Staining by enzymatic conversion of substrate by hPAP was used to detect the presence of recipient-derived cells in the transplanted kidney. Specificity of hPAP staining and adequate blocking of endogenous AP was demonstrated in DA (Figure 2A) and F344 contralateral donor kidneys, showing no expression of hPAP, and in nephrectomized F344-hPAP kidneys (Figure 2B), showing ubiquitous expression of hPAP. Transplantation of DA or F344 donor kidneys into F344-hPAP recipient rats enabled tracking of recipient-derived cells in the transplanted kidney by hPAP staining. The number of recipient-derived cells in the renal interstitium was quantified using computerized morphometry. After F344 to F344-hPAP kidney transplantation a low number of recipient-derived hPAP+ cells infiltrated the kidney, present as single cells, randomly scattered in the renal interstitium (Figure 2C, E). Compared to F344 to F344-hPAP, DA to F344-hPAP transplanted kidneys were infiltrated by a significantly higher number of recipient-derived hPAP+ cells, located in both perivascular and peritubular foci (Figure 2D, E). In this latter model, these cells were mainly macrophages, CD4+ and CD8+ T-cells, whereas after F344 to F344-hPAP transplantation less interstitial CD4+ and sporadically CD8+ T-cells were observed (not shown).
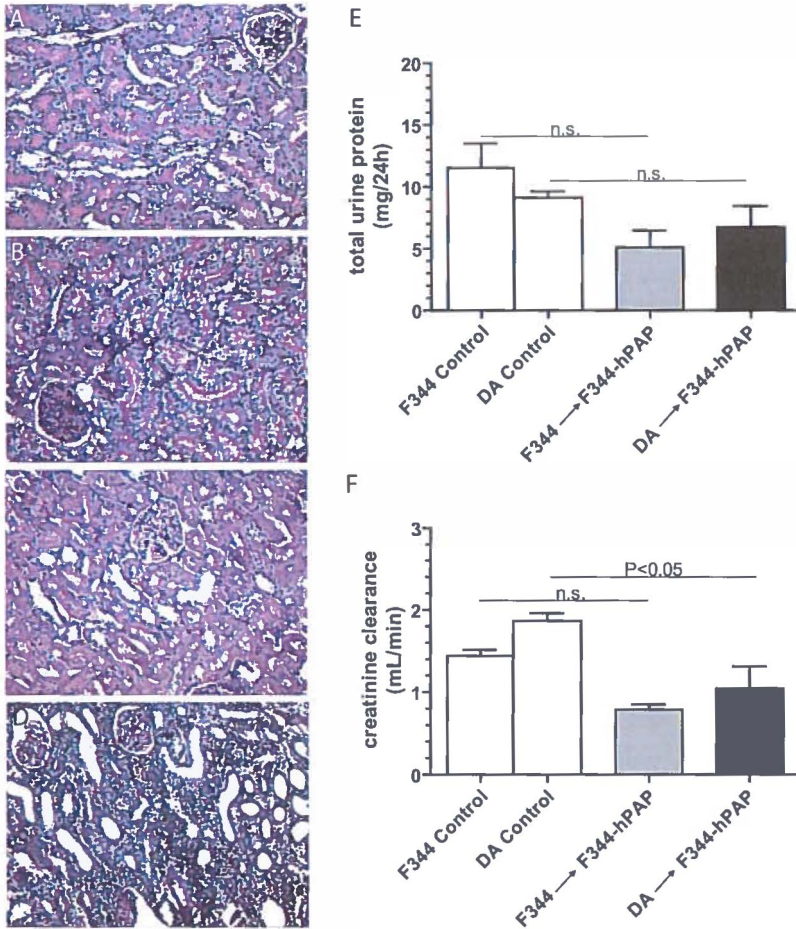
Figure 1. *Renal morphology and function. Representative renal morphology is shown for PAS-stained sections of the contralateral kidney of a DA donor (A), the nephrectomized kidney of a F344-hPAP recipient (B) and kidneys isolated on day 14 after F344 to F344-hPAP (C) or DA to F344-hPAP (D) transplantation. Lens magnification 200x. Renal function was determined by total urine protein (E) and creatinine clearance (F). Bars indicate the mean total urine protein or creatinine clearance per group and SEM.*

Tubular epithelial engraftment of recipient-derived cells

Tubular epithelial engraftment of recipient-derived cells was detected in F344 to F344-hPAP and DA to F344-hPAP kidney transplants using hPAP immunostaining. Occasionally hPAP$^+$, recipient-derived, cells were detected within tubular cross-sections (Figure 3A). Epithelial phenotype of the engrafted recipient-derived cells was demonstrated by immunofluorescence double-staining combining hPAP with the epithelial-specific marker E-cadherin (Figure 3B-D). Moreover, we showed that tubular engrafted recipient-derived cells bound tubular epithelial-specific lectins (Figure 3E-G). These engrafted hPAP$^+$ cells did not express the common leukocyte antigen CD45 (not shown). After DA to F344-hPAP kidney transplantation the percentage of all
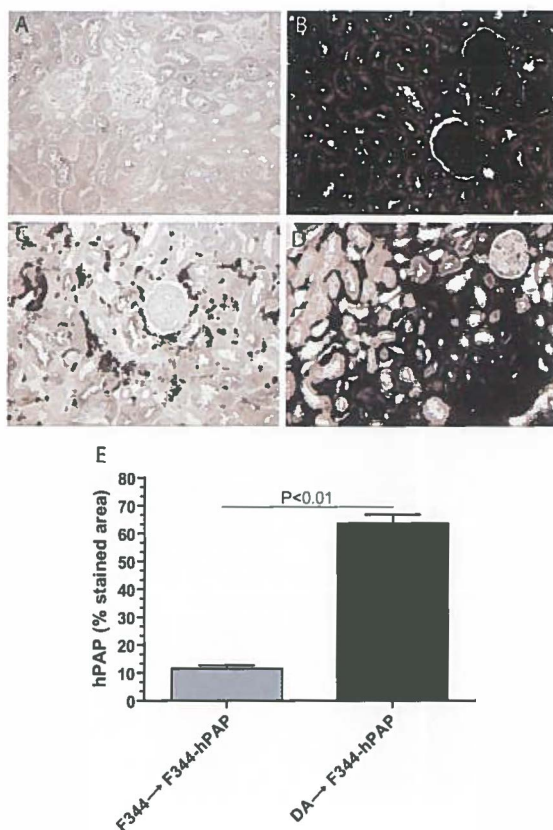
Figure 2. *Renal infiltration of recipient-derived cells. hPAP activity is shown in contralateral non-transgenic DA (A), nephrectomized transgenic F344-hPAP (B) and kidneys isolated on day 14 after F344 to F344-hPAP (C) or DA to F344-hPAP (D) kidney transplantation. Lens magnification 200x. The percentage of hPAP-stained area was quantified by computerized morphometry (E). Bars indicate the mean percentage of hPAP-stained area per group and SEM.*

renal tubular cross-sections containing at least one hPAP+ cell (9.7%) was significantly increased compared to engraftment after F344 to F344-hPAP kidney transplants (4.0%) (Figure 3H). The percentage of recipient-derived tubular cells after DA to F344-hPAP transplantation (0.9%) was increased, albeit not significantly, as compared to the percentage after F344 to F344-hPAP transplantation (0.5%, P=0.0931) (Figure 3I). The extent of recipient-derived cell engraftment did not correlate with the intensity of hPAP+ cell infiltration (not shown).

Renal interstitial myofibroblasts and collagen III deposition

In contralateral F344 (Figure 4A, E) and nephrectomized F344-hPAP (Figure 4B, E) kidneys, α-SMA+ myofibroblasts were sporadically present. F344 to F344-hPAP kidney transplantation elicited compared to contralateral and nephrectomized kidneys, a significant increase in the number of renal interstitial myofibroblasts (Figure 4C, E). A significant increase in renal interstitial myofibroblasts was also observed after DA to F344-hPAP kidney transplantation compared to contralateral DA and nephrectomized
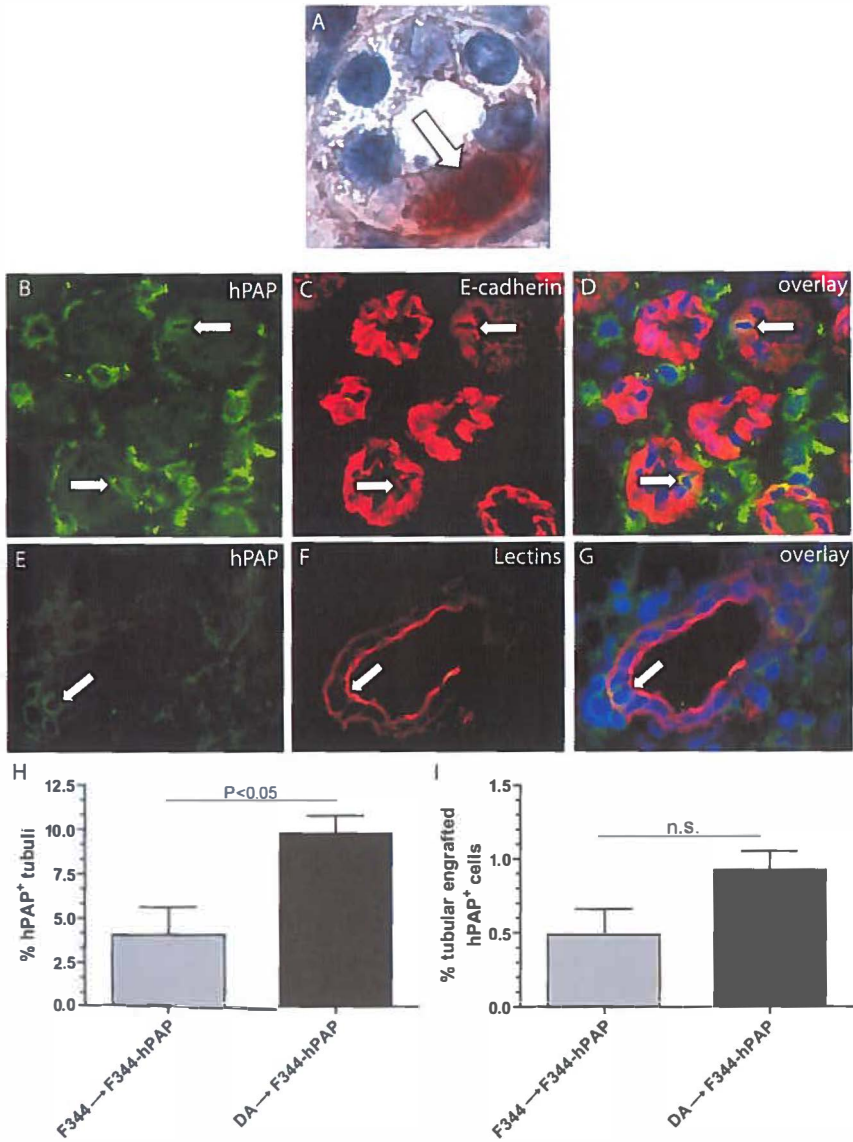
Figure 3. *Tubular epithelial engraftment of recipient-derived cells. hPAP staining was occasionally observed in tubular engrafted cells (A) in kidneys after F344 to F344-hPAP (shown here) and DA to F344-hPAP kidney transplantation. Arrow indicates an example of tubular epithelial recipient-derived cell engraftment. Lens magnification 1000x. Epithelial phenotype of the engrafted recipient-derived cells was demonstrated by double-staining for hPAP (B) and E-cadherin (C). The overlap of signal is shown in the overlay (D). Moreover, tubular engrafted recipient-derived cells (E) expressed tubular epithelial-specific lectins (F). The overlap of signal is shown in the overlay (G). Arrows indicate double-positive cells. Tubular epithelial engraftment of recipient-derived cells was quantified as the percentage of hPAP+ tubuli (H) and as the percentage of hPAP+ tubular engrafted cells (I). Bars indicate the mean percentage of hPAP+ tubuli or of hPAP+ tubular engrafted cells per group and SEM.*

F344-hPAP kidneys (Figure 4D, E). Moreover, the presence of renal interstitial myofibroblasts in the graft was significantly higher after DA to F344-hPAP, compared to F344 to F344-hPAP kidney transplantation (Figure 4E).

Renal interstitial collagen III deposition was similar in the renal interstitium of contralateral F344 kidneys (Figure 4F, J) and nephrectomized F344-hPAP kidneys (Figure 4G, J). After F344 to F344-hPAP kidney transplantation, renal interstitial collagen III deposition was not increased compared to the control kidneys (Figure 4H, J). DA to F344-hPAP kidney transplantation resulted in a significant increase in renal interstitial collagen III deposition compared to contralateral DA kidneys and F344-hPAP nephrectomized kidneys (Figure 4I, J). Moreover, collagen III deposition after DA to F344-hPAP kidney transplantation was significantly increased compared to deposition in F344 to F344-hPAP kidney transplants (Figure 4J).
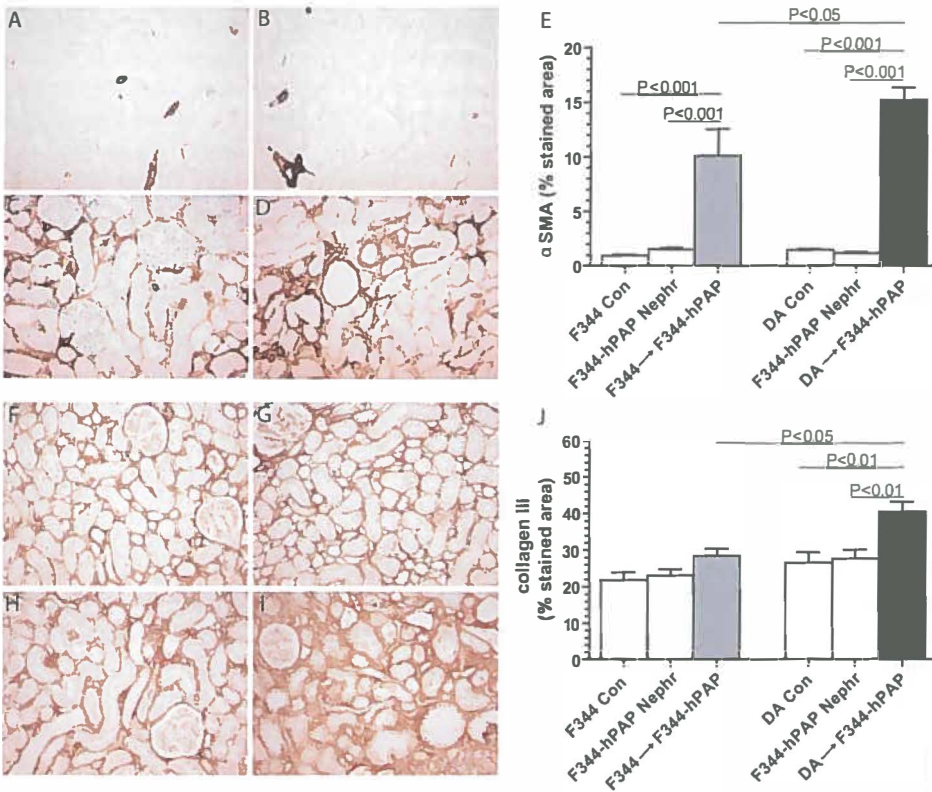
Figure 4. *Renal interstitial myofibroblasts and collagen III deposition. The presence of renal myofibroblasts was detected by staining for a-SMA on a contralateral F344 kidney (A), a nephrectomized F344-hPAP kidney (B) and kidneys isolated on day 14 after F344 to F344-hPAP (C) or DA to F344-hPAP (D) kidney transplantation. Lens magnification 200x. The percentage of α-SMA-stained area was quantified by computerized morphometry (E). Bars indicate the mean percentage of α-SMA-stained area per group and SEM. All α-SMA-positive vascular structures were excluded from quantitative analysis. Renal interstitial collagen III protein deposition is shown in a contralateral F344 kidney (F), a nephrectomized F344-hPAP kidney (G) and kidneys isolated on day 14 after F344 to F344-hPAP (H) or DA to F344-hPAP (I) kidney transplantation. Lens magnification 200x. The percentage of collagen III-stained area was quantified with computerized morphometry (J). Bars indicate the mean percentage of collagen III-stained area per group and SEM. Con = Contralateral, Nephr = Nephrectomized.*

Recipient-derived myofibroblasts

To determine the presence of myofibroblasts originating from extra-renal, i.e. recipient-derived, sources after F344 to F344-hPAP and DA to F344-hPAP kidney transplantation, we used double staining with hPAP, to detect recipient-derived cells (Figure 5A), and α-SMA, to detect myofibroblasts (Figure 5B). After both F344 to F344-hPAP and DA to F344-hPAP kidney transplantation, double-positive, recipient-derived myofibroblasts were observed in the renal interstitium (Figure 5C). In these cells, co-expression of the reporter marker hPAP (FITC) and the myofibroblast marker α-SMA (TRITC) was detected in 8/10 consecutive confocal optical sections of the Z-series, confirming the double-positivity of these cells and excluding the possibility that the two markers were expressed by different, neighboring cells. We expressed the percentage of recipient-derived myofibroblasts in relation to all renal infiltrated recipient-derived cells (Figure 5D) and in relation to all renal myofibroblasts (Figure 5E). Of all interstitial recipient-derived cells, an average of 1.9% after F344 to F344-hPAP transplantation and 2.6% after DA to F344-hPAP transplantation expressed the myofibroblast marker α-SMA (P=0.1775) (Figure 5D). The recipient-derived myofibroblasts constituted up to 28% after F344 to F344-hPAP transplantation and 39% after DA to F344-hPAP transplantation of all renal interstitial myofibroblasts (P=0.2468) (Figure 5E). The presence of recipient-derived myofibroblasts in kidneys after F344 to F344-hPAP and DA to F344-hPAP transplantation were not significantly different (Figure 5D, E).

Discussion

In this study we investigated for the first time tubular engraftment and myofibroblast differentiation of recipient-derived cells in an early window of renal repair and possible onset of fibrosis in a rat model of kidney transplantation. Kidney transplantation resulted in engraftment of recipient-derived cells in the tubular epithelium by day 14 after transplantation. Moreover, recipient-derived myofibroblasts were present in the renal interstitium after transplantation at this time point.

Engraftment and differentiation of recipient-derived cells in human allografts has been studied at long term, but not at short term after transplantation. Yet, using a model of warm IRI, which forms an unavoidable damage hit during transplantation, we previously identified an early window of repair and remodeling, which may determine organ performance. In this model, BMDC sporadically engrafted tubuli (9), while they contributed substantially to the interstitial myofibroblast pool (10). Based on these findings we asked whether, early after transplantation, recipient-derived cells may contribute to tubular epithelial regeneration by tubular engraftment or to the early onset of fibrosis by differentiation to myofibroblasts, in this early time window.

Tubular engraftment of recipient-derived cells was present after both syngeneic and allogeneic transplantation. The low percentage of engrafted tubular cross-sections and engrafted cells observed in this study after syngeneic and allogeneic kidney transplantation was comparable to the sporadic tubular engraftment of BMDC we previously observed after IRI (9). However, in this study, an increased number of tubuliar cross-sections was engrafted by at least one recipient-derived cell after allogeneic transplantation, as compared to syngeneic transplantation. This phenomenon was accompanied by an increased, albeit not significantly, percentage of recipient-derived tubular cells. In the light of our previous results, demonstrating that the severity of
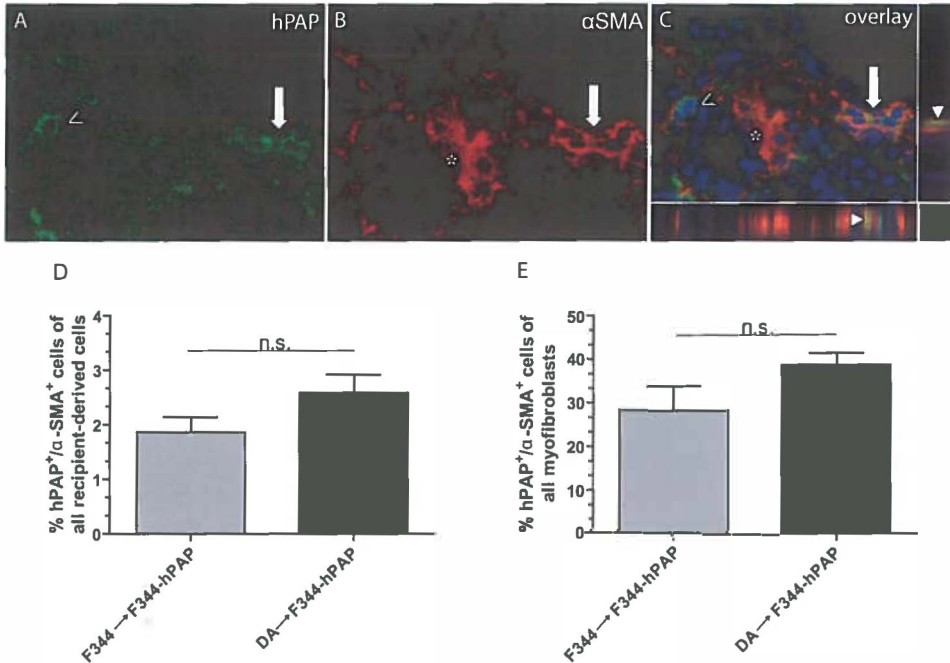
Figure 5. *Recipient-derived myofibroblasts. The presence of recipient-derived myofibroblasts was determined by confocal microscopy of staining for hPAP (FITC) (A) in combination with a-SMA (TRITC) (B) on kidney tissue, isolated on day 14 after transplantation. The overlay shows FITC, TRITC and DAPI channels and the x/z and y/z planes underneath and on the right of the merged picture demonstrate colocalization of the markers (C). Arrow indicates a group of double-positive cells. Open arrowhead indicates hPAP single-positive cell. Asterisk indicates a-SMA single-positive cell. Arrowheads indicate co-expression in the x/z and y/z planes. Co-expression of hPAP and a-SMA was quantified in relation to all renal infiltrated recipient-derived cells (D) and in relation to the renal interstitial myofibroblast population (E). Bars indicate the mean percentage hPAP/a-SMA double-positive cells of all hPAP+ cells or of all a-SMA+ cells per group and SEM.*

6

ischemic damage was associated with an increased number of BMDC-engrafted tubuli (9), it is conceivable that increased tubular damage after allogeneic kidney transplantation accounts for increased tubular engraftment of recipient-derived cells. This concept is in accordance with clinical studies in which the severity of graft damage was shown to correlate with the extent of engraftment of recipient-derived cells in damaged structures (3;5). However, we never observed more than one or occasionally two engrafted recipient-derived cells per tubular cross-section, indicating that the 'per-tubule' amount of damage was similar in both groups. Moreover, the damage inflicted by the combination of ischemia and allogeneic transplantation was possibly amplified by administration of ciclosporin in the allogeneic transplanted rats.

In mouse models of bone marrow transplantation it was shown that BMDC were able to differentiate to myofibroblasts in many tissues, including the gut, lung, and kidney (16-20). Our previous data showed that after an acute ischemic insult, BMDC infiltrated the kidney and, by differentiation to procollagen I-producing myofibroblasts, contributed significantly to the interstitial myofibroblast population (10). Based on these findings, we here asked whether, early after kidney transplantation, recipient-derived cells

derived myofibroblasts were present in the transplanted kidney, constituting up to 40% of all renal interstitial myofibroblasts in both settings. However, after allogeneic transplantation the absolute number of total infiltrating recipient cells is higher than in syngeneic transplanted kidneys. Since this total population of recipient-derived cells comprises myofibroblast progenitors, it is reasonable to conclude that the absolute number of recipient-derived myofibroblasts in the allogeneic transplantation setting is also higher. Regardless of absolute numbers of recipient-derived myofibroblast precursors in the two transplantation settings, the fact that their relative contribution to the interstitial myofibroblast population is similar suggests that the mechanism driving the differentiation of recipient-derived cells towards myofibroblasts must be shared by both settings. Obviously, the quantitative outcome of recipient cell differentiation by this mechanism is higher in the allogeneic transplantation situation, due to increased input of recipient-derived cells in the transplanted kidney. What the impact of this increased population of myofibroblast progenitor cells will be on long-term graft function is not known.

The current study is the first to describe the differentiation fate of recipient-derived cells in the transplanted rat kidney. Using a rat model of kidney transplantation we were able to investigate the short term effects of ischemia-associated (syngeneic) and allogeneic transplantation-associated injury on tubular engraftment and myofibroblast differentiation of recipient-derived cells, in a previously described early window of regeneration and possible onset of renal interstitial fibrosis. Our results indicated that allogeneic transplantation-associated injury, superimposed on ischemic damage, increases tubular engraftment of recipient-derived cells, while it does not affect their relative contribution to the renal interstitial myofibroblast population.

Acknowledgements

References

1) Bai HW, Shi BY, Qian YY, Na YQ, Cai M, Zeng X, Zhong DR, Wu SF, Chang JY, Zhou WQ. Does endothelial chimerism correlate with renal allograft rejection? Transplant Proc 2006 Dec;38(10):3430-3.

2) Grimm PC, Nickerson P, Jeffery J, Savani RC, Gough J, McKenna RM, Stern E, Rush DN. Neointimal and tubulointerstitial infiltration by recipient mesenchymal cells in chronic renal-allograft rejection. N Engl J Med 2001 Jul 12;345(2):93-7.

3) Lagaaij EL, Cramer-Knijnenburg GF, van Kemenade FJ, van Es LA, Bruijn JA, van Krieken JH. Endothelial cell chimerism after renal transplantation and vascular rejection. Lancet 2001 Jan 6;357(9249):33-7.

4) van Poelgeest EP, Baelde HJ, Lagaaij EL, Sijpkens YW, de Heer E, Bruijn JA, Bajema IM. Endothelial cell chimerism occurs more often and earlier in female than in male recipients of kidney transplants. Kidney Int 2005 Aug;68(2):847-53.

5) Sinclair RA. Origin of endothelium in human renal allografts. Br Med J 1972 Oct 7;4(5831):15-6.

6) Gupta S, Verfaillie C, Chmielewski D, Kim Y, Rosenberg ME. A role for extrarenal cells in the regeneration following acute renal failure. Kidney Int 2002 Oct;62(4):1285-90.

7) Mengel M, Jonigk D, Marwedel M, Kleeberger W, Bredt M, Bock O, Lehmann U, Gwinner W, Haller H, Kreipe H. Tubular chimerism occurs regularly in renal allografts and is not correlated to outcome. J Am Soc Nephrol 2004 Apr;15(4):978-86.

8) Poulsom R, Forbes SJ, Hodivala-Dilke K, Ryan E, Wyles S, Navaratnarasah S, Jeffery R, Hunt T, Alison M, Cook T, Pusey C, Wright NA. Bone marrow contributes to renal parenchymal turnover and regeneration. J Pathol 2001 Sep;195(2):229-35.

9) Broekema M, Harmsen MC, Koerts JA, Petersen AH, van Luyn MJ, Navis G, Popa ER. Determinants of tubular bone marrow-derived cell engraftment after renal ischemia/reperfusion in rats. Kidney Int 2005 Dec;68(6):2572-81.

10) Broekema M, Harmsen MC, van Luyn MJ, Koerts JA, Petersen AH, van Kooten TG, van Goor H, Navis G, Popa ER. Bone Marrow-Derived Myofibroblasts Contribute to the Renal Interstitial Myofibroblast Population and Produce Procollagen I after Ischemia/Reperfusion in Rats. J Am Soc Nephrol 2007 Jan;18(1):165-75.

11) Kisseberth WC, Brettingen NT, Lohse JK, Sandgren EP. Ubiquitous expression of marker transgenes in mice and rats. Dev Biol 1999 Oct 1;214(1):128-38.

12) Kunter U, Floege J, von Jurgensonn AS, Stojanovic T, Merkel S, Grone HJ, Ferran C. Expression of A20 in the vessel wall of rat-kidney allografts correlates with protection from transplant arteriosclerosis. Transplantation 2003 Jan 15;75(1):3-9.

13) Marshall T, Williams KM. Total protein determination in urine: elimination of a differential response between the coomassie blue and pyrogallol red protein dye-binding assays. Clin Chem 2000 Mar;46(3):392-8.

14) Guder WG, Hoffmann GE, Hubbuch A, Poppe WA, Siedel J, Price CP. Multicentre evaluation of an enzymatic method for creatinine determination using a sensitive colour reagent. J Clin Chem Clin Biochem 1986 Nov;24(11):889-902.

15) Keppler A, Gretz N, Schmidt R, Kloetzer HM, Groene HJ, Lelongt B, Meyer M, Sadick M, Pill J. Plasma creatinine determination in mice and rats: An enzymatic method compares favorably with a high-performance liquid chromatography assay. Kidney Int 2007 Jan;71(1):74-8.

16) Brittan M, Hunt T, Jeffery R, Poulsom R, Forbes SJ, Hodivala-Dilke K, Goldman J, Alison MR, Wright NA. Bone marrow derivation of pericryptal myofibroblasts in the mouse and human small intestine and colon. Gut 2002 Jun;50(6):752-7.

17) Direkze NC, Forbes SJ, Brittan M, Hunt T, Jeffery R, Preston SL, Poulsom R, Hodivala-Dilke K, Alison MR, Wright NA. Multiple organ engraftment by bone-marrow-derived myofibroblasts and fibroblasts in bone-marrow-transplanted mice. Stem Cells 2003;21(5):514-20.

18) Iwano M, Plieth D, Danoff TM, Xue C, Okada H, Neilson EG. Evidence that fibroblasts derive from epithelium during tissue fibrosis. J Clin Invest 2002 Aug;110(3):341-50.

19) Lin F, Moran A, Igarashi P. Intrarenal cells, not bone marrow-derived cells, are the major source for regeneration in postischemic kidney. J Clin Invest 2005 Jul;115(7):1756-64.

20) Roufosse C, Bou-Gharios G, Prodromidi E, Alexakis C, Jeffery R, Khan S, Otto WR, Alter J, Poulsom R, Cook HT. Bone Marrow-Derived Cells Do Not Contribute Significantly to Collagen I Synthesis in a Murine Model of Renal Fibrosis. J Am Soc Nephrol 2006 Feb 8.

6
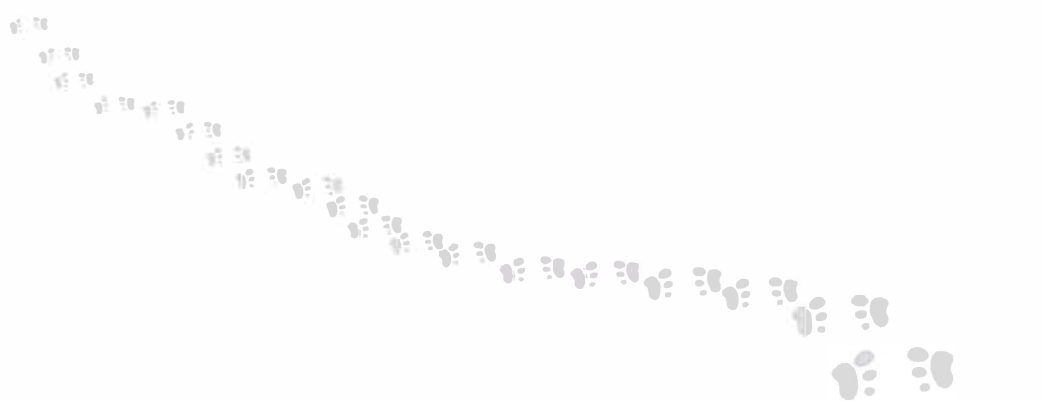
Chapter 7

Decreased Numbers and Partially Impaired Function of Endothelial Progenitor Cells in Kidney Transplant Recipients Early after Transplantation

Eliane R. Popa[1], Martine Broekema[1*], Maartje C. J. Slagman[1*], Jasper A. Koerts[1], Francka J. J. Kloostra[1], Jan-Luuk Hillebrands[3], Marja J. A. van Luyn[1], Willem L. van Son[2], Martin C. Harmsen[1]

[1]Medical Biology Section, Department of Pathology and Laboratory Medicine, [2]Department of Nephrology, [3]Department of Cell Biology, University Medical Center Groningen, University of Groningen, The Netherlands

*Contributed equally

Abstract

Vascular damage in transplanted kidneys may be repaired by engraftment of host endothelial progenitor cells (EPC). However, it is unknown in how far the mobilization and angiogenic function of EPC in kidney transplant recipients early after transplantation (TX) may be affected by previous chronic kidney disease (CKD) and immune suppression. To address this issue we conducted a cross-sectional study in 37 consecutive kidney transplant recipients included ± 14 days after TX, of which 17 patients underwent acute rejection (TX-RX) ± 7 days after TX and 20 patients were complication-free (TX-CF). Twenty-two patients with stage 4 CKD and 22 healthy individuals were included as controls. Circulating CD34-expressing EPC and co-expressing homing receptors VEGFR-2, CXCR4, EPO-R and c-Met were quantified by flow cytometry. The *in vitro* endothelial differentiation capacity of MNC was assessed and transcripts of the E(P)C molecules VE-cadherin, CD31, CD105, VEGFR-2, VEGF-A, eNOS and vWF were identified by RT-PCR. We found decreased numbers and partially impaired function of human EPC at short term after kidney transplantation, and showed that these phenomena are associated with impaired renal function and immune suppression. These findings raise the question whether EPC are able to play a functional role in early vascular repair in kidney grafts.

Introduction

During the peri-transplantation (TX)- and early post-TX period, the kidney (similar to other transplanted solid organs) undergoes a variable amount of damage under the cumulative pressure of insults such as ischemia, inflammation, immune rejection and exposure to immunosuppressive therapy (IST). This damage is reflected by morphological and functional alterations in the graft and sets the scene for the progression of chronic graft failure (1).

In response to acute damage the kidney calls upon a number of innate repair mechanisms, among which proliferation and migration of renal endothelial and epithelial cells, which repopulate denuded areas of these respective tissues (2-4), and extracellular matrix deposition by renal myofibroblasts, which provides structural integrity to the organ (5;6). Moreover, host-derived endothelial, epithelial and myofibroblast cells can be detected in kidney grafts at long time periods after transplantation (7-14), raising the possibility that extra-renal cells may also participate in graft repair. Although the origin of these host-derived cells is under debate, the prevailing scenario states that they are derived from bone marrow stem/progenitor cells. This scenario is corroborated by recent studies that show engraftment of bone marrow-derived cells in various kidney substructures after acute ischemic renal damage (15-18). Importantly, these studies identify an early window of renal bone marrow-derived cell engraftment after acute damage, in which repair is proposed to take place. This early window has received little attention in the setting of clinical and experimental transplantation, where graft repair has been typically studied at long-term follow-up.

In solid organ transplants the primary target of damage is the vasculature, since the endothelium is the first tissue to undergo ischemia, while also forming the interface between the donor organ and the immune system of the host. Indeed, we have shown that graft-derived, circulating endothelial cells, a hallmark of endothelial anoikis, reflect vascular injury in transplanted kidneys (19). Studies in patients with an acute cardiovascular ischemic insult, such as myocardial infarction, have reported a wave of increased mobilization of endothelial progenitor cells (EPC) to the circulation during the first week following the vascular insult (20). These cells can incorporate into regenerating blood vessels and are therefore thought to participate in vascular repair (21-23).

While the phenomenon of EPC mobilization early after graft damage has not been studied in kidney transplant recipients, it is conceivable that, by extrapolation of findings in patients with cardiovascular ischemia, temporary graft ischemia (or acute rejection episodes) should elicit a similar effect. So far, the only indication for mobilization of host-derived EPC is the detection of host-derived endothelial cells in donor vasculature at long term after TX (7;10;13;14). However, a complicating factor in the interpretation of engraftment data in kidney transplant recipients is the finding that a history of chronic kidney disease (CKD), resulting in uremia and long-term exposure to toxic products, is associated with decreased numbers and impaired angiogenic function of EPC (24-30). Thus, it is conceivable that mobilization and angiogenic function in kidney transplant recipients early after TX may be, to an unknown extent, affected by previous CKD.

In the current study we aimed at filling this information gap by investigating numbers and *in vitro* angiogenic function of EPC in kidney transplant recipients at short-term

7

follow-up. To assess the impact of post-TX complications, such as acute rejection, on EPC, patients were stratified by the presence or absence of acute rejection. Moreover, to estimate the impact of a previous history of chronic kidney disease on EPC, patients with stage 4 CKD were included as a control group. To our knowledge, this is the first study documenting EPC numbers and function in kidney transplant recipients in relation to these relevant parameters at short term after TX.

Materials and Methods

Study Groups

In a cross-sectional, prospective study, 17 consecutive renal transplant recipients undergoing biopsy-proven acute graft rejection (TX-AR) were included at 10.5±1.5 days after biopsy, corresponding to 17±2 days after TX (Table 1). All TX-AR patients received a standard immunosuppressive (i.s.) regimen consisting of ciclosporin (CsA; Neoral®, Novartis) (or tacrolimus; Prograf®, Astellas), methylprednisolone and mycophenolate mofetil (MMF; Cellcept®, Roche) (or mycophenolic acid (MPA); Myfortic®, Novartis) supplemented with additional anti-rejection medication consisting of anti-thymocyte globulin, methylprednisolone, or combinations thereof.

Twenty consecutive complication-free renal transplant recipients (TX-CF) (i.e. patients without acute rejection, acute tubulus necrosis or opportunistic infections in the period between transplantation surgery and inclusion) were included at 13±1 days after TX (Table 1). These patients received a standard i.s. regimen (see above). Eleven of these patients were studied again at 146±16 days after TX, after tapering of i.s. medication and/or improvement of kidney function.

Twenty-two consecutive patients with stage 4 chronic renal failure (CKD; mean duration of stage 4 chronic renal failure 57±4 months months, range 9-168 months) were included as controls. These patients had a mean creatinine clearance of 18.1±1.3 ml/min (range 15-29 ml/min) for at least 4 months and thus were uremic. In all study groups, exclusion criteria were the presence of diabetes mellitus, vasculitides or other chronic inflammatory diseases, neoplasms, cardiovascular events and transplantations less than one year prior to kidney TX. Previous medications were continued.

Twenty-two healthy controls (HC; 15 male, 7 female, age 42±3 years) were also included.

The study protocol was approved by the Institutional Review Board of the University Medical Centre Groningen and was consistent with the principles outlined in the Declaration of Helsinki. Informed consent was obtained.

Flow Cytometry

Mononuclear cells (MNC) were isolated from 10 ml of heparinized peripheral blood by lymphoprep density gradient centrifugation (Axis-Shield, Oslo, Norway). Cell counts were performed using Coulter Counter (Beckman Coulter, Mijdrecht, The Netherlands).

CD34-expressing circulating EPC (cEPC) were quantified by flow cytometry (FACScalibur, Becton Dickinson, Sharon, MA), using PERCP-labelled mouse anti-human CD34 monoclonal antibody (moAb) (Becton Dickinson). To assess the expression of homing

Table 1. *Clinical data of kidney transplantation patients*

No.	Clin. Indic.	Gender (m/f)	Age (ys.)	Donor	Isch. t. (min.) c/w	I.s.	C.c. (mL/min.)	$\Delta t_{TX\text{-inclusion}}$ (ds.)	$\Delta t_{TRX\text{-inclusion}}$ (ds.)
1	TX-AR	m	57	LUR	196/50	MMF, CsA, P	36	7	7
2	TX-AR	m	56	LUR	211/52	MPA, CsA, P	31	7	6
3	TX-AR	m	55	NHB	1000/62	MPA, CsA, P	dialysis	40	21
4	TX-AR	m	42	HB	1230/35	MPA, CsA, P	dialysis	16	14
5	TX-AR	m	45	HB	1467/32	MPA, CsA, P	19	19	1
6	TX-AR	m	52	HB	802/49	MMF, CsA, P	21	16	7
7	TX-AR	f	34	HB	30/997	MPA, CsA, P	16	24	12
8	TX-AR	m	18	HB	111/29	MMF, CsA, P	dialysis	14	6
9	TX-AR	m	57	NHB	780/40	MMF, CsA, P	32	64	30
10	TX-AR	f	27	LR	137/43	MPA, CsA, P	dialysis	21	18
11	TX-AR	m	60	NHB	1012/59	MPA, CsA, P	dialysis	15	5
12	TX-AR	m	48	LUR	120/40	MPA, CsA, P	55	14	8
13	TX-AR	m	37	LR	182/51	MPA, CsA, P	81	10	8
14	TX-AR	f	32	HB	796/41	MPA, Tac, P	32	29	7
15	TX-AR	f	68	LUR	150/48	MMF, CsA, P	dialysis	21	13
16	TX-AR	f	28	NHB	u.k	MMF, CsA, P	18	25	9
17	TX-AR	m	41	LR	120/30	MPA, CsA, P	dialysis	9	7
18	TX-CF	f	44	LR	170/45	MMF, CsA, P	72	8	-
19	TX-CF	m	70	HB	1060/40	MMF, CsA, P	63	16	-
19/I	TX-CF						55	126	-
20	TX-CF	m	39	LR	117/41	MMF, CsA, P	47	16	-
20/I	TX-CF						47	113	-
21	TX-CF	m	65	HB	1121/50	MMF, CsA, P	57	16	-
21/I	TX-CF						61	105	-
22	TX-CF	m	41	LR	94/35	MMF, CsA, P	71	16	-
22/I	TX-CF						58	105	-
23	TX-CF	f	48	HB	1440/50	MMF, Tac., P	45	16	-
23/I	TX-CF						49	89	-
24	TX-CF	f	24	LR	144/38	MMF, CsA, P	66	8	-
25	TX-CF	m	67	HB	1590/30	MMF, CsA, P	49	9	-
25/I	TX-CF						65	212	-
26	TX-CF	m	57	LR	176/34	MMF, CsA, P	69	10	-
26/I	TX-CF						64	203	-
27	TX-CF	f	37	HB	1440/42	MMF, CsA, P	38	12	-
27/I	TX-CF						56	77	-
28	TX-CF	m	56	HB	900/34	MMF, CsA, P	76	13	-
28/I	TX-CF						93	213	-
29	TX-CF	m	73	HB	1182/55	MMF, CsA, P	46	14	-
29/I	TX-CF						62	201	-
30	TX-CF	m	65	HB	U.k.	MMF, CsA, P	28	15	-
31	TX-CF	f	46	NHB	801/96	MMF, CsA, P	31	13	-
31/I	TX-CF						46	158	-
32	TX-CF	f	41	HB	28/1084	MMF, CsA, P	43	18	-
33	TX-CF	m	58	LUR	41/149	MMF, CsA, P	61	14	-
34	TX-CF	f	58	LUR	49	MPA, CsA, P	60	14	-
35	TX-CF	m	27	LUR	48	MPA, CsA, P	56	14	-
36	TX-CF	f	58	HB	29	MPA, CsA, P	65	13	-
37	TX-CF	f	47	LUR	120	u.k.	77	49	-

Abbreviations: /I= late re-inclusion (of some TX-CF patients); m: male; f= female; ys.=years; LUR= living unrelated; LR= living related; NHB= non-heartbeating; HB= heartbeating; isch. t= ischemic time; c/w= cold/warm (ischemia); u.k= unknown; i.s.= immune suppression; C.c= creatinine clearance (shown at inclusion); TX=transplantation; RX=rejection; ds= days; MMF= mycophenolate mofetil; CsA= ciclosporin; P= methylprednisolone; MPA= mycophenolic acid; Tac= tacrolimus; Δt = time elapsed between indicated events.

receptors on CD34$^+$ cEPC, double staining for CD34, as described, and VEGFR-2 (mouse anti-human VEGFR-2-biotin, Sigma-Aldrich, St. Louis, USA), CXCR4, (mouse anti-human CXCR4-APC), EPO-R (mouse anti-human EPO-R-PE) or c-Met (mouse anti-human c-Met-biotin; all from R&D Systems, Minneapolis, USA) was performed. As a secondary conjugate we used streptavidin-FITC (DAKO, Glostrup, Denmark). All incubations were performed for 30 min on ice in the dark and were followed by appropriate washing steps. FACS data were analysed using Winlist 5.0 software (Verity, Topsham, ME).

Cell culture

1×10^6 MNC were plated in 24-wells tissue culture plates (Corning Inc., NY, USA) coated with 1% v/v gelatine and 5µg/ml fibronectin (Peprotech, NJ, USA), in RPMI medium containing 20% FCS, 5 µg/mL ECGF, 1 ng/mL VEGF and 10 ng/mL bFGF. Cells were cultured in a humidified incubator at 5% CO_2, 37°C for 6 days, when colony forming units (CFU) were counted. Microscopy was performed using a Leica DMLB microscope, Leica DC300F camera and Leica Qwin 2.8 software (Leica Microsystems, Rijswijk, The Netherlands). Colony size was determined by computer-assisted planimetry, using ImageJ software.

Immunofluorescent stainings

Cultured cells were harvested 6 days after plating, cytospun and double-stained with mouse anti-human CD31 (DAKO) and rabbit anti-eNOS (BD), to assess their endothelial phenotype. DAPI (Sigma-Aldrich) was used as a nuclear dye. Secondary antibodies were donkey anti-mouse-RedX or donkey anti-rabbit-Cy5 (both from Jackson ImmunoResearch, Cambridgeshire, UK). Microscopy equipment was used as described.

RT-PCR

Total RNA was isolated from day 6 cell cultures using the Absolutely RNA Microprep Kit (Stratagene, TX, USA). RNA purity and concentration were measured using Nanodrop equipment (NanoDrop Technologies, NC, USA). After DNase treatment (Absolutely RNA Microprep Kit), copy DNA was synthesized (Kit 1612, Fermentas Vilnius, Lithuania). RT-PCR was performed on a PTC-200 PCR machine (MJ Research Inc, MA, USA), in a final volume of 25 µl, containing 23 µl PCR Master Mix, 1 µl primers for α-SMA and the EC markers VE-cadherin, CD31 (PECAM), CD105 (endoglin), VEGFR-2 (FLK-1), VEGF-A, eNOS, vWF and the housekeeping gene beta-2 microglobulin, and 5 ng cDNA. Amplification conditions were 92 °C for 3 min (denaturation), followed by 35 cycles of 94°C for 45 s (denaturation), 57°C for 45 s (annealing) and 72°C for 1 min (elongation), followed by 72 °C for 3 min. PCR products were visualized on 1% agarose gels by electrophoresis.

Statistics

All statistical analyses were performed using GraphPad Prism 4.0 (GraphPad Software, San Diego California, USA) and SPSS 12.0 software (SPSS Inc., Chicago, USA). One-way ANOVA tests were performed to determine differences between experimental groups.

Differences between paired samples were determined using the Wilcoxon matched pairs test. Pearson or Spearman correlation tests were performed to determine the relationship between different parameters. P-values <0.05 were considered statistically significant. Values exceeding the mean ± 2xSD were excluded from analyses.

Results

Numbers of CD34+ cEPC

Numbers of cEPC were assessed in all groups using flow cytometric analysis of CD34 expression, an accepted marker for cEPC. CD34+ cells were detected within the mononuclear cell gate and typically featured a low side-scatter (not shown).

Healthy controls had an average of 1370 CD34+ cEPC/ml blood (range 800-2360 cells/ml) (Figure 1A). In the TX-AR group, numbers of CD34+ cEPC were app. 4 times lower (mean 350 cells/ml, range 48-1080; P<0.001) than in healthy controls (Figure 1A). Numbers of CD34+ cEPC in TX-AR patients correlated with white blood cell (WBC) numbers (P=0.007; r=0.7).

To test whether the drastic decrease in cEPC numbers in TX-AR patients was attributable to additional immunosuppressive medication (high-dose methylprednisolone, anti-thymocyte globulin), we included a group of TX patients who did not undergo complications after kidney TX (complication-free, TX-CF) and therefore received a standard immunosuppressive regime (CsA, methylprednisolone, MMF or MPA), only. While numbers of cEPC in TX-CF patients were app. 2.5x higher than in TX-AR patients (mean 830 cells/ml blood, range 63-3102, n.s), they were significantly lower than in healthy controls (1.5 times, P<0.01) (Figure 1A). cEPC numbers in TX-CF patients correlated inversely with cold ischemia time (P=0.001; r=-0.68) and positively with warm ischemia time (P=0.0001; r=0.7). Moreover, there was an inverse correlation between cEPC numbers and methylprednisolone dosage (P=0.03; r=-0.44).

Beside the impact of immune suppression on cEPC numbers in TX patients, a history of chronic renal failure has been reported to negatively affect cEPC numbers (24-30). Therefore we included a group of patients with stage 4 renal failure (CKD). Numbers of CD34+ cEPC in this group were significantly lower than in healthy controls (mean 955 cells/ml blood, range 48-1080) (Figure 1A), but significantly higher than in TX-AR patients (2.7 times; Figure 1A). In CKD patients there was a weak inverse correlation between cEPC numbers and serum urea (P=0.04; r=-0.3), but not serum creatinine, creatinine clearance or proteinuria. Moreover, cEPC numbers correlated positively with serum CRP levels (P=0.02; r=0.7) and WBC counts (P=0.02; r=0.4).

To further distinguish between the relative impact of renal function and immunosuppressive medication on cEPC numbers, we followed TX-CF patients longitudinally. Numbers of CD34+ cEPC were reassessed at a mean 146±16 days after TX, if patients had not developed complications (TX-related or other) in the intermittent period and if immune suppression was tapered. Eleven of 18 TX-CF patients fulfilled these criteria. In these patients CsA was significantly tapered in comparison to the first inclusion point from a mean 306 mg/day to a mean 233 mg/day (Figure 1B). Prednisolone was significantly tapered from 18 mg/day to a mean 10 mg/day (Figure 1C). MMF was not tapered. Creatinine clearance improved in 6 of 11 patients but was not significantly higher at long-term follow-up at a group level (Figure 1D). Numbers

7

of CD34+ cEPC were significantly higher at long-term follow-up (mean 1350 cells/ml blood, range 240-3219) than at first inclusion (mean 570 cells/ml blood, range 63-1490) (Figure 1E). cEPC numbers correlated inversely with 24 hour proteinuria (P=0.03; r=-0.54) and serum CRP levels (P=0.01; r=-0.9).

No correlations with relevant parameters (age, gender, duration of disease, weight, use of other medication), other than those reported, were found.
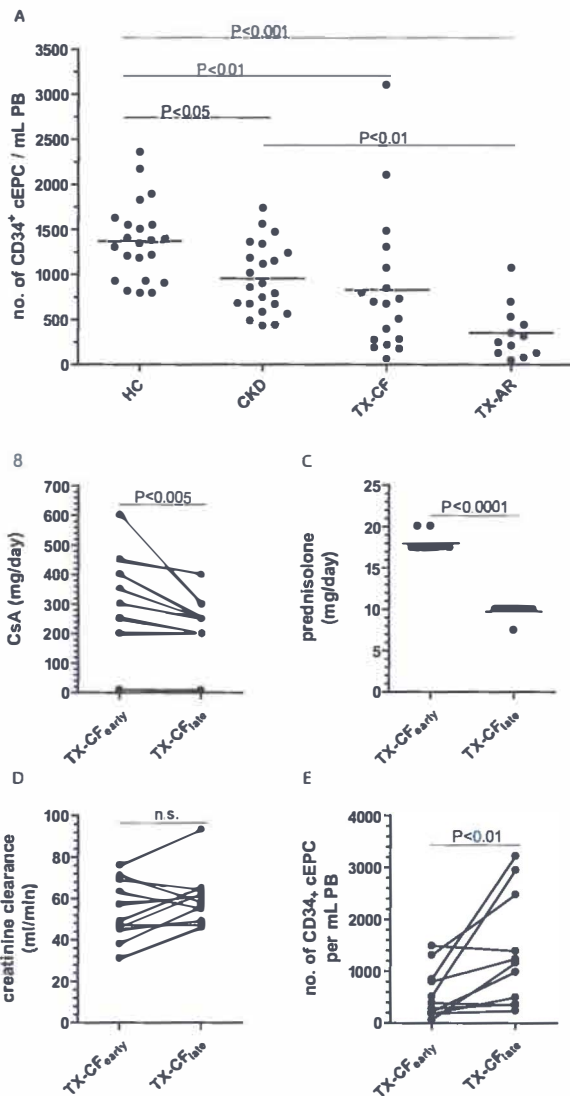
Figure 1: *Numbers of CD34+ cEPC. cEPC were detected in the MNC cell subset by flow cytometric analysis of CD34 expression (A). Patients 12, 14 (TX-AR) and 36, 37 (TX-CF) were excluded from the analysis since they were statistical outliers. Tapering of CsA (B) and prednisolone (C), as well as changes in creatinine clearance (D) and numbers of CD34+ cEPC at long-term follow-up (E) is shown for a subgroup of TX-CF patients followed longitudinally. Dots indicate individual patients, horizontal lines indicate the mean. Abbreviations: HC: healthy controls, CKD: chronic kidney disease; TX-CF: complication-free transplantation patients; TX-AR: transplantation patients with acute rejection.*

Expression of homing receptors on CD34+ cEPC

Since numbers of CD34+ cEPC were significantly lower in TX patients, we asked whether the mobilization of these cells to the circulation was impaired. It has been previously shown that growth factors such as stromal-derived factor-1 (SDF-1), erythropoietin (EPO), vascular endothelial growth factor (VEGF) and hepatocyte growth factor (HGF) can recruit bone marrow-derived cEPC to the circulation (23;31-34). Therefore, we assessed the relative frequency of CD34+ cEPC expressing the corresponding growth factor receptors as a measure of the capacity of these cells to be recruited to the circulation.

In healthy controls, a fraction of CD34+ cells (mean 4.3% of all CD34+ cells, range 1,4-8,6%) expressed CXCR4, the receptor for SDF-1 (Figure 2A). In TX-AR patients, who had the lowest number of CD34+ cells, the percentage of CXCR4+ cells thereof was similar to that in healthy controls (mean 4.0% of CD34+ cells, range 0.5-9.3%) (Figure 2A). The percentage of CD34+/CXCR4+ cells in TX-CF was slightly, albeit not significantly higher than in healthy controls (mean 6.4%, range 0-43.1%) (Figure 2A). In CKD patients the percentage of CXCR4+ cells within the CD34+ cell subset was similar to that in healthy controls (mean 2.3%, range 0.6-4.7%).

Assessment of the relative frequency of EPO-R expressing cells within the CD34+ cell subset again revealed no significant differences between the groups (Figure 2B). The mean percentage of EPO-R+ cells was similar in all groups (85.8% in healthy controls, 78.6% in TX-AR, 80.9% in TX-CF and 80.9% in CKD), with minimum values ranging from 34.73% (CKD) to 79.2% (healthy controls) and maximum values ranging from 90.0% (TX-AR) to 96.5% (TX-CF) (Figure 2B).

More pronounced, albeit not consistently significant differences were present in percentages of CD34+ cells expressing VEGFR-2, the receptor for VEGF-A (Figure 2C). While the frequency of CD34+/VEGFR-2+ cells was comparable in TX-AR patients (mean 12.4%, range 1.6-24.3%) and healthy controls (mean 8.7%, range 4.1-16.2%), the latter was significantly higher than in TX-CF patients (mean 4%, range 1.3-10.7%; $P<0.01$) and CKD patients (mean 5.4%, range 0.3-10.2%; $P<0.05$) (Figure 2C).

Finally, we assessed the percentage of CD34+ cells expressing the HGF receptor c-Met. The mean percentage of c-Met+ cells was similar in healthy controls (mean 4.0%, range 2.7-6.0%), CKD patients (mean 3.1%, range 1.1-6.2%) and TX-CF patients (mean 4.6%, range 0.9-9.1%) (Figure 2D). The percentage of CD34+ cells expressing c-Met was significantly higher in TX-AR patients (mean 10.7%, range 1.6-19.2%) than in healthy controls ($P<0.01$), CKD patients ($P<0.001$) and TX-CF patients ($P<0.01$) (Figure 2D).

In vitro formation of endothelial outgrowth cells

An alternative to phenotypic detection of EPC is their functional characterization as mononuclear cells that can differentiate to endothelial outgrowth cells (EOC) under angiogenic conditions in vitro (35;36).

When cultured under angiogenic conditions for 6 days, MNC from healthy controls developed colonies, as described previously (21). The mean number of colonies in healthy controls (35 colonies/cm^2, range 1.5-61) did not differ significantly from that in TX-AR patients (mean 36 colonies/cm^2, range 0-83.7) or CKD patients (mean 40.5 colonies/cm^2, range 27-81), although in the latter groups the range was larger. In TX-
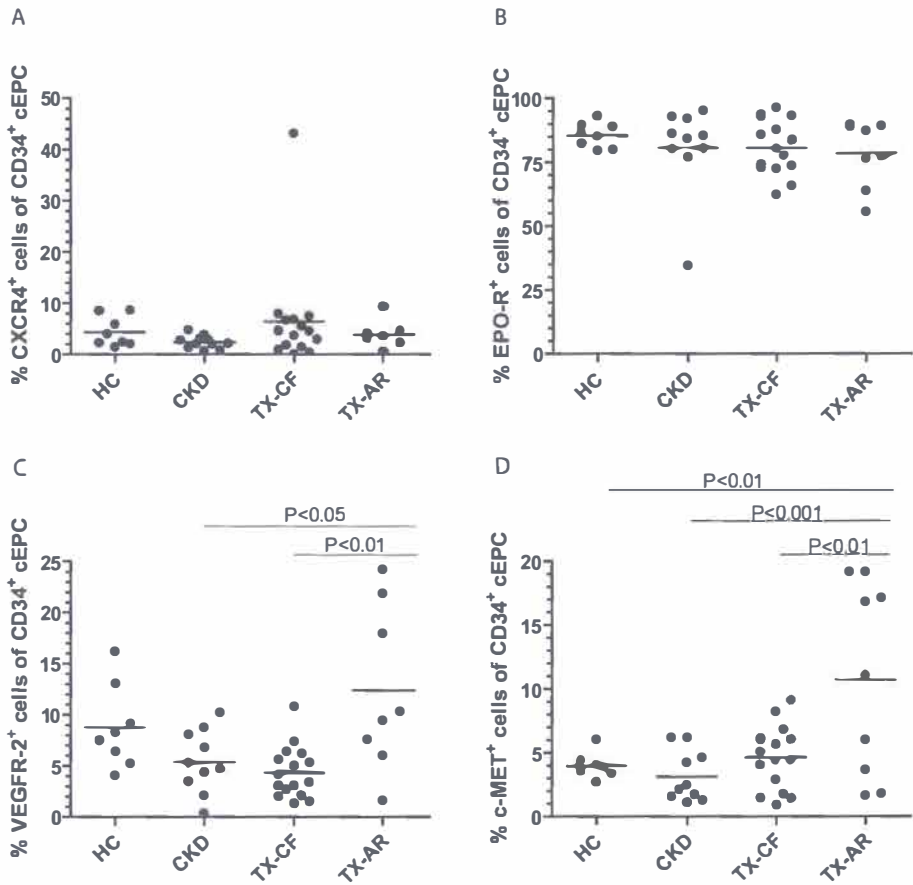
Figure 2: *Expression of homing receptors on CD34⁺ cEPC. The percentage of CD34⁺ cEPC expressing the homing receptors CXCR4 (A), EPO-R (B), VEGFR-2 (C) and c-Met (D) was determined by dual stainings, followed by flow cytometric analysis. Statistical outliers were excluded from graphs (CXCR4: TX-AR # 14, TX-CF #19; EPO-R: TX-AR # 2, 4; VEGFR-2: TX-CF #20; c-MET: TX-CF #20). Dots indicate individual patients, horizontal lines indicate the mean.*

CF patients the number of colonies was app. 3.5 times lower than in healthy controls (mean 10.7 colonies/cm², range 0-32.5), differences with healthy controls or other groups were not statistically significant (Figure 3A).

While the number of colonies did not differ significantly between groups, the morphology and size of colonies clearly indicated lower *in vitro* differentiation capacity of MNC from TX- and CKD patients. MNC from healthy controls formed CFU consisting of spindle-shaped cells (Figure 3B). In CKD patients colonies were smaller in size than in healthy controls, albeit not significantly (Figure 3C,F). Moreover, the typical spindle shape of cells constituting colonies from healthy MNC (Figure 3B) was reduced in CKD colonies (Figure 3C). In TX-CF patients colony size was significantly smaller than in healthy controls (mean 0.01mm², range 0.001-0.03; P<0.05) (Figure 3D,F) and spindle shape of constituting cells was virtually absent (Figure 3D). Similarly, colony size in cultures from TX-AR MNC were significantly smaller than in healthy controls (mean

0.01mm², range 0.004-0.02; P<0.05) (Figure 3E,F) and spindle-shaped cells were absent (Figure 3E). There was no statistical correlation between the number or size of CFU and the number of CD34+ cEPC.

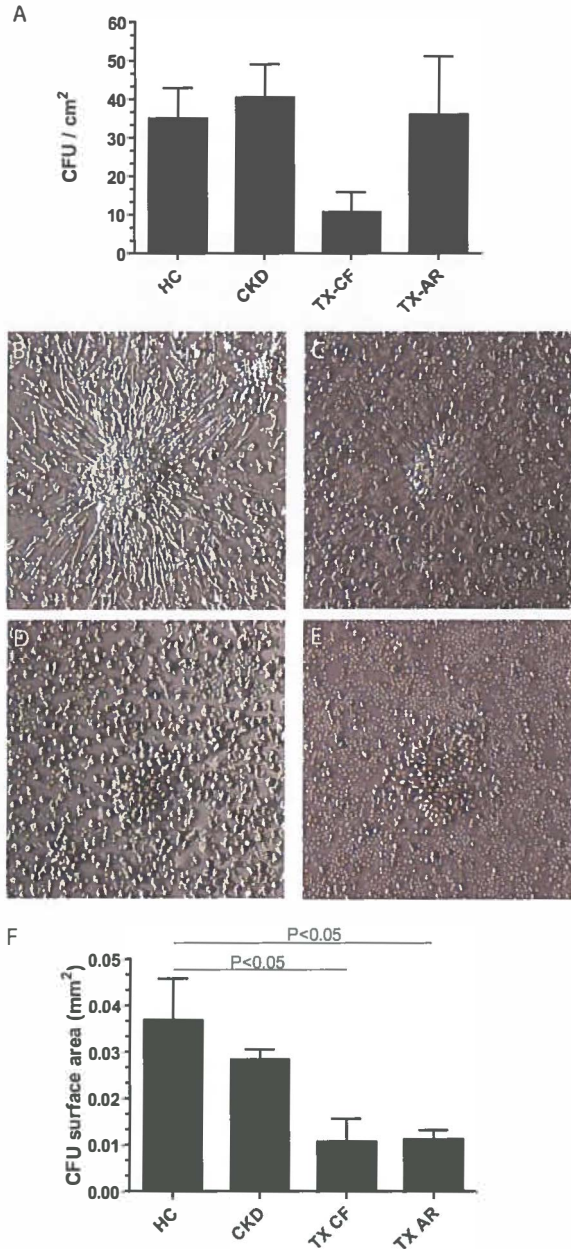**Figure 3:** *In vitro formation of endothelial outgrowth cells. Total MNC were cultured under angiogenic conditions for 7 days, when CFU were quantified (A). CFU from healthy individuals (B), CKD patients (C), TX-CF patients (D) and TX-AR patients (E) differed in morphology and size. CFU size was determined by computer-assisted planimetry (F). Means (bars) and SEM are shown. N=6 individuals/group. Lens magnifications 100x.*

Endothelial characteristics of EOC

EOC from healthy controls were large, flat cells that co-expressed CD31 on the cell membrane and eNOS in intracytoplasmic vesicles (Figure 4B). While EOC from CKD patients were comparable in shape and expression of CD31 and eNOS to healthy EOC (Figure 4C), cells from TX patients retained the morphology of healthy EOC but displayed lower expression of CD31 and eNOS. Moreover, CD31 was no longer confined to the cell membrane but was also detectable in the cytoplasm (not shown). Due to this phenotypic variation of EOC between groups we used morphology as a criterion for quantification. Based on this criterion, numbers of EOC were present at similar frequencies in all groups (Figure 4D).
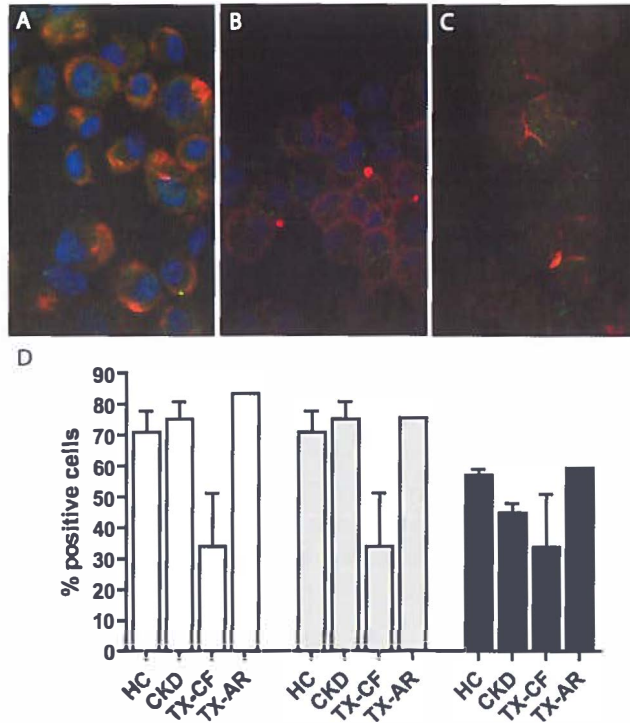
Figure 4: *Endothelial characteristics of EOC. After 7 days of culture under angiogenic conditions, MNC were isolated, cytospun and stained for CD31 (red) and eNOS (green). (A) HUVEC control. (B) MNC from HC. (C) MNC from CKD patients. Lens magnification 400x. Cells expressing CD31 (white bars), eNOS (gray bars) and CD31/eNOS-double positive cells (black bars) were quantified (D). Means (bars) and SEM are shown. Due to poor culture behavior, cells from only 1/5 TX-AR patients could be obtained for staining.*

Since, especially in patients, the number of cultured cells and thus cytospot material for immunophenotyping was limited, we extended our endothelial marker analysis by RT-PCR (Table 2). VEGF transcripts were detected in cultured cells from all healthy controls and CKD patients and in most TX-CF and TX-AR patients. Transcripts for the VEGFR-2 were detected with variable frequency in all groups, confirming previous reports of the instability of this transcript (37). Transcripts of vWF were present in all cultures derived from healthy controls and in all but one cultures from CKD patients,

but only in approximately half of the cultures from TX-CF and TX-AR patients. VE-cadherin was expressed at variable frequency in all groups, while CD105 (endoglin) transcripts were present in all cultures from healthy controls and CKD patients, and in all but one cultures from TX-CF and TX-AR patients. Transcripts for α-SMA were detected in all subjects, irrespective of group (Table 2).

Table 2: *Endothelial transcripts in EOC.*

	HC	CKD	TX-CF	TX-AR
β2M	5/5	6/6	4/4	5/5
αSMA	5/5	6/6	4/4	5/5
VE-cadherin	2/5	3/6	1/4	1/5
CD31 (PECAM)	5/5	5/6	4/4	5/5
CD105 (Endoglin)	5/5	6/6	3/4	4/5
VEGFR-2 (FLK-1)	1/5	5/6	0/4	1/5
VEGF-A	5/5	6/6	3/4	4/5
eNOS	3/5	5/6	1/4	4/5
vWF	5/5	4/6	2/4	3/5

Numbers denote in how many patients out of the total group a transcript was detected by PCR.

Discussion

In the current study, we show decreased numbers and partially impaired function of human EPC at short term after kidney transplantation, and show that these phenomena are associated with impaired renal function and immune suppression.

Based on their vascular engraftment, EPC have been proposed to contribute to blood vessel repair (21-23). Although this contribution is difficult to demonstrate formally, especially in human individuals, EPC are attributed therapeutic value. In conditions associated with acute ischemia (e.g. acute myocardial infarction), EPC are transiently mobilized to the circulation, suggesting that they may be recruited to the site of vascular injury (20). In patients with chronic cardiovascular or renal disease, however, the number and angiogenic capacity of circulating EPC (cEPC) is low (24-30), suggesting that the contribution of these cells to vascular repair may be impaired.

Shortly after transplantation, the donor kidney undergoes vascular damage due to ischemia, immune rejection and immunosuppressive therapy. In this early time window after transplantation, rapid and adequate repair of graft vasculature, e.g. by recipient EPC, is important, since the initial amount of graft damage has been shown to determine long-term graft survival (1). However, kidney recipients typically present with a history of CKD and thus with an impaired EPC compartment (38). Therefore, an assessment of the functional fitness of this compartment during the peri-transplantation period is important and should provide a reflection of the cumulative

7

impact of previous chronic kidney disease, acute ischemia, and immune suppression on EPC quality. Since information on EPC numbers and function in kidney recipients at short-term after transplantation is lacking, the aim of the current study was to study these parameters.

Numbers of EPC, defined as CD34-expressing cells, decreased gradually and significantly with increasing complications (acute rejection and increased immunosuppressive therapy). This decrease appeared to be multifactorial, and probably had its origins in CKD, as suggested by significantly decreased EPC numbers in CKD patients. In these patients, chronic exposure to toxic wastes, particularly to urea, may affect EPC generation or survival, as suggested by the negative correlation between EPC numbers and serum urea. Moreover, the positive correlation between EPC numbers, WBC and CRP suggests an influence of chronic inflammation on EPC.

In complication-free (TX-CF) kidney recipients, EPC numbers were significantly lower than in healthy individuals, but not lower than in CKD patients. Compared to the latter group, TX-CF patients had undergone dialysis prior to transplantation, a procedure that has been associated with fluctuations in numbers of cEPC (24). While dialysis also induces a state of chronic inflammation (39), which, in its turn, may affect EPC, we found no correlations between EPC numbers and inflammatory markers in TX-CF patients, similar to those found in the CKD group. However, it is conceivable that other factors mask the effect of inflammation on EPC in this patient group. Exposure of the graft to acute ischemia may, for instance, lead to increased EPC mobilization, in analogy to acute myocardial ischemia (20). Indeed, EPC numbers in TX-CF patients correlated positively with warm ischemia time, but not with cold ischemia time, suggesting that during reperfusion the graft may start to produce EPC-recruiting chemoattractants that lead to the increased recruitment of EPC.

The group of TX-CF patients allowed us to study possible associations between immunosuppressive treatment and EPC numbers. These patients received a standard immunosuppressive regimen consisting of methylprednisolone, ciclosporin (CsA) and mycophenolate mofetil. While a previous report described the inhibitory effect of CsA on the angiogenic potential of EPC *in vitro* (38), the current patient study could not reveal an association between CsA and EPC numbers. However, EPC numbers did correlate inversely with methylprednisolone dosage. Interestingly, EPC numbers in TX-CF patients at long-term follow-up, when CsA and methylprednisolone were significantly tapered, increased significantly compared to first inclusion at short term after transplantation. Thus, long-term follow-up of TX-CF patients allows us to speculate on the relative impact of ischemia, immunosuppressive therapy, and kidney function on EPC numbers. Since in these patients the period elapsed between the episode of acute ischemia and second inclusion is considerable, and since kidney function was not yet significantly improved at the time point of second inclusion, immunosuppression by methylprednisolone and, possibly, by CsA, is delineated as the most probable cause of decreased EPC numbers. Whether these agents affect the generation or survival of EPC remains to be determined.

In kidney recipients undergoing acute rejection (TX-AR), a dramatic drop in EPC numbers compared to healthy individuals and CKD patients pointed to an altered EPC compartment in the period shortly following transplantation. The effect of immune suppression on EPC was further corroborated by the fact that the dose of

methylprednisolone, which we have proposed to affect EPC numbers, was raised to 1000 mg/day.

While we discussed the possible impact of various factors on EPC numbers, the question remains, which EPC functions are impaired. In the present study, the amount of blood available for experimentation and the number of CD34$^+$ cells therein were limited and did not allow *in vitro* function tests. Therefore, we selected the expression of homing receptors on EPC as a reflection of the homing capacity of these cells, arguing that altered expression patterns may explain the reduced numbers of these cells. Several growth factors have been shown to stimulate recruitment, long- or short-distance migration, and homing of EPC after organ damage, by binding to their receptors on EPC. Among these, SDF-1 and its receptor CXCR4 and EPO/EPO-R elicit increased mobilization of EPC to the circulation when administered systemically (31;33;34). In our study, the percentage of CD34$^+$ cells expressing these receptors was similar in all groups, indicating that the low number of EPC in CKD- and TX patients was not due to alteration in mobilization capacity in response to SDF-1 and EPO. Surprisingly, the percentage of CD34$^+$ cells expressing VEGFR-2 and c-Met, the respective ligands for vascular endothelial growth factor (VEGF) and hepatocyte growth factor (HGF), was significantly higher in TX-AR patients than in the other groups, despite the fact that these patients had the lowest numbers of cEPC. Among other functions, VEGF mediates release of EPC from the bone marrow (23) and long-distance recruitment to the damaged tissue, while HGF, mediates short-distance migration in the tissue (40). The increased percentage of EPC expressing VEGFR-2 and c-Met indicates that recruitment of EPC from the blood into the graft is not a probable reason for the decreased EPC numbers in TX-AR patients. To reconcile decrease numbers of cEPC with increased percentages of VEGFR-2- and c-Met-expressing EPC in this patient group, we propose that, upon cumulative injury by ischemia and acute rejection, the graft releases VEGF and HGF, thus mobilizing increased numbers of EPC. However, immune suppression, superimposed on the previous history of CKD and chronic uremia in the recipient, lead to impaired production of EPC and thus to altogether decreased numbers of cEPC. Interestingly, in TX-AR patients we found a positive correlation between EPC numbers and WBC counts. Despite expression of VEGFR-2 and HGF, this finding suggests that EPC may not be specifically mobilized and recruited upon graft injury, but may rather accompany the inflammatory immune reaction triggered by graft damage and immune incompatibility, as a bystander effect.

Since the number of CD34$^+$ cells was too low to allow isolation and *in vitro* function analysis of these cells, we employed a frequently used alternative strategy to identify cells with angiogenic capacity, i.e. with EPC-like characteristics. According to this strategy, mononuclear cells are cultured under angiogenic conditions, giving rise to colony-forming units (CFU) consisting of cells with spindle-shaped, endothelial-like morphology and expressing endothelial markers (21). This strategy has been formerly used to detect EPC in patients with renal conditions (24-30;38;41-43). Of note, while this strategy allows greater flexibility regarding *in vitro* experimentation, in the current study limitations in numbers of patients fulfilling our inclusion criteria, in blood volume available for experimentation and in numbers of MNC (due to immune suppression), still imposed boundaries on our assays.

No statistical differences in CFU numbers were found between groups, and no correlation was present between CFU number and the number of CD34$^+$ cells, suggesting that the

MNC fraction harbors progenitors of endothelial-like cells that, unlike CD34+ cells, are not affected by the factors discussed above. However, the decreased size and altered morphology of CFU from transplantation patients suggests that the adhesive property of colony-forming cells is impaired in these patients, possibly affecting their engrafting capacity *in vivo*. Interestingly, after 7 days of culture under angiogenic conditions, comparable numbers of cells expressing the endothelial markers CD31 and eNOS were isolated in all groups, indicating that the capacity to differentiate towards endothelial cells was unaffected in transplantation- and CKD patients. Thus, the mononuclear cells fraction harbors a subset of endothelial progenitor cells that, unlike the CD34+ cell subset, appears to be numerically unaffected in transplantation patients and, besides decreased adhesive capacity, displays normal differentiation towards endothelial cells. This subset may consist of monocytes, which have been previously described to display EPC characteristics (44-46).

To our knowledge, this is the first study that investigates numbers and function of EPC in kidney recipients at short term after transplantation. Previous studies have assessed EPC numbers and function in these patients at several months after transplantation, reporting near normal EPC behavior (38;42). Our work complements these studies by showing that early after transplantation, EPC bear the burden of the effects of previous chronic kidney disease, and a high dosage of immunosuppression. We propose that the normal numbers of EPC reported in other studies is due to removal of the chronic uremic environment and tapering of immune suppression. In addition, various studies have reported the presence of endothelial microchimerism in renal allograft biopsies at long term after transplantation (7-14), suggesting that recipient (progenitor) cells participate in vascular repair. Since two definitions of EPC are currently used, i.e. CD34+ cells and MNC with angiogenic properties, and since in the present study we show decreased numbers in the former subset and partially impaired adhesiveness in the latter, a challenging goal for future research will be to determine which recipient cell subset is able to engraft and survive in the donor vasculature at long term.

Acknowledgements

Reference List

1)   Chapman JR, O'Connell PJ, Nankivell BJ. Chronic renal allograft dysfunction. J Am Soc Nephrol 2005 Oct;16(10):3015-26.

2)   Bonventre JV. Dedifferentiation and proliferation of surviving epithelial cells in acute renal failure. J Am Soc Nephrol 2003 Jun;14 Suppl 1:S55-S61.

3)   El Nahas AM. Plasticity of kidney cells: role in kidney remodeling and scarring. Kidney Int 2003 Nov;64(5):1553-63.

4)   Thadhani R, Pascual M, Bonventre JV. Acute renal failure. N Engl J Med 1996 May 30;334(22):1448-60.

5) Gabbiani G, Ryan GB, Majne G. Presence of modified fibroblasts in granulation tissue and their possible role in wound contraction. Experientia 1971 May 15;27(5):549-50.

6) Gabbiani G. The biology of the myofibroblast. Kidney Int 1992 Mar;41(3):530-2.

7) Bai HW, Shi BY, Qian YY, Na YQ, Cai M, Zeng X, Zhong DR, Wu SF, Chang JY, Zhou WQ. Does endothelial chimerism correlate with renal allograft rejection? Transplant Proc 2006 Dec;38(10):3430-3.

8) Grimm PC, Nickerson P, Jeffery J, Savani RC, Gough J, McKenna RM, Stern E, Rush DN. Neointimal and tubulointerstitial infiltration by recipient mesenchymal cells in chronic renal-allograft rejection. N Engl J Med 2001 Jul 12;345(2):93-7.

9) Gupta S, Verfaillie C, Chmielewski D, Kim Y, Rosenberg ME. A role for extrarenal cells in the regeneration following acute renal failure. Kidney Int 2002 Oct;62(4):1285-90.

10) Lagaaij EL, Cramer-Knijnenburg GF, van Kemenade FJ, van Es LA, Bruijn JA, van Krieken JH. Endothelial cell chimerism after renal transplantation and vascular rejection. Lancet 2001 Jan 6;357(9249):33-7.

11) Mengel M, Jonigk D, Marwedel M, Kleeberger W, Bredt M, Bock O, Lehmann U, Gwinner W, Haller H, Kreipe H. Tubular chimerism occurs regularly in renal allografts and is not correlated to outcome. J Am Soc Nephrol 2004 Apr;15(4):978-86.

12) Poulsom R, Forbes SJ, Hodivala-Dilke K, Ryan E, Wyles S, Navaratnarasah S, Jeffery R, Hunt T, Alison M, Cook T, Pusey C, Wright NA. Bone marrow contributes to renal parenchymal turnover and regeneration. J Pathol 2001 Sep;195(2):229-35.

13) Sinclair RA. Origin of endothelium in human renal allografts. Br Med J 1972 Oct 7;4(5831):15-6.

14) van Poelgeest EP, Baelde HJ, Lagaaij EL, Sijpkens YW, de Heer E, 8ruijn JA, Bajema IM. Endothelial cell chimerism occurs more often and earlier in female than in male recipients of kidney transplants. Kidney Int 2005 Aug;68(2):847-53.

15) Broekema M, Harmsen MC, Koerts JA, Petersen AH, van Luyn MJ, Navis G, Popa ER. Determinants of tubular bone marrow-derived cell engraftment after renal ischemia/reperfusion in rats. Kidney Int 2005 Dec;68(6):2572-81.

16) Kale S, Karihaloo A, Clark PR, Kashgarian M, Krause DS, Cantley LG. Bone marrow stem cells contribute to repair of the ischemically injured renal tubule. J Clin Invest 2003 Jul;112(1):42-9.

17) Lin F, Cordes K, Li L, Hood L, Couser WG, Shankland SJ, Igarashi P. Hematopoietic stem cells contribute to the regeneration of renal tubules after renal ischemia-reperfusion injury in mice. J Am Soc Nephrol 2003 May;14(5):1188-99.

18) Lin F, Moran A, Igarashi P. Intrarenal cells, not bone marrow-derived cells, are the major source for regeneration in postischemic kidney. J Clin Invest 2005 Jul;115(7):1756-64.

19) Popa ER, Kas-Deelen AM, Hepkema BG, Van Son WJ, The TH, Harmsen MC. Donor-derived circulating endothelial cells after kidney transplantation. Transplantation 2002 Nov 15;74(9):1320-7.

20) Shintani S, Murohara T, Ikeda H, Ueno T, Honma T, Katoh A, Sasaki K, Shimada T, Oike Y, Imaizumi T. Mobilization of endothelial progenitor cells in patients with acute myocardial infarction. Circulation 2001 Jul 12;103(23):2776-9.

21) Kalka C, Masuda H, Takahashi T, Kalka-Moll WM, Silver M, Kearney M, Li T, Isner JM, Asahara T. Transplantation of ex vivo expanded endothelial progenitor cells for therapeutic neovascularization. Proc Natl Acad Sci U S A 2000 Mar 28;97(7):3422-7.

22) Asahara T, Murohara T, Sullivan A, Silver M, van der Zee R, Li T, Witzenbichler B, Schatteman G, Isner JM. Isolation of putative progenitor endothelial cells for angiogenesis. Science 1997 Feb 14;275(5302):964-7.

23) Asahara T, Takahashi T, Masuda H, Kalka C, Chen D, Iwaguro H, Inai Y, Silver M, Isner JM. VEGF contributes to postnatal neovascularization by mobilizing bone marrow-derived endothelial progenitor cells. EMBO J 1999 Jul 15;18(14):3964-72.

24) Chan CT, Li SH, Verma S. Nocturnal hemodialysis is associated with restoration of impaired endothelial progenitor cell biology in end-stage renal disease. Am J Physiol Renal Physiol 2005 Oct;289(4):F679-F684.

25) Choi JH, Kim KL, Huh W, Kim B, Byun J, Suh W, Sung J, Jeon ES, Oh HY, Kim DK. Decreased number and impaired angiogenic function of endothelial progenitor cells in patients with chronic renal failure. Arterioscler Thromb Vasc Biol 2004 Jul;24(7):1246-52.

26) De Groot K, Bahlmann FH, Sowa J, Koenig J, Menne J, Haller H, Fliser D. Uremia causes endothelial progenitor cell deficiency. Kidney Int 2004 Sep;66(2):641-6.

7

27) Elzawa T, Murakami Y, Matsui K, Takahashi M, Muroi K, Amemiya M, Takano R, Kusano E, Shimada K, Ikeda U. Circulating endothelial progenitor cells are reduced in hemodialysis patients. Curr Med Res Opin 2003;19(7):627-33.

28) Herbrig K, Pistrosch F, Oelschlaegel U, Wichmann G, Wagner A, Foerster S, Richter S, Gross P, Passauer J. Increased total number but impaired migratory activity and adhesion of endothelial progenitor cells in patients on long-term hemodialysis. Am J Kidney Dis 2004 Dec;44(S):840-9.

29) Steiner S, Schaller G, Puttinger H, Fodinger M, Kopp CW, Seidinger D, Grisar J, Horl WH, Minar E, Vychytil A, Wolzt M, Sunder-Plassmann G. History of cardiovascular disease is associated with endothelial progenitor cells in peritoneal dialysis patients. Am J Kidney Dis 2005 Sep;46(3):S20-8.

30) Westerweel PE, Hoefer IE, Blankestijn PJ, de BP, Groeneveld D, van OO, Braam B, Koomans HA, Verhaar MC. End-stage renal disease causes an imbalance between endothelial and smooth muscle progenitor cells. Am J Physiol Renal Physiol 2007 Apr;292(4):F1132-F1140.

31) Bahlmann FH, De Groot K, Spandau JM, Landry AL, Hertel B, Duckert T, Boehm SM, Menne J, Haller H, Fliser D. Erythropoietin regulates endothelial progenitor cells. Blood 2004 Feb 1;103(3):921-6.

32) Fujii K, Ishimaru F, Kozuka T, Matsuo K, Nakase K, Kataoka I, Tabayashi T, Shinagawa K, Ikeda K, Harada M, Tanimoto M. Elevation of serum hepatocyte growth factor during granulocyte colony-stimulating factor-induced peripheral blood stem cell mobilization. Br J Haematol 2004 Jan;124(2):190-4.

33) Moore MA, Hattori K, Heissig B, Shieh JH, Dias S, Crystal RG, Rafii S. Mobilization of endothelial and hematopoietic stem and progenitor cells by adenovector-mediated elevation of serum levels of SDF-1, VEGF, and angiopoietin-1. Ann N Y Acad Sci 2001 Jul;938:36-45.

34) Yamaguchi J, Kusano KF, Masuo O, Kawamoto A, Silver M, Murasawa S, Bosch-Marce M, Masuda H, Losordo DW, Isner JM, Asahara T. Stromal cell-derived factor-1 effects on ex vivo expanded endothelial progenitor cell recruitment for ischemic neovascularization. Circulation 2003 Mar 11;107(9):1322-8.

35) Gulati R, Jevremovic D, Peterson TE, Chatterjee S, Shah V, Vile RG, Simari RD. Diverse origin and function of cells with endothelial phenotype obtained from adult human blood. Circ Res 2003 Nov 28;93(11):1023-5.

36) Lin Y, Weisdorf DJ, Solovey A, Hebbel RP. Origins of circulating endothelial cells and endothelial outgrowth from blood. J Clin Invest 2000 Jan;105(1):71-7.

37) Popa ER, Harmsen MC, Tio RA, van der Strate BW, Brouwer LA, Schipper M, Koerts J, De Jongste MJ, Hazenberg A, Hendriks M, van Luyn MJ. Circulating CD34+ progenitor cells modulate host angiogenesis and inflammation in vivo. J Mol Cell Cardiol 2006 Jul;41(1):86-96.

38) De Groot K, Bahlmann FH, Bahlmann E, Menne J, Haller H, Fliser D. Kidney graft function determines endothelial progenitor cell number in renal transplant recipients. Transplantation 2005 Apr 27;79(8):941-5.

39) Wanner C, Zimmermann J, Schwedler S, Metzger T. Inflammation and cardiovascular risk in dialysis patients. Kidney Int Suppl 2002 May;(80):99-102.

40) Ishizawa K, Kubo H, Yamada M, Kobayashi S, Suzuki T, Mizuno S, Nakamura T, Sasaki H. Hepatocyte growth factor induces angiogenesis in injured lungs through mobilizing endothelial progenitor cells. Biochem Biophys Res Commun 2004 Nov 5;324(1):276-80.

41) Bahlmann FH, DeGroot K, Duckert T, Niemczyk E, Bahlmann E, Boehm SM, Haller H, Fliser D. Endothelial progenitor cell proliferation and differentiation is regulated by erythropoietin. Kidney Int 2003 Nov;64(5):1648-52.

42) Herbrig K, Gebler K, Oelschlaegel U, Pistrosch F, Foerster S, Wagner A, Gross P, Passauer J. Kidney transplantation substantially improves endothelial progenitor cell dysfunction in patients with end-stage renal disease. Am J Transplant 2006 Dec;6(12):2922-8.

43) Steiner S, Winkelmayer WC, Kleinert J, Grisar J, Seidinger D, Kopp CW, Watschinger B, Minar E, Horl WH, Fodinger M, Sunder-Plassmann G. Endothelial progenitor cells in kidney transplant recipients. Transplantation 2006 Feb 27;81(4):599-606.

44) Fujiyama S, Amano K, Uehira K, Yoshida M, Nishiwaki Y, Nozawa Y, Jin D, Takai S, Miyazaki M, Egashira K, Imada T, Iwasaka T, Matsubara H. Bone marrow monocyte lineage cells adhere on injured endothelium in a monocyte chemoattractant protein-1-dependent manner and accelerate reendothelialization as endothelial progenitor cells. Circ Res 2003 Nov 14;93(10):980-9.

45) Rehman J, Li J, Orschell CM, March KL. Peripheral blood "endothelial progenitor cells" are derived from monocyte/macrophages and secrete angiogenic growth factors. Circulation 2003 Mar 4;107(8):1164-9.

46) Urbich C, Heeschen C, Aicher A, Dernbach E, Zeiher AM, Dimmeler S. Relevance of monocytic features for neovascularization capacity of circulating endothelial progenitor cells. Circulation 2003 Nov 18;108(20):2511-6.

7

Chapter 8

General discussion

In this thesis we have investigated the differentiation capacity of bone marrow-derived cells (BMDC) in different models of acute renal injury. Our data showed that, in contrast to what was previously thought, BMDC contribute only marginally to tubular epithelial repopulation. Moreover, we showed that BMDC contributed significantly to the renal interstitial myofibroblast population. In this chapter we will discuss the dual role of BMDC in renal repair and place it in the context of the current understanding of the BMDC. Therefore, the following questions will be addressed;

1. Are BMDC mobilized to the circulation upon kidney injury?
2. Do BMDC home to the injured kidney?
3. Do BMDC differentiate to kidney specific cell types *in vivo*?
4. Which cells from the heterogeneous BMDC population differentiate to kidney specific cell types?

Mobilization of BMDC to the circulation upon kidney injury

For a possible role of BMDC in renal repair by differentiation to renal specific cell types, mobilization of BMDC to the circulation and homing to the injured organ is crucial. We showed an increased number of bone marrow-derived (BMD) progenitor cells, defined as lineage negative (Lin⁻) cells, in the circulation on day 3 after renal ischemia/reperfusion injury (IRI) (*Chapters 3 & 5*) (1). In mice, mobilization of Lin⁻, Sca-1⁺ progenitor cells was reported at 24 hours after IRI in a study by Kale *et al.* (2). The exact composition of the mobilized population of potential progenitor cells in our study and that of Kale needs to be determined. Moreover, the mechanism behind mobilization of BMDC needs to be unraveled. Mobilization is possibly mediated by cytokines that are secreted in large amounts in the inflamed kidney. Several cytokines have been identified that stimulate the mobilization of BMD stem cells, i.e. granulocyte-colony stimulating factor (G-CSF) (3;4), stem cell factor (SCF) (3;5), and granulocyte–macrophage-colony stimulating factor (GM-CSF) (6). Mobilization by G-CSF, the most potent and non-toxic mobilizing agent, was reported to attenuate acute renal failure (7-9) but was also associated with co-mobilization of excessive amounts of granulocytes, resulting in severe worsening of acute renal failure (10). BMDC are released from the bone marrow and mobilized to the circulation by release of proteases and the reduced expression of adhesion molecules on BMDC, e.g. very late antigen-1 (VLA-1) and vascular adhesion molecule-1 (VCAM-1) (11). However, these mobilization mechanisms will not result in specific mobilization of BMD progenitor cells, but inflammatory cells will be mobilized simultaneously. Identification of mobilization mechanisms for specific BMDC subpopulations will allow mobilization of BMDC that can differentiate to tubular epithelial cells without the co-mobilization of inflammatory cells. This approach can be used as a novel therapeutic strategy for renal repair.

Homing of BMDC to the injured kidney

Upon ischemic injury, CD34⁺ progenitor cells were reported to home to the kidney due to decreased expression of stromal cell-derived factor-1 (SDF-1) in the bone marrow and increased SDF-1 in the kidney (12). SDF-1 was also shown to have adverse effects, i.e.

inducing leukocytosis (13) and attracting BMD fibroblasts (14). These findings indicate that SDF-1 does not mediate homing of only CD34+ progenitor cells, but also of other cell types. In our studies, large inflammatory infiltrates were accompanied by BMDC that differentiated towards tubular cells or myofibroblasts. The described mechanisms of mobilization and homing mechanisms for inflammatory cells are also responsible for mobilization and homing of BMD progenitor cells. We speculate that BMD progenitor cells are not specifically recruited and homed to the kidney, but accompany the wave of inflammatory cells that enter the circulation upon renal injury.

Differentiation of BMDC in the injured kidney

Differentiation towards tubular epithelium

Following renal IRI, BMDC engrafted tubuli and expressed tubular epithelial markers (1;2;15-19) (Figure 1). Denudation and disruption of the tubular basement membrane after renal injury might have provided optimal conditions for BMDC to enter the tubule and fill the denuded areas. This was supported by our finding that the extent of tubular BMDC engraftment positively correlated with the severity of post-ischemic renal damage (1). The possibility of migration of cells from the tubular interstitium to the tubular lumen and differentiation was already shown in the opposite direction in a process called epithelial-to-mesenchymal transition (EMT). During EMT, tubular cells respond to injury by loosing their epithelial characteristics, detach from the tubular basal membrane and migrate through the disrupted tubular basal membrane to the renal interstitium where they differentiate to myofibroblasts (20;21).

Interestingly, tubular BMDC engraftment appeared to be a transient process (*Chapter 3*) (1). BMD tubular epithelial cells were possibly cleared by apoptosis during normal epithelial turn-over. In contrast to this finding in rats, tubular engrafted recipient-derived cells were observed in human kidney transplants months after transplantation (19;22;23). The discrepancy between rodent and human models is unclear but can be due to differences in the type of renal injury, the rate of epithelial turn-over or detection techniques.

Our data and those of others indicated that tubular engraftment of BMDC occurred only occasionally, with the number of BMDC-engrafted tubuli ranging between 2 % and 8 % (1;16;19). Although tubular BMDC engraftment was observed only occasional, BMDC might mediate tubular repopulation from within the tubule by secreting growth factors. However, their contribution to repair seems small since, by the time of emerging tubular BMDC engraftment, replacement of damaged tubular cells by proliferation of surviving tubular epithelial cells was already ongoing (*Chapter 3*) (1).

Several factors have been identified that can promote tubular epithelial regeneration in animal models, such as vascular endothelial growth factor (VEGF), hepatocyte growth factor (HGF), insulin-like growth factor-1 (IGF-1), epidermal growth factor (EGF) and fibroblast growth factor (FGF) (24). Possibly, these factors promote epithelial regeneration by increasing BMDC recruitment and homing after injury. This assumption is supported by the finding that HGF is upregulated in serum of healthy humans after G-CSF stem cell mobilization (25). Moreover, VEGF was shown to be involved in recruitment of endothelial progenitor cells (EPC) (26). Although we did not

measure their presence, the increased presence of these growth factors might have caused increased recruitment, homing and tubular engraftment of recipient-derived cells, which we observed after allogeneic kidney transplantation (*Chapter 6*). T cells that infiltrated the allograft might have stimulated tubular engraftment of recipient-derived cells by producing these promoting factors. For example, T cells were shown to produce EGF and FGF and to deliver VEGF to sites of inflammation (27;28). However, increased tubular engraftment by recipient-derived cells might also be explained by the severity of tubular injury after kidney transplantation. This assumption is supported by our previous study in the model of IRI (*Chapter 3*) (1) and by several clinical studies in which the severity of graft damage was associated with increased tubular engraftment of recipient-derived cells (29;30).

BMDC were, upon tubular engraftment, shown to express proximal tubular epithelial-specific proteins, such as cytokeratin (1;15;19), megalin (2), Fx1A (16) or to bind tubular epithelial-specific lectins (1;17-19). This specific protein expression or lectin-binding suggested that BMDC differentiated to tubular epithelial cells. Moreover, expression of adhesion molecules, e.g. e-cadherin (1), and transporter-proteins, e.g. sodium/phosphate transporter type 2 (Na/Pi-2) (16) by BMD tubular epithelial cells indicated that BMD tubular epithelial cells display similar functional properties as resident tubular epithelial cells. Based on these findings BMDC seem capable of mediating renal repair by replacement of tubular cells. Nevertheless, the low numbers and late onset of tubular engraftment of BMDC make the relevance of BMDC in renal repair doubtful.

Differentiation towards myofibroblasts

Since BMDC were reported to differentiate towards myofibroblasts in many tissues (17;21;31-34), the awareness arose that BMDC, by production of ECM, could possibly contribute to the onset of interstitial fibrosis (Figure 1). In *Chapter 4* we showed that BMD myofibroblasts constituted an average 32% of all interstitial myofibroblasts in the post-ischemic kidney (35). Differentiation of BMDC to myofibroblasts preceded tubular engraftment of BMDC and the contribution of BMDC to the myofibroblast population largely exceeded the contribution of BMDC to the tubular epithelial population. Possibly, different BMDC subsets are responsible for differentiation towards myofibroblasts and tubular epithelium and the subset responsible for myofibroblast differentiation exceeds that responsible for epithelial differentiation in number. The observed renal downregulation of the anti-fibrotic bone morphogenetic protein-7 (BMP-7) and upregulation of the pro-fibrotic transforming growth factor-β (TGF-β) (35) could have provided the optimal conditions for this BMDC subset to differentiate to myofibroblasts.

Other pro-fibrotic factors in the renal environment might promote BMD differentiation to myofibroblasts. In *Chapter 5* we studied myofibroblast differentiation of BMDC after administration of the immunosuppressive agent ciclosporin (CsA), which is known for its pro-fibrotic side-effects (36-38). In this study, the profibrotic potential of CsA was shown by increased renal TGF-β expression and interstitial collagen III deposition. However, administration of CsA did not stimulate BMDC differentiation to myofibroblasts in the post-ischemic rat kidney. It is therefore likely that cells other than BMD myofibroblasts were stimulated by CsA to produce TGF-β and ECM. In *Chapter 6*

8
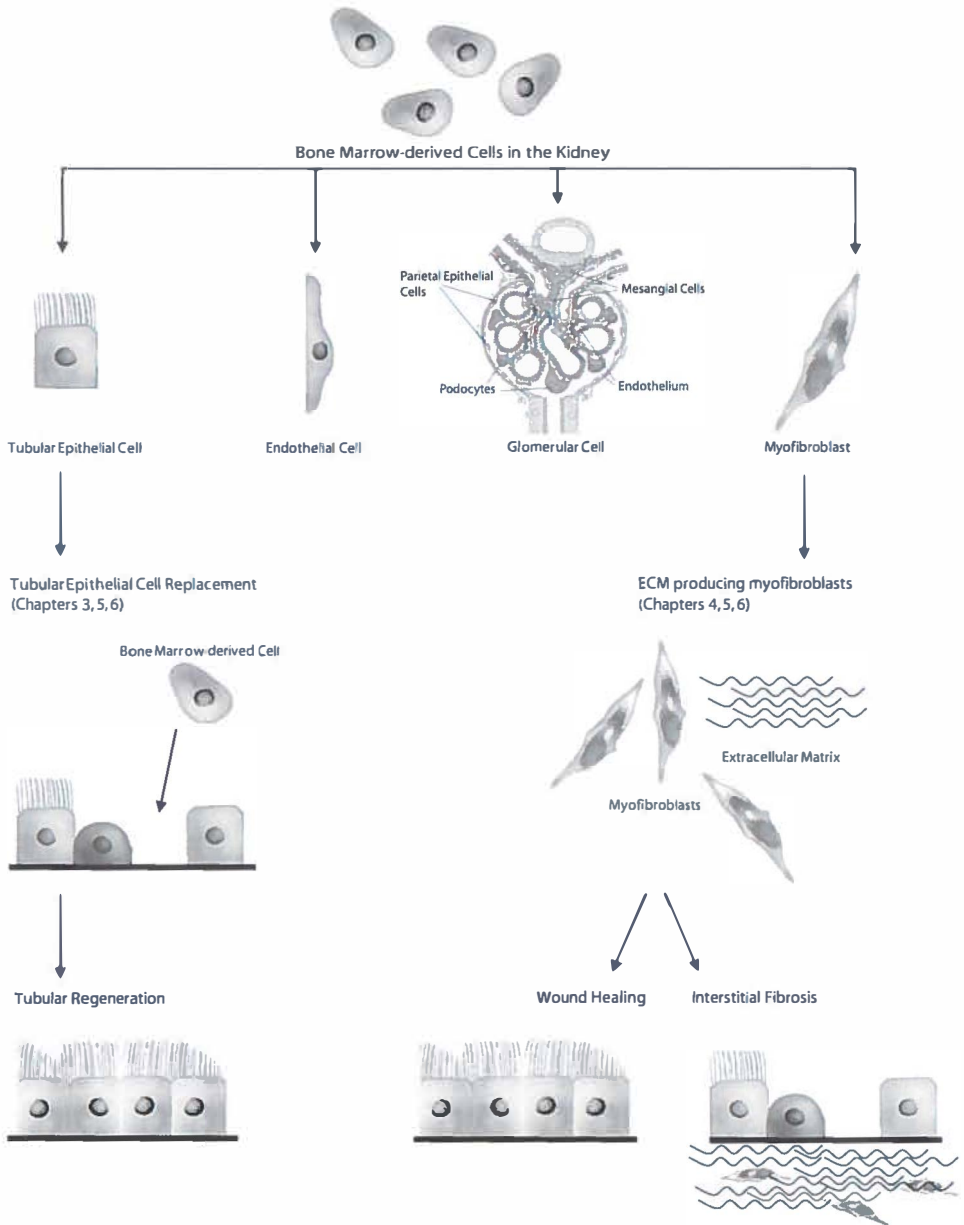
Figure 1. *The role of bone marrow-derived cells in renal repair. Upon infiltration in the injured kidney, BMDC can engraft in and differentiate to tubular epithelial, endothelial and glomerular cells. Moreover, BMDC can infiltrate the interstitium and adopt a myofibroblast phenotype. Tubular epithelial replacement by BMDC can lead to restoration of the tubular epithelium. BMDC myofibroblasts can contribute to tubular repair by wound healing or they can mediate renal scarring by causing the onset of interstitial fibrosis.*

we showed that recipient-derived cell differentiation towards myofibroblast was not promoted after allogeneic kidney transplantation. These allogeneic transplanted rat kidneys were histologically characterized by marked renal infiltration of T cells, which are known to influence the renal environment by secreting soluble factors. Since we did not observe differences in the relative contribution of recipient-derived cells to the myofibroblast population after syn- or allogeneic kidney transplantation, it is not likely that T cell activity and their production of soluble factors influence recipient-derived cell differentiation to myofibroblasts.

Our studies showed that the relative contribution of BMDC or recipient-derived cells to the total renal interstitial myofibroblast population was equal in different injury models with different severity of renal damage (*Chapters 4, 5, 6*). The fact that their relative contribution to the interstitial myofibroblast population is similar in settings with different severity of renal injury, caused by IRI, CsA administration, kidney transplantation or allograft rejection, suggests that the mechanism driving the differentiation of BMDC or recipient-derived cells towards myofibroblasts must be shared by these settings. Nevertheless, BMDC or recipient-derived cells contribute significantly to the interstitial myofibroblast population and might harm renal structure by excessive production of ECM.

The observed expression of α-SMA by renal interstitial BMDC (*Chapter 4*), indicated that these BMDC obtained the contractile properties that are unique for myofibroblasts and vascular smooth muscle cells. We showed that these α-SMA⁺ BMDC produced procollagen I in the post-ischemic kidney, suggesting that BMDC differentiated to myofibroblasts and play an active role in the production of ECM in post-ischemic remodeling (*Chapter 4*) (35). Since in our model of renal IRI is not a model for progressive fibrosis and collagen III deposition was cleared in time, we could not study BMD myofibroblasts in fibrosis. However, Li et al. (39) recently confirmed that BMD myofibroblasts contribute to the development of interstitial fibrosis. This study showed that blockade of the p38 mitogen-activated protein kinase and TGF-β1/Smad signaling pathways, that control the pro-fibrotic action of TGF-β, resulted in a decreased number of BMD myofibroblasts and the attenuation of fibrosis in mice with adriamycine-induced renal fibrosis. The study by Li *et al*. (39) indicates that control of BMDC myofibroblast differentiation, necessary to prevent possible adverse effect of BMDC in therapeutic application, is a feasible option. However, not only the number of BMD myofibroblasts, but that of the resident renal interstitial myofibroblasts was decreased in this study. Since myofibroblasts are essential for wound healing, therapy should be aimed at specific blockade of BMDC differentiation to myofibroblasts.

BMDC populations in the injured kidney

The major question remains which cells of the heterogeneous BMDC population are able to differentiate to renal specific cell types *in vivo*.

In human renal allografts, recipient-derived cells were shown to engraft renal structures and differentiate to renal endothelial and epithelial cells, suggesting that recipient-derived cells mediated repair by replacing damaged graft cells (19;22;23;29;30;40;41). The recipient-derived cells, described in these studies, were assumed to represent

BMDC but can actually be any cell type that was not present in the donor kidney before transplantation.

To investigate if cells from the bone marrow contribute to renal repair, we and others performed bone marrow transplantation in mice or rats to create bone marrow chimeric animals. Since we transplanted whole bone marrow and did not have the tools to distinguish between different BMDC subpopulations, we do not know exactly which cells of the heterogeneous BMDC population are able to differentiate to renal cell types *in vivo*. The majority of the BMDC population that infiltrates the kidney upon injury consists of inflammatory cells, probably accompanied by small subsets of stem- and/or progenitor cells. Several bone marrow stem- and progenitor cells have been identified that possess the capacity to differentiate to renal specific cell types *in vivo*.

The bone marrow contains two stem cell populations, i.e. mesenchymal stem cells (MSC) and the hematopoietic stem cells (HSC), which were reported to contribute to renal repair after acute renal failure. Intravenous infusion of MSC resulted, in contrast to infusion with whole bone marrow (17) and fibroblasts, in functional improvement after glycerol-, cisplatin-, and ischemia/reperfusion-induced acute renal failure (15;18;42-44). Several studies showed that MSC had the potential to engraft and differentiate to tubular epithelial cells, which correlated with functional improvement of the kidney (15;18). Other studies postulated that not engraftment but paracrine actions of MSC, i.e. secretion of renoprotective factors such as VEGF, HGF and IGF-1, were responsible for the observed improvement of renal function (43;44). Functional improvement by paracrine actions of MSC seem feasible mechanisms, since it was also demonstrated in other injury models, such as the hindlimb ischemia model (45;46). Based on these findings, MSC might provide an attractive candidate for therapeutic application after acute renal injury. However, caution is warranted since MSC resemble myofibroblasts in their origin and phenotypical characteristics, suggesting that MSC can easily differentiate towards myofibroblasts. MSC may thereby exert pro-fibrotic rather than regenerative actions, which obviously entails risks. Moreover, the resemblance between MSC and myofibroblasts indicates that the BMDC population, which we showed to differentiate towards myofibroblasts, was derived from MSC.

HSC have also been shown to contribute to post-ischemic tubular regeneration by homing to the injured kidney, engrafting tubular structures and differentiating towards tubular cells in mice (16). These data indicate that HSC might have been part of the BMDC population that differentiated to tubular epithelial cells in our studies.

Circulating endothelial progenitor cells (cEPC) are also part of the BMDC population. EPC are BMDC that are functionally and phenotypically distinct from mature endothelial cells and can differentiate into endothelial cells *in vitro* (47-52). Since in humans the number of cEPC has been shown to correlate with endothelial function and cardiovascular risk (53), the general hypothesis is that a reduction of cEPC results in endothelial dysfunction. We showed in *Chapter 7* that the number of cEPC was decreased in patients with chronic kidney disease. The number of cEPC was further decreased in short term kidney transplant recipients without complications or undergoing acute rejection. Similar data were obtained in other studies, showing reduced numbers of cEPC in patients with different stages of renal failure (54-63). Possibly, long-term exposure of cEPC to uremic toxins during renal failure results in reduced numbers of cEPC. The influence of uremic toxins on cEPC is supported by the fact that improvement of renal function and clearance of uremic toxins after

long-term follow-up in kidney transplant recipients was paralleled by an increase in the number of cEPC (*Chapter 7*). Moreover, other follow-up studies showed that replacement therapy, i.e. dialysis or kidney transplantation, was associated with a normalization of cEPC numbers (55;57;58;61). Since the kidneys of these patients have not been investigated, no causal relationship between reduced cEPC numbers and renal endothelial dysfunction was shown in these studies. Examination of the kidneys of these patients would reveal if the reduction in cEPC after injury reflects increased infiltration of cEPC in the kidney, where EPC can contribute to vascular repair. This is however unlikely, since the reduction of cEPC numbers was not associated with an improvement of renal function.

BMDC differentiation into tubular epithelium or myofibroblasts, which we showed in our studies, possibly represents differentiation of cells from the above mentioned BMDC subpopulations. Identification of the contributors to the BMDC population is necessary to select candidates for therapeutic application in renal repair.

Concluding Remarks

In this thesis we showed that BMDC have the plasticity to differentiate towards tubular epithelium and myofibroblasts (Figure 1). This finding suggests that BMDC might play a dual role in renal repair. BMDC were occasionally shown to engraft the tubular epithelium and differentiate towards tubular epithelial cells (*Chapters 3, 5, 6*), but were largely exceeded by BMDC that infiltrated the renal interstitium and differentiated towards myofibroblasts (*Chapters 4, 5, 6*). By producing ECM BMD myofibroblasts can participate in wound healing, and possibly in the onset of interstitial fibrosis. Identification of the mechanisms that specifically control differentiation of BMDC to myofibroblasts, in order to control and direct this differentiation process, will be important objectives in future studies. Therefore, we propose that, until these mechanisms are identified, the possible therapeutic use of BMDC in patients with renal failure should be approached cautiously.

References

1) Broekema M, Harmsen MC, Koerts JA, Petersen AH, van Luyn MJ, Navis G, Popa ER. Determinants of tubular bone marrow-derived cell engraftment after renal ischemia/reperfusion in rats. Kidney Int 2005 Dec;68(6):2572-81.

2) Kale S, Karihaloo A, Clark PR, Kashgarian M, Krause DS, Cantley LG. Bone marrow stem cells contribute to repair of the ischemically injured renal tubule. J Clin Invest 2003 Jul;112(1):42-9.

3) Orlic D, Kajstura J, Chimenti S, Limana F, Jakoniuk I, Quaini F, Nadal-Ginard B, Bodine DM, Leri A, Anversa P. Mobilized bone marrow cells repair the infarcted heart, improving function and survival. Proc Natl Acad Sci U S A 2001 Aug 2B;98(18):10344-9.

4) de Haan G, Dontje B, Engel C, Loeffler M, Nijhof W. The kinetics of murine hematopoietic stem cells in vivo in response to prolonged increased mature blood cell production induced by granulocyte colony-stimulating factor. Blood 1995 Oct 15;86(8):2986-92.

5) Bodine DM, Seidel NE, Zsebo KM, Orlic D. In vivo administration of stem cell factor to mice increases the absolute number of pluripotent hematopoietic stem cells. Blood 1993 Jul 15;82(2):445-55.

8

6) Brasel K, McKenna HJ, Charrier K, Morrissey PJ, Williams DE, Lyman SD. Flt3 ligand synergizes with granulocyte-macrophage colony-stimulating factor or granulocyte colony-stimulating factor to mobilize hematopoietic progenitor cells into the peripheral blood of mice. Blood 1997 Nov 1;90(9):3781-8.

7) Iwasaki M, Adachi Y, Minamino K, Suzuki Y, Zhang Y, Okigaki M, Nakano K, Koike Y, Wang J, Mukaide H, Taketani S, Mori Y, Takahashi H, Iwasaka T, Ikehara S. Mobilization of bone marrow cells by G-CSF rescues mice from cisplatin-induced renal failure, and M-CSF enhances the effects of G-CSF. J Am Soc Nephrol 2005 Mar;16(3):658-66.

8) Stokman G, Leemans JC, Claessen N, Weening JJ, Florquin S. Hematopoietic stem cell mobilization therapy accelerates recovery of renal function independent of stem cell contribution. J Am Soc Nephrol 2005 Jun;16(6):1684-92.

9) Nishida M, Fujimoto S, Toiyama K, Sato H, Hamaoka K. Effect of hematopoietic cytokines on renal function in cisplatin-induced ARF in mice. Biochem Biophys Res Commun 2004 Nov 5;324(1):341-7.

10) Togel F, Isaac J, Westenfelder C. Hematopoietic stem cell mobilization-associated granulocytosis severely worsens acute renal failure. J Am Soc Nephrol 2004 May;15(5):1261-7.

11) Thomas J, Liu F, Link DC. Mechanisms of mobilization of hematopoietic progenitors with granulocyte colony-stimulating factor. Curr Opin Hematol 2002 May;9(3):183-9.

12) Togel F, Isaac J, Hu Z, Weiss K, Westenfelder C. Renal SDF-1 signals mobilization and homing of CXCR4-positive cells to the kidney after ischemic injury. Kidney Int 2005 May;67(5):1772-84.

13) Hattori K, Heissig B, Rafii S. The regulation of hematopoietic stem cell and progenitor mobilization by chemokine SDF-1. Leuk Lymphoma 2003 Apr;44(4):575-82.

14) Hashimoto N, Jin H, Liu T, Chensue SW, Phan SH. Bone marrow-derived progenitor cells in pulmonary fibrosis. J Clin Invest 2004 Jan;113(2):243-52.

15) Herrera MB, Bussolati B, Bruno S, Fonsato V, Romanazzi GM, Camussi G. Mesenchymal stem cells contribute to the renal repair of acute tubular epithelial injury. Int J Mol Med 2004 Dec;14(6):1035-41.

16) Lin F, Cordes K, Li L, Hood L, Couser WG, Shankland SJ, Igarashi P. Hematopoietic stem cells contribute to the regeneration of renal tubules after renal ischemia-reperfusion injury in mice. J Am Soc Nephrol 2003 May;14(5):1188-99.

17) Lin F, Moran A, Igarashi P. Intrarenal cells, not bone marrow-derived cells, are the major source for regeneration in postischemic kidney. J Clin Invest 2005 Jul;115(7):1756-64.

18) Morigi M, Imberti B, Zoja C, Corna D, Tomasoni S, Abbate M, Rottoli D, Angioletti S, Benigni A, Perico N, Alison M, Remuzzi G. Mesenchymal stem cells are renotropic, helping to repair the kidney and improve function in acute renal failure. J Am Soc Nephrol 2004 Jul;15(7):1794-804.

19) Poulsom R, Forbes SJ, Hodivala-Dilke K, Ryan E, Wyles S, Navaratnarasah S, Jeffery R, Hunt T, Alison M, Cook T, Pusey C, Wright NA. Bone marrow contributes to renal parenchymal turnover and regeneration. J Pathol 2001 Sep;195(2):229-35.

20) Strutz F, Okada H, Lo CW, Danoff T, Carone RL, Tomaszewski JE, Neilson EG. Identification and characterization of a fibroblast marker: FSP1. J Cell Biol 1995 Jul;130(2):393-405.

21) Iwano M, Plieth D, Danoff TM, Xue C, Okada H, Neilson EG. Evidence that fibroblasts derive from epithelium during tissue fibrosis. J Clin Invest 2002 Aug;110(3):341-50.

22) Gupta S, Verfaillie C, Chmielewski D, Kim Y, Rosenberg ME. A role for extrarenal cells in the regeneration following acute renal failure. Kidney Int 2002 Oct;62(4):1285-90.

23) Mengel M, Jonigk D, Marwedel M, Kleeberger W, Bredt M, Bock O, Lehmann U, Gwinner W, Haller H, Kreipe H. Tubular chimerism occurs regularly in renal allografts and is not correlated to outcome. J Am Soc Nephrol 2004 Apr;15(4):978-86.

24) Wang S, Hirschberg R. Role of growth factors in acute renal failure. Nephrol Dial Transplant 1997 Aug;12(8):1560-3.

25) Fujii K, Ishimaru F, Kozuka T, Matsuo K, Nakase K, Kataoka I, Tabayashi T, Shinagawa K, Ikeda K, Harada M, Tanimoto M. Elevation of serum hepatocyte growth factor during granulocyte colony-stimulating factor-induced peripheral blood stem cell mobilization. Br J Haematol 2004 Jan;124(2):190-4.

26) Asahara T, Takahashi T, Masuda H, Kalka C, Chen D, Iwaguro H, Inai Y, Silver M, Isner JM. VEGF contributes to postnatal neovascularization by mobilizing bone marrow-derived endothelial progenitor cells. EMBO J 1999 Jul 15;18(14):3964-72.

27) Yamagishi S, Matsui T, Nakamura K, Yoshida T, Shimizu K, Takegami Y, Shimizu T, Inoue H, Imaizumi T. Pigment-epithelium-derived factor (PEDF) inhibits angiotensin-II-induced vascular endothelial growth factor (VEGF) expression in MOLT-3 T cells through anti-oxidative properties. Microvasc Res 2006 May;71(3):222-6.

28) Workalemahu G, Foerster M, Kroegel C. Expression and synthesis of fibroblast growth factor-9 in human gammadelta T-lymphocytes. Response to isopentenyl pyrophosphate and TGF-beta1/IL-15. J Leukoc Biol 2004 Apr;75(4):657-63.

29) Lagaaij EL, Cramer-Knijnenburg GF, van Kemenade FJ, van Es LA, Bruijn JA, van Krieken JH. Endothelial cell chimerism after renal transplantation and vascular rejection. Lancet 2001 Jan 6;357(9249):33-7.

30) Sinclair RA. Origin of endothelium in human renal allografts. Br Med J 1972 Oct 7;4(5831):15-6.

31) Brittan M, Hunt T, Jeffery R, Poulsom R, Forbes SJ, Hodivala-Dilke K, Goldman J, Alison MR, Wright NA. Bone marrow derivation of pericryptal myofibroblasts in the mouse and human small intestine and colon. Gut 2002 Jun;50(6):752-7.

32) Direkze NC, Forbes SJ, Brittan M, Hunt T, Jeffery R, Preston SL, Poulsom R, Hodivala-Dilke K, Alison MR, Wright NA. Multiple organ engraftment by bone-marrow-derived myofibroblasts and fibroblasts in bone-marrow-transplanted mice. Stem Cells 2003;21(5):514-20.

33) Roufosse C, Bou-Gharios G, Prodromidi E, Alexakis C, Jeffery R, Khan S, Otto WR, Alter J, Poulsom R, Cook HT. Bone Marrow-Derived Cells Do Not Contribute Significantly to Collagen I Synthesis in a Murine Model of Renal Fibrosis. J Am Soc Nephrol 2006 Feb 8.

34) Deb A, Wang SH, Skelding K, Miller D, Simper D, Caplice N. Bone marrow-derived myofibroblasts are present in adult human heart valves. J Heart Valve Dis 2005 Sep;14(5):674-8.

35) Broekema M, Harmsen MC, van Luyn MJ, Koerts JA, Petersen AH, van Kooten TG, van Goor H, Navis G, Popa ER. Bone Marrow-Derived Myofibroblasts Contribute to the Renal Interstitial Myofibroblast Population and Produce Procollagen I after Ischemia/Reperfusion in Rats. J Am Soc Nephrol 2007 Jan;18(1):165-75.

36) Andoh TF, Burdmann EA, Bennett WM. Nephrotoxicity of immunosuppressive drugs: experimental and clinical observations. Semin Nephrol 1997 Jan;17(1):34-45.

37) Calne RY, White DJ, Thiru S, Evans DB, McMaster P, Dunn DC, Craddock GN, Pentlow BD, Rolles K. Cyclosporin A in patients receiving renal allografts from cadaver donors. Lancet 1978 Dec 23;2(8104-5):1323-7.

38) de Mattos AM, Olyaei AJ, Bennett WM. Nephrotoxicity of immunosuppressive drugs: long-term consequences and challenges for the future. Am J Kidney Dis 2000 Feb;35(2):333-46.

39) Li J, Deane JA, Campanale NV, Bertram JF, Ricardo SD. The contribution of bone marrow-derived cells to the development of renal interstitial fibrosis. Stem Cells 2007 Mar;25(3):697-706.

40) Bai HW, Shi BY, Qian YY, Na YQ, Cai M, Zeng X, Zhong DR, Wu SF, Chang JY, Zhou WQ. Does endothelial chimerism correlate with renal allograft rejection? Transplant Proc 2006 Dec;38(10):3430-3.

41) van Poelgeest EP, Baelde HJ, Lagaaij EL, Sijpkens YW, de Heer E, Bruijn JA, Bajema IM. Endothelial cell chimerism occurs more often and earlier in female than in male recipients of kidney transplants. Kidney Int 2005 Aug;68(2):847-53.

42) Duffield JS, Park KM, Hsiao LL, Kelley VR, Scadden DT, Ichimura T, Bonventre JV. Restoration of tubular epithelial cells during repair of the postischemic kidney occurs independently of bone marrow-derived stem cells. J Clin Invest 2005 Jul;115(7):1743-55.

43) Togel F, Hu Z, Weiss K, Isaac J, Lange C, Westenfelder C. Administered mesenchymal stem cells protect against ischemic acute renal failure through differentiation-independent mechanisms. Am J Physiol Renal Physiol 2005 Feb 15.

44) Togel F, Weiss K, Yang Y, Hu Z, Zhang P, Westenfelder C. Vasculotropic, paracrine actions of infused mesenchymal stem cells are important to the recovery from acute kidney injury. Am J Physiol Renal Physiol 2007 Jan 9.

45) Kinnaird T, Stabile E, Burnett MS, Shou M, Lee CW, Barr S, Fuchs S, Epstein SE. Local delivery of marrow-derived stromal cells augments collateral perfusion through paracrine mechanisms. Circulation 2004 Mar 30;109(12):1543-9.

46) Kinnaird T, Stabile E, Burnett MS, Lee CW, Barr S, Fuchs S, Epstein SE. Marrow-derived stromal cells express genes encoding a broad spectrum of arteriogenic cytokines and promote in vitro and in vivo arteriogenesis through paracrine mechanisms. Circ Res 2004 Mar 19;94(5):678-85.

8

47)   Asahara T, Murohara T, Sullivan A, Silver M, van der Zee R, Li T, Witzenbichler B, Schatteman G, Isner JM. Isolation of putative progenitor endothelial cells for angiogenesis. Science 1997 Feb 14;275(5302):964-7.

48)   Gehling UM, Ergun S, Schumacher U, Wagener C, Pantel K, Otte M, Schuch G, Schafhausen P, Mende T, Kilic N, Kluge K, Schafer B, Hossfeld DK, Fiedler W. In vitro differentiation of endothelial cells from AC133-positive progenitor cells. Blood 2000 May 15;95(10):3106-12.

49)   Hur J, Yoon CH, Kim HS, Choi JH, Kang HJ, Hwang KK, Oh BH, Lee MM, Park YB. Characterization of two types of endothelial progenitor cells and their different contributions to neovasculogenesis. Arterioscler Thromb Vasc Biol 2004 Feb;24(2):288-93.

50)   Peichev M, Naiyer AJ, Pereira D, Zhu Z, Lane WJ, Williams M, Oz MC, Hicklin DJ, Witte L, Moore MA, Rafii S. Expression of VEGFR-2 and AC133 by circulating human CD34(+) cells identifies a population of functional endothelial precursors. Blood 2000 Feb 1;95(3):952-8.

51)   Quirici N, Soligo D, Caneva L, Servida F, Bossolasco P, Deliliers GL. Differentiation and expansion of endothelial cells from human bone marrow CD133(+) cells. Br J Haematol 2001 Oct;115(1):186-94.

52)   Yin AH, Miraglia S, Zanjani ED, Almeida-Porada G, Ogawa M, Leary AG, Olweus J, Kearney J, Buck DW. AC133, a novel marker for human hematopoietic stem and progenitor cells. Blood 1997 Dec 15;90(12):5002-12.

53)   Hill JM, Zalos G, Halcox JP, Schenke WH, Waclawiw MA, Quyyumi AA, Finkel T. Circulating endothelial progenitor cells, vascular function, and cardiovascular risk. N Engl J Med 2003 Feb 13;348(7):593-600.

54)   Bahlmann FH, DeGroot K, Duckert T, Niemczyk E, Bahlmann E, Boehm SM, Haller H, Fliser D. Endothelial progenitor cell proliferation and differentiation is regulated by erythropoietin. Kidney Int 2003 Nov;64(5):1648-52.

55)   Chan CT, Li SH, Verma S. Nocturnal hemodialysis is associated with restoration of impaired endothelial progenitor cell biology in end-stage renal disease. Am J Physiol Renal Physiol 2005 Oct;289(4):F679-F684.

56)   Choi JH, Kim KL, Huh W, Kim B, Byun J, Suh W, Sung J, Jeon ES, Oh HY, Kim DK. Decreased number and impaired angiogenic function of endothelial progenitor cells in patients with chronic renal failure. Arterioscler Thromb Vasc Biol 2004 Jul;24(7):1246-52.

57)   De Groot K, Bahlmann FH, Sowa J, Koenig J, Menne J, Haller H, Fliser D. Uremia causes endothelial progenitor cell deficiency. Kidney Int 2004 Sep;66(2):641-6.

58)   De Groot K, Bahlmann FH, Bahlmann E, Menne J, Haller H, Fliser D. Kidney graft function determines endothelial progenitor cell number in renal transplant recipients. Transplantation 2005 Apr 27;79(8):941-5.

59)   Eizawa T, Murakami Y, Matsui K, Takahashi M, Muroi K, Amemiya M, Takano R, Kusano E, Shimada K, Ikeda U. Circulating endothelial progenitor cells are reduced in hemodialysis patients. Curr Med Res Opin 2003;19(7):627-33.

60)   Herbrig K, Pistrosch F, Oelschlaegel U, Wichmann G, Wagner A, Foerster S, Richter S, Gross P, Passauer J. Increased total number but impaired migratory activity and adhesion of endothelial progenitor cells in patients on long-term hemodialysis. Am J Kidney Dis 2004 Dec;44(5):840-9.

61)   Herbrig K, Gebler K, Oelschlaegel U, Pistrosch F, Foerster S, Wagner A, Gross P, Passauer J. Kidney transplantation substantially improves endothelial progenitor cell dysfunction in patients with end-stage renal disease. Am J Transplant 2006 Dec;6(12):2922-8.

62)   Steiner S, Schaller G, Puttinger H, Fodinger M, Kopp CW, Seidinger D, Grisar J, Horl WH, Minar E, Vychytil A, Wolzt M, Sunder-Plassmann G. History of cardiovascular disease is associated with endothelial progenitor cells in peritoneal dialysis patients. Am J Kidney Dis 2005 Sep;46(3):520-8.

63)   Steiner S, Winkelmayer WC, Kleinert J, Grisar J, Seidinger D, Kopp CW, Watschinger B, Minar E, Horl WH, Fodinger M, Sunder-Plassmann G. Endothelial progenitor cells in kidney transplant recipients. Transplantation 2006 Feb 27;81(4):599-606.

8

Chapter 9

Nederlandse samenvatting voor niet-ingewijden

Nierfalen

Bij nierfalen zijn de nieren niet in staat om afvalstoffen en overtollig vocht uit het lichaam te verwijderen. In zulke gevallen kan door middel van dialyse of niertransplantatie de nierfunctie vervangen worden. Momenteel zijn er echter geen therapiëen beschikbaar die de schade aan de nier zelf kunnen herstellen. Het onderzoek beschreven in dit proefschrift richt zich op de mogelijkheid om herstel van beschadigde nieren te bewerkstelligen.

De nier kan beschouwd worden als een afvalverwerkingsbedrijf in het lichaam. Dankzij de ongeveer 1 miljoen filtratie-eenheden, de nefronen, waaruit de nier bestaat, plassen wij dagelijks zo'n 1000-2500 ml urine met daarin diverse afvalstoffen uit. Elk nefron is opgebouwd uit een kluwen van haarvaatjes, de glomerulus, met daarop aansluitend een buisvormig systeem, de tubulus, die uitmondt in de verzamelbuis. De verzamelbuis staat in verbinding met de urineleider en de blaas (Figuur 1). In de glomerulus vindt de filtratie van het bloed plaats. Afvalstoffen en overtollig vocht worden uit het bloed gefilterd en via de tubulus verder vervoerd richting urineleider. Alvorens het daar aankomt worden er door de cellen van de tubulus, de tubulaire epitheelcellen, grote hoeveelheden water en stoffen die voor het lichaam behouden moeten blijven, opgenomen en teruggetransporteerd naar de bloedbaan. Het resterende filtraat zal als urine via de blaas het lichaam verlaten. Dit filtratiesysteem functioneert dusdanig dat grote moleculen, zoals eiwitten, niet in de urine terechtkomen. Wanneer schade aan de nier optreedt kan er "lekkage" van eiwitten naar de urine optreden, waardoor kostbare stoffen voor het lichaam verloren gaan. Lekkage van eiwitten kan bovendien de afvoerbuisjes beschadigen, waardoor nierfunctieverlies optreedt en het lichaam vergiftigd wordt met afvalstoffen.
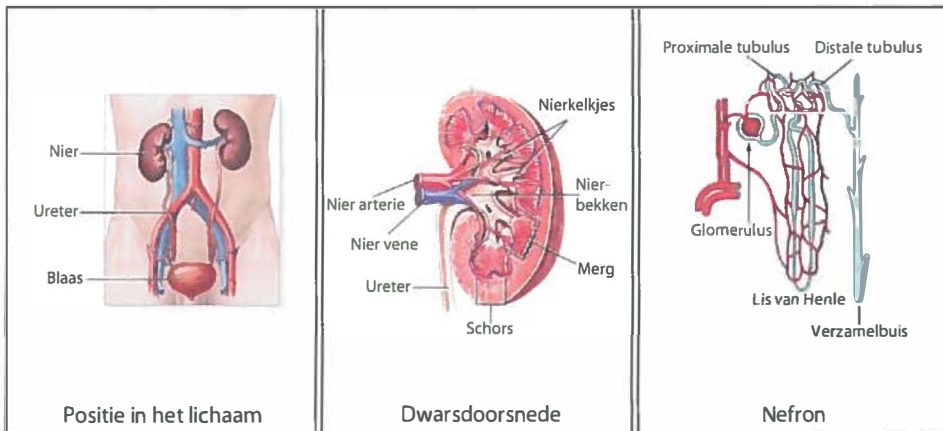
Figuur 1. *De nier*

Fibrose

Een van de mogelijke oorzaken van nierfalen is fibrose. Men spreekt van nierfibrose wanneer er overmatige hoeveelheden bindweefsel worden gevormd in de nier,

waardoor de nier zijn functie niet meer goed kan uitoefenen. Myofibroblasten zijn cellen die bindweefsel-eiwitten produceren en daardoor betrokken zijn bij het ontstaan van fibrose. Myofibroblasten hebben echter normaliter een nuttige rol, omdat bindweefselformatie ook onmisbaar is voor wondheling.

Interne herstelmechanismen van de nier

De nier is in staat om, tot op zekere hoogte, te herstellen na schade. Dit is mogelijk door twee mechanismen. Ten eerste kunnen cellen van de tubulus die de schade hebben overleefd zich vermeerderen en vervolgens verplaatsen naar plaatsen waar cellen door schade verdwenen zijn om daar deze "gaten" op te vullen. In de tweede plaats maakt de nier extra bindweefsel aan na schade. Dit proces wordt wondheling genoemd en zorgt ervoor dat de structuur van de nier behouden blijft. Als er te veel bindweefsel wordt gevormd, treedt fibrose op (zie hierboven). Normaal gesproken functioneren deze interne herstelmechanismen dusdanig dat de nier na veel vormen van schade volledig zal herstellen. Bij zeer ernstige schade kan echter het herstelmechanisme van de nier te kort schieten, waardoor nierschade, en verlies van nierfunctie resteert. Bij een zeer slechte nierfunctie is kunstnierbehandeling (dialyse) noodzakelijk is om te overleven. Nadeel daarvan is dat weliswaar de nierfunctie wordt overgenomen door de kunstnier, maar dat de eigen nierschade niet hersteld wordt. Gelukkig is vaak transplantatie mogelijk, waardoor de patiënt weer nierfunctie heeft. Zowel bij dialyse als bij transplantatie kunnen echter complicaties optreden, en de sterfte is dan ook hoger dan in de gezonde populatie. Voor transplantatie bestaat bovendien een lange wachtlijst door het tekort aan donor-organen.

Therapie die herstel van ernstige nierschade kan bewerkstelligen zou daarom een grote vooruitgang zijn, en in ons onderzoek willen wij een bijdrage leveren aan het ontwikkelen daarvan.

Mogelijke rol van beenmergafkomstige cellen in nierherstel na schade

In dit proefschrift onderzoeken we de mogelijke rol van cellen uit het beenmerg in het herstel van de nier na nierschade. Het beenmerg is de sponsachtig rode substantie die zich bevindt in het binnenste van botten; in deze substantie bevinden zich de zogenaamde stamcellen. Dit zijn cellen waaruit zich allerlei verschillende soorten cellen kunnen ontwikkelen. Naast het vormen van botweefsel is het vormen van bloedcellen een belangrijke functie van het beenmerg. Witte bloedlichaampjes (leukocyten), rode bloedlichaampjes (erythrocyten) en bloedplaatjes (thrombocyten), worden gemaakt uit de bloedvormende, hematopoietische, stamcellen die zich in het beenmerg bevinden. Botweefsel wordt gevormd uit een andere type stamcellen dat zich ook in het beenmerg bevindt, namelijk de mesenchymale stamcellen. Hematopoietische en mesenchymale stamcellen kunnen niet alleen bloed-cellen en botcellen vormen, maar ze kunnen zich ook specialiseren (= differentiëren) tot weefsel-specifieke cellen, zoals niercellen. Men neemt aan dat stamcellen in het beenmerg na schade van een orgaan een signaal krijgen waardoor ze losgemaakt worden uit het beenmerg en zich, via de bloedbaan verplaatsen, naar de plaats van de schade. In het geval van nierschade is de hypothese (veronderstelling) dat beenmergafkomstige cellen zich, na aankomst in de nier, onder invloed van het omringende nierweefsel, kunnen specialiseren tot

niercellen om daarmee de beschadigde niercellen te vervangen en de schade te herstellen. Deze hypothese hebben wij proefondervindelijk onderzocht.
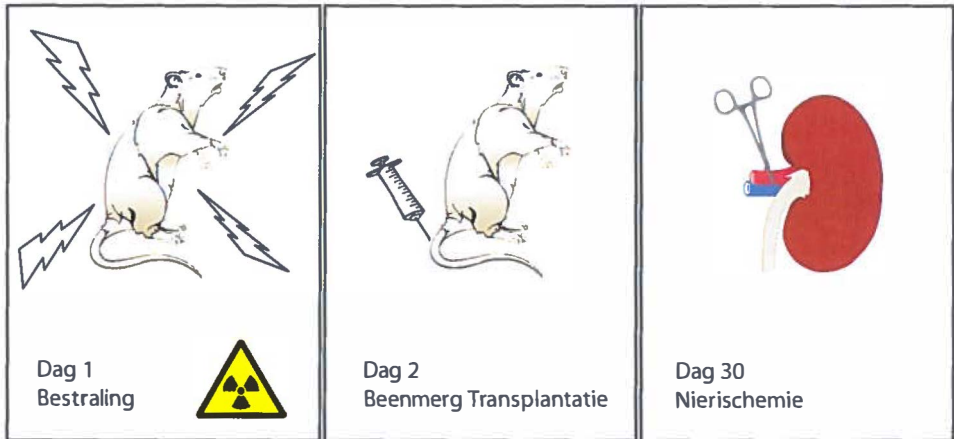
Proefdiermodellen

Deze hypothese hebben we onderzocht in proefdiermodellen. In de eerste plaats moesten we daartoe een model opzetten waarin het mogelijk was om aan cellen in de nier te kunnen zien dat ze oorspronkelijk uit het beenmerg afkomstig waren. Om dit te bewerkstelligen werd het beenmerg van ratten voorzien van een makkelijke herkenbaar label, door eerst het eigen beenmerg te verwijderen door bestraling en vervolgens een beenmergtransplantatie te doen met gelabeld beenmerg (Figuur 2). Het gelabelde beenmerg was afkomstig uit transgene ratten. Het kenmerk van transgene ratten is dat in al hun lichaamscellen een bepaald, normaal niet-voorkomend, eiwit tot expressie komt. Wij hebben gebruik gemaakt van het beenmerg van transgene ratten waarin het eiwit hPAP (humaan Placentaal Alkalische Phosphatase) in alle lichaamscellen tot expressie komt. Door dit hPAP beenmerg te transplanteren naar niet-transgene ratten konden we het hPAP eiwit gebruiken om beenmergafkomstige cellen in de nier te detecteren met simpele histologische technieken.

Vervolgens hadden we een model nodig dat nierschade in de mens simuleert. In hoofdstuk 3 t/m 5 beschrijven we processen die optreden na ischemie/reperfusie schade. Deze schade is het gevolg van een tijdelijke onderbreking van de doorbloeding van de nier (ischemie) en het daarop volgende herstel van de bloedstroom (reperfusie). Deze vorm van schade vindt bijvoorbeeld plaats tijdens niertransplantatie wanneer de nier van het ene lichaam naar het andere wordt verplaatst. We hebben ischemie/reperfusie schade in ratten geïnduceerd door de nierarterie gedurende 45 minuten af te klemmen, gevolgd door herstel van de bloedstroom (Figuur 2). In hoofdstuk 6 hebben we niertransplantaties in ratten uitgevoerd. Aan de hand van dit model konden we de schade na het onderbreken van de bloedstroom onderzoeken, maar ook wat er gebeurt wanneer een nier uit een donor met een andere genetische achtergrond dan de ontvanger (=allogene transplantatie) wordt getransplanteerd en er een immunologische reactie optreedt die tot afstoting kan leiden.

Het uitgevoerde onderzoek – per hoofdstuk

Hoofdstuk 1 geeft een overzicht van de vragen die we in dit proefschrift willen beantwoorden. Dit wordt gedaan aan de hand van een beschrijving van de biologische processen die optreden bij acuut en chronisch nierfalen, de interne herstel mechanismen van de nier en de mogelijke rol van beenmergafkomstige cellen in het herstel na nierschade.

Voor een goede interpretatie van de rol van beenmergafkomstge cellen in nierherstel is het cruciaal om deze cellen in het lichaam te kunnen detecteren. Zoals gezegd hebben we gebruik gemaakt van een diermodel voor beenmergtransplantatie om de beenmergafkomstige cellen te kunnen detecteren in de nier. In de literatuur worden echter vele verschillende detectiesystemen om beenmergafkomstige cellen mee te traceren beschreven. Daarom geven we in hoofdstuk 2 een overzicht van deze verschillende detectiesystemen en hun voor- en nadelen bij het gebruik in modellen van experimentele nierschade.

Figuur 2. *Schematische weergave van de gebruikte proefdiermodellen. Door middel van bestraling wordt het beenmerg van een rat vernietigd. Vervolgens wordt een beenmerg transplantatie uitgevoerd waarmee het vernietigde beenmerg wordt vervangen door transgeen hPAP beenmerg. De ratten herstellen gedurende 30 dagen voor volledige reconstitutie van het beenmerg. Na de herstelperiode wordt nierschade aangebracht door afklemming van de nierarterie gedurende 45 minuten (=ischemie). Vervolgens kunnen de transgene hPAP beenmerg afkomstige cellen in de nier gedetecteerd worden met simpele histologische technieken.*

De capaciteit van beenmergafkomstige cellen om na nierschade te differentiëren tot niercellen hebben we onderzocht in *hoofdstuk 3*. Hiervoor hebben we in ratten met hPAP⁺ beenmerg nierschade aangebracht door hun nierarterie gedurende 45 minuten af te klemmen. Op verschillende tijdstippen na de schade-inductie hebben we de nier onderzocht op de aanwezigheid van beenmergafkomstige (hPAP⁺) cellen. In de nier vonden we beenmergafkomstige cellen die ingebouwd waren in de tubulus. Met verdere analyses konden we vaststellen dat deze cellen ook daadwerkelijk niercellen waren geworden. Bovendien vonden we dat er meer beenmergafkomstige cellen ingebouwd werden in de nier tubulus naar mate de nierschade erger was. Een zeer onverwachte bevinding was dat op lange termijn de ingebouwde cellen ook weer verdwenen. Onze resultaten suggereren dat de beenmergafkomstige cellen de beschadigde niercellen kunnen vervangen maar dat ze, wanneer de schade herstelt is, weer verdwijnen. Het inbouwen van beenmergafkomstige cellen in de tubulus gebeurde echter slechts op kleine schaal, en kon daarom onmogelijk verantwoordelijk zijn voor het herstel van de nier dat we in de loop der tijd observeerden. Aangezien het bekend is dat de nier zichzelf tot op zekere hoogte kan herstellen, onderzochten we of cellen uit de nier zelf verantwoordelijk waren voor het geobserveerde herstel proces. Het bleek dat het merendeel van de beschadigde niercellen inderdaad vervangen werd door vermeerdering van niet-beschadigde niercellen.

In de tubulus van beschadigde nieren werden dus slechts sporadisch beenmergafkomstige cellen werden ingebouwd. In de ruimte tussen de nefronen, de interstitiële ruimte, werd daarentegen een grote hoeveelheid beenmergafkomstige cellen aangetroffen. Voor het merendeel waren dit ontstekingscellen, die aangemaakt worden in het beenmerg en na orgaanschade vanuit het beenmerg naar de plaats van schade bewegen om daar lichaamsvreemde en dode cellen op

te ruimen en de wondheling te bevorderen. In *hoofdstuk 4* hebben we onderzocht of de beenmergafkomstige cellen in de interstitiële ruimte van de beschadigde nier in staat zijn om differentiëren tot myofibroblasten. Zoals eerder genoemd zijn myofibroblasten in staat om bindweefsel eiwitten te produceren en zijn ze kort na het moment van beschadiging op de plaats van de schade aanwezig om een bijdrage leveren aan wondheling. In het geval van overtollige productie van bindweefsel kunnen myofibroblasten bijdragen aan het ontstaan van fibrotische nierschade. Uit ons onderzoek bleek dat beenmergafkomstige cellen inderdaad in staat waren om te differentiëren tot myofibroblasten en dat ruim 30% van alle myofibroblasten in de nier van afkomstig was uit het beenmerg. Additionele analyses wezen uit dat myofibroblasten die ontstaan waren uit beenmergafkomstige cellen bindweefsel konden produceren en dus functioneel waren. In ons nierschade model toonden we daarmee indirect aan dat beenmergafkomstige cellen een bijdrage leveren aan wondheling. Omdat in ons model geen nier fibrose optrad, konden we geen uitspraak doen over een eventuele bijdrage van beenmergafkomstige cellen aan fibrose, maar andere onderzoekers hebben inmiddels een bijdrage van de beenmerafkomstige cellen aan nierfibrose kunnen bevestigen.

Om afstoting van de getransplantateerde nier te voorkomen, worden de ontvangers van een donor nier behandeld met immunosuppressieve medicatie. Een veel gebruikt immuunosuppressief medicijn is ciclosporine (CsA). Een bijwerking van CsA is echter dat CsA het ontstaan van nier fibrose stimuleert. Om te onderzoeken of die pro-fibrotische bijwerking komt doordat CsA de differentiatie van beenmergafkomstige cellen tot myofibroblasten stimuleert, hebben we ratten behandeld met CsA. In *hoofdstuk 5* beschreven we dat CsA behandeling inderdaad leidt tot een verhoogde afzetting van bindweefsel in de interstitiële ruimte, maar de differentiatie van beenmergafkomstige cellen naar myofibroblasten werd niet gestimuleerd. CsA geïnduceerde fibrose, zoals die vaak optreedt in CsA behandelde niertransplantatie patiënten, wordt dus niet veroorzaakt door beenmergafkomstige cellen.

In alle tot nu toe beschreven experimenten hebben we beenmergafkomstige cellen bestudeerd na ischemische nierschade, d.w.z. na schade die veroorzaakt wordt door het tijdelijk onderbreken van de bloedtoevoer naar de nier. Deze schade treedt op tijdens niertransplantatie, wanneer het donor orgaan van de donor naar de ontvanger wordt verplaatst en daarmee de bloedtoevoer tijdelijk onderbroken wordt. Echter, een getransplanteerde nier wordt ook aan andere schade prikkels blootgesteld. Zo worden immunologische afstotingsreacties in gang gezet door het immuun systeem van de ontvanger als gevolg van de aanwezigheid van het lichaamsvreemde donor orgaan. Vandaar dat we de differentiatie mogelijkheden van beenmergafkomstige cellen wilden onderzoeken in een model waarin ook een reactie van het immuun systeem optreedt, omdat dat meer overeenkomst vertoont met de situatie bij de nierpatient. Om dit te bewerkstelligen hebben we niertransplantaties uitgevoerd in ratten. In dit model hebben we geen gebruik gemaakt van beenmerg transplantatie om beenmergafkomstige cellen te kunnen detecteren. In plaats daarvan hebben we een nier uit een gewone rat getransplanteerd naar een transgene ontvanger rat. Zoals eerder beschreven, brengen alle lichaamscellen van de transgene rat een eiwit, in ons geval hPAP, tot expressie. Door met histologische technieken hPAP in de getransplanteerde nier aan te tonen, kunnen we cellen detecteren die van buiten de nier afkomstig zijn. We spreken in dit geval dus niet van beenmergafkomstige cellen

maar we noemen de cellen die van buitenaf de nier infiltreren ontvangerafkomstige cellen. In *hoofdstuk 6* hebben we het inbouwen van ontvangerafkomstige cellen in de nier tubulus en differentiatie tot myofibroblasten bestudeerd na niertransplantatie in ratten. We hebben de processen na 2 vormen van transplantatie bestudeerd, namelijk syngene (donor en ontvanger zijn genetisch identiek) en allogene (donor en ontvanger zijn genetisch verschillend) niertransplantatie. Het inbouwen van ontvangerafkomstige cellen in de nier tubulus werd gevonden in de syngene getransplanteerde nier, 14 dagen na transplantatie. Na allogene niertransplantatie vonden we dat een groter aantal tubuli ontvangerafkomstige cellen bevatten. Aangezien de nier na allogene transplantatie ernstiger beschadigd is, geeft dit aan dat, vergelijkbaar met onze bevindingen in *hoofdstuk 3*, het aantal ingebouwde ontvangerafkomstige cellen toeneemt met toenemende mate van schade. Eveneens vergelijkbaar met onze voorgaande bevindingen was het lage aantal ingebouwde ontvangerafkomstige cellen. Een groter deel van de ontvangerafkomstige cellen bleek te differentiëren tot myofibroblasten. Na allogene transplantatie was het aantal myofibroblasten in de nier verhoogd in vergelijking met de situatie na syngene transplantatie. Echter, percentueel was er geen verschil in de bijdrage van ontvangerafkomstige cellen aan de totale myofibroblast cel populatie. Deze resultaten suggereren dat allogene niertransplantatie, in vergelijking met syngene niertransplantatie, tot gevolg heeft dat ontvangerafkomstige cellen in grotere aantallen inbouwen in de nier tubulus, terwijl er geen verschil is in de relatieve bijdrage van ontvangerafkomstige cellen aan de myofibroblast cel populatie in de nier.

Alle bovenstaande experimenten zouden moeilijk, danwel onmogelijk, uit te voeren zijn in mensen. In *hoofdstuk 7* hebben we met de beperkte mogelijkheden die we voor handen hadden, getracht de rol van de beenmergafkomstige cellen te onderzoeken in de humane situatie. Hierbij hebben we de aanwezigheid van beenmergafkomstige cellen onderzocht in het bloed van patiënten met nierfalen die nog geen dialyse behandeling nodig hadden en in het bloed van patiënten die recentelijk een niertransplantatie hebben ondergaan. We hebben ons hierbij gericht op een specifiek type beenmergafkomstig cel, de endotheel voorloper cel (endothelial progenitor cell, EPC). EPC kunnen inbouwen in beschadigde bloedvaten en daarmee zijn deze beenmergafkomstige cellen mogelijk betrokken bij het herstel van bloedvaten na schade. Gedacht wordt dat een verminderde hoeveelheid EPC in het bloed duidt op een verminderde capaciteit tot bloedvat herstel en daarmee een verhoogde kans op slecht functionerende bloedvaten. Uit ons onderzoek bleek dat patiënten met nierfalen een verlaagd aantal EPC in hun bloed hadden in vergelijking met gezonde mensen. Doordat de nieren van deze patiënten niet goed functioneren, blijven afvalstoffen (uremische toxines) achter in het lichaam. Mogelijk worden de cellen in het bloed blootgesteld aan deze toxines waardoor ze afnemen in aantal. Het aantal EPC was nog verder verlaagd in het bloed van patiënten die recentelijk een niertransplantatie hadden ondergaan. Deze patiënten hebben vaak een voorgeschiedenis van langdurig nierfalen, wat mogelijk verklaart waarom hun aantallen EPC nog verder verlaagd zijn. Wanneer we het bloed van deze ontvangers van een niertransplantatie op een later tijdstip, en met een verbeterde nierfunctie nogmaals onderzochten, bleek dat het aantal EPC was verbeterd ten opzichte van de eerste meting. Deze resultaten suggereren dat niertransplantatie, met een verbetering in nierfunctie tot gevolg, kan leiden tot normalisatie van het aantal EPC in het bloed.

In *hoofdstuk 8* worden de resultaten van dit proefschrift geplaatst in het kader van het huidige internationale onderzoek naar beenmergafkomstige cellen in nierherstel. Verder wordt in dit hoofdstuk bediscussieerd waar het toekomstige onderzoek zich op zou moeten richten.

Conclusies

In dit proefschrift hebben we aangetoond dat beenmergafkomstige cellen de mogelijkheid hebben om te differentiëren tot andere celtypen, te weten nier tubulus cellen en myofibroblasten. Onze bevindingen suggereren dat de rol van beenmergafkomstige cellen in nierherstel twee-ledig is. Enerzijds hebben we aangetoond dat beenmergafkomstige cellen soms inbouwen in de nier tubulus en differentiëren tot tubulus cel (*hoofdstukken 3, 5, 6*). Anderzijds, en in veel grotere aantallen troffen we beenmergafkomstige cellen in de interstitiële ruimte aan die differentiëerden naar myofibroblasten (*hoofdstukken 4, 5, 6*). Door de productie van bindweefsel eiwitten kunnen myofibroblasten, die ontstaan zijn uit beenmergafkomstige cellen, bijdragen aan wondheling maar mogelijk ook aan het ontstaan van nier fibrose.

Gebaseerd op bovenstaande bevindingen lijkt de toepassing van beenmergafkomstige cellen om nierherstel te bewerkstelligen in patiënten met nierfalen niet geheel zonder gevaar. Zo zou het inbrengen van grote hoeveelheden beenmergafkomstige cellen in nierpatiënten kunnen leiden tot nierfibrose. Daarom zijn wij van mening dat het gebruik van beenmergafkomstige cellen voor therapeutische doeleinden niet zonder het nodige vervolgonderzoek kan plaatsvinden. De mechanismen die verantwoordelijk zijn voor de differentiatie van beenmergafkomstige cellen tot myofibroblasten zullen moeten worden geïdentificeerd om controle en sturing van deze differentiatie stap te kunnen bewerkstelligen. Tot deze mechanismen ontrafeld zijn, is de therapeutische toepassing van beenmergafkomstige cellen in patiënten met nierfalen niet verantwoord.

9

Het recept voor een succesvol AIO-schap

Het Recept voor een Succesvol AIO-schap
Men neme:

Een inspirerende begeleider.

Eliane, dankjewel voor... te veel om op te noemen! Ik was jouw "kindje" en in 4 jaar tijd heb je me opgevoed tot wetenschapper. Bedankt dat je jouw passie voor de wetenschap met mij hebt willen delen en me begeleid hebt op de, soms hobbelige, weg naar mijn promotie. Eigenlijk is het niet mijn, maar ons proefschrift en ik hoop dat je net zo trots bent op ons eindproduct als ik.

Een werklustige analist

Jasper, jouw medewerking aan het project was absoluut onmisbaar! Als er een analist-van-het-jaar-verkiezing was, zou ik je nomineren. Bedankt voor je flexibiliteit, enorme werklust, je nuchtere houding en dat je er altijd was!

Een intellectueel ondersteuningsteam.

Marco, bedankt voor je waardevolle inbreng bij de intellectuele ondersteuning van het project en alle "teammomenten". Op een vaak plagende, maar altijd leuke, manier stimuleer je mensen tot nadenken en ik heb dat als enorm leerzaam beschouwd! Dat professoren niet onbereikbaar hoeven te zijn, bewijzen Gezan en Marja. Gezan, jouw enthousiasme werkt aanstekelijk! Daarnaast wil ik je bedanken voor al je hulp en je enorme betrok- kenheid. Marja, allereerst bedankt voor het creëren van

zo'n fijne werkomgeving en prachtig lab voor de stamcel en
toxiciteit engineering-club. En, naast al het andere, bedankt voor
het houden van overzicht met de "helicopter view".

Een bekwame micro-chirurg
Arjen, door al je "Mac Gyver" acties werden moeilijk uitvoerbare
experimenten toch mogelijk. En naast de vele dierexperimenten, bleek
even een "bakkie" doen op het CDL een prima therapie voor een
gestreste AIO! Bedankt voor alles!

Een enthousiaste groep dierverzorgers & biotechnici
Vooral Harm en Natasha hebben mij in de eerste jaren "bijgestaan",
want werken op AOLO8 was zoiets als wild kamperen: je moest alles
zelf meezeuwen. Maar het ging prima, dankzij jullie. Ook op het
CDL heb ik altijd veel hulp gehad met het werk dat ik zelf niet kon,
wilde of durfde te doen... bedankt allemaal!

Begripvolle AIO "lotgenoten"
Machteld, 10 jaar geleden zijn we begonnen met kletsen, en zijn
nooit meer opgehouden. Onze AIO-collega's zijn er vast wel eens gek
van geworden, maar ik vond het super! Bedankt ook voor je hulp
en vriendschap. Monika, jouw Poolse temperament zorgde voor
leven in de brouwerij en was een prima toevoeging aan onze, tot dan
toe, hollandse AIO kamer. Guido, niet alleen je Sorsto was erg
welkom op onze kamer: het was vooral erg gezellig ouwehoeren
over mooie vakantiebestemmingen en leuke restaurantjes.

Maike, je sleurde me mee in je enthousiasme en liet me juichen voor het Duits voetbal elftal. Geloof me als ik zeg dat dat een hele prestatie is! Bedankt voor je gezelligheid!

Daniël, Susanne, Jasper, Dirk, Caroline, Jan-Renier, allemaal in hetzelfde schuitje en dat schept een band!

Heleen en Patricia, de andere "nier-vrouwen" met wie ik nog lang niet uitgekletst ben!

Een goede werkomgeving gecombineerd met een flinke dosis gezelligheid Harry, Theo en Jan-Luuk, bedankt dat ik een kijkje in jullie 'keukens' mocht nemen en daarvan kon profiteren! Barry & Martin, bedankt dat jullie me altijd zo goed van alles op de hoogte gehouden hebben! Sigga, Alieda, Linda, Xavier, Corien, Josée, Jelle, Flooke, Maartje, Greetje, Alice, Marja, Ieneke, Henriëtte, Hans en de "nieuwelingen" Ali, Xing-Song, Annemarie en Miriam, bedankt voor alle raad en daad en al het andere dat de werksfeer zo aangenaam maakte.

Leergierige flex-werkers

Reshma, Ingrid en Yvonne, de studenten die bruisend van energie bij mij op het lab kwamen om iets te leren. Ik hoop dat dat gelukt is, jullie hebben in elk geval heel wat stukjes van mijn proefschrift bijelkaar gepipetteerd. Bedankt!

163

Een technisch support-team

Arja, bepaalde dingen kan je maar beter aan andere mensen over laten. Chris, Arjen en Martijn: dankzij jullie ziet mijn boekje er zo flitsend en strak uit, bedankt jongens!

Verder neme men een ruime hoeveelheid tijd voor ontspanning, en laat men zich omringen door:

Een Posse

Wij groeiden samen op en volgen elkaar al jaren, waar dan ook. Met al onze posse-avonturen zou ik een tweede boekje kunnen vullen! Hoewel we stiekem allemaal harstikke ambitieus zijn in ons werk, is het heerlijk dat het met jullie niet altijd over werk hoeft te gaan. Wij begrijpen elkaar volkomen! Marloes, Helga, Jelle, Arja en Patrick... bedankt!

Bioloogjes

Machteld en Lysanne, wij zijn met z'n drieën afgestudeerd en nu ook gepromoveerd. Alledrie op onze eigen manier maar de tips, steun en begrip tijdens de hobbels op de weg waren onontbeerlijk! Bovendien waren die spelletjesavonden, de (vedal vegetarische) culinaire hoogstandjes, kroegavonden en leuke trapjes samen met Martijn, Roos, Arja en Martijn een perfecte afwisseling op onze promotie-perikelen. Bedankt allemaal!

164

Een stabiele thuisbasis

Pap en mam, jullie hebben me altijd een luisterend oor, een helpende hand en een bemoedigend woord geboden. Bedankt! En vooral voor al die keren dat jullie me even "uit kwamen laten" als ik ernstige behoefte had aan afleiding van het werk. Chris, als grote broer ben je een belangrijke "adviseur" op vele fronten voor me, dankjewel voor al je goede raad!

Het geheime ingrediënt

(hiervan kan men nooit teveel toevoegen...)

Martijn, bedankt dat je er altijd voor me was, bent er hopelijk altijd zult zijn!

Voor het beste resultaat dient men alle bovengenoemde ingrediënten samen te voegen. Vier jaar pruttelen en er staat u een smaak-sensatie te wachten!

Martine